The development of a graphene-copper composite for use in drinking water treatment

A thesis submitted to Dublin City University in fulfilment of the requirements for the award of the degree of Doctor of Philosophy

By

Declan McGlade B.Sc.

School of Biotechnology,

Dublin City University,

Dublin 9,

Ireland.

Research Supervisors: Dr. Bríd Quilty, Dr. Kieran Nolan, Dr. Jenny Lawler & Dr. Anne Morrissey

January 2017

Declaration

I hereby certify that this material, which I now submit for assessment on the programme of study leading to the award of Doctor of Philosophy is entirely my own work, that I have exercised reasonable care to ensure that the work is original, and does not to the best of my knowledge breach any law of copyright, and has not been taken from the work of others save and to the extent that such work has been cited and acknowledged within the text of my work.

Declan McGlade	Date
(57375328)	

Acknowledgements

I would like to thank my whole supervisory panel; Dr. Kieran Nolan, Dr. Jenny Lawler and Dr. Anne Morrissey for their work over the years across the different aspects of the project.

The most profound and deepest thanks must of course go to my supervisor Dr. Bríd Quilty. Without whom this would never have been completed and without whom I would not have been given the opportunity in the first place.

My lab mate Thayse Marques Passos who has been a tremendously positive influence on me throughout my time in DCU. Not only has she given invaluable advice with regards to work but she has helped me grow as a person.

All of the staff across the different schools who have helped me over the years. In particular the technical staff in both the school of biotechnology and the school of chemical sciences who have facilitated my work so willingly; Allison, Theresa, Deirdre, Graham, Monica, David, Kasia, Veronica, Vinny and Aisling but to name a few.

All of my friends at DCU, both old and new, from undergraduate all the way through the PhD who have given their support. My parents and my family who have given encouragement from start to finish, their help in any way was always appreciated.

Contents

List of abbreviations

AA – Ascorbic acid

AFM – Atomic force microscopy

BRGO – Biologically reduced graphene oxide

BSA – Bovine serum albumin

CFU – Colony forming units

CNT – Carbon nanotube

Cu-rGO – Graphene-copper composite

CVD – Chemical vapour deposition

GFM – Graphene family materials

GO – Graphene Oxide

LB – Langmuir-Blodgett

LB-broth – Luria-Bertani broth

MFC – Microbial fuel cell

MIC – Minimum Inhibitory Ceoncentration

MWCNT – Multi-walled carbon nanotube

NBT – Nitro blue tetrazolium

PBS – phosphate buffered saline

PLL – Poly-L-lysine

rGO – Reduced graphene oxide

ROS – Reactive oxygen species

SEM – Scanning electron microscopy

SWCNT – Single-walled carbon nanotube

TEM – Transmission electron microscopy

XTT – 2, 3-Bis-(2Methoxy-4-Nitro-5-Sulfophenyl)-2H-Tetrazolium-5-Carboxanilide

ZOI – Zone of Inhibition

List of Figures

List of Tables

Abstract

The development of a graphene-copper composite for use in drinking water treatment

Declan McGlade, School of Biotechnology, Dublin City University

It was of interest to investigate the use of graphene as both an antibacterial agent and an absorbent to treat drinking water. The use of l-ascorbic acid as a reducing and capping agent was developed as a novel method for the immobilisation of the graphene-copper composite. Graphene oxide (GO), reduced graphene oxide (rGO) and a graphene copper composite (Cu-rGO) were produced and characterised using ultraviolet-visible spectroscopy (UV-vis), thermogravimetric analysis (TGA), dynamic light scattering (DLS), scanning electron microscopy (SEM) and energy-dispersive x-ray spectroscopy (EDX). Graphene oxide (GO) and reduced graphene oxide (rGO) showed no antibacterial activity. The graphene-copper composite showed antibacterial activity against *E. coli* and *B. subtilis* at 10^5CFU/ml at 100ppm. Scanning electron microscopy (SEM) showed membrane damage as the most likely mechanism of antibacterial action and fluorescent microscopy showed adherence of bacterial cells to graphene particles. The effectiveness of the composite was attributed to the antibacterial activity of the copper and the adsorptive potential of the graphene. Immobilisation of the composite was of interest to apply the material in a practical manner to a water treatment prototype. Two methods, one using sodium borohydride ($NaBH_4$) and another using l-ascorbic acid were used for composite production. The composite was immobilised as free standing films and as a coating on commercial glass fibre membranes. The immobilised composite inhibited *E. coli* and *B. subtilis* at 10^8 CFU/ml within forty minutes of contact and had maximum adsorption capacities of 482 mg/g and 183 mg/g for methylene blue and famotidine respectively. A prototype incorporating the composite coated membranes was capable of inactivating *E. coli* at 10^2 CFU/ml and removing *Cryptosporidium* at 10 oocysts/L at a flow rate of 90 ml/min. Testing following the filtration of 100L showed that copper leaching was minimal with a maximum concentration of 1.3mg/L and no mutagenic activity was detected using the AMES test.

1. Introduction

1.1 Water treatment in the modern age

Historically, human settlements have been established close or adjacent to water sources in order to facilitate ease of access to water for drinking, cooking and other everyday activities. This ease of access focused on the availability of water rather than quality. While certain qualities of water can be overtly undesirable, such as odour, cloudiness or an unpleasant taste, more important characteristics are not obvious to human senses. The chemical and microbiological quality of water in particular can have a profound impact on human health and the analysis of these two characteristics did not become possible until the late 1800's. While contamination with chemical and microbiological contaminants was not widespread historically, the increased level of human activity and habitation across the globe has led to spoiling of reliable sources of drinking water. Removing bacteria and other microorganisms from water, for sanitation or drinking, is an extremely topical issue worldwide for both "western" and developing countries (Li et al. 2008) (Narayan 2010). A recent WHO report has shown that 38% of health-care facilities in 54 developing countries do not have access to an adequate water supply, significantly increasing the chance of infection due to water-borne microorganisms (WHO 2015). Even developed countries such as Ireland, despite being famed for its clean water, also suffer with microbiological issues in water bodies. The continued *Cryptosporidium* outbreaks and boil water notices being served across more rural areas of the country are a prime example of how there exists a requirement for new, more effective, treatment systems (Duffy 2015). The most recent drinking water report from the Irish EPA has stated that improving disinfection standards in water treatment is a key and immediate issue (The Environmental Protection Agency 2013). Disinfection is now a poignant example of how traditional water treatment methods are becoming insufficient in the modern age. Cryptosporidium for example, a protozoa which requires low numbers to incur a pathogenic response, is typically not effected by standard levels of chlorination, even in bathing waters (Carpenter et al. 1999). While it can be effectively inactivated by other treatment methods such as ozonation, these carry their own risks in the form of disinfection by-products. Although ozonation is an effective form of disinfection it can lead to the production of carcinogenic bromates and other undesirables; Driedger *et al.* (2001). Even chlorination, the traditional form of tertiary treatment for water disinfection, can result in the production of trihalomethanes and haloacetic acids, both of which can be carcinogenic from prolonged exposure (Chauret et al. 2001). In addition to these modern disinfection issues, the removal of new and emergent chemical contaminants is also a consideration for contemporary water treatment systems. Pharmaceuticals, personal care products (PCPs) and antibiotics are being used in increasing amounts, are not removed by traditional water treatment systems and are

entering waterways in volumes not seen in the past. While the long-term health effects of many of these contaminants are not known, they do represent an emergent hazard which needs to be addressed. The European-union (EU) has already drafted a watch list of contaminants of emerging concern which includes antibiotics (Azithromycin) and anti-inflammatories (Diclofenac) among others (Carvalho et al. 2015). Indeed, the more prevalent use of antibiotics has resulted in their presence in increasing concentrations within activated sludge systems, traditionally seen as the work-horse of waste-water treatment. These increased antibiotic levels within waste water treatment plants (WWTP) has seen the rise of anti-biotic resistant bacteria and their spread into the environment through the water course (Yang et al. 2013). These bacteria may also prove more resilient to standard disinfection methods and it highlights the need for new methods of disinfection at the tertiary stage of drinking water treatment. The current "gold standard" within water treatment is the reverse osmosis system which relies on a semi-permeable membrane and hydrostatic pressure to remove contaminants (Yoon et al. 2003). It has been shown to be effective at removing small molecules of emergent concern such as endocrine disruptors at greater than 95% and can remove both bacteria, viruses and other potential pathogens (Uang & Edlak 2001). While an effective method for the removal of both potential pathogens and chemical contaminants reverse osmosis systems are susceptible to fouling and do not inactivate microorganisms. An ideal system would be capable of removing chemical contaminants and inactivated retained microorganisms. These issues are of particular importance to smaller rural treatment plants rather than their larger counterparts. The ability of smaller group water schemes or public sources to deal with existing and emergent issues can be limited by both funding and man-power compared to the treatment systems of larger urban centres. This has been highlighted in Ireland with the public / private group schemes having the poorest microbiological quality with 95% compliance to *E. coli* standards compared to 100% of public water supplies (The Environmental Protection Agency 2017). These schemes would benefit from the implementation of new technology which would be capable of dealing with these issues cheaper and more effectively. The requirement for new materials and methods of water treatment, for both disinfection and chemical contaminant removal, is apparent. Graphene is a relatively new material which shows potential as an adsorptive agent for organic material and other chemical pollutants from water (S. Wang *et al.* 2013) (Yang et al. 2011) (Maliyekkal et al. 2013). Graphene, in its many forms, is also purported to be an effective antibacterial agent particularly when composited with other biocides like metals. It may be that graphene, as an adsorptive agent for chemical removal and as an antibacterial agent for disinfection may be an effective material to deal with these rising issues in water treatment.

1.2 The graphene family

Graphene is a single-atom thick sheet of carbon atoms in a honeycombed structure (Allen *et al.* 2010), (Meyer et al. 2007) which is being heralded in popular media as the "wonder material" of the century (Peplow 2013), (Shukman 2013), (Macguire *et al.* 2013). Initiatives such as the graphene flagship have seen funding levels in the region of billions of euro being made available for graphene related research in recent years (Graphene-Flagship.eu 2013). Graphene shows great potential in the electronics industry and may play a pivotal role in the next generation of electrical devices. The amount of graphene focused research has been burgeoning consistently since 2004, when Novoselov and Geim first isolated and reported the material; they were subsequently awarded the noble prize in chemistry in 2010 for the work (Novoselov *et al.* 2004). Graphene has seen intensive use across varying scientific disciplines from controlled drug delivery (Yang *et al.* 2009), to photo-catalysis (Xiang *et al.* 2012) (Zhang *et al.* 2010). The primary research focus for graphene remains electronics however. The high surface-to-volume ratio present in graphene lends it an incredibly high adsorptive capacity and has led to its application in the removal of contaminants and other undesirable components in water (Nguyen *et al.* 2012) (Kemp *et al.* 2013). As such graphene represents a promising material for environmental applications like water treatment.

Graphene oxide (GO) is chemically exfoliated from graphite and is easily dispersed in water due to the numerous hydroxyl, carboxyl and epoxyl functional groups present on its surface. It is typically produced using various modifications to the Hummer's method; the chemical exfoliation of graphite using concentrated acid and potassium permanganate (Hummers Jr & Offeman 1958). This easily applied bench-top synthesis is seeing high popularity in terms of research application as it does not require expensive equipment as is needed in the chemical vapour deposition (CVD) method of graphene production and results in a more readily usable material compared to methods such as mechanical exfoliation, in which the sheets of graphene will typically be attached to a substrate following isolation. Reduced graphene oxide (rGO) commonly produced via reduction of GO and these two materials form the basis for the majority of graphene related microbiological and adsorptive studies. In addition, both GO and rGO can easily be composited with other materials such as metals, polymers or biomolecules allowing for the addition of specific tailored functionality. The production of graphene-composite materials has allowed the widespread application of graphene as a carrier molecule in many fields of study and research. As the production of graphene materials via chemical means is more easily achieved, cheaper and can be up-scaled compared to mechanical exfoliation (Novoselov & Jiang 2005) or chemical vapour deposition (Li *et al.* 2009), it is the method of choice for the majority of microbiologically focused studies.

However, the physical and mechanical differences between chemically synthesised graphene materials and the more pristine graphene sheets produced mechanically or by CVD have already been highlighted and their response should not be taken as a direct representation of the antibacterial efficacy of pristine graphene (Loh *et al.* 2010).

Furthermore, during the chemical exfoliation of graphene from graphite, the resulting surface functionalisation and the average sheet size produced are not homogenous; the process is not a typical organic synthesis in the classic sense, as a definitive molecule is not produced. Rather, the product is a colloidal suspension of oxidised graphene sheets of varying lateral size, thickness and surface functionalisation. This raises issues when considering biological applications of these materials, as batch-to-batch variations in their fundamental characteristics will impact significantly on their interaction with biological systems. It is important to note the potential issue in comparability between individual studies using chemical synthesis. Additionally, this also represents a potential problem when attempting to provide definitive information as to the toxicity of graphene related materials (GRMs) such as composites of metals, polymers and other additions. This is a particularly relevant point as there is currently no standard or guidelines for the characterisation of GRMs and those sold commercially will often be certified / characterised on a batch-to-batch basis. The biological availability and potential toxicity of GRMs would be dependent on their surface functionalisation as well as several other physical and chemical characteristics including particle size and oxidative potential.

1.3 The emergence of antibacterial graphene

As graphene is a carbon nanomaterial, it is reasonable to look to the antibacterial and toxic potential of other carbon nanomaterials in order to glean an understanding of the expected level of toxicity of graphene and its potential mechanisms of action. Therefore, we can look to other members of the carbon nanomaterial family such as carbon-60 and carbon nanotubes. Carbon nanotubes can be single or multi-walled and the different biological response between the two varieties highlights how variation in structure can impact the biological availability of nanomaterials. Two studies from (Jia *et al.* 2005) and (Kang *et al.* 2009) suggested that the cytotoxic potential of carbon nanomaterials is inversely proportional to the mass, i.e. the greater the complexity of the carbon nanomaterial, the less toxic and vice versa. They suggested that this relationship may be due to the available surface-to-volume ratio of the materials. They proposed that single walled carbon nanotubes would be the most toxic, followed by multi-walled nanotubes and finally carbon-60, which would have a negligible effect. A study from (Kang *et al.* 2008) supports this suggestion, in terms of antibacterial action, where it was found that single walled carbon nanotubes were more effective at

inactivating *E. coli* than their multi-walled counterparts. (Fang *et al.* 2007) showed that colloidal suspensions of carbon-60 were capable of altering the membrane composition of both gram-positive *B. subtilis* and gram-negative *P. putida* resulting in a more fluid membrane and that the *B. subtilis* was the more susceptible of the two organisms suggesting that the membrane composition of the target organism plays a key role in the susceptibility to the toxic effect of carbon nanomaterials. A report from (Lyon & Alvarez 2008) suggested that direct contact with carbon-60 could result in non-reactive oxygen species (non-ROS) mediated oxidative stress in microorganisms which would disrupt cellular function and a further study from (Kang *et al.* 2007) suggested that direct contact between carbon nanotubes and *E. coli* was required to incur antibacterial action via cell membrane damage. As the majority of these studies suggest that carbon nanomaterials incur antibacterial action via membrane damage and oxidative stress it is not unreasonable to expect that graphene may operate via a similar mode of action.

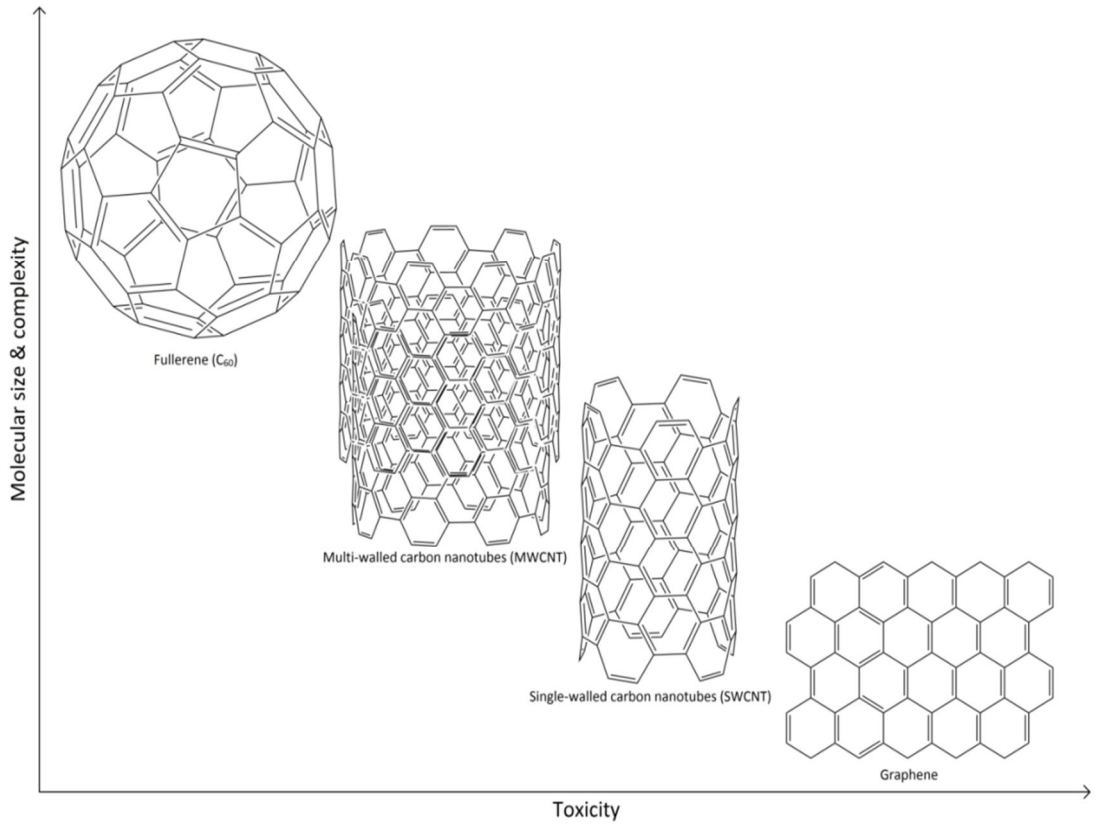

Figure 1.1 The potential mass-to-toxicity relationship which may exist within the carbon nanomaterial family as suggested by both (Jia *et al.* 2005) and (Kang *et al.* 2009) It is suggested that the smaller and less complex nano-materials like graphene would be more toxic than their larger counter parts like Carbon-60. Should this relationship hold true, graphene would be the most potent material in terms of its toxicity.

Additionally, with the idea that the more molecularly simple forms of carbon nanomaterials possess the greater toxic potential, it would be reasonable to assume that graphene, as the simplest form of any carbon nanomaterial, could possess the greatest toxic potential and

consequently may be the most useful in terms of antibacterial applications. Graphene materials may express their antibacterial activity via similar channels to those mentioned above and it is useful to consider the family of materials as carbon nanomaterials are fundamentally similar in terms of their elemental composition. Examining the timeline of published work in terms of antibacterial graphene materials will give an insight into the process by which the field has evolved, its focus and the fundamental issues in examining their microbiological response. While composite materials are a heavy feature in this area of research and make up the majority of work done, focusing on the studies which examine stand-alone graphene materials will allow an understanding of how and why they may exert an antibacterial response. The number of contradictory reports as to the level of antibacterial activity, the dose and time-dependent response and the mechanisms of action highlights why the research thrust of the research moved toward composite materials.

The first study to report on the antibacterial activity of graphene materials was published by (Akhavan *et al.* 2009) and reported on the photoinactivation of *E. coli* using a titanium-dioxide (TiO_2)-graphene film. While unique in terms of its use of a graphene-TiO_2 hybrid, the study was focused on the improvement to the already high photocatalytic potential of TiO_2 rather than the anti-bacterial effects of graphene materials alone. There was no comparative work done on the antibacterial effect of stand-alone graphene materials against the TiO_2 composite. The quantity of investigative work into the antibacterial potential of graphene materials has increased steadily over subsequent years since with 70 studies published in 2014 alone and numbers moving to and above the one hundred mark over the following two years. In 2010, the publication of two studies, one from (Hu *et al.* 2010) and a second study from (Akhavan *et al.* 2010) catalysed the interest in the use of graphene materials as potential antibacterial agents and set the scene, with their suggestions as to the mechanisms of antibacterial action. (Hu *et al.* 2010) described the use of a free-standing graphene paper for the inactivation of *E. coli* which also appeared to possess very little cytotoxic action against human epithelial cells, bringing forward the idea that antibacterial graphene may be useful in clinical applications where they may come into contact with humans as well as microorganisms. Additionally, it was stated that the graphene paper could be easily formed via a one-step filtration process, an attractive concept for the creation of antibacterial surfaces and more easily handled items compared to suspensions of graphene formed via chemical exfoliation. They reported that both graphene oxide (GO) and reduced graphene oxide (rGO) were effective antibacterial agents in solution at concentration ranges of less than 100mg/L. The second study from (Akhavan *et al.* 2010) showed that graphene sheets, both oxidised and reduced, could be deposited in a perpendicular manner on a stainless steel substrate and that the available

"sharp edges" of the sheets would result in membrane damage to both gram positive *S. Aureus* and gram-negative *E. coli* that came into contact with them. They reported that the *S. Aureus* was more susceptible to damage than the *E. coli* to which they assigned the more robust nature of the cell envelope of *E. coli* due to the presence of the outer membrane.

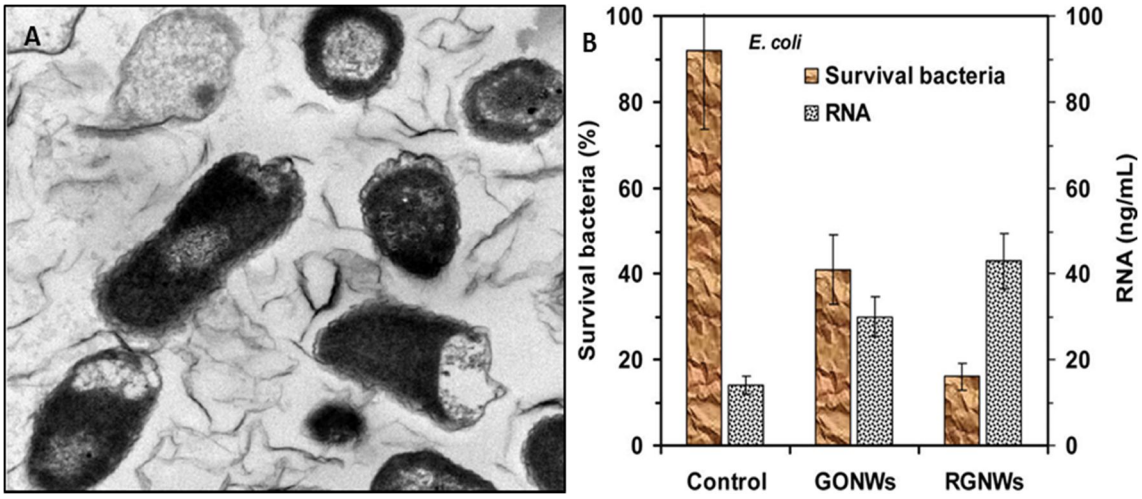

Figure 1.2 Results from the investigations by [A] (Hu *et al.* 2010) and [B] (Akhavan *et al.* 2010) which were pivotal in forming the idea that membrane damage was a key mechanism of action in the antibacterial activity of graphene materials. Hu et al. claimed that their TEM observations [A] showed *E. coli* with membrane damage following exposure to graphene oxide (GO) sheets in solution. Akhavan et al. used an RNA efflux assay [B] to show that intracellular material was being ejected into the surrounding media from cells due to membrane damage following exposure to fixed GO and rGO sheets.

Both of these studies were integral in establishing the proposed mechanisms of antibacterial action of graphene materials, as both described the membrane damage which was occurring in cells coming into contact with graphene sheets. Hu *et al.* showed apparent membrane damage occurring in *E. coli* cells via both scanning electron (SEM) and transmission electron (TEM) microscopic analysis. (Akhavan *et al* 2010. reported the efflux of RNA from cells following exposure to deposited graphene sheets, which was suggestive of membrane damage and the loss of intracellular material into the surrounding environment. While (Akhavan *et al.* 2010) stated that their reduced graphene oxide (rGO) nanowalls were more effective at inactivating *E. coli* than their graphene oxide (GO) counterparts, (Hu *et al.* 2010) found that the GO was more effective, albeit marginally, than rGO when introduced into solution. The difference in toxicity may be due to the fixation of the material and the availability of the surface in relation to the organisms present. It is difficult to directly compare the toxic effect in each case as one study deals with free particles in solution and the other with graphene materials fixed to a surface. Taken together however, these studies would seem to suggest that both graphene oxide and reduced graphene oxide showed potential as antibacterial agents.

In parallel to these studies, which were examining the effect of stand-alone graphene materials, a study by (Shen *et al.* 2010) examined the effect of a graphene-silver nano-composite on several microorganisms. This study was the first to examine the potential synergistic effect between biocidal heavy metals and graphene materials against microorganisms. They found that the composite material was effective at completely inhibiting three separate microorganisms at concentrations as low as 0.05mg/L in solution, several orders of magnitude less than that required for stand-alone graphene materials as reported by (Hu *et al.* 2010) at that point. Though no comparative work with GO or rGO was carried out within the same study, the antibacterial potential of the graphene-silver composite was clear. This initial study by (Shen *et al.* 2010) was the first of what was to become the most investigated graphene-metal composite for antibacterial applications.

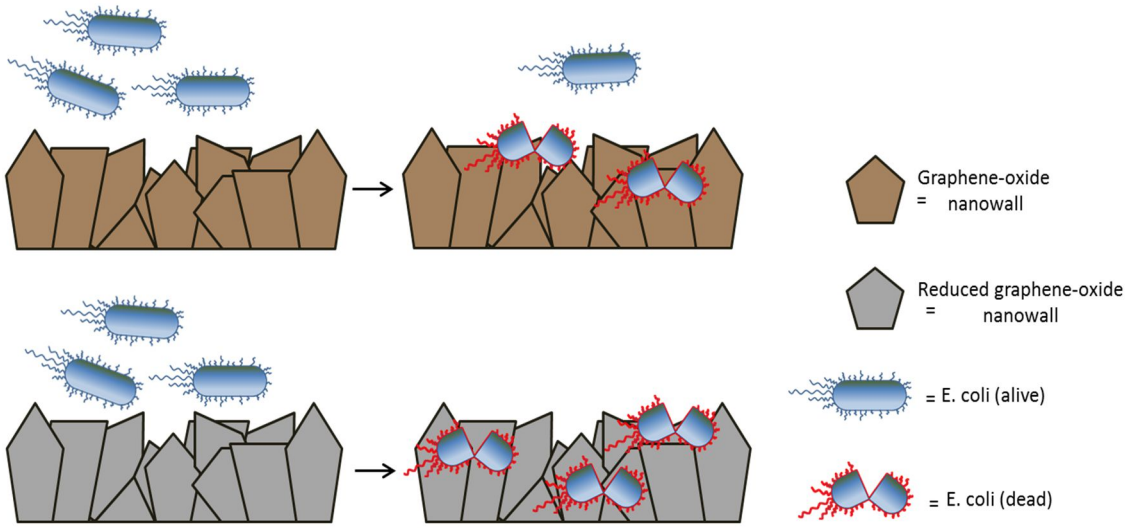

Figure 1.3 The mechanism of action proposed by (Akhavan *et al.* 2010) as to the antibacterial activity of fixed graphene sheets as "nanowalls". Bacteria coming into contact with the edges of the graphene sheets have their membranes damaged and are killed. Their results showed that reduced graphene oxide (rGO) nanowalls were more effective that those formed using graphene oxide (GO).

With the advent of these studies, pushing graphene into the area of antibacterial applications and away from traditional electronic investigations which were garnering the most attention, a catalysis within this field of research occurred in subsequent years. The primary focus of antibacterial graphene based materials would move more toward composite materials, with their apparent superior effectiveness, and away from the application of stand-alone graphene. Composites of silver in particular would garner the most attention in the following years.

1.4 Toward composite use and the understanding of mechanisms

While the majority of studies examining the antibacterial potential of graphene materials focus on the use of composites, silver is by far the most used material in terms of composite production. This is due to the well-established biocidal effect of silver against bacteria and other microorganisms, as well as the relative ease by which graphene-metal composites could be produced (Morones *et al.*(2005) (Oberdörster *et al.* 2007) (Durán *et al.* 2010). In 2011 for example, almost half of the total studies published which addressed the subject of antibacterial graphene materials dealt with silver composites (Xu *et al.* 2011) (D. Zhang *et al.* 2011) (L. Liu *et al.* 2011) (Das *et al.* 2011), (Dai *et al.* 2011) (Bao *et al.* 2011) (Ma *et al.* 2011). The incorporation of non-heavy metal materials into graphene for antibacterial applications was also coming to light at this time, with the emergence of graphene as a possible carrier in a drug delivery system (Gao *et al.* 2011) (Pandey *et al.* 2011) and the incorporation of other well-established biocidal compounds such as phosphonium salts (Cai *et al.* 2011).

A more keen interest into the actual mechanism of action was also coming into focus with a study from (Liu *et al.* 2011) examining the antibacterial effect of both graphene oxide (GO) and reduced graphene oxide (rGO) compared to its parent materials; graphite and graphite oxide. The effect of these materials against *E. coli* was examined via shake flask studies in saline solution and cell structure following incubation was subsequently examined via scanning electron microscopy (SEM). They examined whether or not graphene materials would exert oxidative stress on cells via a γ-L-glutamyl-L-cysteinyl-glycine (GSH) oxidation assay and an XTT assay for the detection of reactive oxygen species (ROS). The effect of each material was examined for both time and concentration dependant activity and it was found that graphene oxide possessed the greater anti-bacterial effect between itself and the reduced graphene oxide with almost 70% loss in bacterial population over 2 hours at 40mg/L. Over a four hour period, the effect was more pronounced, with the GO achieving a 90% reduction and the rGO achieving 75% reduction. The antibacterial effect of the two parent graphitic materials was found to be negligible. They stated that the antibacterial effect was also concentration dependant, with an increase in GO concentration up to 80mg/L resulting in almost total reduction in population after two hours. With their microscopic examination, Liu *et al.* observed that bacterial cells were becoming wrapped in GO sheets and they suggested that this wrapping would result in isolation from the surrounding environment and the inhibition of normal cellular function. However, the larger more aggregated rGO particles, having lost much of their sheet like structure, were incapable of performing this action and as such were less effective as an antibacterial material. One of the more interesting assertions from this study was that while there was observed oxidation of glutathione in the GSH assay, suggestive of oxidative stress, there was no observable production of reactive oxygen species via the XTT

assay. They suggested that the oxidative stress exerted by graphene materials was ROS-independent and that direct contact between graphene sheets and the cells was required in order to incur a response. This would rationalise the lesser observed antibacterial effect of the rGO, as the larger aggregates would have reduced surface area compared to that of the GO. The more aggregated particles would have a lower overall available surface area, thereby reducing the potential interaction between the material and the bacterial cells in solution. However, the use of tetrazolium salt based assays such as the XTT method has been shown to be interfered with by other carbon nanomaterials like carbon nanotubes previously, though this interference has predominantly resulted in false positives rather than false negative results (Wörle-Knirsch *et al.* 2006) (Casey *et al.* 2007). This may be a contributing factor in the observation from Liu *et al.* in terms of the disparity between the oxidative potential of the materials and the lack of ROS production. However, as mentioned previously, carbon-60 has been shown to exhibit non-ROS mediated oxidative stress and this may be the case for graphene materials.

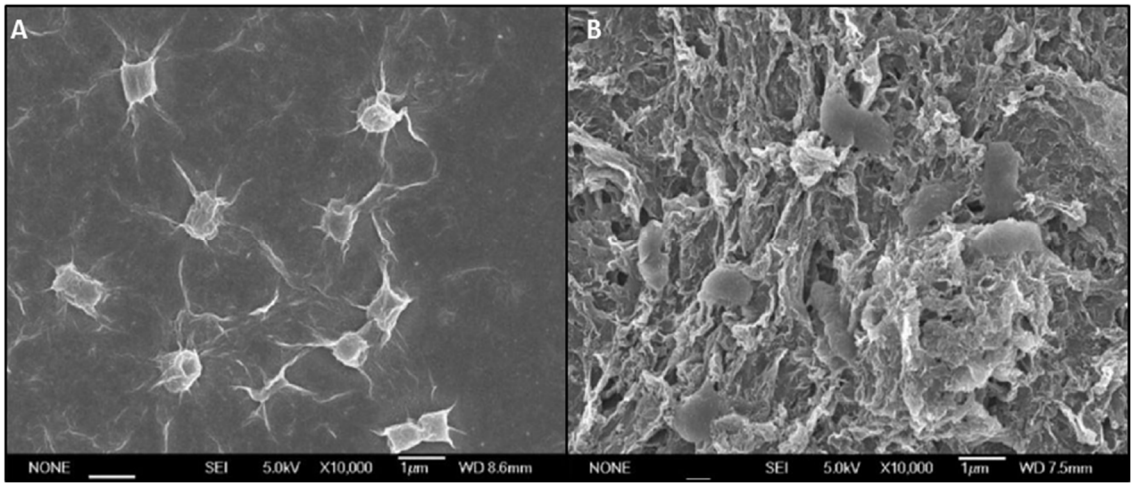

Figure 1.4 Scanning electron micrograph (SEM) images from (Liu *et al.* 2011) showing *E. coli* cells [A] supposedly wrapped in GO sheets and [B] on the surface of rGO aggregates.

The concept of cell wrapping would further be supported by another study from (Akhavan *et al.* 2011), whereby cells were specifically wrapped in graphene oxide sheets for targeted photo-inactivation. They suggested that the wrapped cells were more easily inactivated by near infrared radiation (IR), as the captured cells could be specifically targeted and that the wrapping process isolated them from the surrounding environment thus inhibiting their ability to perform normal cellular function. Additionally, a study from (Ma *et al.* 2011), examining the effect of a graphene-silver composite suggested that this bacterial wrapping or attachment to the material would promote contact between cells and the biocidal material with which it was composited, resulting in a synergistic effect. Thus the composite would have enhanced performance compared to either of the materials alone due to the fact that contact with the cells was more likely.

The attachment and association of bacterial cells with carbonaceous surfaces such as activated carbon has already been well documented for many years (LeChevallier 1988) (Camper 1986).

At this point the suggested mechanisms by which graphene materials may exert their antibacterial effect were beginning to take shape. Cells coming into contact with the thin edges of graphene sheets were likely have their membranes damaged. Direct contact between the sheets, regardless of orientation, would result in oxidative stress to cellular components. It was suggested that sheets of graphene in suspension could wrap cells thereby isolating them from the environment and inhibiting normal function. The suggestion that bacterial cells would adhere to graphene sheets decorated with biocidal metals such as silver and thus enhance the effect of those materials was also supporting the idea that biocidal metal composites of graphene were more effective than the metals alone. Taking all of the proposed mechanisms at this point together, it is clear that the antibacterial effect of any graphene material is reliant on direct contact of the organism with the material.

1.5 Questions of toxicity

During the same period however, a study from (Ruiz *et al.* 2011) sought to address the apparent disparity between the antibacterial potential of graphene materials and their inherent lack of cytotoxic potential to mammalian cells which was also being reported (Chen *et al.* 2008), (Agarwal *et al.* 2010) (Park *et al.* 2010). They questioned the assertion from (Hu *et al.* 2010) that their produced graphene paper was both biocompatible and antibacterial. In their study they stated categorically that "*graphene oxide does not have antibacterial properties*". They examined not only the growth of *E. coli* with the addition of a colloidal suspension of graphene oxide, but also the effect of a graphene oxide coated PVDF membrane on bacterial growth; similar to the paper produced in the study by Hu *et al.* They found that *E. coli* cells grown with the addition of a colloidal suspension of graphene oxide (GO) at 25mg/L resulted in a higher optical density than control samples grown without and scanning electron microscopic (SEM) analysis showed the apparent formation of a thick biofilm on the GO with the production of extracellular polymeric substances (EPS). The PVDF-graphene membranes, coated in both 25 and 75mg/L solutions of GO, showed apparent preferential growth of bacteria in areas of higher GO concentration and qPCR analysis showed that the total number of bacteria present on the GO filters was two and three times higher than that of the control paper. Taking these observations in the context of the concentration dependent observations made by (Hu et al. 2010), where almost total loss of viability was observed after 2 hour incubation with 85mg/L, and the observations from (Liu *et al.* 2011) where incubation over 2 hours with 40mg/L resulted in a 70% reduction in population, it is surprising that no inhibition of bacterial growth *in any way* was observed, particularly with graphene oxide, as in both of

those studies the GO was shown to be the more effective agent compared to the reduced graphene oxide (rGO). It should be noted that there is a disparity between the methods employed by the different studies. Where both Hu and Liu examined the effect of graphene materials in saline solution, which is a non-growth scenario, Ruiz *et al.* examined the antibacterial effect in a growth media. It is possible that the growth media, which would contain not only salts but also amino acids, sugars as well as other constituents to promote growth, would inhibit or limit any possible antibacterial effect from the graphene. If we consider the proposed mechanisms of action, that the thin edges of graphene would damage the cellular membrane and that direct contact with the sheets would induce oxidative stress. It is possible that the incorporation of the graphene sheets into a rich media, such as LB, would result in the occupation of edges and active oxidative sites by other material present and limit the potential contact with bacterial cells, inherently reducing any antibacterial potential.

In the examination of a graphene-silver composite that year, two studies from (Tai *et al.* 2012) and (Das *et al.* 2011) also showed that graphene oxide possessed no antibacterial effect when applied in solid growth media against *S. Aureus* and *E. coli*. A similar study from (Bao *et al.* 2011) however showed a clear zone of inhibition against each of the same two organisms. These observations bring into focus the state of the bacterial cells at the time of exposure to the material as well as the exposure scenario. Each study from Tai, Das and Bao *et al.* examine the effect of graphene materials in solid media. These examinations are based on the disk diffusion method of anti-bacterial action, which is dependent on the diffusion of a biocide into the surrounding media. Considering the already proposed mechanisms of antibacterial action of both GO and rGO, it would be reasonable to assume that they would be incapable of acting in a biocidal manner in this scenario, unless the production of ROS would result in diffusion into the surrounding media. It may be that the antibacterial effect of graphene materials is dependent on the growth state of the organism at the time of exposure as both Hu and Liu applied their graphene materials in a non-growth saline solution. Das, Tai and Ruiz applied GO to a growth media in which bacteria would be in a more active state metabolically, it could be that this more vigorous metabolic state allows the organism to either circumvent or better cope with the antibacterial action of the materials. Both the matrix in which the organism is found and the state of the organism at the time of exposure are extremely important aspects which should be taken into consideration for any microbiological assay and making a direct comparison of concentration dependant response between a growth and non-growth scenario is difficult. The strain of the organism employed and its ability to cope with different environmental stresses is also of paramount consideration. While all of the studies mentioned

used *E. coli* as a model organism, each employed a different strain which also may contribute to the disparity between them.

Another influencing factor which may explain the lack of inherent antibacterial activity observed by (Ruiz *et al* 2011) is the washing procedure employed. This may also account for the obvious contradictory results reported by (Bao *et al* 2011) compared to the results observed by (Tai *et al*. 2011) and (Das *et al.* 2011) using not only the same material but also the same organisms and exposure conditions. While all of the studies mentioned make use of the same preparation method for graphene oxide, chemical exfoliation via the Hummers' method, (Ruiz *et al.* 2011) describe a thorough seven day washing procedure via dialysis to remove residual material from the production step. The washing of chemically exfoliated graphene is renowned as a lengthy process and if not carried out completely will result in residual potentially toxic material which would colour any response observed during a biological assay. Materials used in the production process such as permanganates, concentrated acid and strong reducing agents would have a profound effect on any biological assay even at low concentrations.On the subject of exposure times and matrixes, another use for graphene in terms of microbiological application was also emerging at this time; in microbial fuel cells. Microbial fuel cells, which make use of bacteria to generate an electrical current are often limited by the available surface area within the device for bacterial colonisation (Verstraete *et al.* 2006). It was at this time that (Zhang *et al.* 2011) first suggested a graphene based anode for use within a microbial fuel cell (MFC) to improve performance and (Feng *et al.* 2011) suggested that nitrogen doped graphene would also work well in improving a MFC system. The line of reasoning behind this application is that the graphene, as a carbonaceous, conductive material with high surface area, would act as a large area for bacterial attachment as well as better facilitating electron transfer for current generation. They found that the graphene, specifically reduced graphene oxide (rGO) from chemical exfoliation, did indeed improve the performance of the cell and facilitated the growth of a significant bacterial biofilm with *E. coli* (figure 1.5 [A]). This observation from (Zhang *et al* 2011) called into question the antibacterial efficacy of reduced graphene oxide (rGO) which, while not as effective as GO, was still purported to be antibacterial by both (Hu *et al.* 2010) and (Liu *et al.* 2011). The disparity between the report by (Akhavan *et al.* 2010) with regards to the antibacterial activity of the graphene nanowalls deposited on the stainless steel surface and the graphene decorated surface of the MFC is particularly interesting. Both reports deal with a stainless steel surface which is decorated with graphene and exposed to *E. coli*, where one reports loss of bacterial viability and the other reporting a significant amount of growth, especially as (Akhavan *et al.* 2011) reported that the rGO was the more effective of the two

graphene materials. It may be that the orientation of the graphene sheets, as claimed by (Akhavan et al. 2011), is significant and that only their perpendicularly orientated graphene sheets would exhibit antibacterial activity. As MFCs make use of growth media, it may be that the different media compared to the saline solution employed by (Akhavan et al. 2011) is responsible for the bacterial growth.

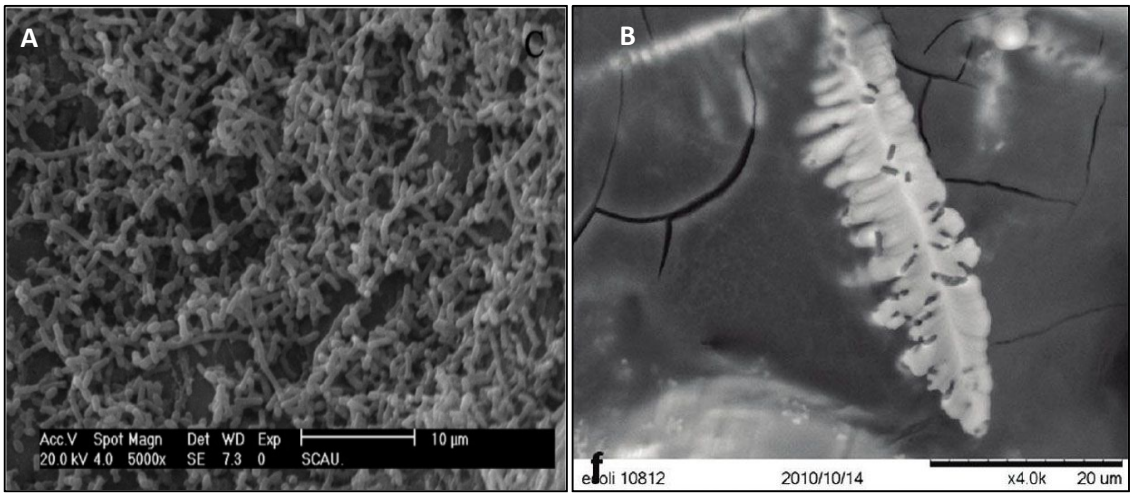

Figure 1.5 scanning electron micrograph (SEM) images from [A] (Zhang *et al.* 2011) shows the growth of an *E. coli* biofilm over a graphene anode in a microbial fuel cell and [B] (Ruiz *et al.* 2011) shows a biofilm growth following *E. coli* incubation with GO sheets.

With the observations from (Ruiz *et al.* 2011) strongly questioning whether or not graphene oxide possessed any anti-bacterial activity at all and the emergence of reduced graphene oxide for microbial fuel cells, the original reports on the strong antibacterial activity of graphene materials began to come into question. Certainly, it would seem that the environment in which bacteria are exposed to graphene materials is an important parameter, as the studies which seem to purport a lack of antibacterial effect exposure examine the organism within a growth scenario. The organisms, being in a more vigorous metabolic state, may be more capable of coping with the stress induced by the exposure to the graphene materials than they would be in a non-growth scenario like saline solution. The examination of the characteristics which influence the antibacterial potential of graphene materials would continue in earnest into the following year with the publication of several studies specifically examining the effect of different and hitherto unexamined exposure parameters.

1.6 On oxidative stress, particle size and bacterial growth

The use of graphene materials for antibacterial purposes continued its focus on composite materials with a further influx of silver based studies being published throughout the following year (Shen *et al.* 2012) (Cai Lin *et al.* 2012) (L. Liu *et al.* 2012) (Chook *et al.* 2012) (Tai *et al.* 2012) (Nguyen *et al.* 2012) (Jiang *et al.* 2012) (Cai *et al.* 2012) (Kholmanov *et al.* 2012). The development of other metal composites for antibacterial purposes was also emerging with composites of zinc (Kavitha *et al.* 2012) being produced as well as the investigation of

graphene polymer and textile composites to form free-standing materials containing graphene for biomedical applications such as antibacterial wound dressings (Lu *et al.* 2012) and antibacterial surfaces (Lim *et al.* 2012) (Carpio *et al.* 2012) (Some *et al.* 2012).

With the publication of another study from (Liu *et al.* 2012) which addressed the potential impact of lateral sheet size on the antibacterial effect of graphene oxide sheets, an additional layer was added to the potential factors influencing the antibacterial capabilities of graphene materials. They sought to ascertain whether their previous assertion as to the cell-wrapping capabilities of GO sheets held true for sheets of different lateral sizes. It is important to consider that graphene sheets, while nanoparticles in the strictest sense can have widely varying lateral sizes. It is reasonable to assume that the size, and the average variability across different sheet sizes in a colloidal suspension of GO, would have a profound effect on how it may interact with a biological system and would obviously impact on the more available plane of interaction, whether edge or face-on i.e. sheets of larger lateral size would have more availability in terms of the basal-plane and those of smaller size would have more available edges. If the assertion that the edges of the graphene sheets are the active site of antibacterial action were to hold true, then colloidal suspensions which contain larger numbers of sheets with a smaller lateral size would then possess the greater antibacterial efficacy than their larger counterparts. Particle size is an extremely important aspect to the potential biological interaction of nanoparticles and the size and shape of other types of nanoparticles such as metals has already been shown to have a profound effect on their antibacterial activity and bioavailability (Martínez-Castañón *et al.* 2008) (Wang *et al.* 2008) (Simon-Deckers *et al.* 2009).

The size of graphene particles had already been shown to affect their toxicity in mammalian cells and the same dependence may hold true for bacterial interaction (Akhavan *et al.* 2012). In their study (Liu *et al.* 2012) examined how graphene oxide sheets sonicated for longer or shorter periods of time affected *E. coli* cells in both saline solution and deionised water. As in their previous study examining the difference between graphene and its parent materials, they examined the effect of lateral sheet size on the ability of GO to oxidise glutathione in a GSH assay to assess oxidative potential. They also examined the physical effect of the different sized GO sheets on *E. coli* cells via atomic force microscopy (AFM). They found that sheets of larger lateral size were more effective at reducing the bacterial population in a short period of time with almost 90% loss in viability after one hour. Sheets of smaller sizes, which were sonicated for up to four hours prior to inoculation, resulted in a much milder but steady decline in bacterial population, up to 56% over four hours, as compared to the sharp initial reduction observed from the larger sheets. From their microscopic analysis they claimed that

laterally large GO sheets were clearly able to wrap and entirely enfold *E. coli* cells in solution. In contrast, the smaller sheets were seen to interact with the bacterial membrane, disrupting and damaging it which resulted in rough pockmarked cells (Figure 1.6 [B]) indicative of membrane damage.

The oxidation assay showed little to no variation in the oxidative potential of the GO sheets of different lateral sizes. Liu *et al.* concluded that the oxidative potential of GO was more a function of the surface functionalisation rather than the available edge sites of the sheets.

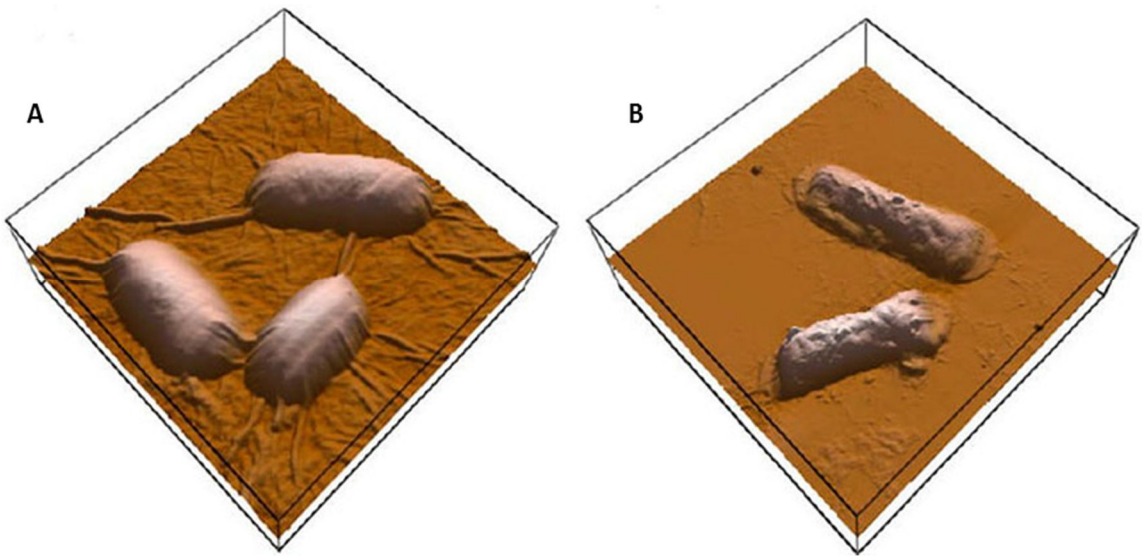

Figure 1.6 Atomic force micrograph (AFM) images captured by (Liu *et al.* 2012) showing [A] *E. coli* cells enwrapped within laterally large GO sheets and [B] *E. coli* cells following incubation with GO sheets of low lateral size showing pocked and damaged membranes.

As GO sheets are invariably molecularly thin, an increase in the available edge sites would not result in a large increase in available surface area. The observation that laterally smaller sheets do not possess inherently greater antibacterial activity questions the earlier observation from Akhavan *et al.* (2010) that it is the available edges of graphene sheets, damaging the bacterial membrane, which is the primary mechanism of antibacterial action.

The previous findings of (Liu *et al.* 2011) that the oxidative stress induced by graphene materials was non-reactive oxygen species (non-ROS) dependent was also brought into question with the publication of a study from (Gurunathan *et al.* 2012). They examined the effect of both graphene oxide and reduced graphene oxide on *P. aeruginosa*, a gram-negative bacterium which had not been challenged with graphene materials up to that point. They examined the effect of suspensions of both graphene oxide and reduced graphene oxide against *P. aeruginosa* in non-growth (saline) and growth (Luria-Bertani) media. In addition they examined whether or not either of the materials would generate reactive oxygen species via a nitroblue tetrazolium (NBT) assay. They showed that the response of *P. aeruginosa* to both GO and rGO was entirely linear in terms of both concentration and time dependant responses with

up to 150mg/L resulting in 90% reduction in population after two hours and 75mg/L resulting in 90% reduction after four hours. The difference in response between GO and rGO was negligible with GO having a marginally stronger effect than the rGO in saline solution. This observation is unique in terms of the level of comparability between the two materials, where most studies which have examined both GO and rGO have reported a more pronounced response from one of the two materials. However the most significant finding in this study pertained to the oxidative stress response. It was reported that both GO and rGO resulted in ROS production 3.8 and 2.7 times higher than that of the control sample. This finding is particularly relevant as (Liu *et al.* 2011) reported no generation of reactive oxygen species from their XTT assay kit. As previously mentioned, some carbon nanomaterials have been shown to interact and disrupt tetrazolium salt based assays. Both the XTT and the NBT assay are based on the reduction of the tetrazolium salt to formazan, resulting in a colour change. The adsorptive nature of graphene oxide, along with its many surface functional groups may have a significant impact on the colour expression from these assays. Whether the adsorption of the formazan products would result in localised concentration and thereby the observation of false positives, as has been shown in carbon nanotubes, would occur or not remains to be seen. It is also possible that graphene oxide could adsorb the functional components within the assay and prevent them from interacting with the molecules of interest, in this case reactive oxygen species, thus inhibiting the expression of the assay which would result in a false-negative. There have been no systematic investigations into the interaction of graphene with different established biological assays for reactive oxygen species as has been done with carbon nanotubes. It is difficult to rationalise either result, particularly in light of the known issues of tetrazolium based assays with other carbon nanomaterials. Categorically saying that graphene materials do or do not result in the production of reactive oxygen species based on the published literature becomes difficult in light of these issues.

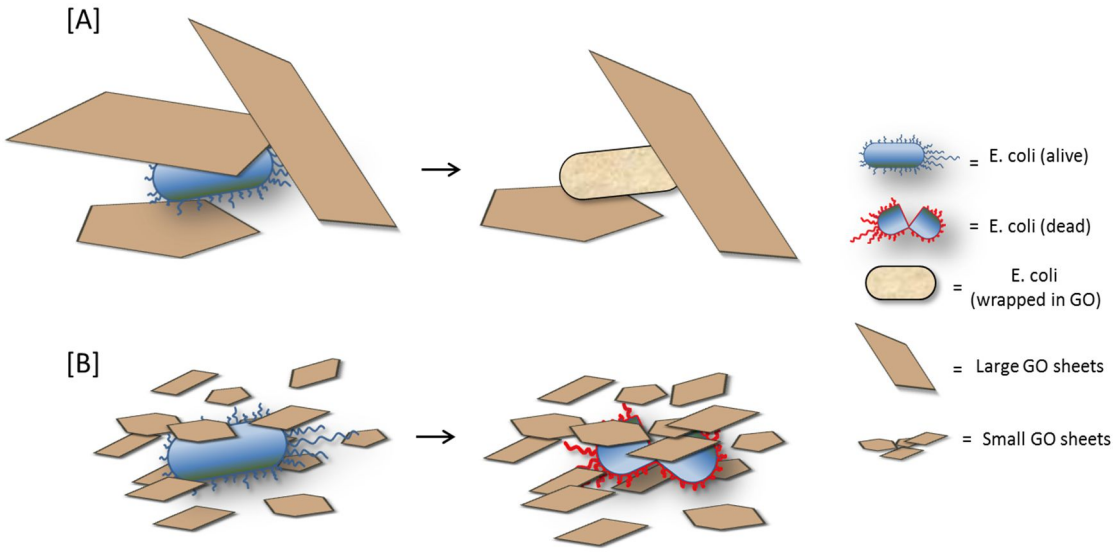

Figure 1.7 The antibacterial mechanism of action proposed by (Liu *et al.* 2012) for graphene oxide sheets of different lateral sizes in suspension. Larger sheets will completely wrap cells and isolate them from the environment, where smaller sheets will pock and damage the cellular envelope.

On the subject of the oxidative potential of graphene, a study from (Krishnamoorthy *et al.* 2012) the following year examined both the antibacterial activity of what they referred to as "graphene nanosheets" produced via the reduction of graphene oxide by hydrazine. For the sake of comparison to the studies already mentioned, these nanosheets can be considered comparable to reduced graphene oxide, as hydrazine reduction is one of the commonly applied methods for the production of rGO from GO. They examined the effect of these nanosheets against several organisms; *E. coli* and S. typhimurium as gram-negative models and *E. faecalis* and *B. subtilis* as gram-positive models. They used the standard broth dilution method to investigate the minimum inhibitory concentration (MIC) against each organism, scanning electron microscopic analysis to investigate the effect of the sheets against the bacterial membrane and most notably they used an ultrasound-induced lipid peroxidation assay to examine they ability of the material to cause lipid peroxidation. The minimum inhibitory concentrations, and indeed the antibacterial response to the material, found by Krishnamoorthy *et al.* were much lower than any other previously observed. The minimum inhibitory concentration is the concentration at which no bacterial growth is observed and as such all the organisms present can be deemed to be inhibited. It was claimed that both *E. coli* and S. typhimurium had an MIC value of just 1mg/L and that *E. faecalis* and *B. subtilis* had values of 8 and 4mg/L respectively, which are orders of magnitude lower than previously reported.

In contrast to the report from (Akhavan *et al.* 2011*)* which claimed that gram-positive bacteria were more susceptible than gram-negative, the opposite is claimed by the authors in this case. As the MIC values for both *E. coli* and S. typhimurium were lower than their gram-positive

counterparts. The authors attribute this greater resistance to the thicker peptidoglycan layer present in the cellular envelope of the gram-positive bacteria. It is also notable that the broth dilution method for minimum inhibitory concentration analysis is carried out in Luria-bertani (LB) broth, a rich growth media. Up to now, the trend in reports showed that only suspensions of graphene materials introduced into non-growth scenarios would exhibit an antibacterial effect against microorganisms present. The report from (Krishnamoorthy *et al. 2012)* showed not only that graphene was effective at inhibiting the growth of several microorganisms in growth media but that their as produced "nanosheets" had MIC values orders of magnitude lower than the already reported concentrations of GO and rGO used previously. Though brief, their investigation into the lipid peroxidation potential showed that the graphene nanosheets, at concentrations of 10 and 5mg/L, increased the level of peroxidation compared to control samples by 117% and 109% respectively. Though no separate assay was performed; the authors claimed this was indicative of ROS production. Whether the production of reactive oxygen species was responsible, or that the lipid peroxidation was due to direct contact non-ROS mediated oxidative potential of the graphene was unconfirmed.

This investigation highlights another fundamental issue in terms of comparison between different studies; terminology. While GO and rGO are terms which are sufficient to encompass the materials which are being dealt with by the majority of microbiologically focused studies, the above example shows that a definitive set of nomenclature is needed to define more strictly the different features of the materials which would help in carrying out a more valid comparison between different studies.

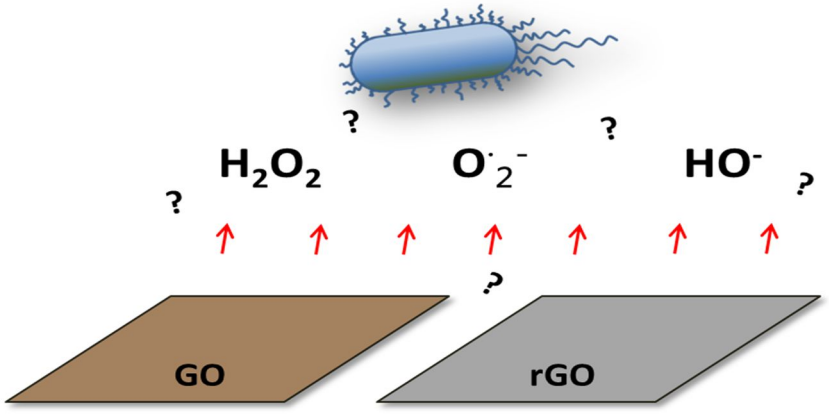

Figure 1.8 Whether or not graphene materials are capable of producing reactive oxygen species still remains to be seen. While (Liu et al. 2011), (Gurunathan et *al.* 2012) and (Krishnamoorthy *et al.* 2012) have all reported the ability of either graphene oxide or reduced graphene oxide to incur oxidative stress, whether or not the production of reactive oxygen species (ROS) or some sort of non-ROS mediated mechanism is responsible is still unknown.

In addition to these studies, which were questioning the already proposed mechanisms of action of antibacterial activity, another study from (Akhavan *et al.* 2012) sought to examine

whether or not *E. coli* could be used to produce reduced graphene oxide from graphene oxide via incubation in anaerobic conditions. The idea of biologically reduced graphene oxide (BRGO) had been investigated previously albeit only with shewanella, a particularly electro-active genus of bacteria which is commonly applied in microbial fuel cells for example (Salas *et al.* 2010) (Wang *et al.* 2011) (Jiao *et al.* 2011). It has been suggested that graphene oxide may act as a terminal electron acceptor in the respiratory pathway and as such benefit any colonising bacteria present. The concept of using a bacterial organism to reduce GO to rGO is somewhat at odds with some of the previous statements from (Akhavan *et al.* 2011) (Liu *et al.* 2011) and (Hu *et al.*2011) who have all claimed that direct contact with the materials will result in bacterial inhibition. However, as this study examined the effect in a growth media and under anaerobic conditions the ability of the organism to cope with, or possibly even benefit from the material may be very different due to the exposure conditions. The observations made by (Ruiz *et al.* 2011) mentioned earlier for example, seemed to suggest that bacteria present in a growth media along with a colloidal suspension of GO would have improved growth unlike the antibacterial effects observed in saline solutions. In their study (Akhavan *et al.* 2012*)* grew *E. coli* in LB broth along with a GO film and examined the effect on the electronic state of the film and the bacterial population over time. They showed that the bacterial growth in the solution with the added GO was comparable to that of the control but at 24 hours a sharp decline in population was observed. They attributed this sudden loss of bacterial viability to the detachment of bacteria from the already reduced surface or the alteration in the electronic structure of the material. Following the production of their BRGO surface they examined the anti-bacterial effect that the surface would have compared to that of GO. They found that the GO surface had little to no effect in terms of bacterial kill and that the BRGO resulted in a 24% reduction following two hours.

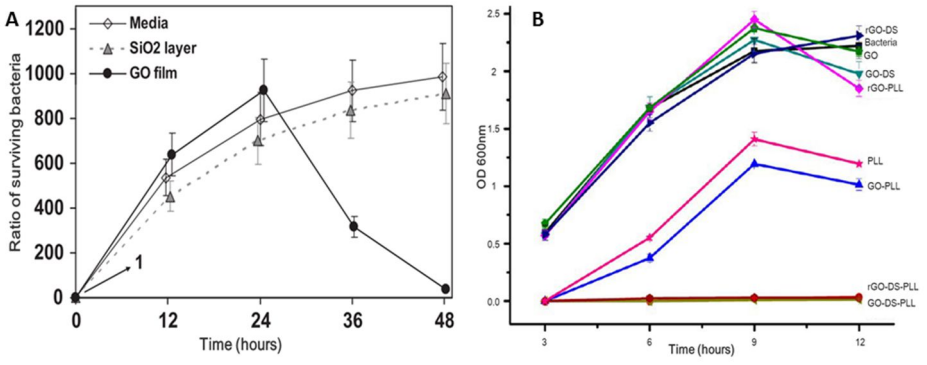

Figure 1.9 [A] The response of *E. coli* in an anaerobic growth scenario with a graphene oxide (GO) film, as published by (Akhavan *et al.* 2012) with a sharp decline in bacterial population after 24 hours. [B] The lack of inherent antibacterial effect from both GO and rGO highlighted by (Some *et al.* 2012) when introduced into a growth media (LB) with *E. coli* at 25mg/L: Green and Navy series. The difference between two studies highlights just how different exposure scenarios and indeed the focus of the investigation can have a profound impact on the results observed.

They used this response to rationalise that it was the detachment from the surface due to the change in surface electronic state of the graphene that resulted in the sudden drop during the growth scenario rather than the minor antibacterial effect of the material. They concluded that, as in their previous study, reduced graphene oxide can have a more profound antibacterial effect than graphene oxide and that under the correct conditions graphene oxide can benefit the bacterial population. This particular study is an excellent example of the dynamic nature of the biological interactions of graphene materials; not only in terms of the culture media used but also in terms on the exposure conditions, whether aerobic or anaerobic. It also emphasises the level of variety which exists in terms of reduction methods and material manipulation which can be carried out on graphene. The effect of the environment in which microorganisms are exposed to graphene materials would be highlighted once again with the publication of a study from (Some *et al.* 2012). They examined the effect of GO and rGO against *E. coli* in growth media (LB broth) and compared their effects to various poly-l-lysine (PLL) composites of each material. In terms of comparability, the study is very similar to that performed by (Ruiz *et al.* 2011) with *E. coli* as a target organism and LB broth as a growth media, albeit with the examination of rGO in addition to GO.

Similar to the results obtained by (Ruiz *et al.* 2011), it was found that neither GO nor rGO had any significant inhibitory effect when introduced into LB media inoculated with *E. coli*. However, it should be noted that no concentration dependant analysis was carried out and that only 25mg/L of each material was tested and observations were carried out over twelve hours, a lengthier period compared to most previous examinations.

Making definitive statements on the antibacterial efficacy of different graphene materials becomes difficult based on the studies done up to this point. Not only do the characteristics of the material; such as lateral size, thickness and surface functionalisation, have a profound influence on their potential interaction, but it is clear that the material can have a dynamic nature dependant on the exposure scenario and the conditions of the environment involved during exposure. The reports from Ruiz and Das *et al.* would seem to have supported the assertion that the antibacterial activity of graphene materials was limited or indeed completely inhibited by its introduction into a growth media as opposed to a saline solution as reported by (Hu *et al.* 2011), (Liu *et al.* 2011) and (Akhavan *et al.* 2011) This media-dependent response was then further supported by the observations of Some et al., for rGO as well as GO, whereby they had no observable effect from either material in their case. However the study by (Krishnamoorthy *et al.* 2012) showed that not only were their graphene nanosheets effective in growth media but that they were profoundly more effective than previous reports had shown. This blatant contradiction only highlights the difficulty in comparing studies that may

have variance in the preparation method of their graphene materials. The report from (Gurunthan *et al.* 2012) also contradicts the initial report from (Liu *et al. 2011)* that the observed oxidative stress induced by graphene materials is ROS independent, however the use of tetrazolium salt based assays throws doubt over both reports. The investigation carried out by (Liu *et al.* 2012) into the effect of lateral sheet size would seem to suggest that the size of graphene oxide sheets will only affect the time-dependant toxicity and not its oxidative stress potential, this suggests that the availability of the edges of the graphene sheets is not a primary mechanism in terms of its antibacterial activity as was suggested in the original work by (Akhavan *et al.* 2010). The importance of defining the material with a suitable naming system which more directly reflects the specific features was also highlighted with the contrasting report on the dose-dependent response from Krishnamoorthy *et al.* and their "graphene nanosheets". An attempt to address the issue of nomenclature and a naming system for the different carbon materials which are all encompassed within the "graphene family" was done in an editorial from *Carbon* (Bianco et al. 2013), though this unified naming system is on-going, with several different institutions vying for their naming system to be the primary one.

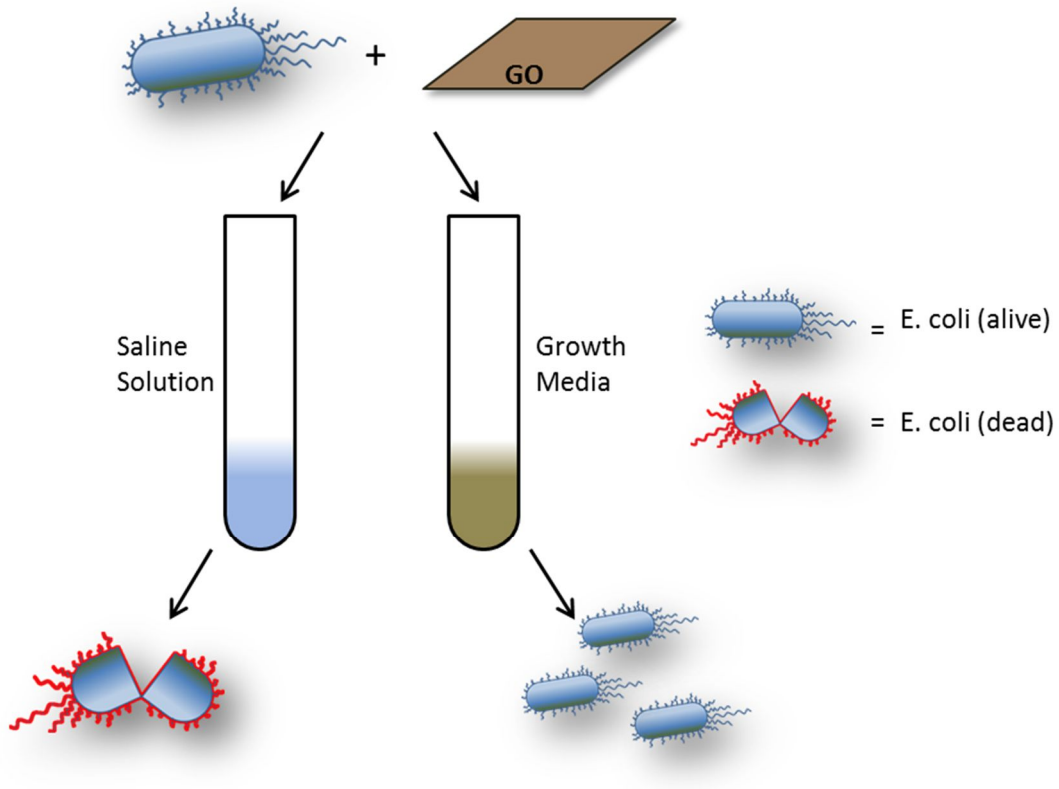

Figure 1.10 A graphical representation of the disparity between the reports showing an antibacterial effect from graphene materials and a lack-thereof, which seemed to depend on the media in which the organism was exposed. Reports from (Ruiz *et al.* 2011) and (Some *et al.* 2012) showed no apparent antibacterial effect from

both GO and rGO against *E. coli* when introduced into a growth media compared to other studies which showed antibacterial activity occurring in saline or buffer solutions.

1.7 Ascertaining mechanisms

The number of investigations which examined the antibacterial potential of graphene materials increased significantly within the following years and the main thrust of this field would continue to find itself in the direction of graphene-silver composites, with numerous composites of silver being investigated and the focus on novel production methods (Tang *et al.* 2013) (Ocsoy *et al.* 2013) (Li *et al.* 2013) (Vijay Kumar *et al.* 2013) (G. He *et al.* 2013) (Han *et al.* 2013) (Jiang *et al.* 2013). A study published in 2013 focused on the production of a new citrate modified graphene oxide-silver composite which once again showed the lack of antibacterial activity of graphene oxide (Das *et al.* 2013). The contradictions in reports as to the antibacterial efficacy of stand-alone graphene materials are most likely the driver in the greater level of interest in composite materials for antibacterial purposes. The addition of a well-established biocidal material such as silver guarantees antibacterial functionality and is a more attractive concept, particularly for practical applications. The emergence of multi-metal as well as multi-material composites such as graphene-polymer-metal composites was also occurring with the advent of multi-purpose graphene materials with antibacterial functionality (Bora *et al.* 2013) (W. He *et al.* 2013) (W. Wang *et al.* 2013) (H. Wang *et al.* 2013) (Yu *et al.* 2013) (Zhang *et al.* 2013) (Zhao *et al.* 2013). Additionally, a thrust into the areas of enhanced photo inactivation of microorganisms using graphene-composites of TiO_2 and other photo catalytic materials was emerging with several publications focusing on this field along with combination materials for both antibacterial and organic pollutant removal (Cao *et al.* 2013) (Gao *et al.* 2013) (W. He *et al.* 2013) (Veerapandian *et al.* 2013) (Raj Pant *et al.* 2013) (Liu *et al.* 2013). To highlight the variation in composite type and use, the application of graphene based antibacterial materials such as membranes and electrically actived materials for water treatment was also an emerging field at this time (Kumar *et al.* 2013) (Hong *et al.* 2013).

However the outstanding study which emerged in 2013, in terms of the antibacterial investigation of graphene materials, was one which addressed the interaction of the edges of graphene sheets with the bacterial envelope. The study from (Tu *et al.* 2013), published in Nature Nanotechnology, examined the effect of graphene oxide nanosheets against *E. coli* in saline solution using traditional counting methods, transmission electron microscopy (TEM) and most uniquely, the application of computer simulations to examine the possible molecular interactions of the edges of the graphene sheets with the cellular membrane. Not only that but they also examined the effect of lateral sheet size on the antibacterial efficacy of the material as well as how it would affect its interaction with the cellular membrane in the simulation experiments. They sought to validate the observations from (Akhavan *et al.* 2010)

with regards to the “sharp edges” of graphene sheets as well as the assertion from (S. Liu *et al.* 2012) that the lateral size of the graphene sheet was an important feature in terms of its antibacterial efficacy. This application of computer modelling is particularly relevant as membrane damage is one of the principal mechanisms of action proposed by many of the investigations which had been carried out up to this point. The assertion that membrane damage would be a principal mechanism of action in the antibacterial potential of graphene materials was based primarily on the previously observed membrane damage which occurred in single walled carbon nanotubes (SWCNTs). However an in-depth study into the membrane damage of graphene had not been carried out as had been done with SWCNTs (Liu *et al.* 2010).

From their microscopic analysis the authors determined that the antibacterial activity of graphene oxide sheets against *E. coli* cells was based not only on kinetic membrane damage but also on the gradual dissolution of the cellular membrane from interaction with the GO sheets which resulted in the extraction of lipids from the phospholipid bi-layer in the cellular envelope.

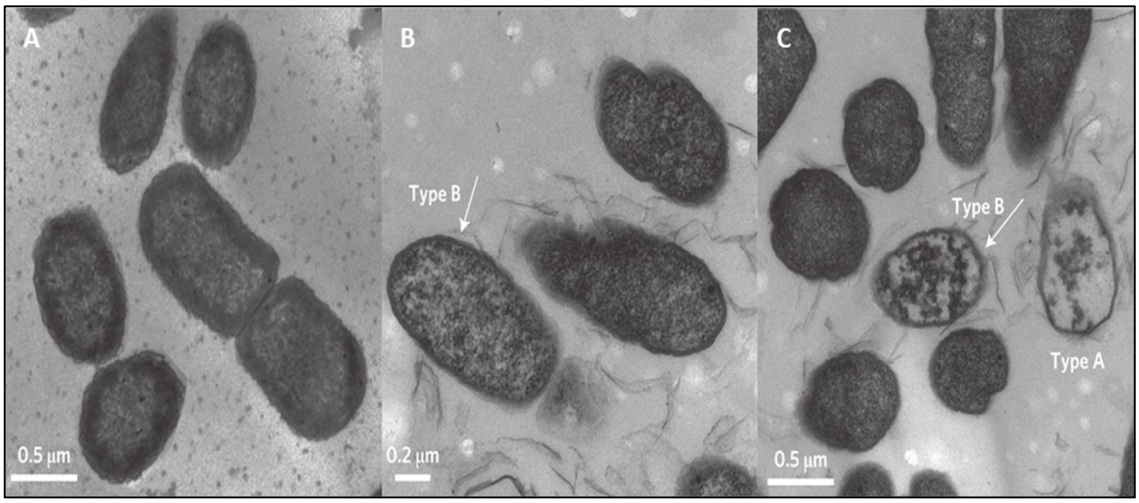

Figure 1.11 The three stages of membrane dissolution, as well as the two types of interaction of GO sheets with the bacterial membrane as described by (Tu *et al.* 2013). Stage I [A] Initial inoculation whereby the cells are unaffected. Stage II [B] with visible thinning of the cellular membrane occurring. Stage III [C] with a “cut” cell of Type A visible and a Type B cell with a membrane having suffered dissolution due to lipid extraction by the GO sheets.

Three stages of membrane dissolution are described during a 2.5 hour incubation with 100mg/L of GO. During the first stage, directly following inoculation, the cells are capable of coping with the GO present in solution and are unaffected with no visible membrane damage. During stage two however, a thinning of the cellular envelope is visible, though no ruptures or leakage of cellular contents has occurred. In the final stage, cells can be observed to have lost cellular integrity entirely which results in what the authors refer to as “empty nests” whereby the intracellular material has almost entirely been evacuated and an empty vessel remains. They divided the potential interaction of the graphene oxide sheets into two types; Type A whereby the GO sheets would become inserted into the bacterial envelope and “cut” the

membrane via kinetic shear and Type B, whereby the insertion of the graphene sheet into the membrane results in vigorous extraction of the phospholipids from the cellular membrane. The authors described the Type A interaction as being representative of the original model proposed by (Akhavan *et al.* 2010), where the "sharp edges" of the GO sheets will cut the membrane via kinetic interaction. The Type B interaction however was a hitherto unseen mechanism and was more clearly described by the computer modelling rather than the TEM analysis. In fact the authors state that they had not hypothesised the Type B interaction from their initial microscopic observations but rather re-evaluated them following the computer modelling simulations. The authors' claim that the extraction of lipids from the cellular membrane is due primarily to the Van der Walls attractions between the edges of the graphene sheet and the membrane lipids, whereby once interaction occurs, the tail end of the sheet becomes trapped within the membrane. The phospholipids then begin to "climb" along the graphene sheet resulting in the eventual dissolution of the membrane. This extraction process continues as the lipids spread across the graphene sheet surface.

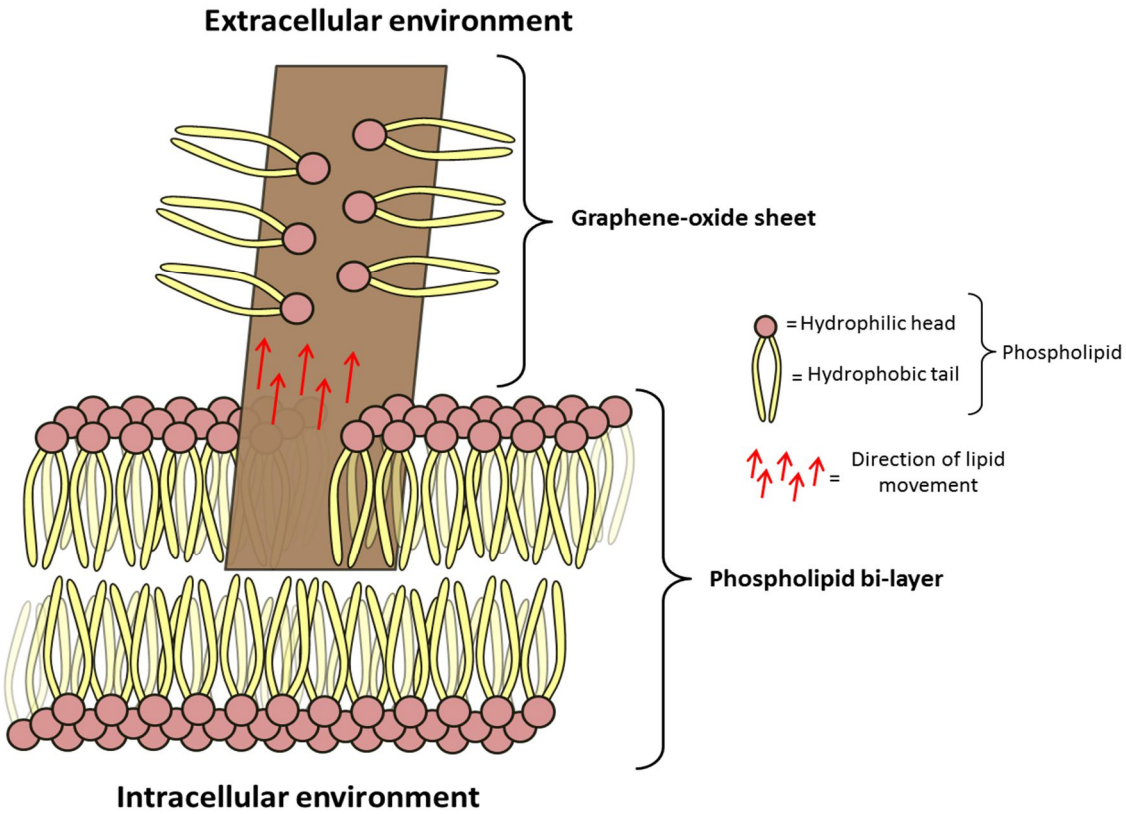

Figure 1.12 The mechanism by which graphene oxide sheets exert antibacterial action as proposed by (Tu *et al.* 2013). From their computer modelling they proposed that graphene oxide sheets will be inserted into the phospholipid bi-layer and extract lipids resulting in membrane dissolution.

They showed, in their simulations, that sheets of larger lateral size would result in a more vigorous extraction of lipids from the membrane. It was claimed that the un-oxidised regions on the GO sheets, more akin to that of pristine graphene, would attract the hydrophobic heads

of the lipids while the oxidised regions would attract the hydrophilic tails. They claimed that the larger un-oxidised regions would promote a greater level of cell dissolution due to the stronger attraction compared to that of the oxidised regions. As such, GO sheets of greater lateral size, which were more likely to contain larger un-oxidised regions than their smaller counter parts, would have the greater potential for lipid extraction. They supported this hypothesis by examining the effect of GO sheets of different lateral size (~500, ~200 and ~50nm) against *E. coli* and found that the largest sheets resulted in the greatest reduction in bacterial population; 90% after 2.5 hours incubation with 100mg/L. This assertion that the larger un-oxidised regions were responsible for the greater antibacterial effect was further rationalised with the characterisation of each suspension of GO via UV-vis. The authors showed that a shift in the absorption spectrum of the material from 238 to 218nm as the size of the GO reduced was indicative of a loss of these large un-oxidised areas which would only be present in laterally large sheets. The authors claimed that this phenomenon held true for both the inner and outer membranes of gram negative *E. coli*. Whether this would occur in the membranes of gram positive organisms, with their thick peptidoglycan layer was not investigated. The relationship between the antibacterial effectiveness of graphene materials and organisms with different membrane structure still requires further investigation as reports already mentioned have shown conflicting results in that regard. The model proposed by (Tu *et al.* 2013) appears robust in explaining the interaction of GO sheets with microorganisms. They established not only the lateral size dependant response but also explained their microscopic observations with computer modelling. Whether the computer model employed accounts for all the variables of this relatively new material is difficult to say, as all of the physical characteristics of graphene are yet to be understood fully. Following the report from (S. Liu *et al.* 2012) where it was found that GO sheets which were laterally large were more effective, it seemed that the original assertion by (Akhavan *et al.* 2010) that the sharp edges of the graphene sheets were responsible was incorrect. With smaller sheets and more available edges, one would expect a greater antibacterial effect but that was not the case. However the above investigation from (Tu *et al.* 2013) provides a rationalisation as to why both laterally large and smaller GO sheets can incur an antibacterial effect and why the relationship is proportional to the available basal planes and not just the edges alone. While the thin edges of the graphene sheets will interact with the cellular membrane regardless, the larger sheets have areas which are more akin to that of pristine graphene. These large areas of sp^2 hybridisation promote the movement of the lipids from the cellular membrane to the graphene sheet moreso than the oxidised regions present on the GO sheets. As such the laterally larger sheets have the greater potential for movement of lipids and thus the greater antibacterial efficacy. However this activity of lipid extraction while promoted by laterally

larger sheets is still dependant on the availability of the edges of GO sheets for the initial interaction with the cellular envelope.

1.8 Edges, planes and charge transfer

In more recent years there have been several reports of a more robust nature which have attempted to define the specific modes of antibacterial action of graphene, particularly in terms of its orientation. In addition, some investigations have been carried out to examine whether or not pristine graphene produced via chemical vapour deposition (CVD) possesses similar attributes to that of its chemically derived cousins. The examination of the antibacterial efficacy of CVD graphene has not been carried out in depth despite it being one of the more reliable methods for producing pristine graphene sheets. The more complex and expensive equipment required to produce CVD graphene is most likely the limiting factor in this regard. Comparison with chemically derived graphene for antibacterial studies becomes difficult as CVD graphene will be inherently bound as a surface to a substrate.

A particularly interesting report from (Li *et al.* 2014) sought to examine the effect of CVD grown graphene sheets on different substrates for antibacterial effectiveness. They examined the effect of monolayer graphene sheets grown on copper (Graphene@Cu), germanium (Graphene@Ge) and graphene grown on a metal substrate which was subsequently transferred onto silicon dioxide (Graphene@SiO_2). They examined the materials against *E. coli* and *S. Aureus* using both plate counting techniques and live/dead fluorescent microscopy.

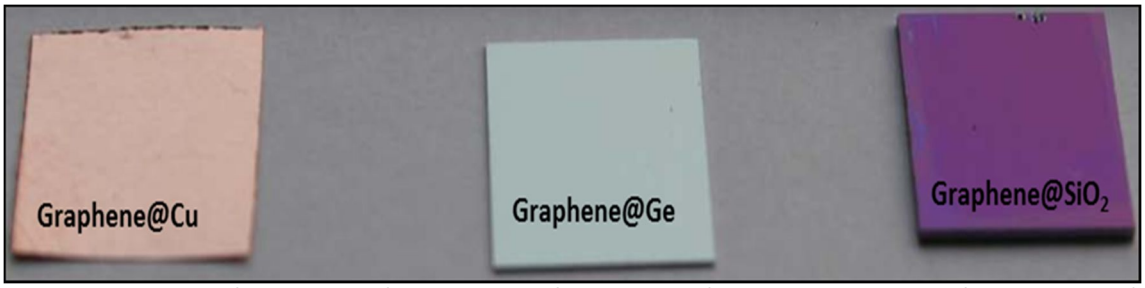

Figure 1.13 Copper (Graphene@Cu), Germanium (Graphene@Ge) and Silicon Dioxide (Graphene@SiO_2) substrates each coated with monolayers of graphene grown via CVD as reported by (Li *et al.* 2014).

Their line of investigation was to examine if electron transfer across the graphene sheets was a driving mechanism for the antibacterial action of pristine sheets. The three substrates would represent the three different types of electrically active materials; conductors (copper), semiconductors (germanium) and insulators (SiO_2). Their model of antibacterial activity via electron transfer was based on graphene forming a junction with the underlying substrate, which would serve to actively transfer electrons from the bacterial cells via the graphene and thus perturb normal cellular function due to the loss of energy, in the form of electrons, in their respiratory pathway.

If correct, this would represent the first such example of this particular mode of action in terms of antibacterial activity of graphene materials. They found that the graphene on the copper substrate was the most effective, followed by the germanium and finally the silicon dioxide against both *E. coli* and *S. Aureus*. Their experimental results proved their hypothesis as copper as a conductor, showed the greatest antibacterial effect and there was no visible effect from the SiO_2 with germanium in the middle. However, it should be noted that the three substrates alone would have expressed this response in any case as copper is known as a more effective biocide than germanium and SiO_2 is not known to be antibacterial. The authors were keen to point out the lack of copper ions being released from their material as they had observed no Cu released after 72 hours in saline solution via inductively coupled plasma mass spectrometry (ICP-MS), though this data was not shown. Examining the as produced graphene films on each of the substrates (Figure 1g), it is difficult to imagine that no interaction between the substrates and the surrounding solution would occur and that there would be no release of biocidal ions with a monolayer of graphene covering only one side.

This electron transfer model would subsequently be refuted with the publication of a study by (Dellieu *et al.* 2015). In order to verify the electron transfer model as proposed by (Lit *et al.* 2014), they examined the effect of CVD graphene partially and fully grown on copper (Cu) and gold (Au) substrates against the same organisms; *E. coli* and *S. Aureus* using Live/Dead and counting techniques in the same manner as the previous study. In terms of the examination of the graphene on a copper substrate, the studies are identical. The purpose of examining the fully and partially grown graphene monolayers was to ascertain whether or not the release of ions into the surrounding media was occurring and how that would affect any observed anti-bacterial effect from the graphene. The authors proposed that copper, in being n-doped, will be inclined to have electrons transferred to it from the graphene monolayer rather than the opposite, as was proposed by (Li *et al.* 2014) additionally; gold, being p-doped, would be more inclined to receive electrons from the attached graphene. This comparison would further serve to prove whether or not the electron transfer model held true as gold possesses a much lower antibacterial potential than copper. As such any dramatic antibacterial effect from the graphene coated gold substrate could be attributed to the electron transfer phenomenon and not to the metal support. Additionally, they performed atomic absorption spectroscopy (AAS) to examine whether or not any metal ions were released into the bacterial solution during incubation. Their result categorically disproves the idea of electron transfer as a mode of antibacterial action in CVD produced graphene monolayers. They found that there was no observable antibacterial effect from the graphene layer grown on the gold substrate against either *E. coli* or *S. Aureus*, or from the gold substrate with no graphene; indicating that even

though the gold would be a viable substrate for electron transfer from the bacterial cells via the graphene that this phenomenon does not occur.

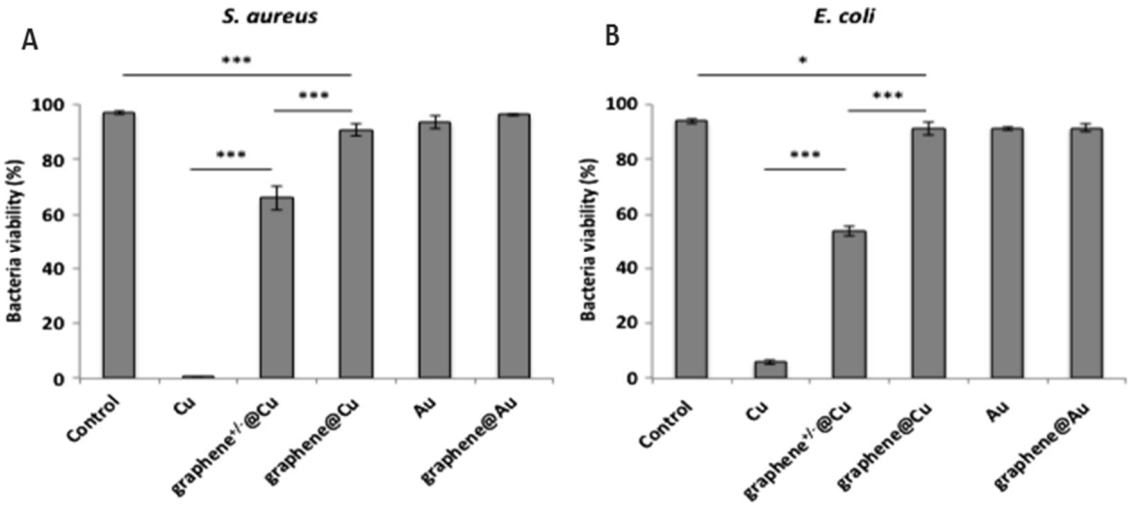

Figure 1.14 The results of cell viability analysis carried out by (Dellieu *et al.* 2015) in which CVD grown graphene layers on copper and gold substrates were tested against *E. coli* and S. Aureus. The results discount the assertion fron (Li *et al*. 2014) that electron transfer is a principal mechanism of action in the antibacterial potential of CVD grown graphene monolayers.

The fully grown monolayer of graphene on the copper substrate showed a less than 10% reduction in bacterial viability against both organisms indicating that the graphene was not eliciting an antibacterial response and the minor reduction was attributed to the release of cupric ions from the underlying substrate. It was also clear that the ability of the copper to release its active ions was limited by the graphene covering the surface. This argument was supported by the much higher reduction, 34% for *S. Aureus* and 46% for *E. coli*, which was caused by the partially grown monolayer. As the bare copper substrate resulted in almost total reduction of the bacterial population for both organisms, the authors surmised that any observed antibacterial effect of the CVD grown graphene was from the underlying substrate and not from the interface between it and the graphene. The results clearly indicate that CVD grown graphene on a copper substrate will limit the release of cupric ions and reduce the biocidal effect of the copper, but that the graphene does not inherently possess any antibacterial potential itself. It is interesting to note that the CVD graphene grown on these substrates would have little to no oxidative groups present on their surface due to the method of production. Taking into account the earlier observation from (Tu *et al.* 2013), in their computer modelling, they observed a greater efflux of lipids from the bacterial membrane with laterally larger sheets of GO which had greater areas of sp^2 hybridisation and thus lower areas of oxidative groups. As the pristine sheets formed via CVD should be composed entirely of un-oxidised regions. The lack of antibacterial activity observed by (Dellieu *et al.* 2015) despite this would seem to suggest that the availibility of the edges of the graphene sheet in order to perform lipid extraction is required for antibacterial action to occur. These two studies

represent the beginnings of a shift in the publication landscape of antibacterial graphene studies. Up to this point the proposed mechanisms of action were very numerous and despite contradictions between reports there had been no studies performed in order to directly refute the claims of another in this line of investigation.

This availability of the different planes of graphene had come into particular focus with the publication of two studies examining how the isolation of graphene oxide sheets via different methods impacts on their antibacterial potential. A study from (Hui *et al.* 2014) sought to examine why, up to this point, there appeared to be contradictory reports as to the antibacterial effects of graphene in differing media, they proposed that removing the availability of the basal planes, the flat surfaces of GO, would inhibit its antibacterial effectiveness. This investigation was in response to those carried out by (Ruiz *et al.* 2011) for example, who had found that the addition of GO into Luria-Bertani (LB) broth improved the growth of organisms present. They examined this phenomenon by tweaking the availability of the basal planes using an occupying protein, bovine serum albumin (BSA), and tryptophan, a basic amino acid as well as examining the effect of the LB-broth itself on the antibacterial efficacy of GO.

Initially they evaluated the effect of GO against *E. coli* in saline solution and found that a concentration of 200mg/L was required to elicit an almost total reduction in bacterial population. However when supplemented with LB broth at 5%, the authors found that a reduction of less than 20% was achieved and that up to 300mg/L only 61.4% of the population was killed; indicating that the addition of the LB broth does indeed inhibit the bactericidal capability of the GO. Following incubation with LB supplemented saline, AFM analysis showed that the average thickness of the GO sheets had increased by 60% to which the authors attributed components from the broth having become adsorbed to the GO sheet surface. As they were unsure what components were responsible, the authors sought to quantify to what extent known components adsorbing to the surface of the GO inhibited its antibacterial efficacy. Suspensions of GO were saturated with BSA in order to ensure total adsorption of the protein to the surface of the GO sheets. Under AFM analysis, the authors found that the average thickness of the sheets was over four times higher, indicating that the GO sheets had totally adsorbed the BSA to their surface. Subsequent antibacterial assays showed that the BSA saturated GO resulted in a reduction of only 34% with 200mg/L. The authors indicated that due to the size of the BSA, only up to 84% of the GO surface would be occupied and as such some surface area would still remain available. The reduction in the antibacterial efficacy was obvious. In order to examine if total coverage of the GO sheet would result in complete inhibition the authors then examined the effect of tryptophan saturated GO in a similar

manner. As tryptophan is a much smaller molecule, but would still readily adsorb to the GO surface, it would be more able to completely occupy the entirety of the GO surface. Following saturation with tryptophan, GO at 200mg/L showed little to no antibacterial action against *E. coli* in saline solution. The authors had shown categorically that occupying the basal planes of GO can render it innocuous as an antibacterial agent. In order to verify the mechanism of action the authors performed a live/dead fluorescent assay, dependant on membrane damage for staining of dead cells, which showed that membrane damage was indeed occurring. While the authors did not hypothesise an exact mode of action, they stated that it was clear that membrane permeabilisation (the creation of a more permeable bacterial membrane) or membrane damage was a key contributor. They also did not rule out the possibility of the edges of GO sheets still being available following BSA saturation as a possible explanation for the remaining antibacterial action observed. This robust investigation shows that the antibacterial efficacy of GO is highly dependent on the environment in which it is introduced and as such the limitations on the application of GO as an antibacterial agent are apparent. Applying any sort of biocide in an already "pristine" environment or scenario seems almost counter intuitive and severely limits potential antibacterial application of GO.

This rationalises the high number of composite focused studies being carried out, as adding a known biocide such as a metal is relatively simple in terms of graphene-composite production and guarantees antibacterial functionality regardless of environment.

The second study which examined the availability of these basal planes did so via a mechanical rather than an occupying method. The study from (Mangadlao *et al.* 2015), isolated flat GO sheets onto a polyethylene terephthalate (PET) surface via the Langmuir-Blodgett (LB) deposition method and examined the response of *E. coli* brought into contact with the fixed GO. Their study sought to not only rationalise the assertion from (Hui *et al.* 2014) as to the availability of the flat surfaces of the GO but also addressed the issue of available edges which was a primary mechanism as suggested by (Akhavan *et al.* 2010) (S. Liu *et al.* 2012) and (Tu *et al.* 2013). The surfaced fixed sheets would also be immobile and unable to wrap the cells and isolate them from the environment as had been previously suggested previously. Though short, their study examined the effect of these flat fixed GO sheets against *E. coli* via Live/Dead fluorescent microscopy and showed that PET with a greater deposition of GO, i.e. more available flat planes had a higher level of antibacterial action than surfaces with less. The use of the LB method for the deposition of GO would make certain that no edges of any of the GO sheets were available for interaction with the organisms. As they surmised that the availability of the edges of the GO sheets is not a primary mechanism of action of the antibacterial activity. This refutes the assertions by (Akhavan *et al.* 2010) and (S. Liu *et al.* 2012) and also

throws doubt of the lipid extraction model as proposed by (Tu *et al.* 2013). While the authors claim that their findings are in line with the lipid extraction model of (Tu *et al.* 2013), the computer modelling suggests that insertion of the edges of the graphene sheets is an essential element in order for lipid extraction to occur. The GO sheets in this case are fixed with their edges unavailable and as such the lipids cannot be extracted as suggested. The authors also state that their findings are in line with the charge transfer model of monolayer graphene as proposed by Wang. As already mentioned this model has since been refuted by the investigation performed by (Dellieu *et al.* 2015) and cannot be applied in this case. Comparing the LB fixed GO sheets to the findings of (Dellieu *et al.* 2015) also raises some serious questions. Why did (Mangadlao *et al.* 2015) observe antibacterial activity with flat GO sheets but the opposite was recorded by (Dellieu *et al.* 2015) with the CVD grown graphene monolayer? It is possible that GO may possess antibacterial capabilities in this format, unlike the CVD grown graphene but there was no suggested model up to that point to explain this mechanism of action.

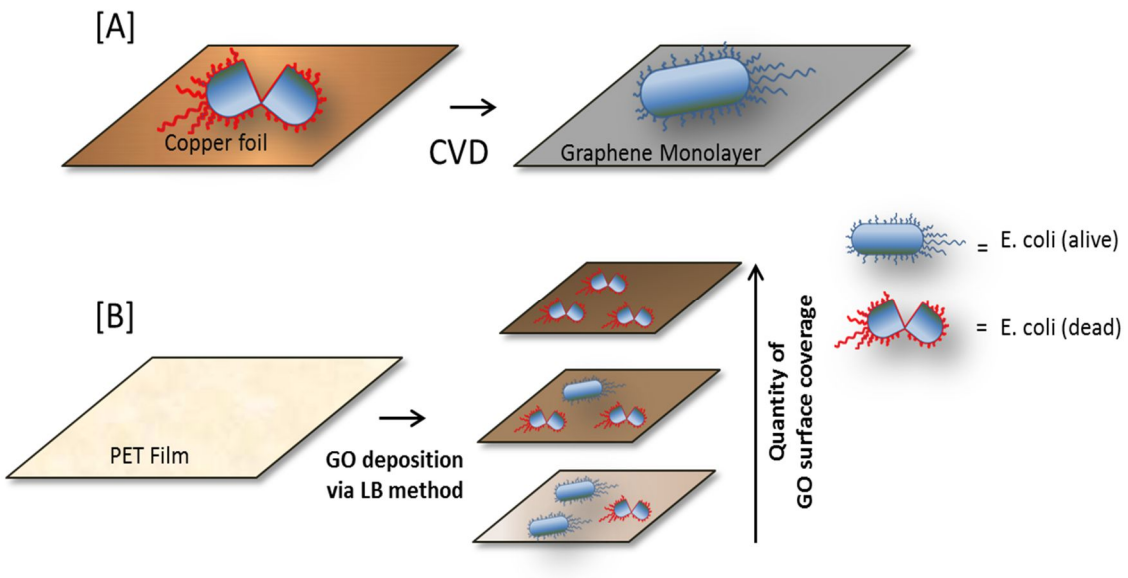

Figure 1.15 [A] (Dellieu *et al.* 2015) had shown that graphene monolayers grown on metallic substrates such as copper possessed no inherent antibacterial effect when completely covering the surface. This questioned the logic of (Tu *et al.* 2015) lipid extraction model due to the larger areas of sp^2 hybridisation on wider GO sheets. Their work disputed the electron transfer model as proposed by (Li *et al.* 2014) [B] The Langmuir-Blodgett deposition method employed by (Mangadlao *et al.* 2015) showed that GO sheets deposited on a flat surface with no edges available were still capable of incurring an antibacterial effect against *E. coli*. This would suggest that the flat planes of GO alone could be antibacterial.

A more recent report, from the latter half of 2016, published in conjunction with Konstantin Novosolev (the winner of the Nobel Prize for the discovery of graphene) has suggested that the majority of the antibacterial activity observed in the studies up until now is a result of material contamination following the graphene production process (Barbolina *et al.* 2016).

Although different laboratories may be performing washing steps following the production of their graphene materials, trace amounts of acids and reducing agents (while alone not in concentrations high enough to elicit an anti-bacterial response) all contribute to a change in pH resulting in the observed antibacterial effects. They displayed this through assays conducted using both as-produced and commercially available graphene at different sheet sizes, in growth and in non-growth media as well as at different concentrations. These assays showed that the antibacterial activity of the GO was dependant on the number of washes that had been carried out and that when cleaned thoroughly, no antibacterial activity was observed in any of the samples, regardless of graphene sheet size or concentration. In addition they showed TEM images of *E. coli* and *S. aureus* following incubation with GO with no apparent membrane damage caused by contact with the GO sheets.

They stated that:

"…the data in this study has for the first time generated definitive data that clearly demonstrates that under the in vitro conditions used here no antibacterial properties could be assigned to highly purified GO. It was neither bactericidal nor bacteriostatic over a broad concentration range against planktonic cultures of either E. coli or S. aureus in a number of assays."

Certainly an unambiguous statement, definitive in its assertion that much of the studies carried out up to this point have suffered from a fundamental flaw in their experimental design. These findings are supportive of the study by (Ruiz *et al.* 2011) (which had found no antibacterial effect from GO) several years previous, as they had emphasised the extent to which their GO had been washed. While this study deals with GO, the question as to the efficacy of rGO and graphene produced via non-chemical methods still remains. The publication of this study along with a critical review article on the disparity seen within the literature has cast a much needed critical eye upon this field of investigatio; (Hegab *et al.* 2016). It is no surprise that dealing with a newly discovered nano material across a multi-disciplinary line of research (from material science to microbiology) has resulted in such disparity. It must also be considered that there is less than ten years of research carried out into this field and that our understanding of graphene interactions with bacterial cells may change drastically as more information comes to light.

1.9 Is graphene antibacterial?

Based on the studies done up to this point, the question as to whether graphene materials are antibacterial or not does not have a straightforward yes or no answer. Rather there have been several hypotheses based on cumulative data over time, which have themselves evolved as more data has become available. The parameters which govern the antibacterial efficacy are still not well known but there are certain elements which have been established to some degree. Each of the elements mentioned below represent primary routes which predominantly require further investigation in order to ascertain how they fully impact on the antibacterial potential of graphene materials. No doubt the investigation into the antibacterial application of graphene materials will continue in earnest over the coming years. The focus should be on how each of the different parameters of the material mentioned up to now impacts on its effectiveness as a biocide.

It will not be enough to examine graphene for antibacterial effectiveness through a single route, as it has been shown just how dynamic the nature of the material and its interaction with the surrounding environment and with microorganisms can be. In light of the more recent work carried out by (Barbolina *et. al* 2016) many of the studies over the past seven years will have to be revisited with a more critical eye in terms of material production.

1. **Charge Transfer**

Charge transfer, as proposed by (Li *et al.* 2014) does not play an active role in the antibacterial activity of graphene monolayers grown via CVD. The work by (Dellieu *et al.* 2015) disproved this hypothesis categorically and showed that graphene monolayers grown via CVD possess no inherent antibacterial activity.

2. **Edges**

On the subject of edges, the study from (Mangadlao *et al.* 2015) has shown that the availability of the edge sites of graphene oxide sheets does not govern its antibacterial potential. This data is supported heavily by the work done by (Hui *et al.* 2014) and disproves the first hypothesis proposed by (Akhavan *et al.* 2010) that it is the edge sites of the sheets that are responsible for the primary mode of action via membrane damage through kinetic shear.

3. **Basal planes**

The lack of required edge interaction raises concerns over the lipid extraction model proposed by (Tu *et al.* 2013) which, while robust as a mode of action, is dependent on the insertion of the edge of the graphene sheets into the membrane in order for lipid extraction to occur. It

may be that the basal planes of graphene sheets are capable of performing lipid extraction in a manner different to that described by (Tu *et al.* 2013) when fixed on a substrate in a horizontal manner. How horizontally orientated graphene sheets incur an antibacterial effect requires further investigation.

4. Surface functionalisation

Additionally the disparity between the reports of (Dellieu *et al.* 2015) and (Mangadlao *et al.* 2015) on the activity between LB-fixed GO sheets and CVD grown pristine graphene raises questions on the surface functionalisation of graphene. If larger areas of pristine-like graphene are more antibacterial as suggested by the computer models of (Tu *et al.* 2013) then the CVD graphene should be the more effective agent. Research on the antibacterial activity of CVD graphene is limited and requires further investigation. The number of reports showing the varying responses of GO and rGO begets the requirement for a systematic robust comparative study of each material and their antibacterial potential (S. Liu et al. 2011) (Wang et al. 2012) (Gurunathan et al. 2013) (Hu et al. 2010), (Gurunathan et al. 2012).

5. Membrane Damage

Membrane damage is a key feature in the antibacterial action of graphene materials. SEM, TEM and fluorescent microscopy dependant on membrane damage have categorically shown that different members of the graphene family can cause membrane damage in bacterial cells. How this occurs and whether kinetic or membrane permeabilisation is responsible still requires further study (Hu *et al.* 2010) (S. Liu *et al.* 2011) (Tu *et al.* 2013) (Mangadlao *et al.* 2015).

6. Lateral Size

Laterally larger sheets of graphene oxide, when added to a solution inoculated with microorganisms, cause a more acute antibacterial effect than their smaller counterparts. Cell wrapping may be an explanation in solution but the greater availability of the basal planes most likely plays a key role in this regard (Liu *et al.* 2012) (Tu *et al.* 2013).

7. Media

The effect of different media on the antibacterial efficacy has been highlighted without question in the work by (Hui *et al.* 2014). This offers an explanation as to the original investigations by (Ruiz *et al.* 2011) (Das *et al.* 2011) and (Tai *et al.* 2011) whereby they

observed no antibacterial effect whatsoever. The adsorption of elements such as amino acids onto the graphene sheets removes the surface availability and thus reduces the chance of direct contact between the graphene and the organisms.

8. Oxidative stress

It is clear that graphene materials may exert some sort of oxidative stress as evidence by the reports of (Gurunathan *et al.* 2012) (S. Liu *et al.* 2010) (Musico *et al.* 2014) (Deng *et al.* 2014) and (Krishnamoorthy *et al.* 2012). The results of glutathione and lipid peroxidation assays clearly show that some sort of oxidation of functional materials is occurring when these assays are performed with graphene materials. Whether or not this is as a result of reactive oxygen species remains to be seen. The conflicting results between the XTT of (Liu *et al.* 2011) and the NBT assay of (Gurunathan *et al.* 2012) show that there is and is not a production of ROS in each case.

1.10 The filling of a niche

In considering the application of a graphene material for water treatment and antibacterial purposes, the trend in publications as well as the practicality of the application needs to be considered. In terms of graphene composite materials as biocides, there is currently an over-saturation of graphene-silver composites, with over 50 publications dealing specifically with the antibacterial applications of graphene-silver composites published throughout 2015/16. In addition, when considering a clinical or human health application the concern over the cytotoxic effect of silver nanoparticles has been highlighted and is a subject of concern in terms of their potential health impact (Marambio-Jones *et al.* 2010) (Ahamed *et al.* 2010) (Wijnhoven *et al.* 2009). The level of interest in silver stems from the low concentration required to achieve an acute antibacterial effect. The focus of silver based composites is entirely on novel production of composites which are multi-functional. However, the high cost associated with both silver and graphene production limits the scope of these composites in terms of practical applications significantly.

Copper based graphene composites however have seen almost no use in terms of antibacterial applications with only a single investigation examining the effect of a graphene-poly-l-lysine composite which included copper nanoparticles (Ouyang *et al.* 2013). Copper has been shown to be an effective antibacterial surface and has found application in clinical situations (Grass *et al.* 2011). Copper nanoparticles have even been shown to be almost as effective as silver nanoparticles in terms of their antibacterial efficacy in some cases (Yoon *et al.* 2007). The

production of graphene-copper composites has been carried out by several different investigations but the focus of these studies have been on sensing technology (Chen *et al.* 2011), Raman scattering (Zhang 2012) and material-strength (Chu *et al.* 2014). There has been no investigative work into the application of a graphene-copper composite as an antibacterial agent done up to this point. The potential synergy between graphene and copper may offer a cost-effective alternative which is equally as efficacious as its much more expensive silver equivalent.

Graphene has also been shown to be an effective agent for the adsorption of organic and environmental pollutants from water much like other carbonaceous materials and represents a potential agent for water remediation (S. Wang *et al.* 2013) (Yang *et al.* 2011) (Maliyekkal *et al.* 2013). Combining the adsorptive potential of graphene materials for pollutant removal with the antibacterial potential of biocidal metals such as copper represents a niche line of investigation which has not been carried out up to now and may offer an effective material for multi-purpose water treatment. The need for new disinfection technologies for water treatment has been highlighted in the past few years with concerns over by-products from current disinfection technologies such as chlorination and ozonation. The production of trihalomethanes, bromates and haloacetic acids from these processes present a potential long-term adverse effect to human health (Richardson *et al.* 2008) (Richardson *et al.* 2007). The inability of current chlorination regimes to remove non-bacterial pathogenic organisms such as Cryptosporidium has been highlighted with outbreaks and boil-water notices in Ireland (Chauret *et al.*(2001) (Driedger *et al.* 2001). Other issues such as the spread of antibiotic resistance in activated sludge populations highlights the need for new treatment process capable of dealing with these modern issues (Rizzo *et al.* 2013) (Yang *et al.* 2013). New water-treatment technologies including a variety of biocidal tools and materials offer a potential solution to these issues. The over-reliance on certain water treatment processes for many years has given rise to modern issues which will require a suite of new technologies if they are to be dealt with. Composites of graphene and non-specific biocides such as copper may be useful materials in this regard if they can be fabricated in a cost-effective manner which can be applied practically.

1.11 Project Aims and objectives

The objective of the project was to investigate if graphene could be applied as both an anti-bacterial and adsorptive agent in a prototype drinking water treatment unit. Given the conflicting reports as to the antibacterial efficacy of graphene materials, it was of interest to examine the antibacterial activity of graphene oxide (GO), reduced graphene oxide (rGO) and, given the lack of investigation into that area, if a graphene-copper composite (Cu-rGO) would offer any advantages as a potential anti-bacterial agent. While there have been studies examining the application of graphene films or papers for water treatment, the production of an immobilised graphene-copper composite has not been done up to this point.

The aims of the project were:

- To produce graphene oxide (GO), reduced graphene oxide (rGO) and a graphene-copper composite (Cu-rGO) and to examine their physio chemical characteristics.

- To investigate the anti-bacterial efficacy of each of these materials against various organisms via a variety of methods including solid and liquid culture.

- To examine whether or not a graphene-copper composite offered any advantage over commonly applied copper containing anti-bacterial compounds such as copper salts.

- To ascertain the adsorptive potential of the graphene oxide (GO), reduced graphene oxide (rGO) and the copper-composite (Cu-rGO) using a number of potential chemical contaminants in water and to examine how immobilisation would impact upon their adsorptive capacities.

- To construct a drinking water treatment prototype incorporating an immobilised graphene-copper composite and to challenge it with the removal of microorganisms and chemical contaminants.

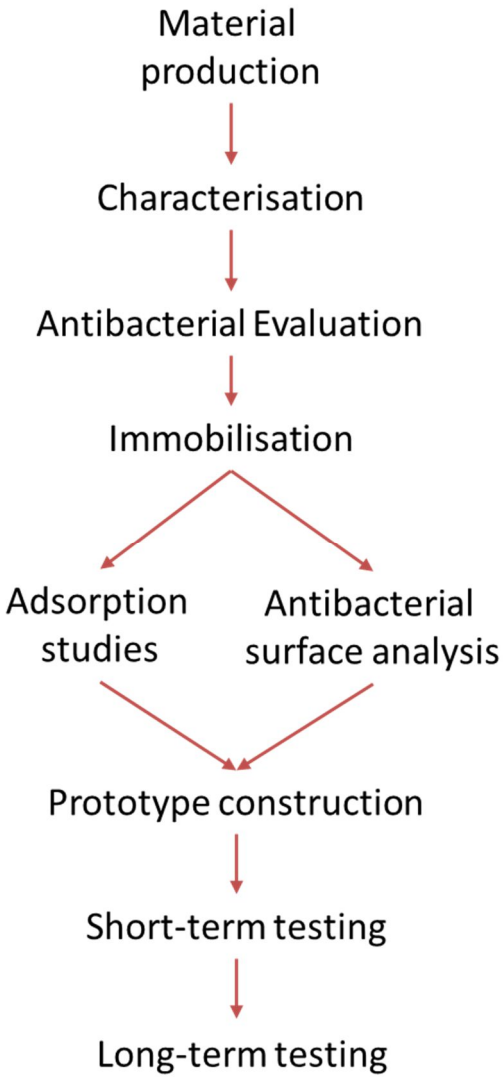

Figure 1.16. A simple diagrammatic representation of the work-flow carried out throughout the project

2. Materials and Methods

2.1 Materials

2.1.1 Media and Buffers

Nutrient agar, nutrient broth, tryptone broth, bacteriological agar, TBX agar and phosphate buffered saline (PBS) were all obtained from Thermo-Fischer scientific (Dublin, Ireland). Solutions were sterilised by autoclaving at 121°C for 15 minutes.

2.1.2 Chemicals and Reagents

Acid washed graphite flakes (#699131) were purchased from Anthricite Industries Inc. (Sunbury, United States). Chemicals and reagents, e.g. HCl, $CuCl_2$, $CuSO_4$, H_2SO_4, $NaBH_4$ etc. were all purchased from Sigma Aldrich (Dublin, Ireland).

2.1.3 Bacterial cultures

Bacterial cultures; *E. coli* (T37-1) and *B. subtillis* (DSM10) were maintained on nutrient agar at 4°C and bacterial stock solutions were stored in glycerol at -80°C. *Escherichia coli* (T37-1) was an environmental isolate coded for its location of isolation, the Tolka River, the temperature at which it was isolated 37°C, and the sample number from which it was taken. *Bacillus subtilis* (DSM10) was purchased from DSMZ GmbH, Germany. Routine sub-culturing was carried out every 4 weeks whereby a loopful of culture was transferred to a fresh nutrient agar plate and grown overnight at 30°C. Following overnight incubation, cultures were then stored at 4°C.

2.2 Methods

2.2.1 Material preparation

Graphene materials were produced via chemical exfoliation and reduction. Three materials were produced to examine their efficacy as both adsorbants for chemical contaminants and as antibacterial agents; graphene oxide (GO), reduced graphene oxide and a graphene copper composite (Cu-rGO).

2.2.1.1 Preparation of Graphene Oxide

2g of graphite flakes were placed in a 700W microwave for 15 seconds to produce expanded graphite (EG) as the precursor for graphene oxide (GO) synthesis. 2g of EG and 250ml of sulphuric acid (H_2SO_4) were then mixed and stirred in a round bottomed flask. Next, 10g of $KMnO_4$ was gradually added to the mixture. After 24 hours of stirring at room temperature, the mixture was then transferred into an ice bath and 500ml of de-ionised water (DI) and 100ml of H_2O_2 was added slowly to the mixture resulting in a colour change to golden brown. Following 30 minutes of stirring, the resulting oxidised EG particles were washed with a HCL solution (9:1 water:HCL) and centrifuged three times, then centrifuged and washed with

deionized water. Repeated centrifugation washing steps with deionised water were carried out until a solution pH >5 was achieved. During the washing process, oxidised EG particles were exfoliated to GO sheets with gentle shaking resulting in a viscous aqueous solution with a concentration of 4.5mg/ml.

2.2.1.2 Preparation of Graphene-Copper Composite (Cu-rGO)

A graphene-copper composite (Cu-rGO) was subsequently produced via the sodium borohydride reduction method described by (Zhang et al. 2012).

GO (30mg), $CuCl_2$ (18mg) and DI water (200ml) were mixed in a 500ml round bottom flask, the mixture was ultra-sonicated at low energy for 1hr. 10ml of 1% Sodium borohydride ($NaBH_4$) solution, was then added slowly, and the reaction mixture was stirred at 100^{o}C for 24hrs. After being cooled to 50^{o}C, the resulting composite was collected by centrifugation and dried at 100^{o}C under vacuum to give the Cu-rGO composite.

2.2.1.3 Preparation of Reduced Graphene Oxide (rGO) and Copper Nanoparticles (CuNPs)

Reduced graphene oxide (rGO) was produced via the method as described in Section 2.2.1.2 above, without the addition of copper chloride to the mixture. Additionally, the effect of the reduction process of the oxidative state of the copper present in the composite was also investigated via the reduction of $CuCl_2$ in the absence of graphene to produce processed Cu.

2.2.1.4 Preparation of Immobilised Graphene-copper composite

In order to produce free-standing graphene composite films and a stable coating for membrane filters, a method for the production of a graphene-copper composite using l-ascorbic acid was developed based on two methods described by (Zhang et al. 2010) and (Xiong et al. 2011).

20ml of graphene oxide (1mg/ml) and 20ml $CuCl_2$ (7.5mg/ml) were added to a round bottomed flask and ultra-sonicated for one hour. 20ml ascorbic acid (0.1M) was added drop-wise and the mixture was heated at 80^{o}C under stirring for 24 hours. This resulting mixture was then washed repeatedly with water via centrifugation and dried at 60^{o}C.

To produce free-standing composite films, 10mg of Cu-rGO was dispersed in 10ml of de-ionised water and sonicated for one hour to produce a 1mg/ml suspension; this was vacuum filtered onto a nitrocellulose filter (pore size 0.2µm) and the resulting films peeled from the surface. To produce composite coated membrane filters, 10ml of a 1mg/ml suspension of Cu-rGO was drop cast onto glass fibre membranes (Whatman-GC 47mm diameter) and dried at 60^{o}C.

2.2.2 Material characterisation

The chemical composition of each material was analysed via Ultraviolet-visible (UV-vis) spectrophotometric analysis, thermo-gravimetric analysis (TGA) and Fourier-transform infrared spectroscopy (FTIR). Principally, the loss of oxidative groups following the reduction process was examined for. Energy-dispersive X-ray Spectroscopy (EDX) was used to confirm the elemental composition of each material and in particular, the quantity of copper present within the composite (Cu-rGO). Dynamic light scattering (DLS) was used to establish the particle size distribution within aqueous suspensions of each material and the morphological profile of each material was evaluated via optical and scanning electron microscopic (SEM) analysis. Transmission electron microscopy (TEM) was used to compare the aggregation of the materials produced using different reducing agents.

2.2.2.1 Ultraviolet-visible (UV-vis) spectrophotometric analysis

Ultraviolet-visible (UV-vis) spectra were obtained using a UV-3100PC (VWR, Ireland) spectrophotometer. Aqueous solutions of GO, rGO and Cu-rGO at 100ppm were used as samples for UV-vis analysis with de-ionised (DI) water as a blank sample. UV-vis spectra were obtained from 200 to 500nm at 1nm stepwise.

2.2.2.2 Thermogravimetric analysis (TGA)

TGA analysis was performed using a TGA Q50 (TA Instruments, United Kingdom). Solids of each material were added to the decomposition chamber, a temperature ramp of 20 to 800^{o}C was used at an increase rate of 20^{o}Cmin^{-1}, with weight loss denoted as percentage weight (W%), under a nitrogen atmosphere.

2.2.2.3 Size distribution analysis via dynamic light scattering (DLS)

Particle size distribution analyses' on dispersions of GO, rGO, Cu-rGO and CuNPs was measured by Zetasizer Nano ZS90 (Malvern, UK). Aqueous solutions of 100ppm were used as samples and measured in disposable capped cuvettes. Temperature settings were set at 25^{o}C with a dispersant refractive index of 1.330 and a viscosity of 0.8872. The refractive index was set at 1.50 and material absorption at 0.1.

2.2.2.4 Optical Microscopic Analysis of graphene materials

A wet mount consisting of 10µl of GO, rGO and Cu-rGO suspensions at 100ppm were dropped onto glass microscopic slides and spread evenly using a glass cover slip. Images were captured using a Nikon Ti Eclipse inverted microscope (Nikon, Ireland) under bright field conditions using lenses at x10 and x40 magnification.

2.2.2.5 Scanning Electron Microscopic (SEM) Analysis of graphene materials

For scanning electron microscopic analysis, samples were mounted on aluminium stubs (AGG3313) using carbon conductive tape (G3939) purchased from Agar Scientific (Stansted, United Kingdom). Samples were imaged with a Hitachi-S3400 SEM (Hitachi, Japan) at an acceleration voltage of 20KV and a probe current of 35μA. Samples were imaged with a Hitachi-S3400 SEM (Japan) and a Hitachi S5500 FESEM (Hitachi, Japan) for both secondary and transmission electron imaging.

2.2.2.6 Fourier transform infrared spectroscopy

The attenuated total reflection-Fourier transform infrared (ATR-FTIR) spectrum was recorded on a Perkin Elmer Spectrum100 spectrometer. The spectrum was recorded over a range from 650 to 4000 cm−1 with 32 scans at a resolution of ±4 cm^{-1}.

2.2.2.7 Energy dispersive x-ray spectroscopy (EDX) Analysis

A Hitachi S5500 FESEM (Hitachi, Japan) was used to carry out EDX analysis on graphene and composite samples. Samples were mounted onto a dual-stub aluminium holder along with a cobalt (Co) standard. Calibration was carried out using the cobalt standard as a reference and analysis performed thereafter. Five regions were analysed per sample. The corresponding spectra were recorded and the percentage weight composition of each element noted. The elemental composition for each sample was taken as the average of the five regions recorded.

2.2.3 Isolation and Identification of environmental *E. coli* strain

2.2.3.1 Sampling and growth on selective media

Water was sampled aseptically from the river Tolka using a Sterilin (331-0063) sample bottle. 0.1ml of the water sample was spread, in triplicate, across the surface of tryptone bile x-glucoronide (TBX) agar (Oxoid CM0945) to select for *E. coli* which appear as blue/green colonies. These were then selected and grown on nutrient agar.

2.2.3.2 Gram staining

A gram-stain procedure was carried out as described by (Harley & Prescott 1990), the stained smear was then observed using a Nikon Ti Eclipse inverted microscope. Gram-negative cells were observed as red in colour and Gram-positive cells appeared purple

Laboratory strains of bacteria were used as controls for each; *Bacillus subtilis* DSMZ10 (positive) and *Pseudomonas putida* CP1 (negative).

2.2.3.3 Oxidase test

The oxidase test is a biological assay used to identify bacterial cultures via the presence or absence of the cytochrome c oxidase enzyme. An oxidase test was also carried out using oxidase strips (Oxoid). One colony of pure culture grown on nutrient agar was transferred via sterile inoculation loop to an oxidase strip and the result recoded as blue colour generation or lack-of.

2.2.3.4 Indole test

The indole test is a biochemical test which examines the ability of bacteria to convert tryptophan to indole and is used for the identification of an organism. An indole test was carried out by growing the isolated bacteria in tryptone broth and three to four drops of Kovacs reagent were gently run down the side of the test tube; results were recorded as the production of a red/pink interface at the surface of the liquid.

2.2.3.5 Catalase test

The catalase test is a biological test which examines for the presence or absence of the catalase enzyme via the use of hydrogen peroxide and is used for bacterial identification. A catalase test was perfomed by adding 1 drop of a 3% H_2O_2 solution to isolated colonies grown on a nutrient agar plate. The production of bubbles indicated a positive result.

2.2.3.6 API-20E Identification

The analytical profile index (API) 20E test from Biomerieux (France) was used in the identification of the environmental *E. coli* strain and the identification was carried out as per the manufacturers' specifications.

2.2.4 Antibacterial studies

Antibacterial studies were carried out in solid media via various approaches to examine the potential diffusive nature of the materials, in liquid growth media to examine their potential inhibitory effect and in a non-growth saline solution to examine their biocidal potential as would be found in a water treatment scenario. *E. coli* (T37-1) was used as a model Gram-negative organism and *B. subtilis* (DSM-10) as a Gram-positive organism. Graphene Oxide (GO), Reduced graphene oxide (rGO) and the graphene-copper composite (Cu-rGO) were each tested via each method. During the antibacterial investigations, two copper containing salts, copper chloride ($CuCl_2$) and copper sulphate ($CuSO_4$) as well as copper nano particles (CuNPs) were used as controls for comparison with the copper containing graphene-composite. The

CuNPs, produced via the same method would be analogous to the copper present in the composite material.

2.2.4.1 Solid media studies

GO, rGO, CurGO and CuNPs were tested in a number of different ways in solid media to examine how different exposure methods would affect their antibacterial potential and if the materials could be applied in a more free-standing form for antibacterial applications

The four methods employed were:

- Wells were cut into agar inoculated with bacteria and suspensions of each material added.
- Disks impregnated with each material were added to the surface of agar inoculated with bacteria.
- Solid pieces of each material were placed onto the surface of agar inoculated with a lawn of bacteria
- Vacuum filtered disks with known concentrations of material were added to agar inoculated with a lawn of bacteria.

Results in all cases were observed as zones of inhibition, categorised as an area of exclusion around the material whereby no bacterial growth is observed. The zone of inhibition is the diameter of the full zone given in mm. For the vacuum-filtered disk assay, $CuCl_2$ and $CuSO_4$ were also used for comparison with the copper containing composite. Disks impregnated with 5µg of gentamicin would be used as positive control samples.

Inoculum preparation

A loopful of bacterial culture was transferred from a maintained agar plate using a sterile inoculation loop to a 10ml aliquot of nutrient broth and grown overnight on a shaking incubator at 150rpm and 30^{o}C. Following overnight growth, the broth was centrifuged at 4000rpm for 15 minutes and the pellet washed twice and re-suspended in 10ml of PBS. Optical densities were adjusted to 0.5 McFarland standard (Mcf) equating to a cell number of ~10^8 CFU/ml. For the well and disk diffusion studies 1ml of the bacterial suspension was added to a sterile petri dish with 20ml molten agar and allowed to solidify before exposure to materials. For solid and vacuum-filtered disk diffusion studies a bacterial lawn was prepared on solid agar by dipping a sterile cotton swab into the bacterial suspension and drawing it over the surface to create an even coverage of organism.

Preparation of materials

1000ppm suspensions of GO, rGO, Cu-rGO and CuNPs were prepared by adding 10mg of each material to 10ml of sterile de-ionised water and sonicating for one hour, 1000ppm concentrations were used for these materials in all cases unless otherwise specified. Solutions of $CuCl_2$ and $CuSO_4$ were prepared by dissolving powders of each in sterile de-ionised water.

- **Well diffusion assay**: 10mm wells were cut into the agar using a heat sterilised agar cutter. 200µl of each material suspension at 1000ppm was added, in triplicate, to wells on individual agar plates.

- **Disk diffusion assay**: sterile 6mm whatman disks (Grade AA 2017-006) impregnated with 20µl of each material suspension were placed onto the inoculated agar.

- **Solid exposure assay**: suspensions of GO and rGO were dried at 60°C in a fan assisted oven to form films, 5mm sections which weighed ~5mg were cut and applied directly to inoculated agar plates. For comparison, and as the other materials did not form free-standing films, 5mg of each of Cu-rGO and CuNPs were placed, in triplicate, directly onto the surface of plates.

- **Vacuum-filtered disks:** 20ml of each material suspension were filtered using a Supelco filtration apparatus (58062-U) onto Whatman cellulose acetate filters (pore size 0.2µm) with a diameter of 35mm. 5mm disks were then cut and placed, face down, onto inoculated agar plates so that the material was in direct contact with the organism. The final concentration on each of the particulate loaded disks was ~0.4mg. Standard whatman disks were loaded with equivalent quantities of $CuCl_2$ and $CuSO_4$ for comparative purposes. The concentration of material on each vacuum filtered disk was established via the below calculation:

Total Area

$d = 35mm \ \therefore r = 17.5mm$

$A = \pi r^2$

$A = 962.11mm^2$

$$\frac{20mg}{962.11mm^2}$$

$Concentration = 0.02mg/mm^2$

5mm vacuum-filtered disks

$r = 2.5mm$

$A = 19.63mm^2$

$(19.63mm^2)(0.02mg/mm^2)$

$= 0.3926 \ or \sim 0.4mg \ per \ disk$

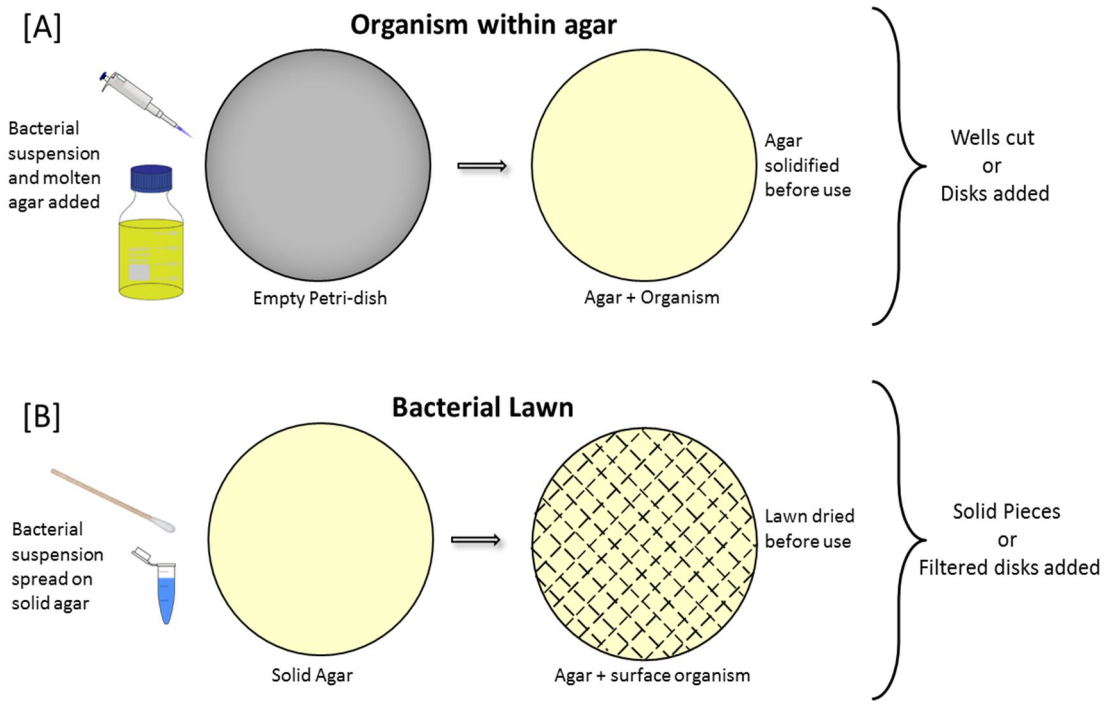

Figure 2.1 The two inoculation methods employed for the exposure of micro-organisms in solid media. [A] Organism incorporated directly into molten agar and [B] the creation of a bacterial lawn on the surface of the media.

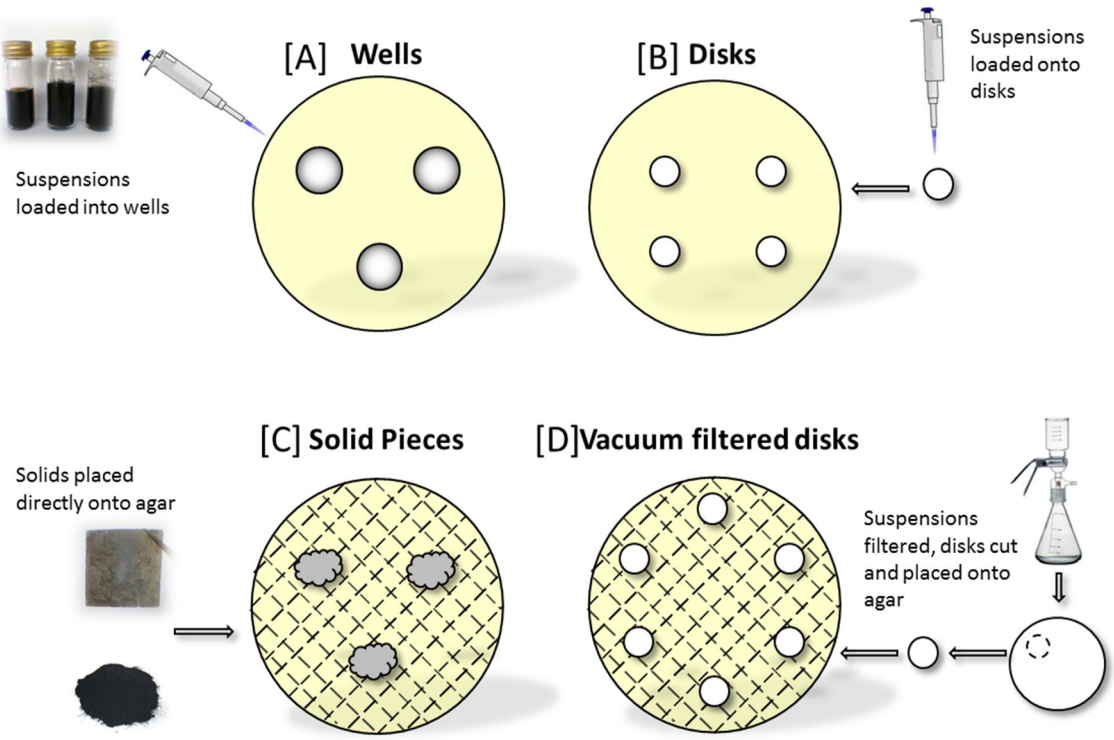

Figure 2.2 The four methods employed in examining the effect of materials in solid media. [A] Suspensions added to wells cut into agar [B] Disks loaded with suspensions added onto the surface of the agar [C] Solid pieces of material added to agar with a bacterial lawn and [D] disks cut from membranes vacuum filtered with suspensions of material added to the surface of the agar.

2.2.4.2 Liquid Media Studies

Inoculum preparation

A loopful of bacterial culture was transferred from a maintained agar plate using a sterile inoculation loop to a 10ml aliquot of nutrient broth and grown overnight on a shaking incubator at 150rpm and 30°C. Following overnight growth, the broth was centrifuged at 4000rpm for 15 minutes and the pellet washed twice and re-suspended in 10ml of PBS.

For the minimum inhibitory concentration analysis, the optical density of bacterial suspensions was adjusted to 0.07 at 660nm equating to 10^8CFU/ml.

For the shake flask studies, the optical density of *E. coli* suspensions was adjusted to 0.015 and suspensions of *B. subtilis* to 0.025 at 660nm, equating to 10^7 CFU/ml. 1ml of a 1:100 dilution of the bacterial suspension was added to 100ml of PBS to give a final cell concentration of 10^3CFU/ml.

Antibacterial analysis in non-growth media

Shake flask studies were carried out in 250ml Erlenmeyer flasks with a final volume of 100ml of PBS. Materials were added to each flask in order to bring them to the desired concentration in parts per million (mg/L). After the addition of particulates, flasks were sonicated for 40 minutes to disperse the materials. Following inoculation with organism, flasks were incubated up to 24 hours at 30°C on an orbital shaking incubator at 150rpm. 1ml samples were taken at 1.5 hour intervals up to 6 hours and again at 24 hours. Samples were then serially diluted and enumerated.

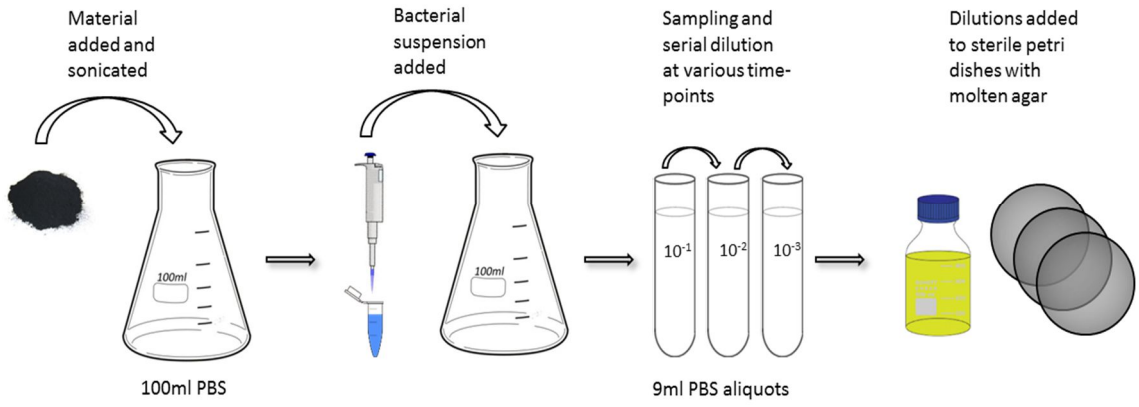

Figure 2.3 The method employed in the shake flask studies. Materials were added to 100ml aliquots of PBS and dispersed via sonication. Following inoculation with bacterial suspensions, 1ml aliquots were taken periodically, serially diluted and plated in triplicate.

Determination of bacterial numbers

For shake flask studies colonies were enumerated using the pour plate technique. Cell suspensions were serially diluted to 10^{-2} using 9ml aliquots of sterile PBS. 1ml of each dilution of 10^{-1} and 10^{-2} were added, in triplicate, to sterile petri dishes and 20ml of molten nutrient agar added. Plates were incubated overnight at 30°C and colonies counted. The change in bacterial population was expressed as percent loss from the initial inoculum.

$$\%\ change\ in\ population = \frac{Cell\ count}{(\frac{Initial\ cell\ count}{100})}$$

Antibacterial analysis in growth media

The minimum inhibitory concentration (MIC) of $CuCl_2$, $CuSO_4$ and CuNPs was determined using the standard 96-well-plate method as described by (Andrews 2001). Two-fold dilutions were carried out from an initial concentration of 1000mg/L.

Due to the particulate nature of GO, rGO and Cu-rGO, MIC determination was carried out for these materials in a larger volume (1ml) in test tubes. An initial concentration of 1000mg/L was used and two-fold dilutions carried out in a series of nine test-tubes. A tube containing no material would act as a control for bacterial growth. A series of tubes without bacteria would act as controls for the materials for optical density measurements. Following serial dilution, 50µl of a suspension of bacteria at an optical density of 0.07 (10^8CFU/ml) was added to each tube. The tubes were then incubated at 30°C for 24 hours. Results were recorded as optical density measurements at 660nm. Streak plates were carried out from each well/tube on to nutrient agar in order to validate whether or not the organism had been completely inhibited.

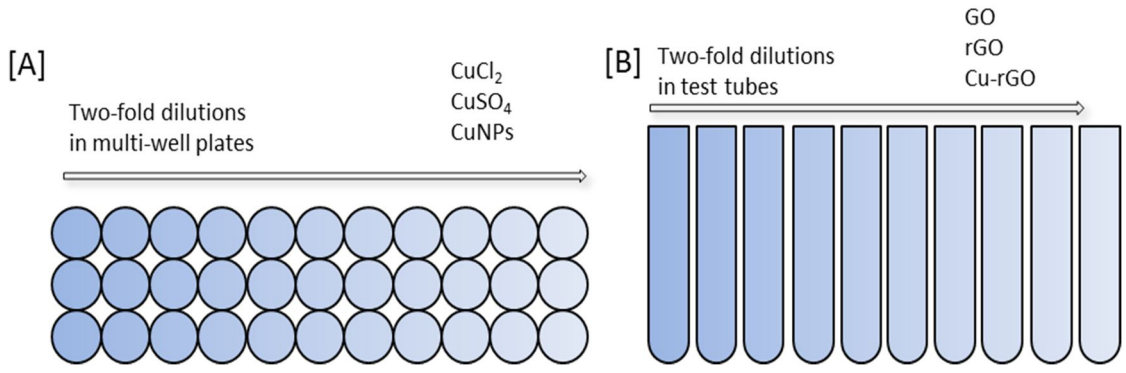

Figure 2.4 The two methods employed to evaluate the minimum inhibitory concentrations of the various materials tested, two-fold dilutions were carried out in series in both cases. $CuCl_2$, $CuSO_4$ and CuNPs [A] were tested via the standard 96-well plate method. GO, rGO and Cu-rGO [B] were tested in larger volumes due to their particulate nature.

2.2.4.3 Scanning Electron Microscopic Analysis

Disks of each of GO, rGO and Cu-rGO prepared via vacuum filtration as in Section 2.2.4.1 were placed into 5ml nutrient broth inoculated with 1ml of *E. coli* suspension adjusted to 0.07 optical density in a 6-well cell-culture plate which was incubated overnight at 30^{o}C. Following incubation, disks were removed from well plates and microorganisms were fixed with 5% glutaraldehyde for 30 minutes at 4^{o}C and dehydrated step-wise using a gradient of ethanol solutions (50, 60, 70, 80, 90 & 100%) for 10 minutes each. Following dehydration, microbiological samples were sputter-coated with gold using a Quorum 750T (Sussex, United Kingdom) for 90s at 20µA. Samples were viewed using an acceleration voltage of 20KV and a probe current of 35mA.

2.2.4.4 Optical Microscopic Analysis

500µl aliquots of a suspension of *E. coli* (T37-1) were adjusted to 0.6 optical densities at 660nm were added to each of three sterile 1ml microfuge tubes. The tubes were then brought to concentrations of 500mg/L of each of GO, rGO and Cu-rGO respectively. To investigate the level of agglomeration in different concentrations of the composite tubes of 1000, 400 and 0mg/L of Cu-rGO were prepared. These tubes were then incubated at 30^{o}C for 24 hours. Following incubation, 1.5 µl of SYT09 dye was added to each tube, these were then incubated for 15 minutes in the dark. 10µl aliquots from each tube were added to a clean microscopic slide and a cover slip added. Images were captured using a Nikon Ti Eclipse inverted microscope (Nikon, Ireland) under bright field and fluorescent conditions using lenses at x40 magnification.

2.2.4.6 Evaluation of graphene mutagenicity via the Ames test

The mutagenic potential of the graphene compounds was evaluated using an AMES-mod ISO kit test purchased from EBPI Inc. Canada. Lyophilised *salmonella typhimurium* TA-100 was grown overnight at 37^{o}C in nutrient broth and adjusted to an optical density of 0.05 at 600nm. In a 24 well plate 1.6ml of 0.1, 1 and 10ppm of graphene oxide, reduced graphene oxide and the graphene-copper composite were mixed with 200µl exposure solution as well as 200µl of the adjusted bacterial culture in triplicate. Sodium azide (NaN_3) was used as a positive control for mutagenicity and positive control wells were performed in duplicate. Following incubation at 37^{o}C for 100 minutes, 1.6ml from each well was added to 8.7ml of bromocresol reversion media. Each mixture was then plated into 48 wells on a 96 well-plate (a total of 144 replicates) and incubated for 72 hours at 37^{o}C. Plates were scored visually with yellow wells as positive and purple as negative.

2.2.5 Adsorption studies

In order to examine the adsorptive potential of the graphene materials in a water treatment scenario, three materials of interest; methylene blue, famotidine and diclofenac were used as model contaminants for removal from water. *Famotidine* is a widely available and used pharmaceutical used to inhibit acid production within the stomach and used to treat ulcerous conditions and acid-reflux, its fate in waterways is unknown and it represents a novel material for investigation. *Diclofenac* is a widely used anti-inflammatory medication which is available over the counter, is a classified as a "substance of emerging concern" and as such is of interest in light of water treatment. *Methylene Blue* is a commonly used compound in both research and medical applications is a possible teratogen which is undesirable in the water course. It is a commonly applied dye to examine the adsorptive potential of material.

2.2.5.1 Time-dependant adsorption analysis

For both the free-standing films and the composite coated membranes, a time-dependant analysis was carried out over 8 hours to examine the rate of adsorption. 10mg free-standing films of each of GO, rGO and Cu-rGO were added to 10ml aliquots of methylene blue (0.0048mg/ml), famotidine (0.032mg/ml) and diclofenac (0.03mg/ml). The coated membranes, due to their larger size and available surface area were added to 100ml of each of the chemicals at the same concentrations. Samples were shaken at 150rpm at room temperature and monitored at 664nm (MB) 281nm (famotidine) and 276nm (diclofenac) via UV-visible spectroscopy.

2.2.5.1 Adsorption capacity analysis

In order to ascertain the total adsorption capacity of each of the graphene materials; GO, rGO and Cu-rGO were examined for their adsorptive potential over a range of concentrations. All three materials would be examined in two different formats; as disperse particles in suspension and as vacuum filtered films. The Cu-rGO would also be examined as the glass-fibre membrane coating. Diclofenac adsorption was investigated at 0.03, 0.3 and 3mg/L, famotidine at 0.032, 0.32 and 3.2mg/L and methylene blue removal at 0.0048, 0.048 and 0.48mg/L. The change in absorbance was monitored via UV-visible spectroscopy and the total adsorption at each concentration.

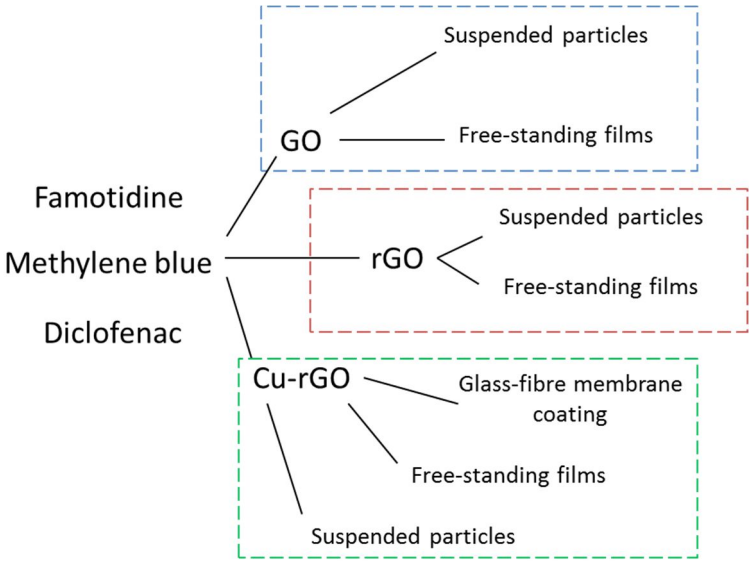

Figure 2.5. Breakdown of the different physical parameters tested to examine the adsorptive potential of the graphene materials

2.2.6 Prototype studies

Prototype studies would serve as a means of examining the efficacy of the graphene materials as both antibacterial and adsorptive agents in a potential water treatment unit. The immobilised material would be incorporated into prototype units in varying formats in order to examine its performance and robustness

2.2.6.1 Antibacterial analysis of immobilised graphene-copper composite surfaces

In order to examine the antibacterial efficacy of the fixed graphene-copper composite as a surface, an agar slurry method, used to ascertain the antibacterial efficacy of surfaces was employed (ASTM standard E2180-07 2012). 0.85g NaCl and 0.3g bacteriological agar were added to 100ml deionised water and autoclaved at 121^{o}C for 15 minutes to produce gelatinous agar slurry. This was cooled to 44^{o}C in a water bath and inoculated with *E. coli* to a final concentration of 10^{6}CFU/ml. 10 x 10mm square of Cu-rGO films were prepared and 150µl of inoculated agar slurry added to the surface. Following incubation at 10 minutes intervals up to one hour, the slurry was then removed from the surface, dispersed into sterile PBS and enumerated via pour plate technique.

2.2.6.2 Prototype construction

Technical drawings for the prototypes were created using AutoCAD 2012 and Solid Works 2011. The material used for manufacturing the flow prototypes was Poly-methyl-methacrylate (PMMA) tubing at 1000 mm (L) x 50 mm (OD) x 40 mm (ID) (Radionics, Ireland). Support structures were cut from 2 mm thick PMMA sheets using a Zing Laser cutter (Epilogue, USA). Chambers were cut using a DWE7491 Table saw (Dewalt, Ireland) and internal rebates were

cut using a RP0900 router (Makita, Ireland), the final height of all prototypes was 500mm. Internal bonding of films and membranes was performed using and inert polyvinyl-siloxane dental glue (Coltene, Ireland). External and structural bonding was done using Bostik clear silicone sealant (Radionics, Ireland). Three varieties of prototype were produced; incorporating 4 free-standing composite films, 3 composite coated glass fibre membranes and finally 9 composite coated membranes. All prototypes had a final internal volume of ~620ml.

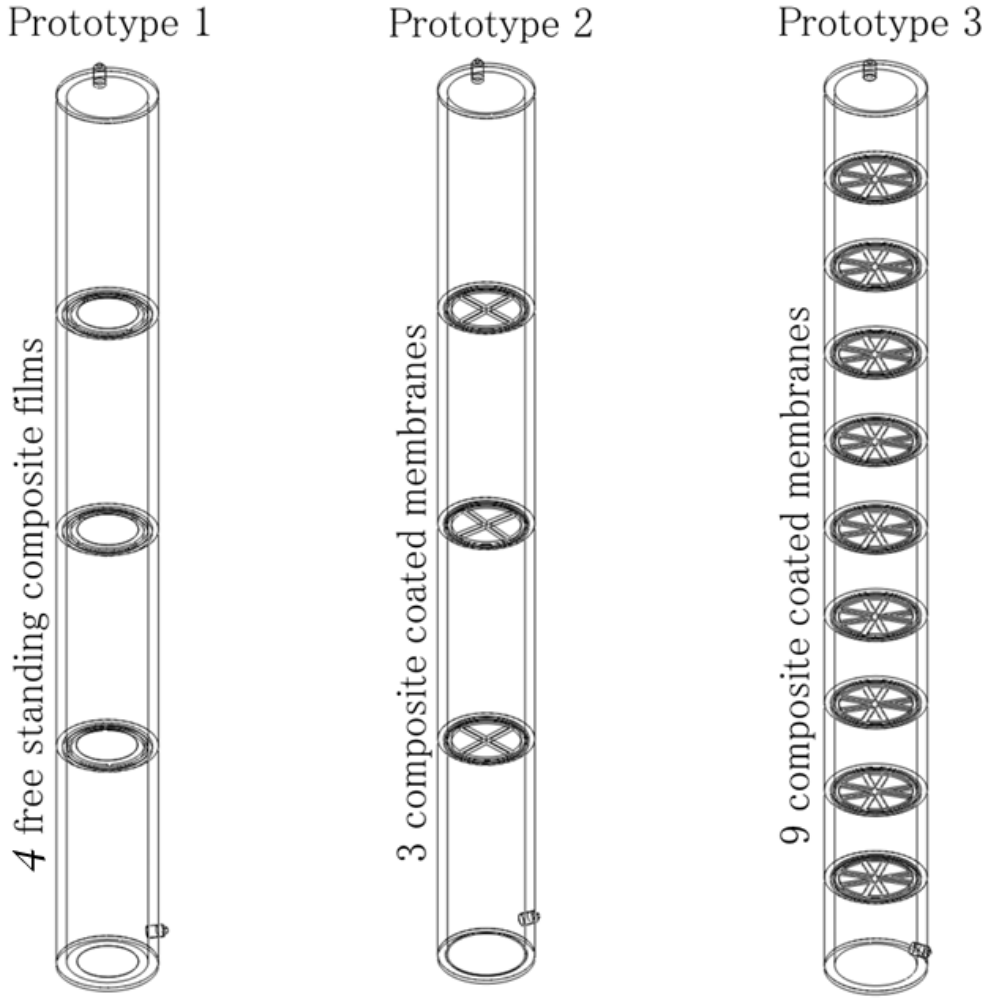

Figure 2.6 Simple representations of each prototype variety which incorporated; 4 composite films, 3 coated membranes and the final version incorporating 9 composite coated membranes with greater support structures.

2.2.6.3 Bacterial removal by prototype

Bacterial removal by the prototype was carried out using units which incorporated both the free-standing graphene-copper composite films as well as the composite coated glass fibre membranes.

All prototypes were cleaned, sterilised with 70% IMS and flushed with 1 L of sterile de-ionised water before microbiological assays were carried out. 700 ml or 5 L of sterile saline solution

(0.85% NaCl) were inoculated with *E. coli* to a final concentration of 10^2CFU/ml. In the preliminary run, using 700 ml, a Watson-marlow 114DV peristaltic pump (Watson-marlow, Ireland) was used at a flow rate of 22 ml/min to give a ramp-up time (i.e. initial filling of the unit) of 30 minutes. 1 ml samples were taken in triplicate at 30 minutes, at each hour thereafter up to 6 hours and bacteria were enumerated using the pour plate technique.

For the larger volume examination of 5 and 10 litres, samples were taken after initial ramp-up time and then after each litre eluted until the total volume had passed through the prototype. 1 ml Samples were taken at each point and enumerated in triplicate via pour plates. Following the experiment, each membrane was removed from the prototype, cut into two halves and placed into each of R2A broth and nutrient broth to examine the viability of the bacteria retained on the surface; results were recorded as positive or negative growth within each media.

2.2.6.4 Chemical contaminant removal by prototype

In order to examine the adsorption potential of the composite coated membranes within the prototype 700ml of methylene blue 0.0048mg/ml (absorbance = 1) and famotidine 0.032mg/ml (absorbance = 1) were passed through two prototypes at a flow rate of 22ml/min to provide a residence time of 30 minutes. Removal was monitored via UV-visible spectroscopy at 664nm for methylene blue and 281nm for famotidine. Continuous circulation was carried out and samples taken at thirty minute intervals up to eight hours, an additional sample was also collected following 24 hours of circulation.

2.2.6.5 Removal of Cryptosporidium by prototype

To examine the removal of Cryptosporidium by the prototype, 100 oocysts (provided by City Analysts Ltd. Dublin) of Cryptosporidium parvum were added to 10 L of sterile saline solution (0.85% NaCl) to give an inoculum size of 10 oocysts/L. This was passed through prototype #3, collected and passed through a filtramax filtration unit for collection. Microscopic analysis was carried out by City Analysts Ltd. for the presence or absence of oocysts following passage through the unit.

2.2.6.6 Long-term testing of prototype

In order to examine the long-term robustness of the prototype, up to 100L of tap-water was filtered at a maximum flow-rate of 90ml/min through prototype #3. The prototype was examine visually for the structural and membrane integrity, spiking with *E. coli* was carried out at set intervals to examine for bacterial retention and samples were taken for AAS analysis to examine for copper leachate from the graphene-copper composite into the permeate.

Operating parameters

The long-term flow testing was carried out using tap water. A constant flow-rate of 90ml/min was achieved through the use of a peristaltic pump attached to a tap-fed reservoir. This flow rate was used as the maximum rate, as any higher was found to physically damage the membranes.

Copper leachate analysis

The leaching of copper from the composite within the prototype was investigated during the long-term testing. 15ml samples were taken every 5 litres, acidified to below pH2 with nitric acid (HNO_3) and examined for the presence of copper using atomic adsorption spectroscopy (AAS). A Varian Spectra AA 50 (Agilent, Ireland) was used to carry out copper leachate analysis. A mark seven air-acetylene burner was used and a lamp current of 4mA was employed during analysis. Copper standards (0.4, 0.6, 0.8, 1, 2 and 3ug/ml) were used to perform a standard curve.

Bacterial removal during long-term testing

6.2ml aliquots of *E. coli* at 10^5CFU/ml were prepared and added to the flow at 10L intervals. After spiking, 1ml samples were taken at 3 minute intervals up to 10 minutes and added, in triplicate, to 10ml of nutrient broth to examine for the presence or absence of growth.

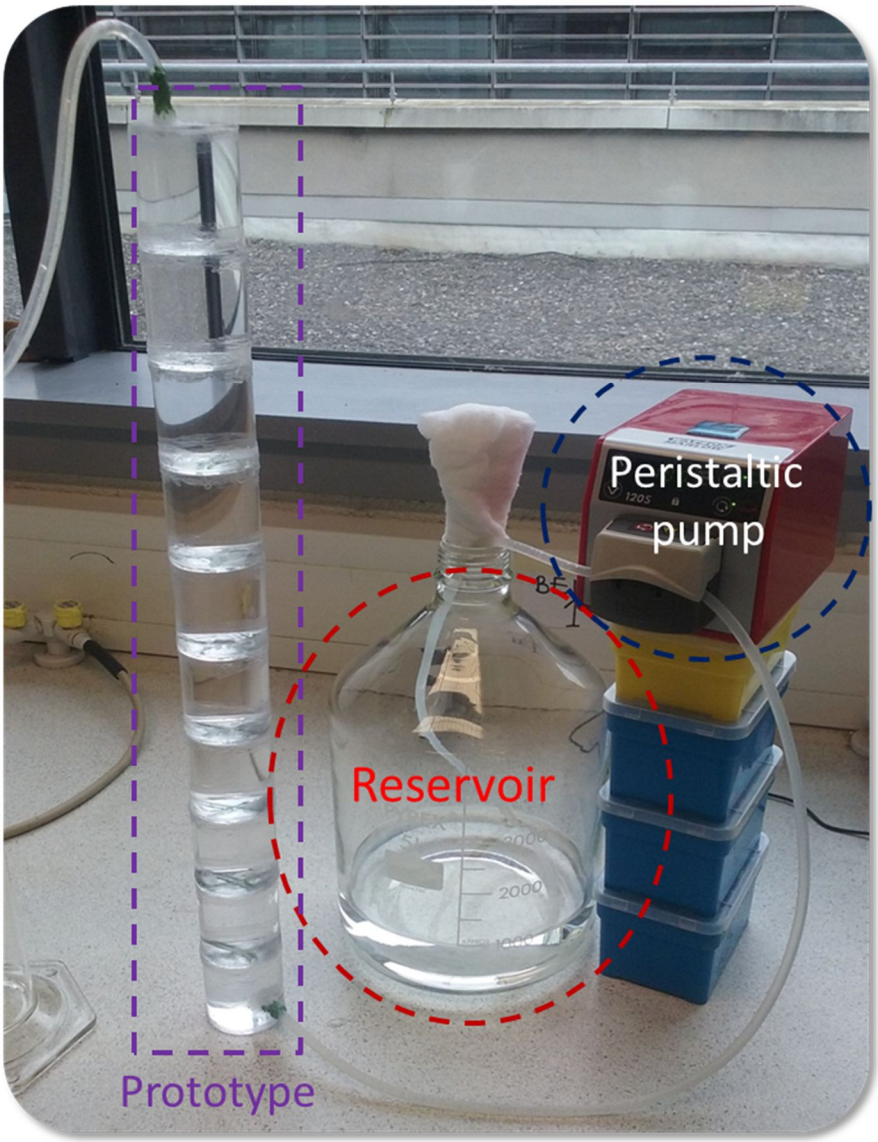

Figure 2.7. The experimental set-up used with the prototype highlighted (purple square), the reservoir (red circle) and the peristaltic pump (blue circle). The flow is pumped from the inlet at the bottom of the unit, upward through each membrane dividing each section.

2.2.7 Statistical Analysis

All experiments were carried out in triplicate with statistical analysis, data analysis and graphing conducted using Microsoft Excel.

3. Results

3.1 Characterisation of materials

The characterisation of each of the graphene materials was an important initial phase of the project for several reasons;

1) Verifying that the materials were produced correctly and conformed to characteristics seen within the literature.
2) Understanding, in particular, the physical and chemical differences between each material so as to provide a better understanding of their performance as antibacterial agents and adsorbents.
3) Examining the physical morphology of each material and how this can impact on their immobilisation.

While the production of graphene oxide is well established and applied using the hummers' method, the variation in characteristics of graphene produced by different laboratories, and even between batches, necessitates thorough characterisation each time any graphene materials are produced. In order to produce graphene oxide (GO), potassium permanganate ($KMnO_4$) and sulphuric acid (H_2SO_4) were used to oxidise graphite to graphite oxide which gave a purple-brown paste. The addition of water resulted in a colour change to orange-brown and a noticeable increase in volume. The addition of hydrogen peroxide (H_2O_2) reduced the excess permanganate present for removal during washing. This process results in a golden brown paste which then requires repeated centrifugal washing with deionised water to remove excess acid and unreacted material. After washing, GO was seen as a viscous brown suspension. Initially, sodium borohydride ($NaBH_4$) was used as a reducing agents to produce reduced graphene oxide and the graphene-copper composite (Cu-rGO). L-ascorbic acid would also be used as both a reducing agent and stabiliser to produce a homogeneous composite for immobilisation. The reduction process resulted in solutions which were noticeably black, compared to the brown of the GO solution which is indicative of reduction. The chemical composition of each material was analysed via Ultraviolet-visible (UV-vis) spectrophotometric analysis, thermo-gravimetric analysis (TGA) and Fourier-transform infrared spectroscopy (FTIR). Principally, the loss of oxidative groups following the reduction process was examined for. Energy-dispersive X-ray Spectroscopy (EDX) was used to confirm the elemental composition of each material and in particular, the quantity of copper present within the composite (Cu-rGO). Dynamic light scattering (DLS) was used to establish the particle size distribution within aqueous suspensions of each material and the morphological profile of each material was evaluated via optical and scanning electron microscopic (SEM) analysis. The presence of sheet-like structures, indicative of graphene exfoliation from graphite was examined for. Transmission electron microscopy (TEM) was used to compare the aggregation of the materials produced using different reducing agents.

3.1.1 Ultraviolet-visible (UV-vis) spectrophotometric analysis

UV-vis spectra of GO, rGO and Cu-rGO were taken for characterisation. GO (blue) shows a characteristic peak at ~230nm, indicating the successful exfoliation and oxidation of graphite to GO. Subsequent chemical reduction results in a characteristic red-shift of the absorption peak from 230 to 260nm, indicative of the loss of oxygen containing functional groups on the surface of GO and the restoration of the electronic conjugation across the sheets. Cu-rGO displays a much broader band from 260nm to 400nm compared to that of rGO, indicative of the presence of oxidised copper nanoparticles.

In order to create stable dispersions of rGO and Cu-rGO for immobilisation, l-ascorbic acid was used as an alternative reducing agent which would also act as a stabiliser within the suspension. The characteristic red shift of the GO to rGO can be seen to occur from 230nm to 250nm (purple line) indicative of the loss of the oxygen containing functional groups within the GO albeit to a lesser extent compared to that of the sodium borohydride ($NaBH_4$) reduction.

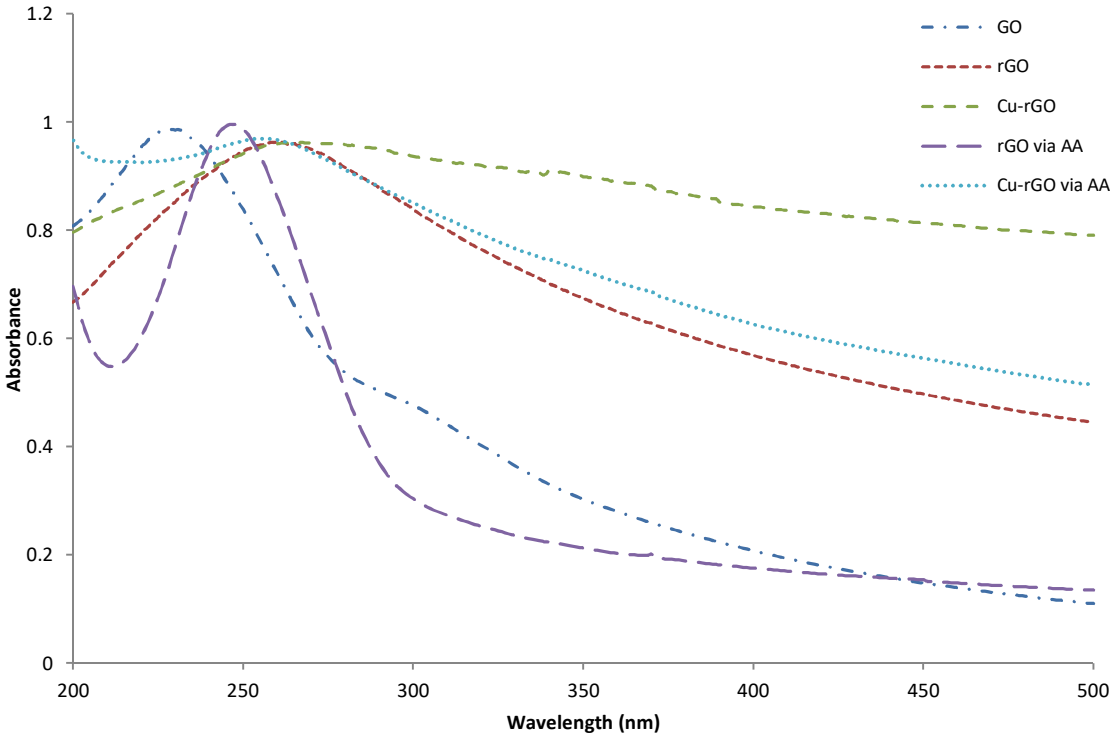

Figure 3.1 UV-vis specta of GO (blue), rGO (red) and Cu-rGO (green).

3.1.2 Thermogravimetric analysis (TGA)

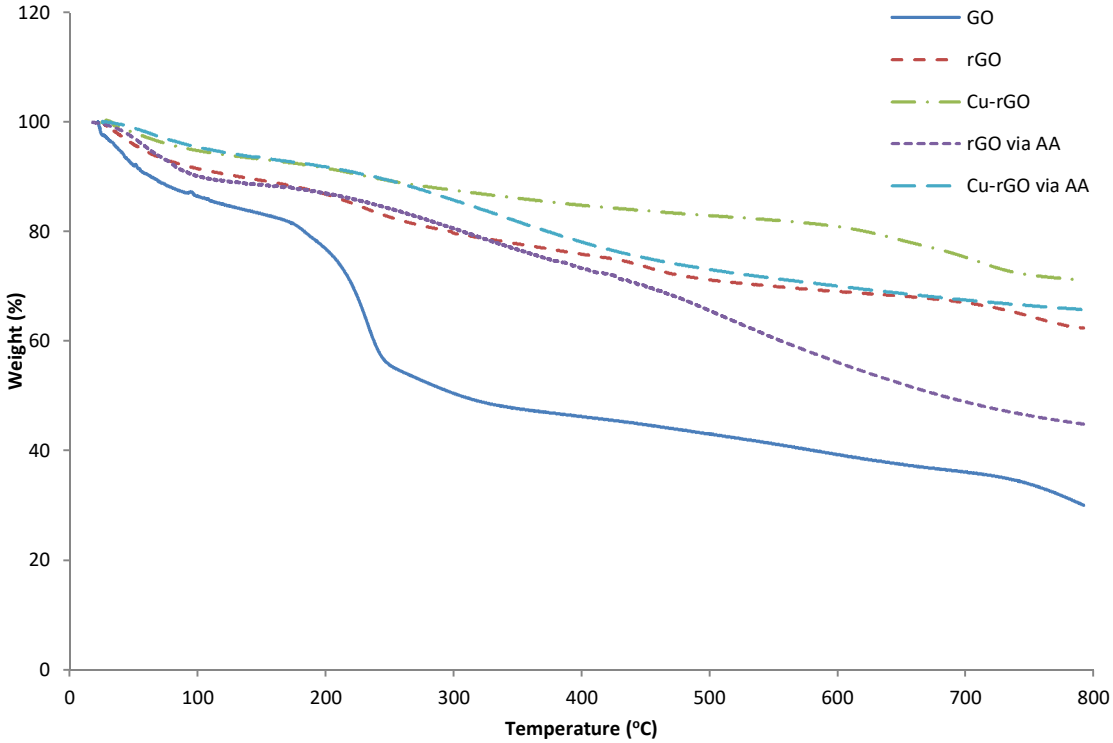

Figure 3.2 Thermogravimetric analysis carried out on graphene oxide (GO), reduced graphene oxide (rGO) and the graphene-copper composite (Cu-rGO).

Solids of GO, rGO and Cu-rGO were characterised for their thermal stability via thermogravimetric analysis (TGA). GO showed a significant drop in mass at ~200°C and showed a more rapid decline in weight loss compared to the other two materials with less than 30% remaining at 800°C. rGO showed a mild yet steady decline from 0 to 800°C, losing only 30% weight in total which is suggestive of much greater thermal stability compared to that of GO. The graphene-copper composite showed the greatest thermal stability of the three materials losing only 25% of its total weight up to 800°C.

The l-ascorbic acid derived rGO can be seen to be more thermally stable than the original GO, losing 56% of its total weight, but less so than the borohydride ($NaBH_4$) derived rGO, which indicates that while reduction has occurred, it is to a lesser extent than that of the borohydride method. Interestingly, the Cu-rGO derived l-ascorbic acid reduction is as stable as the more reduced rGO via borohydride reduction, losing ~34% of its total weight, which is most like a result of the thermal stability of the copper present; though it is still not as thermally stable as its borohydride derived counter-part with less oxygen content and higher copper concentration.

3.1.3 Particle size analysis via dynamic light scattering (DLS)

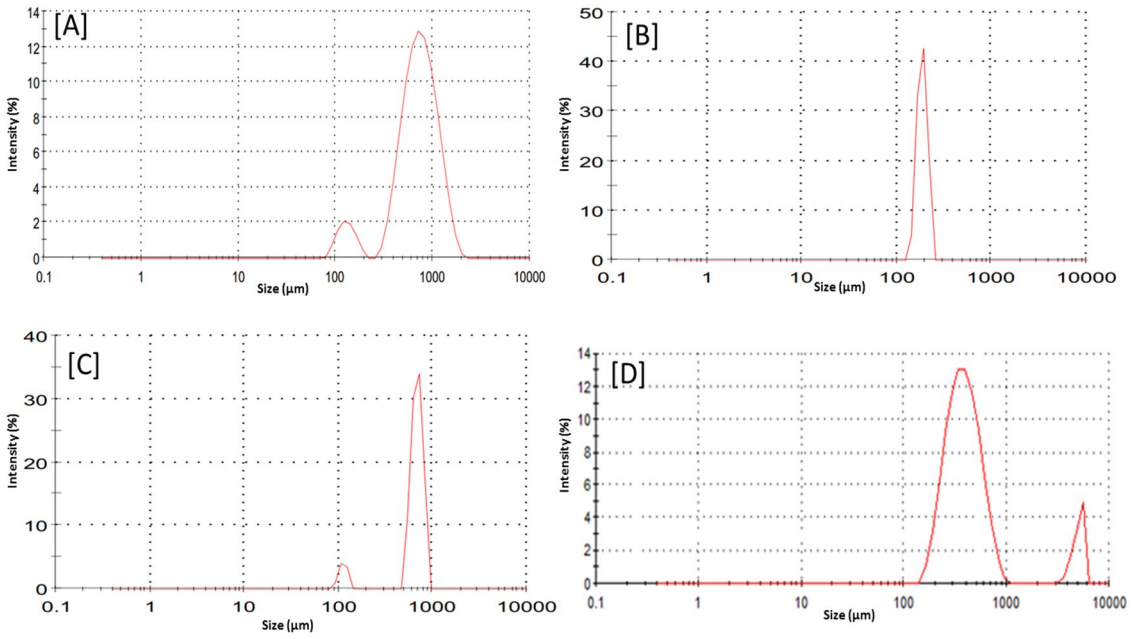

Figure 3.3 Size distribution analysis of [A] GO solution. Two peaks, each pertaining to sizes of 0.131 and 0.793µm respectively, were resolved. Size distribution analysis of the CuNPs solution [D]. Two peaks, each pertaining to 0.39 and 5.0µm respectively were resolved. While the data for rGO [B] and Cu-rGO [C] is shown, this can only be taken qualitatively as the poly-dispersity within the sample inhibited accurate particle measurement.

Aqueous solutions of GO, rGO, Cu-rGO and CuNPs were further characterised via dynamic light scattering (DLS) to examine the range of particle sizes present in solution. The examination of GO showed the predominant presence of two sizes of particles; 0.793µm and 0.131 µm. Particles of 0.793µm contributed to 91.8% of the particles present, with the remaining 8.2% being 0.131 µm in size - Figure 3.3 [A]. While the majority of particles present within the GO solution are of these sizes, the relatively broad peaks present suggest a high level of poly-dispersity within the solution, meaning that while these are the predominant sizes present the homogeneity of the solution in relation to particles size is low.

The suspension of copper nanoparticles was found to consist of two sized particles: 90.2% at 0.398µm and the remaining 9.8% at ~5µm [D]. This remaining 10% is most likely agglomerates of copper rather than individual particles. Again, while the most numerous particles may be ~0.398µm, the broad peak would suggest that a high level of variability (most likely due to aggregation) is present. Due to the high level of aggregation (which could be observed visually), settling and poly-dispersity present in solutions of both rGO and Cu-rGO, measurements taken of each solution via DLS were considered invalid, thus the requirement for further characterisation of these solutions via microscopic techniques.

3.1.4 Optical microscopic analysis of material dispersions

Following the confirmation of GO, rGO and Cu-rGO production, further characterisation was required to investigate the particle size distribution present in the solutions of rGO and Cu-rGO as well as the morphological profile of all three materials. Optical microscopic analysis was used to examine and compare the size of particle aggregates present in solutions of rGO and Cu-rGO. In the GO solution, small barely visible translucent sheets, immeasurable through light microscopy due to their small size can be seen throughout the solution along with much larger sheets from 50-100µm (Figure 3.4). Contrastingly, the rGO and Cu-rGO solution both show large agglomerated particles in the 100's of µm range throughout. The large agglomerates can be seen to be composed of many much smaller particles (Figure 3.5 [B]). The Cu-rGO solution shows much denser particles compared to the translucent sheets visible in the GO, indicative of high levels of particle agglomeration.

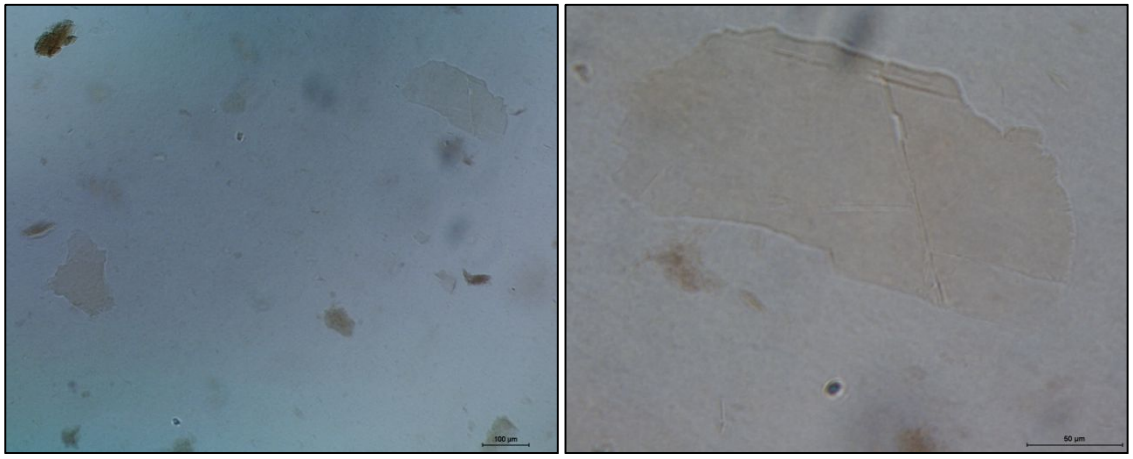

Figure 3.4 Optical microscopic images of GO at [A] x10 magnification and [B] x40 magnification.

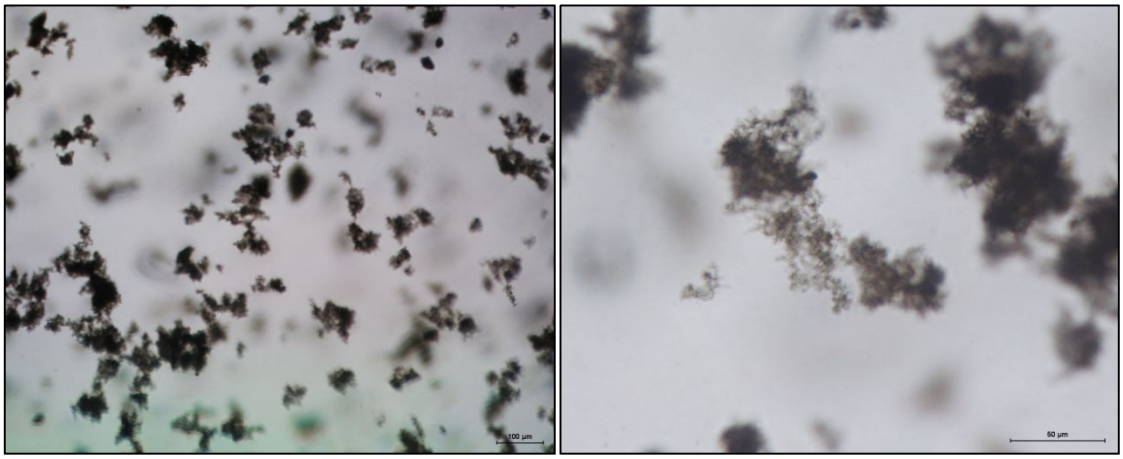

Figure 3.5 Optical microscopic images of rGO at [A] x10 magnification and [B] x40 magnification.

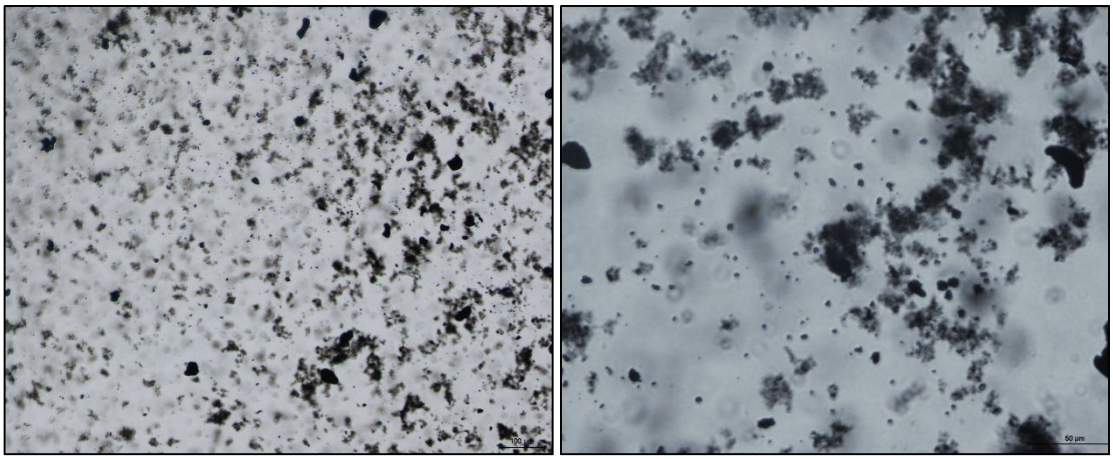

Figure 3.6 Optical microscopic images of Cu-rGO at [A] x10 magnification and [B] x40 magnification.

3.1.5 Scanning electron microscopic analysis

Graphene Oxide (GO)

The exfoliation of graphene oxide sheets from expanded graphite was confirmed by the presence of lustrous silk-like sheets which were visible under SEM analysis (Figure 3.7). Under low-magnification, x500, large sheets of >100um width were visible. Sheets also appeared crumpled in some areas and translucent in others, suggesting a variance in the sheet thickness across the sample.

Reduced Graphene Oxide (rGO)

The physical characteristics of reduced graphene-oxide (rGO) sheets was also observed under SEM (Figure 3.8) to examine changes occurring following chemical reduction. While a sheet-like structure was visible, similar to the observation of GO, the veil-like appearance of low-number sheets was absent suggesting the agglomeration of sheets during the reduction process.

Graphene-Copper Composite (Cu-rGO)

Cu-rGO morphology was also examined via SEM analysis and yielded images with a very apparent morphological difference compared to both the GO and rGO samples. Due to the presence of copper, the promotion of particulate agglomeration is clearly visible in the Cu-rGO sample. Large agglomerates of sheets can be seen (Figure 3.9 [B]) clearly decorated with copper particles accross the surface.

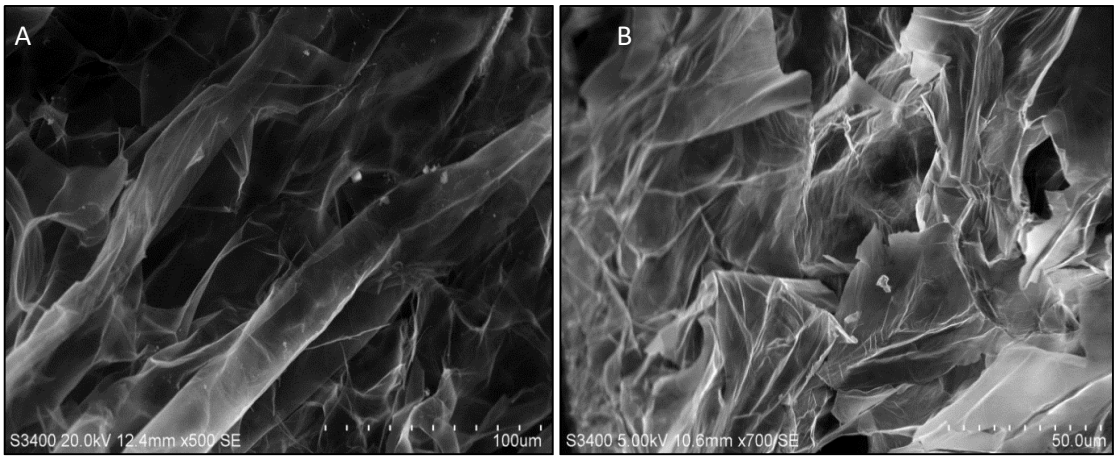

Figure 3.7 Scanning electron micrographs of chemically exfoliated graphene oxide sheets at [A] x700 magnification and [B] x500 magnification.

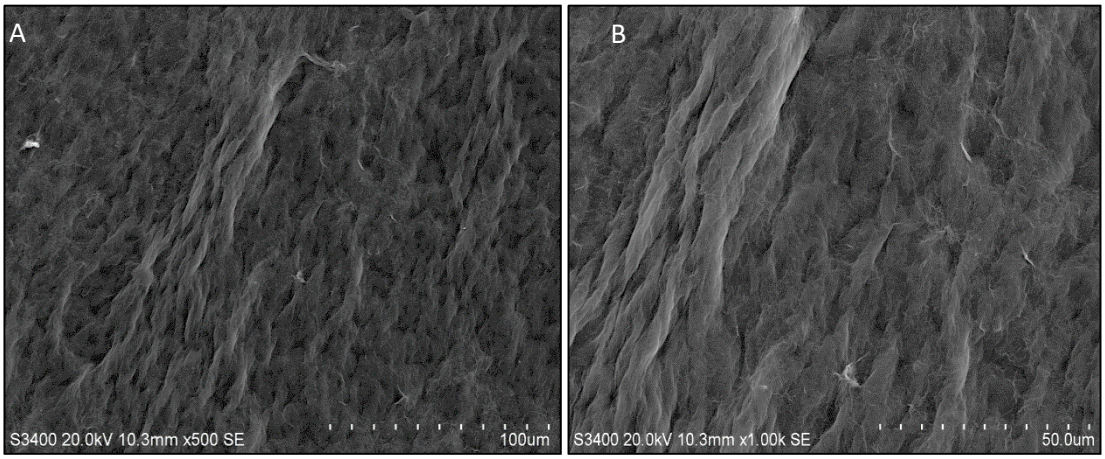

Figure 3.8 Scanning electron micrographs of exfoliated graphene oxide sheets following chemical reduction at [A] x500 magnification and [B] x1.0k magnification.

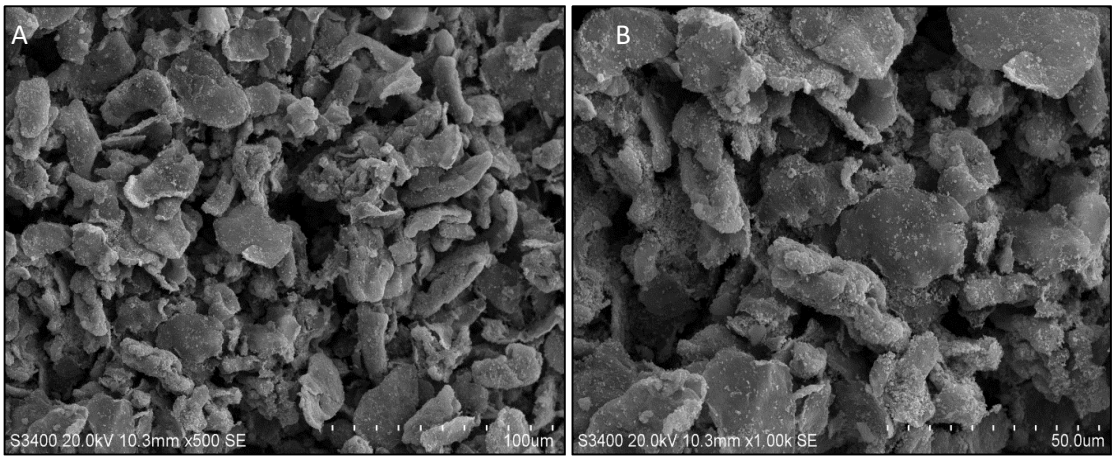

Figure 3.9 Scanning electron micrographs graphene-copper composite at [A] x500 magnification and [B] x1.0k magnification.

3.1.5.1 Scanning transmission electron microscopic (STEM) analysis

Scanning transmission electron images were captured using a Hitachi S5500 to examine the internal structural variation of the different materials, in particular to examine the difference between the aggregation of the rGO and Cu-rGO produced via the different reduction methods.

Graphene oxide (GO)

Unlike the images captured via scanning electron microscopy the use of transmission electrons shows very clearly the thin gossamer sheet-like nature of the graphene oxide (Figure 3.10 [A]). Images captured of individual sheets showed a large variation in sheet size from 10's of nanometres to 1 micron and few larger sheets in the 10's of micron range as had been seen during optical microscopic analysis.

Copper nanoparticles (CuNPs)

Transmission images captured of the copper nano-particles showed a distribution in their size between 10 and 25nm (Figure 3.10 [B]) with the majority being circular or oval in shape. The nano-particles can be seen to form clusters which are echoed in the images captured of the composite material with nano particles cluster visible attached to graphene sheets.

Reduced graphene oxide (rGO)

Figure 3.11 [A] and [B] highlight the difference in imaging conditions formed by the two preparation methods employed for the reduced graphene oxide. Figure 3.11 [A] shows the reduced graphene oxide via sodium borohydride ($NaBH_4$) reduction with large aggregates covering the substrate and a difficulty in distinguishing individual sheets. Figure 3.11 [B] demonstrates the dispersity of the l-ascorbic acid prepared reduced graphene oxide with some aggregates of three to four microns visible but far more disperse than the borohydride preparation.

Graphene-copper composite (Cu-rGO)

The difference in morphology between the sodium borohydride ($NaBH^4$) prepared CU-rGO and the l-ascorbic acid prepares Cu-rGO can be seen in figure 3.12 [A] and [B]. The first material can be seen to have large chunks in the 10's of micron range while the l-ascorbic acid prepared Cu-rGO facilitates to observation of individual small aggregates of sheets over the carbon substrate with clusters of copper nano particles attached to the surface of those sheets.

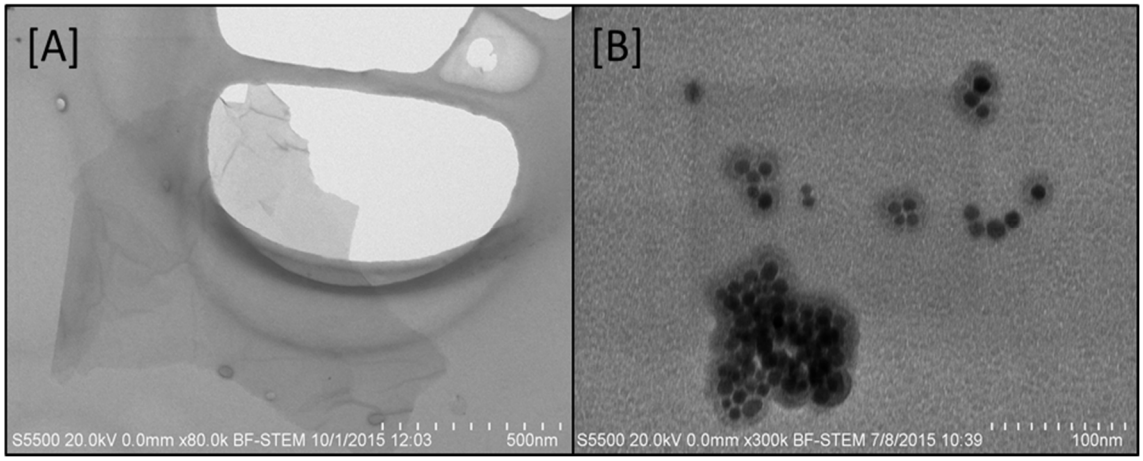

Figure 3.10 Scanning transmission electron (STEM) microscopic images of [A] Graphene oxide on holey carbon substrate and [B] copper nano particles derived via l-ascorbic acid reduction on holey carbon substrate

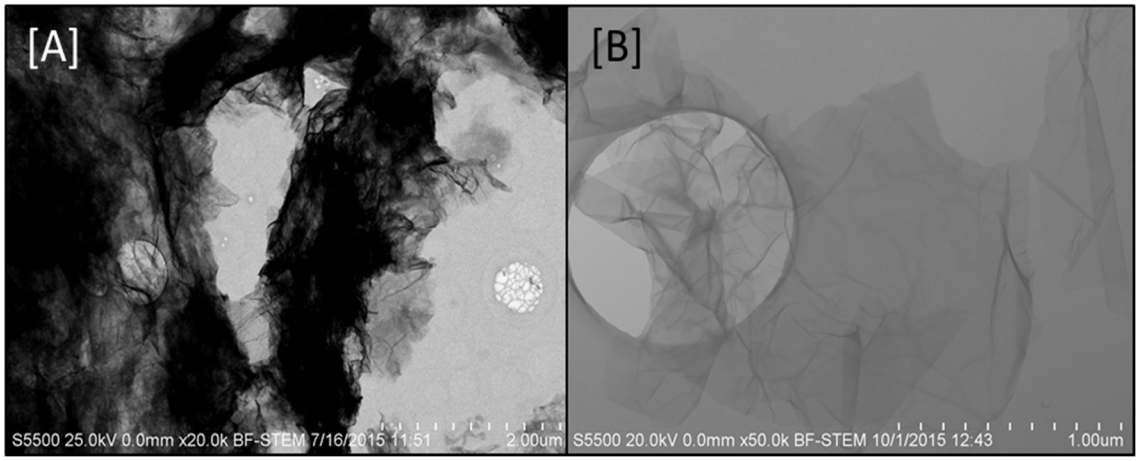

Figure 3.11 Scanning transmission electron (STEM) microscopic images contrasting the difference between [A] the reduced graphene oxide prepared via sodium borohydride ($NaBH_4$) reduction and [B] via l-ascorbic acid reduction

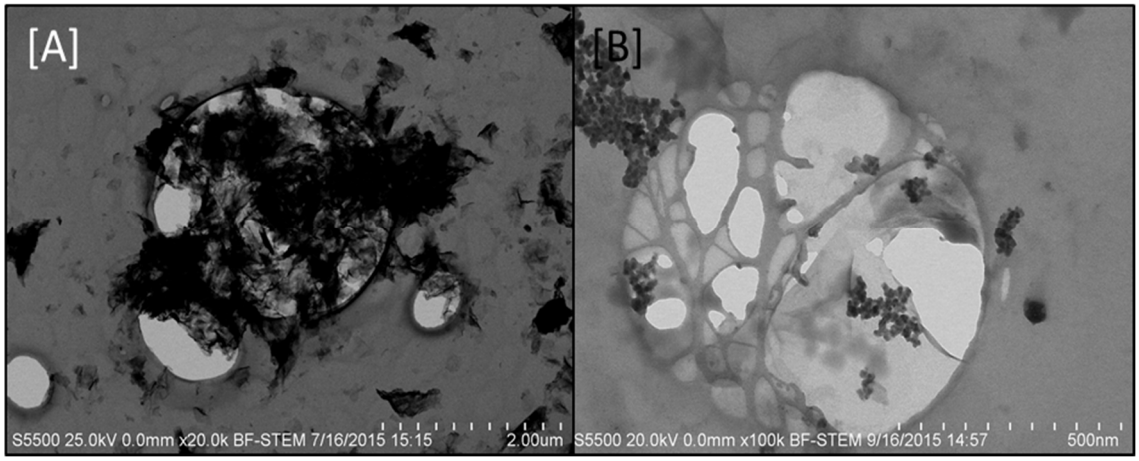

Figure 3.12 Scanning transmission electron (STEM) microscopic images contrasting the difference between [A] the copper composite prepared via sodium borohydride ($NaBH_4$) reduction with large aggregates and [B] via l-ascorbic acid reduction with nano particle cluster visible on the graphene sheets

3.1.6 Fourier-transform infrared spectroscopy (FTIR)

Fourier-transform infrared spectroscopy (FTIR) was used to gauge the different functional groups, and the loss thereof following reduction, within the graphene materials. Adsorption bands of GO are observed at 3204, 1729 and 1046 cm^{-1} and can be attributed to O-H deformation, C=O carbonyl stretching and C-O stretching respectively. The remaining peaks at 1362cm^{-1} (O-H deformations in the C-OH groups) and 1220cm^{-1} (C-OH) correspond to the carboxyl groups present in the GO. The peak at 1619cm^{-1} is still under debate and may represent either absorbed water molecules or unreacted graphitic regions (Mei *et al.* 2011), (Stankovich *et al.* 2006), (Fuente *et al.* 2003), (Szab *et al.* 2006).

The significant reduction in these bands can be seen in both the rGO (red line) and the Cu-rGO (blue line) following reduction by sodium borohydride ($NaBH_4$) or l-ascorbic acid with little to no absorption visible following the reduction processes. The significantly lower transmittance occurring during analysis of the composite can be attributed to the presence of the copper within the structure of the graphene.

The observation of these adsorption bands as well as the change observed following the reduction process are in-line with those observed in the literature from previous productions of graphene-copper composites (Xu *et al.* 2009), (Chen *et al.* 2011).

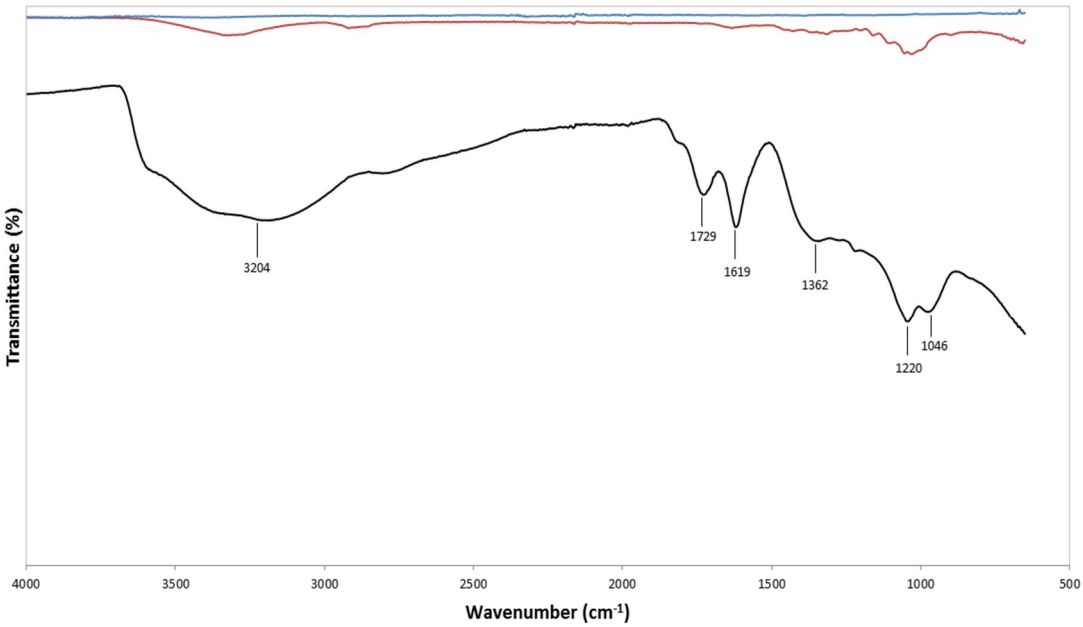

Figure 3.13: FTIR spectrum of GO (black), rGO (red) and Cu-rGO (blue)

3.1.7 Evaluation of elemental composition via Energy-dispersive X-ray Spectroscopy (EDX)

Graphene Oxide (GO)

Graphene Oxide showed a typical elemental composition as seen in Table 3.1. The carbon oxygen ratio was ~1:1, showing the high level of oxidation of the graphene following chemical exfoliation. No other constituents were present indicating a thorough removal of any residual material from the production process.

Reduced graphene Oxide (rGO)

The reduced graphene oxide showed a markedly lower carbon oxygen ration moving from 50%-50% to ~70%-30% in favour of carbon. This would suggest that the borohydride ($NaBH_4$) reduction is effective at removing the oxidative groups present on the surface of the graphene oxide.

Graphene-copper Composite (Cu-rGO)

The graphene-copper composite showed a markedly lower level of oxidation compared to graphene oxide, indicative of the loss of oxidative groups present on the surface during the borohydride reduction process, from 46% in GO to 22% in the Cu-rGO. The average copper composition was found to be 40% with an obvious variance across the surface, from 28% up to 49% depending on the site observed. This variance indicates the inhomogeneity of copper attachment across the graphene sheets during production. This inhomogeneity can also been seen from the SEM analysis in Figure 3.9.

Copper Nanoparticles

In addition to the production of the composite, a separate process excluding the addition of graphene was also performed to examine the effect of the reduction process on the $CuCl_2$ used to produce the composite. The form of copper present, i.e. copper metal (Cu), cuprous oxide (Cu_2O), cupric oxide (CuO) or the highest copper oxide (Cu_2O_3), in the composite is of importance as different forms of copper will possess different levels of anti-bacterial efficacy. The copper and oxygen content present was found to be 74.31 and 26.69% by weight respectively.

Reduced Graphene Oxide via l-ascorbic acid

As the sodium borohydride ($NaBH_4$) reduction resulted in an inhomogeneous suspension which was not useful for immobilisation an additional method which utilised l-ascorbic acid as both a reducing and capping agent was developed. The reduced graphene oxide (rGO) produced via l-ascorbic acid reduction was shown to have a higher oxygen content compared to the borohydride reduction with ~34% oxygen present indicating that the l-ascorbic acid may act as a milder reducing agent.

Graphene-copper composite (Cu-rGO) via l-ascorbic acid.

Several formulations of graphene-copper composite were prepared in order to examine the suspension stability. A final method, producing a stable dispersion with ~25% copper content was used to produce the composite to be used for immobilisation. Compared to the sodium borohydride ($NaBH_4$) reduction method the l-ascorbic acid reduction process resulted in a far more homogeneous material with the copper spread evenly throughout the structure.

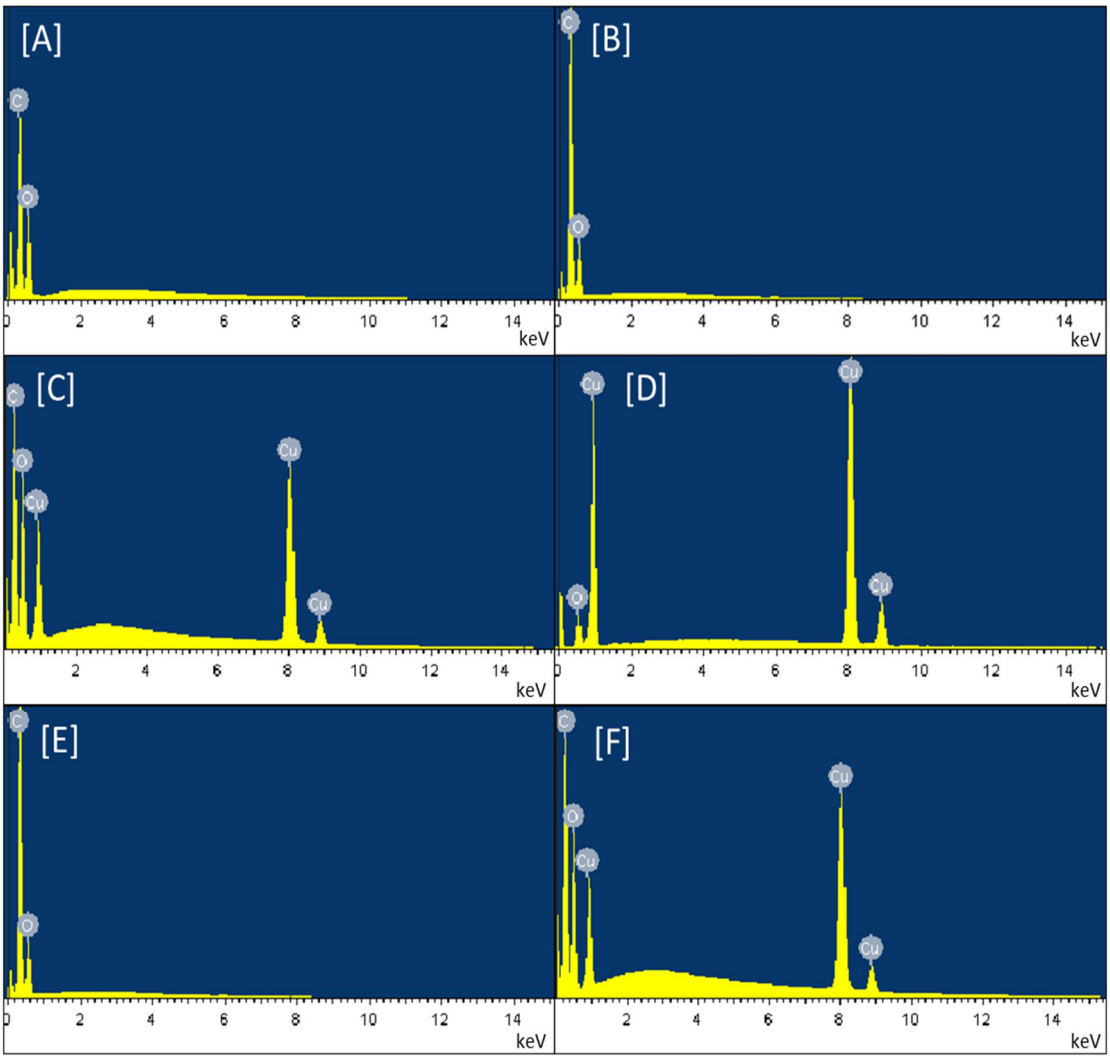

Figure 3.14 EDX spectra of [A] Graphene Oxide (GO) [B]Reduced Graphene Oxide (rGO) [C] Graphene copper composite (Cu-rGO) [D] Copper nanoparticles (CuNPs) [E] Reduced graphene oxide using l-ascorbic acid (rGO via AA) and [F] The graphene copper composite using l-ascorbic acid (Cu-rGO via AA)

Table 3.1 Average values of EDX analyses taken for the graphene oxide, reduced graphene oxide, graphene-composite and copper nanoparticles.

Material	Carbon (%)	Oxygen (%)	Copper (%)
Graphene Oxide	50.1	49.9	-
Reduced Graphene Oxide	70.49	29.51	-
Copper Compoiste (Cu-rGO)	37.16	22.42	40.04
Copper Nanoparticles (CuNP)	-	26.69	74.31
Reduced Graphene Oxide via AA	66.03	33.97	-
Copper Composite (Cu-rGO) via AA	47.63	27.43	24.94

3.2 Antibacterial testing

Graphene oxide was tested to ascertain whether or not it possessed any antibacterial efficacy as was claimed by some of the literature. The copper composite (Cu-rGO) was examined to investigate whether or not the conjoining of the copper with graphene would offer any particular advantage in terms of antibacterial efficacy. The rGO would serve as a control material for comparison with the Cu-rGO to examine the level of efficacy added by the copper. The antibacterial testing of the graphene materials was carried out in two ways; in solid media and liquid media.

In solid media, various methods of exposing the bacteria to each of the materials was investigated as, due to their various physical natures, the standard Kirby-bauer disk diffusion was unsuitable. As such, suspensions of each material were loaded into wells, onto disks and powders of each were placed onto the surface of agar inoculated with *E. coli* and *B. subtilis*. The effect of direct contact of organisms with the material was investigated by incorporating bacteria within the agar as well as creating bacterial lawns on the surface. The effect of contact with the materials on the bacterial envelope was examined via scanning electron microscopy in order to ascertain if membrane damage was occurring.

In liquid media, non-growth buffer solutions of PBS were used under shaking to examine if there was any physical damage caused, by the edges of sheets as suggested in the literature, by graphene materials. It would also shed light on the potential performance of the materials in a water treatment-like scenario. These analyses were also carried out over various concentrations of the three materials to examine the dose-response of the organisms. The aggregation and adsorption of bacterial cells onto the surface of graphene sheets was examined for via optical and fluorescent microscopy to see whether or not bacterial cells would “stick” to the sheets. The different response of bacteria in growth media as opposed to a non-growth scenario was also investigated as there were conflicting reports within the literature as to how organisms respond to graphene materials depending on the matrix of exposure.

Finally, the mutagenicity of each of the materials was examined via the AMES test. The purpose of examining the mutagenicity of each of the materials was to examine whether or not this would represent a concern when the material was applied to a prototype drinking water treatment system. As the permeate from any prototype would ideally be for human-consumption the mutagenicity of the materials and their potential impact on human health are of concern. In addition, the investigation of the mutagenic potential of graphene materials via the Ames test represents a novel line of investigation which has not been explored before.

3.2.1 Isolation and identification of environmental *E. coli* strain

A bacterial culture was isolated as described in section 2.2.9 and identified as *E. coli*. The results of the various identification methods employed are listed in Table 3.2. This environmental isolate was termed *E. coli* (T37-1) coded for its location of isolation, the Tolka River, the temperature at which it was isolated; 37°C and the sample number from which it was taken. It was then subsequently used in all antibacterial testing as a model organism.

Table 3.2 Results of the various identification methods employed to isolate an environmental strain of *E. coli* for use in antibacterial testing.

Isolation	
Growth on TBX agar	Formation of Blue/Green colonies
Gram-stain	Red pigmentation
Cell morphology	Rod
Oxidase Test	Negative
Indole Test	Positive
Catalase Test	Positive
API-20E Identification	99.9% confidence

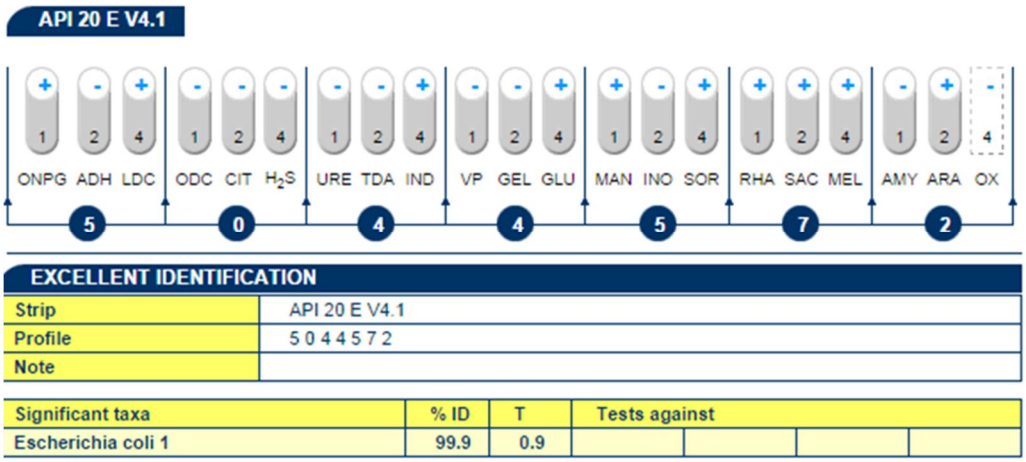

Figure 3.15. The positive and negative results (+ /-) results of each of the individual tests found within the API-20E kit and the associated identification (*E. coli* @ 99.9% confidence) attributed by the online database.

3.2.2 Solid Media Testing

Well-diffusion assay

Antibacterial studies were carried out in solid media using a number of approaches. Initially, the well diffusion assay was employed whereby wells were cut into nutrient agar incorporated with bacteria. 200µl of each material suspension, GO, rGO, Cu-rGO and CuNPs were added to each well. This approach was used to examine the diffusion of each material into the surrounding media. There was no observable zone from any of the particulate suspensions via this method.

Disk-diffusion assay

As no response was observed from the particulates in the well diffusion assay, the disk diffusion method was employed to examine the effect of more localised concentration on the antibacterial efficacy of each material. Disks impregnated with 20µl of each material suspension were applied to nutrient agar incorporated with bacteria. Once again, there was no observable zone from any of the materials employed in this case.

Solid exposure

In order to examine the effect of more direct contact between the materials and the organism, 5mg of solids of each material were applied to the surface of nutrient agar plates with a lawn of bacteria spread on the surface. The formation of a lawn on the surface of the agar would greater facilitate the direct contact with the organism and the material.

In the case of GO and rGO no response was observed once again for either organism. Clear zones of inhibition were present for the composite and the copper nanoparticles. The size of the zones was not measured as the shape and size of the applied solids varied and results were recorded as a positive or negative response.

Vacuum-filtered disk assay

As the need for direct contact was apparent and to examine the effect of exposure in solid media in a quantifiable manner, cellulose membranes were vacuum filtered with suspensions of each material to create disks of known concentration. Disks containing 0.4mg of each material were applied to nutrient agar plates covered with a lawn of bacteria. For comparative purposes standard Whatman disks impregnated with 0.4mg of $CuCl_2$ and $CuSO_4$ were also used as well. Table 3.3 shows the zones of inhibition of each material. A disk impregnated with 5µg of gentamicin, which served as a positive control, showed expected results in line with those within the literature Landrygan et al. (2002).

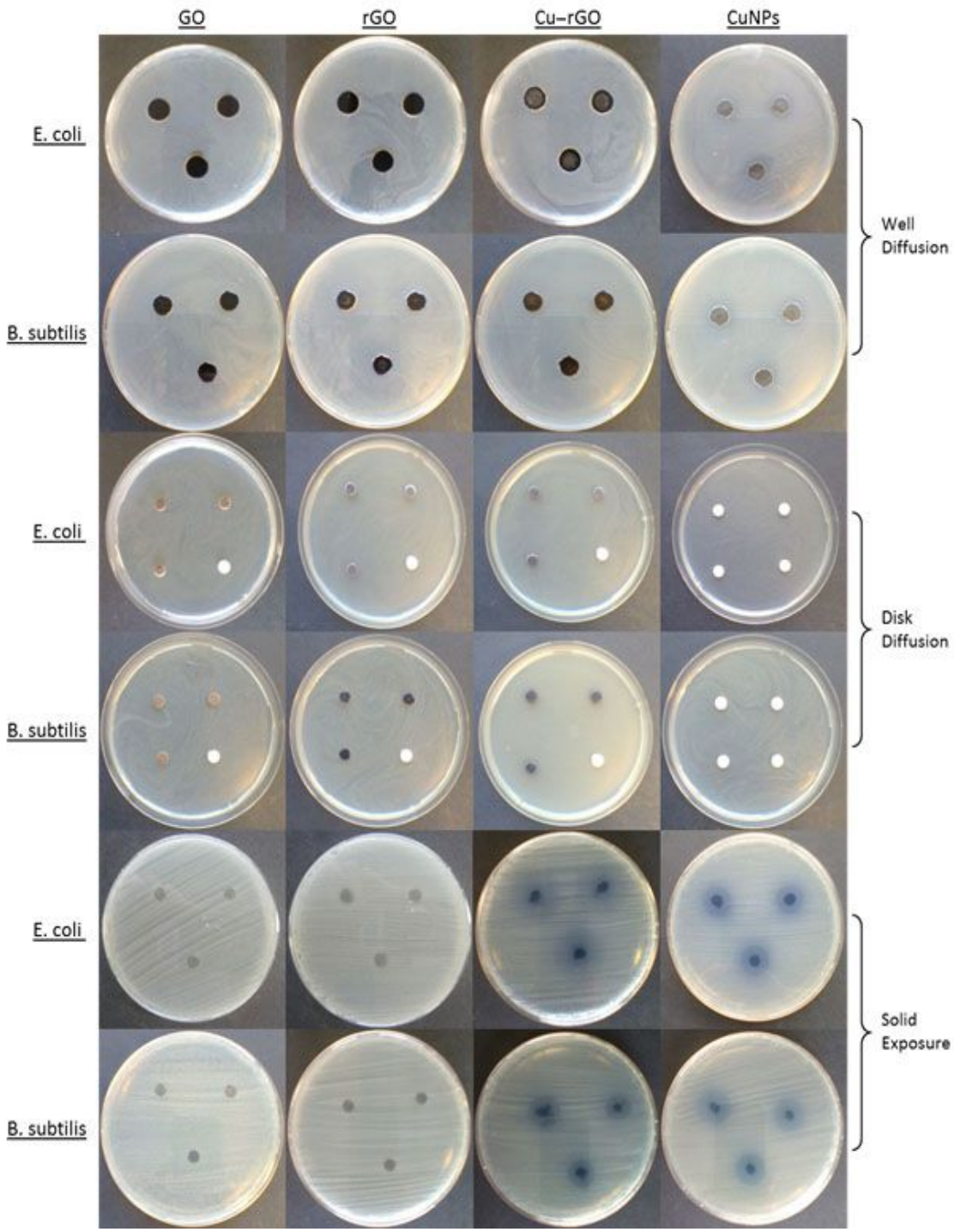

Figure 3.16 The results of the first three exposure methods employed during the solid media testing against *E. coli* and *B. subtilis*. Rows 1-2 the well diffusion method with wells cut into inoculated agar and aliquots of suspensions added. Rows 3-4 the disk diffusion method, disks loaded with material were added to the surface of agar inoculated with bacteria. Rows 5-6 the solid exposure assay, solid pieces of each material were added to agar with a bacterial lawn on the surface. Zones of inhibition can be seen only around the copper composite (Cu-rGO) and the copper nano particles (CuNPs) in the solid exposure assay.

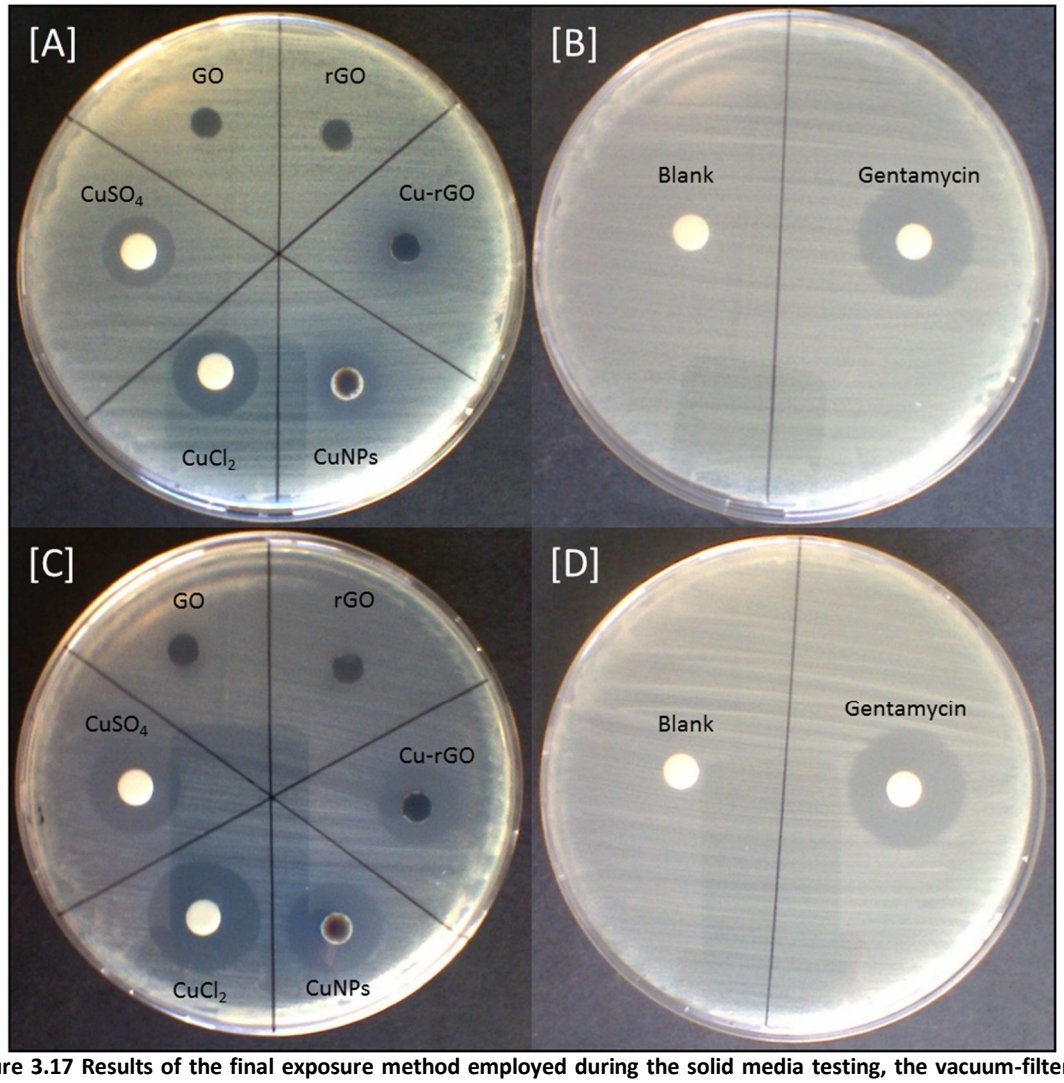

Figure 3.17 Results of the final exposure method employed during the solid media testing, the vacuum-filtered disks as well as the control experiment using a blank and disk impregnated with gentamycin. There was no observable zone of inhibition from either the GO or rGO with either organism. *B. subtilis* showed larger zones than *E. coli* in all cases.

Table 3.3 The zones of inhibition for each of the material employed in the vacuum-filtered disk assay against both *E. coli* and *B. subtilis*.

Zone size (mm)	*E. coli*	*B. subtilis*
Blank	No zone	No zone
GO	No zone	No zone
rGO	No zone	No zone
Cu-rGO	11mm	14mm
$CuCl_2$	14mm	19mm
$CuSO_4$	10mm	15mm
CuNPs	12mm	16mm
Gentamycin	19mm	20mm

3.3.3 Scanning Electron Microscopic (SEM) analysis of cell morphology

E. coli exposure to vacuum filtered disks was carried out as per Section 2.2.4.3 and surface exposure examined via SEM analysis. In the case of both GO and rGO, *E. coli* on the surface appear convex and proud of the surface with defined membranes and are unperturbed by surface contact. *E. coli* can be seen to be numerous across the surface of both the GO and rGO suggesting the surface of each material does not possess innate anti-microbial activity when in direct contact with micro-organisms. *E. coli* exposed to the surface of Cu-rGO however show clear membrane damage, looking deflated and conforming to the surface of the material rather than standing proud of it.

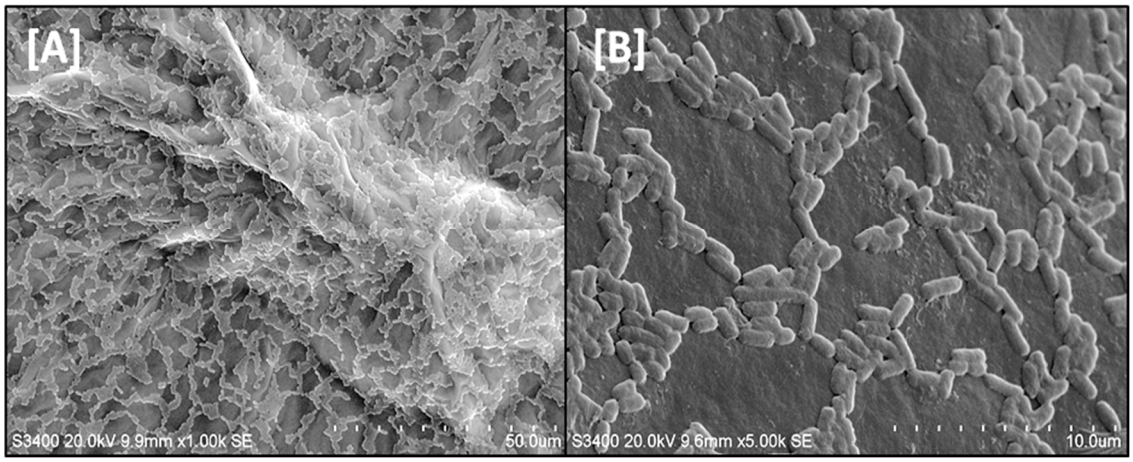

Figures 3.18 *E. coli* exposure to the surface of GO at [A]x1k magnification and [B]x5k magnification. *E. coli* can be seen to be numerous across the surface of GO and appear unperturbed by contact with the surface, having intact membranes and standing proud of the surface.

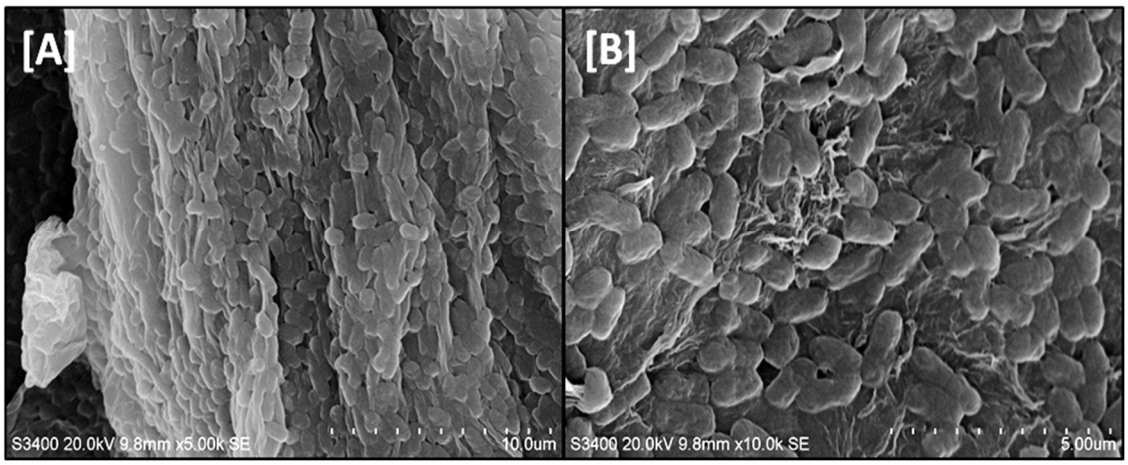

Figure 3.19 *E. coli* exposure to the surface of rGO at [A]x5k magnification and [B]x10k magnification. Much like GO, *E. coli* are numerous and appear intact and unperturbed across the surface of the rGO.

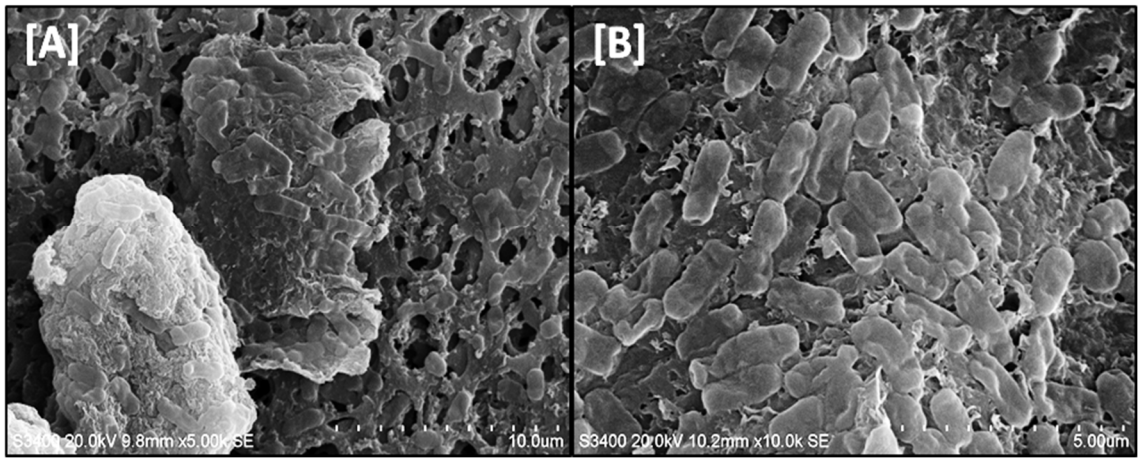

Figure 3.20 *E. coli* exposure to the surface of Cu-rGO at [A]x5k magnification and [B]x10k magnification. In contrast to both GO and rGO *E. coli* in contact with the surface of Cu-rGO appear to have lost membrane integrity. Rather than looking convex as in Figures 2.20 [A] and [B], *E. coli* are deflated looking and conform to the surface.

3.3.4 Anti-bacterial evaluation in non-growth liquid media

In order to examine the effect of free particles of graphene materials, liquid media studies with agitation were carried out. These studies were designed to mimic those in the literature which had reported a kinetic or shear-based antibacterial effect on planktonic bacterial cells. PBS, a saline buffer solution was used as a non-growth media. Both *E. coli* and *B. subtilis* were used and challenged with 100mg/L of each material over a 6 hour period along with 24 hour sampling. There was no statistically significant reduction in the population of *E. coli* cells during the 6-hour incubation period with either the GO or rGO, with cell counts comparable to the control sample in both cases. The copper-composite resulted in a reduction of 25±2%, greater than the same concentration of copper nanoparticles which resulted in 14±3%. In the six hour period, it was shown that the copper-containing salts, $CuCl_2$ and $CuSO_4$, had a more acute effect than the particulates, achieving 35±2 and 36±4% reduction in population size respectively (Figure 3.21). There was still no statistically significant reduction in population over a 24 hour period from the GO or rGO, though a higher cell count was achieved in each case which can be attributed to a combination of endogenous respiration and cell localisation on the particulate matter. The results over a 24 hour period showed a markedly different trend for the salts and other particulates. The Cu-rGO and CuNPs achieved a reduction in population of 81±1 and 80±3% respectively. The $CuCl_2$ and $CuSO_4$ showed a final reduction in population of 57±3 and 47±1% in each case (Figure 3.20). As with the *E. coli*, there was no statistically significant reduction in the population of *B. subtilis* cells with either GO or rGO over 24 hours (Figure 3.21).

The *B. subtilis* was shown to be more susceptible to the copper containing compounds than the *E. coli* however with total loss of cell viability occurring in 6 hours with all of the materials. The CuNPs, CuSO4 and CuCl2 had all achieved a greater than 99% reduction within 3 hours with the Cu-rGO requiring 6 hours for a complete kill to occur (Figure 3.22).

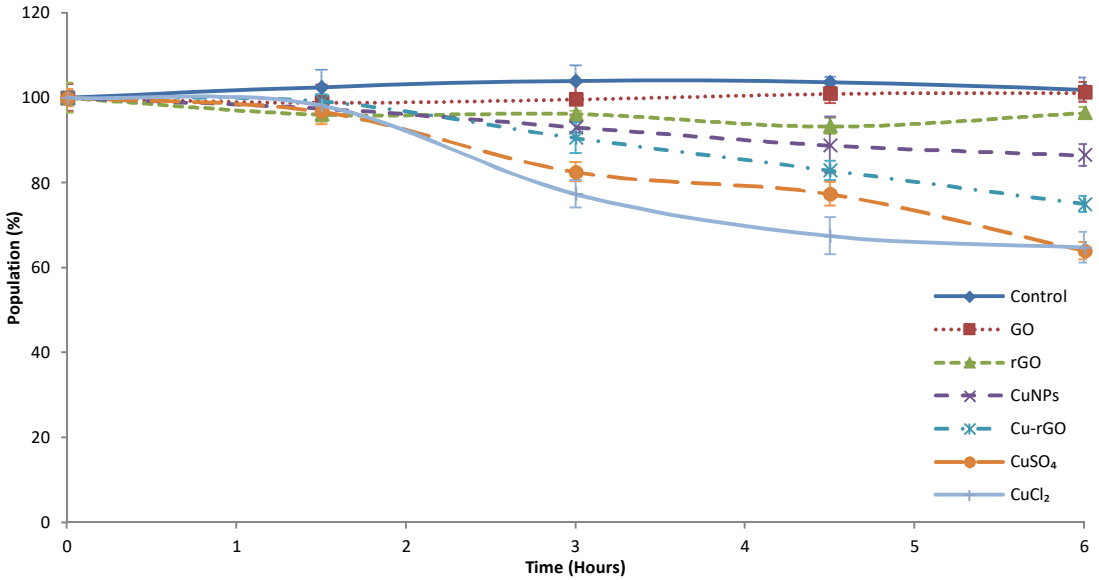

Figure 3.21 *E. coli* exposure to the various materials: GO, rGO, Cu-rGO, CuNPs, $CuCl_2$ and $CuSO_4$ in PBS over a 6 hour period at 100mg/L.

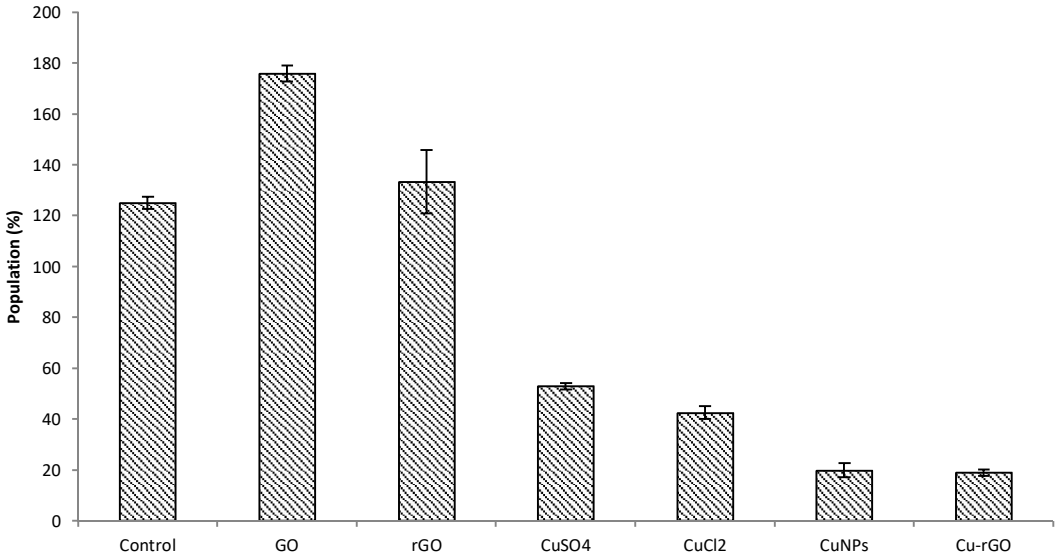

Figure 3.22 *E. coli* exposure to the various materials: GO, rGO, Cu-rGO, CuNPs ,$CuCl_2$ and $CuSO_4$ in PBS following a 24 hour period at 100mg/L.

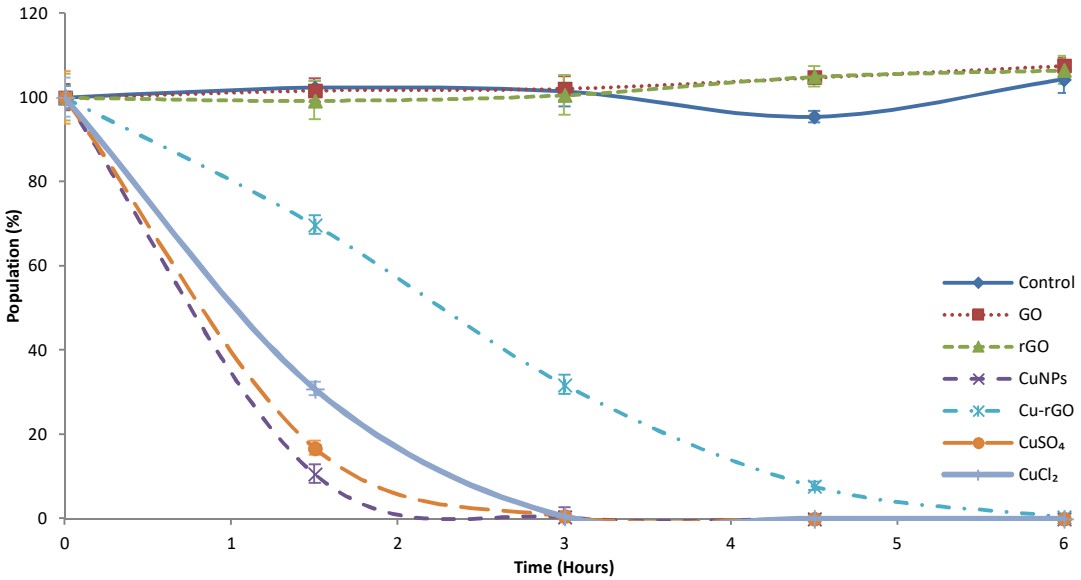

Figure 3.23 *B. subtilis* exposure to the various materials: GO, rGO, Cu-rGO, CuNPs ,$CuCl_2$ and $CuSO_4$ in PBS over a 6 hour period at 100mg/L.

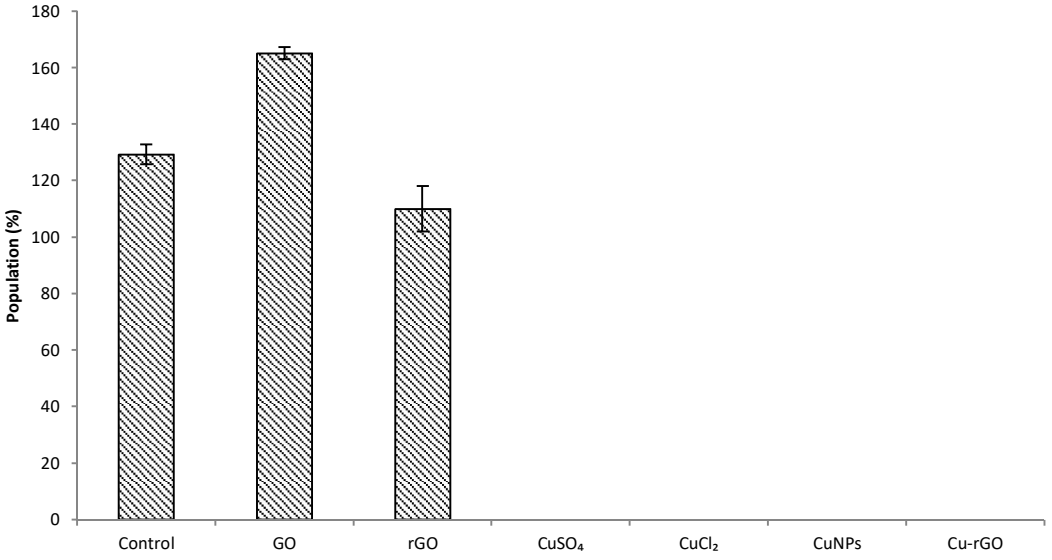

Figure 3.24 *B. subtilis* exposure to the various materials: GO, rGO, Cu-rGO, CuNPs ,$CuCl_2$ and $CuSO_4$ in PBS following a 24 hour period at 100mg/L.

3.3.5 Antibacterial evaluation in liquid growth media

In order to examine the dose-dependent response of both organisms in liquid growth media, as well as to establish the minimum concentration required to inhibit all bacterial growth, an MIC determination was carried out in nutrient broth. Concentrations of up to 1000mg/L were tested for all materials as these are the upper limits found within previous reports for the antibacterial testing of graphene materials. Following incubation, streak plates onto nutrient agar were carried out to check for positive or negative growth. Neither of the stand-alone graphene materials, GO nor rGO, showed any inhibition to either of the organisms up to 1000mg/L. There was increased optical density in the inoculated samples compared to controls and the formation of a thick bacterial deposit (inset of figure 3.22). The combination of particulates and bacterial growth in the higher concentrations (500mg/L and above) led to high optical density readings, beyond the limit of quantification and as such were unreliable in terms of measurement. Streak plates carried out from each of the tubes showed levels of growth comparable to that of the control sample.

All of the control materials $CuCl_2$, $CuSO_4$ and CuNPs possessed MIC values of 400mg/L for both organisms with the exception of the *B. subtilis* and CuCl2, resulted in complete inhibition at 200mg/L (Figures 3.26 and 3.27). A concentration of 1000mg/L of Cu-rGO was required to totally inhibit the growth for both organisms (Figure 3.28).

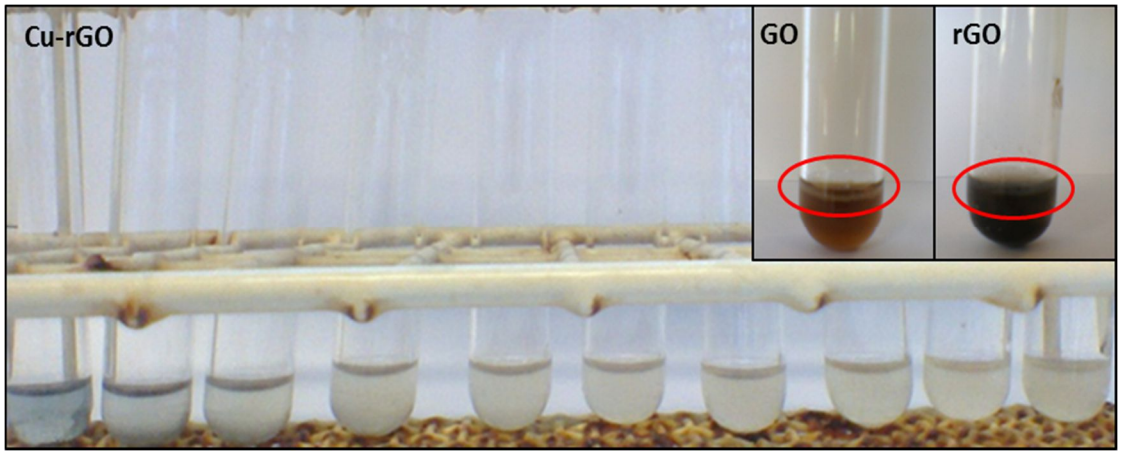

Figure 3.25 The MIC determination set-up employed for the particulate suspensions of GO, rGO and Cu-rGO. Concentration of Cu-rGO increasing from right to left without a noticable clarity at higher concentrations due to the lack of bacterial growth. Inset – The formation of thick films of micro-organism occurred even with the highest concentrations of GO and rGO, 1000mg/L, used.

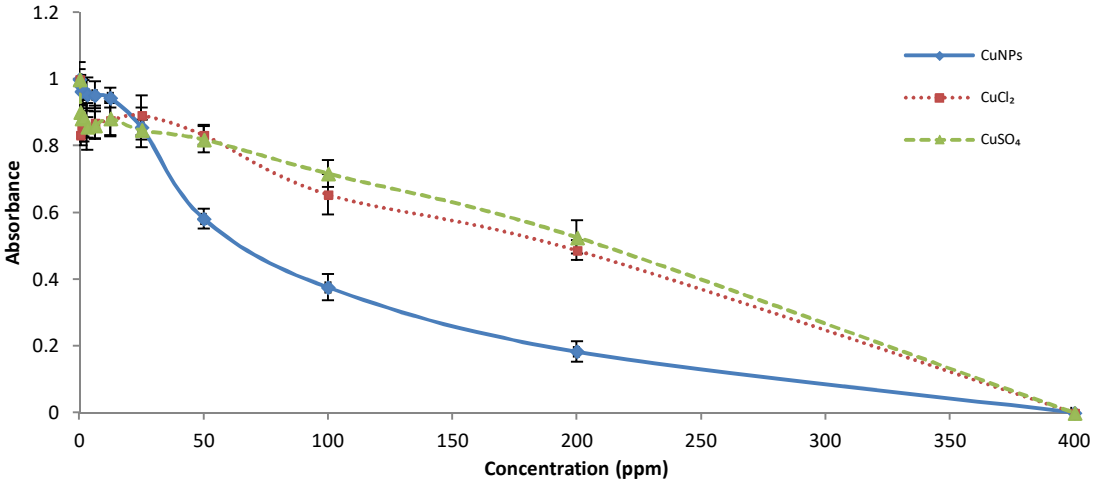

Figure 3.26 Determination of MIC values for *E. coli* for each of the copper containing compounds via the broth microdilution method: CuNPs, $CuCl_2$ and $CuSO_4$.

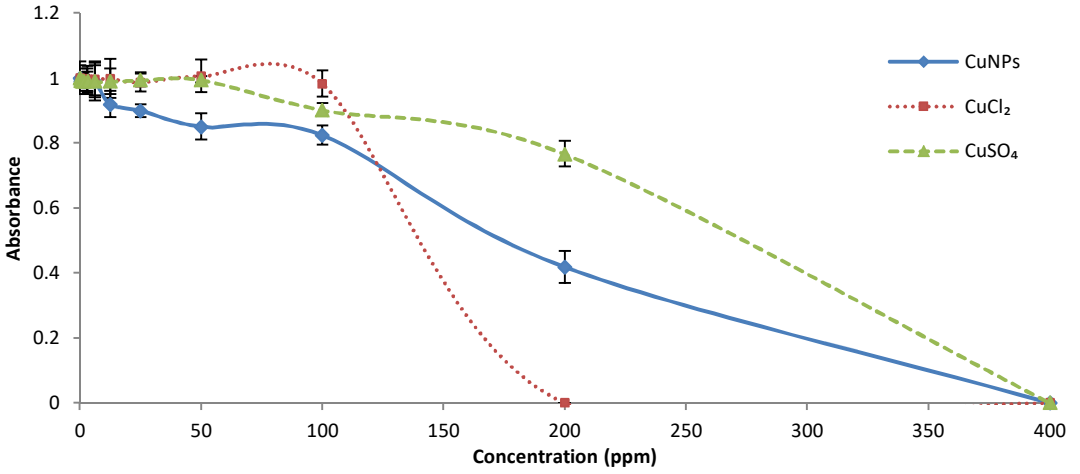

Figure 3.27 Determination of MIC values for *B. subtilis* for each of the copper containing compounds via the broth microdilution method: CuNPs, $CuCl_2$ and $CuSO_4$.

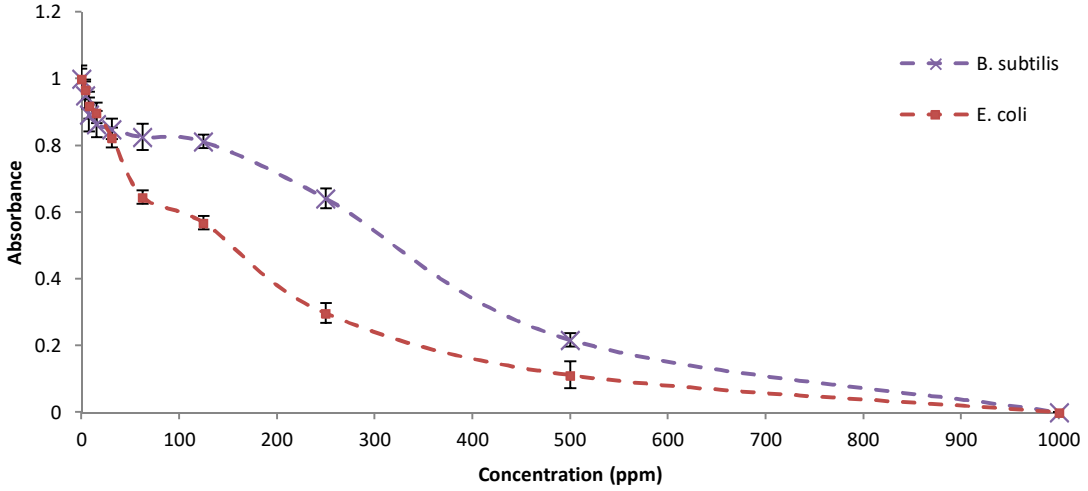

Figure 3.28 Determination of the MIC values for each organism, *E. coli* and *B. subtilis*, for the Cu-rGO using the large volume method as shown in figure 3.25.

3.3.6 Optical and fluorescent microscopic analysis

Fluorescent microscopic analysis was carried out as described in Section 2.2.4.4. Cells appear as green points due to the fluorescent stain. In the case of all materials, bacterial cells can be seen to have attached or become associated with graphene particles present in solution. This can be seen to be true for each of GO, rGO and Cu-rGO, though rGO and Cu-rGO showed higher tendency toward greater localised cell density compared to GO, as can be seen in figures 3.30 and 3.31. This agglomeration and localisation of cells clearly demonstrates the tendency of the bacterial cells to preferentially attach or become associated with the graphene materials as opposed to remaining in the free solution. In order to examine how the concentration of graphene particulates in solution effected the agglomeration of materials buffer solutions at concentrations of 0, 400, and 1000mg/L of Cu-rGO were prepared and inoculated with *E. coli*. Figures 3.32, 3.33 and 3.34 show concentrations of 0, 400 and 1000mg/L of Cu-rGO following exposure to *E. coli* (T37-1) in buffer solution and following staining with SYT09. The level of agglomeration in terms of both particles and bacterial agglomerates is highlighted with the increase in Cu-rGO concentration. The control sample (0mg/L) shows an even dispersion of cells across the field of view with little to no aggregated cells visible. By comparison the middle concentration of 400mg/L shows high levels of agglomerated Cu-rGO with bacterial cells obviously attached to the larger particles. The level of both particulate and cell agglomeration is particularly evident when comparing the bright-field images between the different concentrations. The highest concentration of 1000mg/L shows much agglomerated particles, as is particularly evident in the brightfield image of figure 3.34 [A], with large thick particles obstructing the passage of light to the objective. In addition, cell aggregates can be observed around these much larger particles as is particularly evident in the bottom left quadrant of the image.

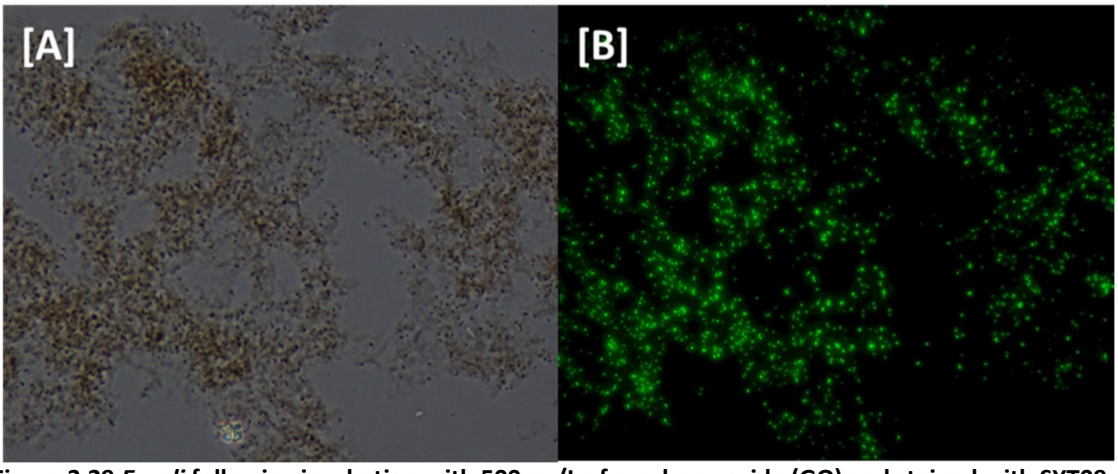

Figure 3.29 *E. coli* following incubation with 500mg/L of graphene oxide (GO) and stained with SYT09. Images captured via [A] brightfield and [B] fluorescent green channel.

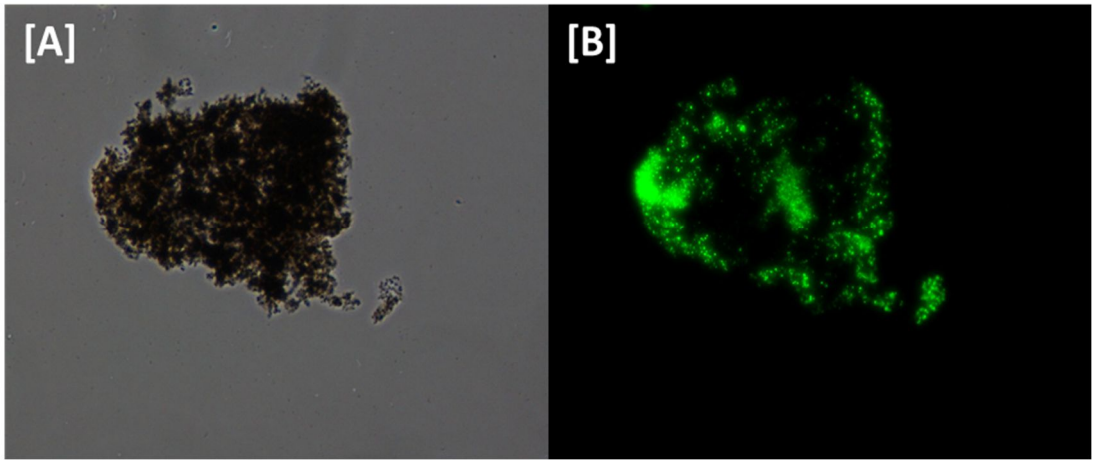

Figure 3.30 *E. coli* following incubation with 500mg/L of reduced graphene oxide (rGO) and stained with SYT09. Images captured via [A] brightfield and [B] fluorescent green channel.

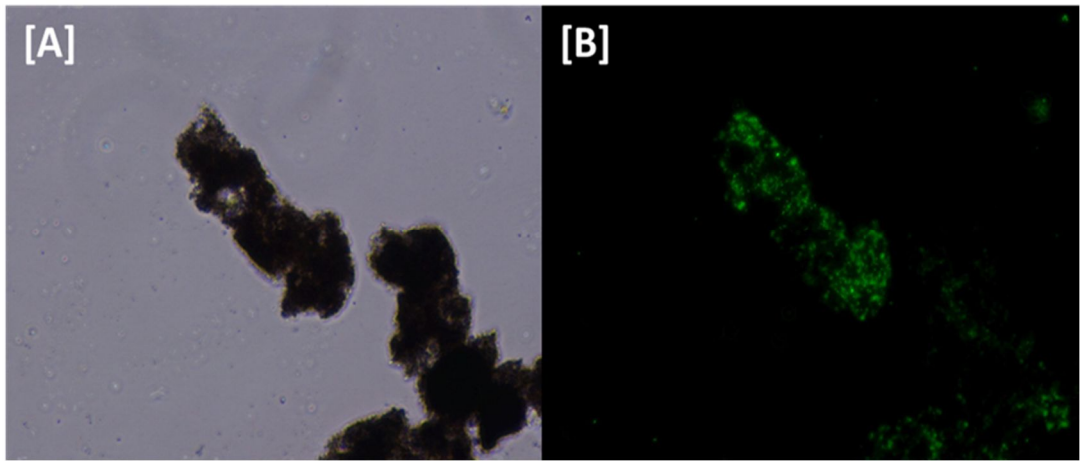

Figure 3.31 *E. coli* following incubation with 500mg/L of copper-graphene composite (Cu-rGO) and stained with SYT09. Images captured via [A] brightfield and [B] fluorescent green channel.

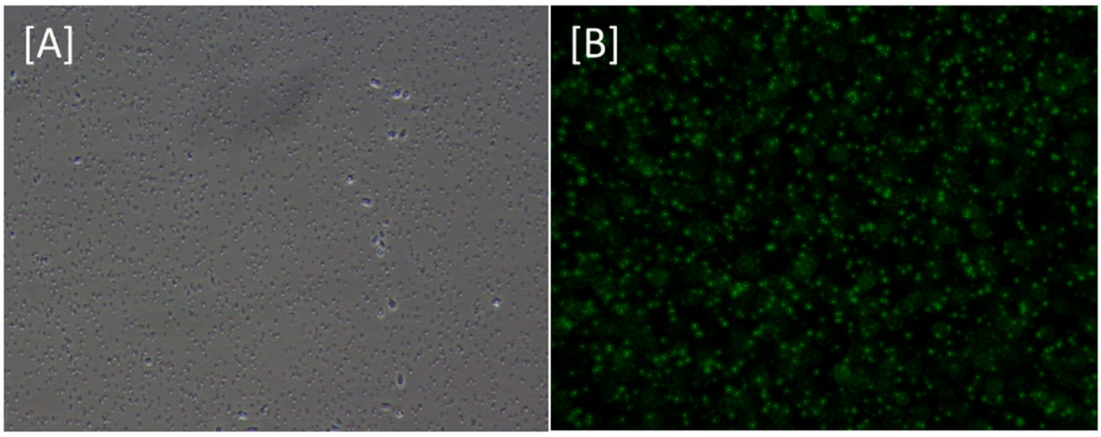

Figure 3.32 Brightfield [A] and fluorescent [B] images of the control sample containing no Cu-rGO at x40 magnification. There is an even distribution of cells throughout the image.

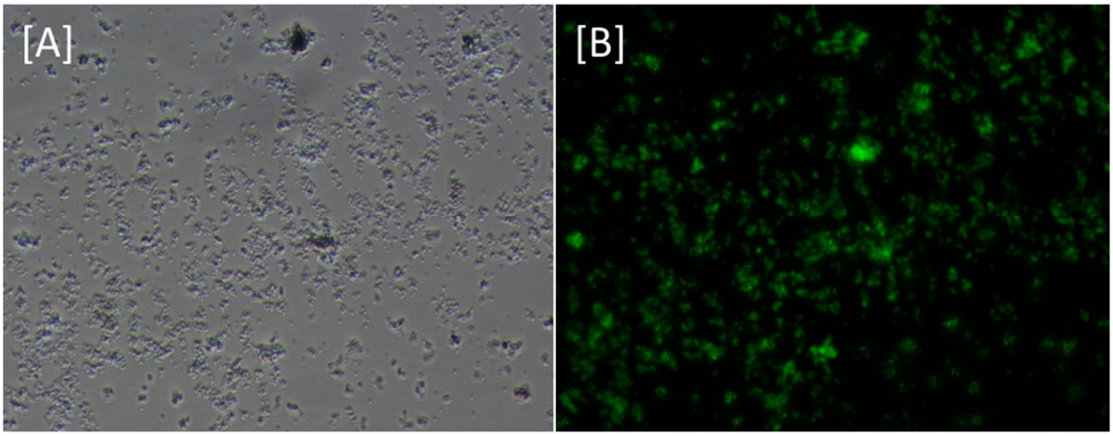

Figure 3.33 Brightfield [A] and fluorescent [B] images of the sample containing 400mg/L of Cu-rGO at x40 magnification. A more profound level of particulate and cell aggregation is occurring with an increase in the Cu-rGO concentration.

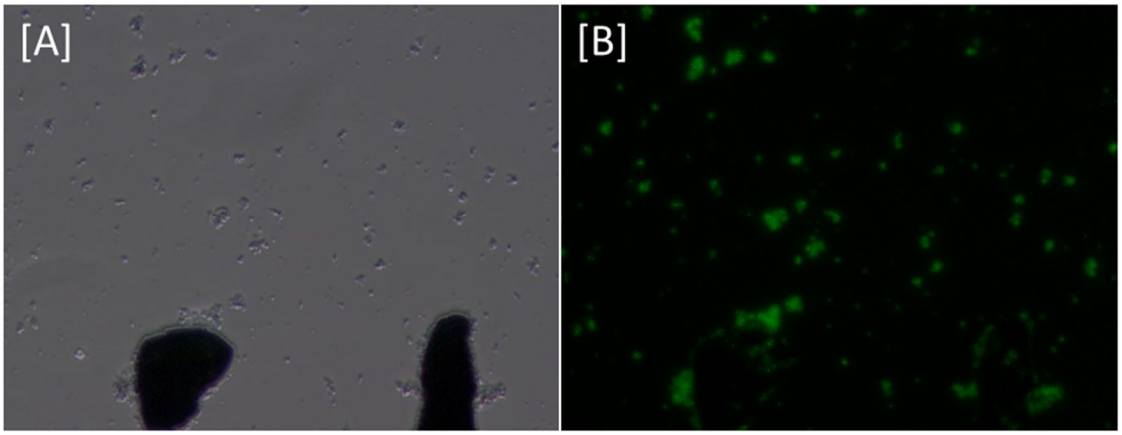

Figure 3.34 Brightfield [A] and fluorescent [B] images of the sample containing 1000mg/L of Cu-rGO at x40 magnification. The large agglomerates of Cu-rGO particles can be seen in the brightfield image [A] and have become thick enough to obstruct light transmission. The localisation of cells can be clearly seen in the fluorescent image [B] with large groupings present on the agglomerated Cu-rGO particles.

3.3.7 Evaluation of graphene mutagenicity via the Ames test

The potential mutagenic impact of the graphene materials (GO, rGO and Cu-rGO) were evaluated using the AMES test as described in section 2.2.4.6. As the ideal end-point of the project was the production of drinking water, the potential mutagenicity of the graphene compounds was of interest due to the fact that they may come into human contact via direct consumption. Each compound was tested at concentrations of 0.1, 1 and 10ppm (mg/L). Across the three compounds and the concentrations tested the level of observed mutagenicity was equivalent to that of the negative control sample. The expected value for the negative control is ≤15 revertants which was observed in this case and was the observed values for all of the compounds tested.

The expected value for a known mutagen, such as Sodium Azide (NaN_3), the positive control in this case, is ≥25 revertants. Based on the observed results, each of the graphene materials can be said to be non-mutagenic at the concentrations tested.

Table 3.4. Results of the mutagenicity testing carried out on the GO, rGO and Cu-rGO at concentrations of 0.1, 1 and 10ppm

Concentration	GO	rGO	Cu-rGO	Positive Control (Sodium Azide)	Negative Control
N/A	-	-	-	33	12
0.1ppm	10 ± 1	11 ± 3	10 ± 2	-	-
1ppm	9 ± 2	9 ± 2	8 ± 3	-	-
10ppm	10 ± 2	10 ± 4	7 ± 1	-	-

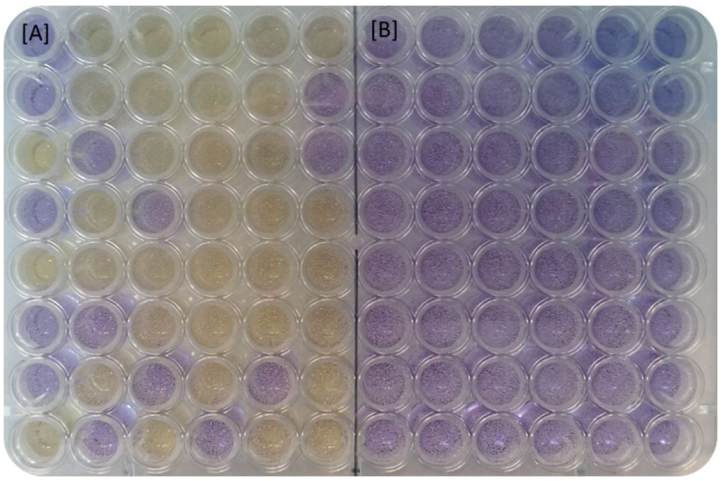

Figure 3.35 An example of a 96-well plate used for carrying out the AMES test. The positive control [A] shows a high level of revertant wells (yellow) while the sterility control [B] can be seen to have no growth in any of the wells (purple). Colour change is brought about by a change in pH due to bacterial growth.

3.3 Immobilisation of graphene-copper composite

Through the use of l-ascorbic acid as both a reducing agent and a stabiliser to promote formation a homogeneous suspension the copper composite was immobilised in two formats; as free-standing films and as a coating on a glass fibre membrane. A copper content of 24-25% was the maximum copper content possible while still achieving a stable dispersion. Higher copper contents were found to result in aggregation and the inability to form a homogenous film or coating.

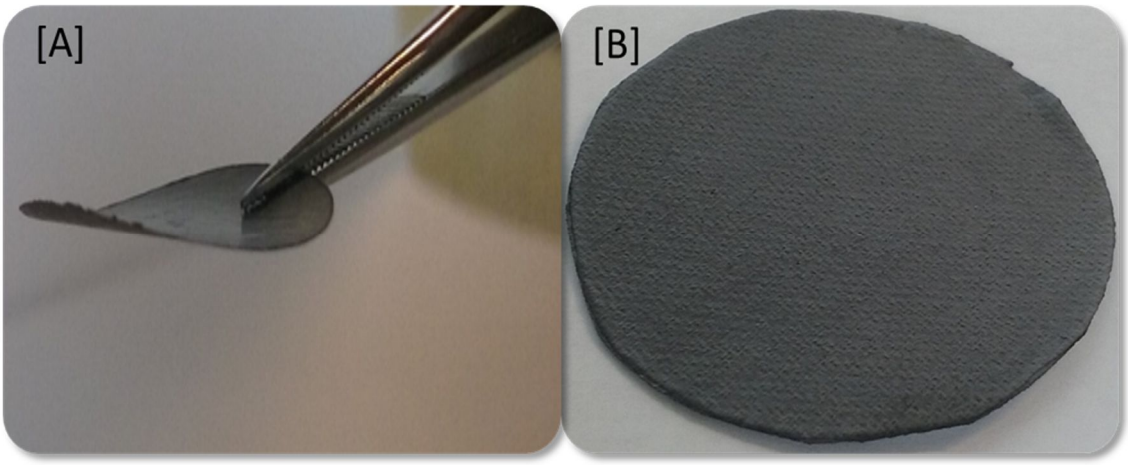

Figure 3.36 The two varieties of immobilisation employed for the graphene composite. [A] As a 15mm diameter free-standing film and [B] as a coating on the surface of a 40mm glass fibre membrane.

The immobilisation of the graphene composite was an essential step in the context of the overall aims of the project. While a graphene-copper composite could be easily formed through the established sodium borohydride ($NaBH_4$) reduction method found within the literature, it was ill suited to any immobilisation due to the high level of aggregation, low suspension dispersity and the inhomogeneity of the copper throughout the material. The issue of aggregation when creating a graphene-copper composite from graphene oxide is two-fold:

1) Folding and aggregation of graphene oxide sheets plays a vital role in their adsorption of metals.

2) Reduction of graphene oxide removes the oxidative groups which provide the water dispersibility and inherent workability of the material.

The folding and aggregation of graphene oxide sheets when mixed with solutions of $CuCl_2$ has been documented and has been attributed as a main factor to its ability to adsorb copper from aqueous solutions (S. Yang et al. 2010). Indeed, the aggregation of GO sheets can be observed visually and occurs almost instantaneously when a solution of $CuCl_2$ is added to GO (Figure 3.37). Unsurprisingly, a GO-$CuCl_2$ mix is an unsuitable mixture for the production of a homogenous immobilised composite. This issue of metal nano-particles aggregation within graphene-metal composites has been raised across other disciplines such as in the application of graphene-silver composites for photo-catalysts for example (Wang et al. 2017).

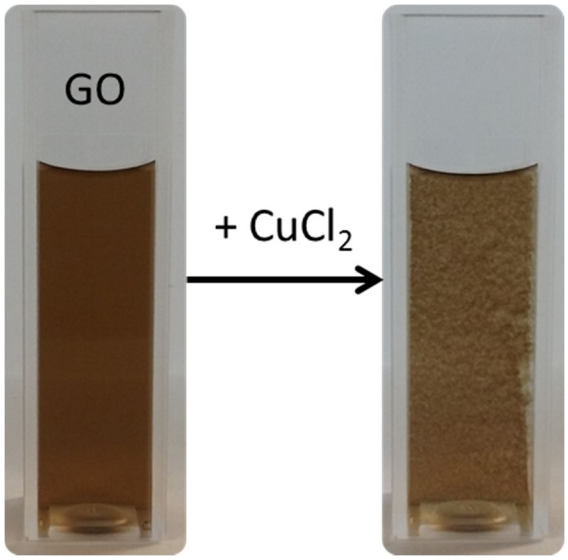

Figure 3.37 Graphene oxide solution before (left) and after (right) the addition of CuCl2. The aggregation of the sheets of graphene oxide occurs instantaneously upon the addition of the metal salt.

While the sodium borohydride ($NaBH_4$) reduction process is effective at reducing the metal salt and forming copper nanoparticles, it also removes a large proportion of the oxidative groups from the graphene oxide which can be seen from both the UV-vis and EDX analyses. In the context of this project this effect can be described as a "double edged sword". The reduction process inherently reduces the homogeneity of the rGO suspension compared to the GO, causing it to be a more difficult suspension to work with due to the aggregates. This issue can be overcome by sonication of rGO suspensions but the dual aggregation of functional group loss and metal particles addition causes this to become more difficult. In the context of water treatment, water dispersible GO suspensions are unsuitable for immobilisation, as after they are returned to an aqueous environment (in the form of a vacuum-filtered film for example), the GO will inherently re-disperse. This re-dispersion of free-formed GO films can be seen

clearly in figure 3.38 where a 10mg vacuum-filtered GO film was added to a solution of de-ionised water. The break-up of the immobilised graphene once it is *in-situ* is obviously undesirable. Conversely, the difficulty in forming a stable film due to the aggregates formed by the sodium borohydride reduced copper-composite also poses an issue in forming a homogenous immobilised graphene-copper composite.

So a workable suspension of a graphene-copper composite which maintains integrity when returned to an aqueous environment was required.

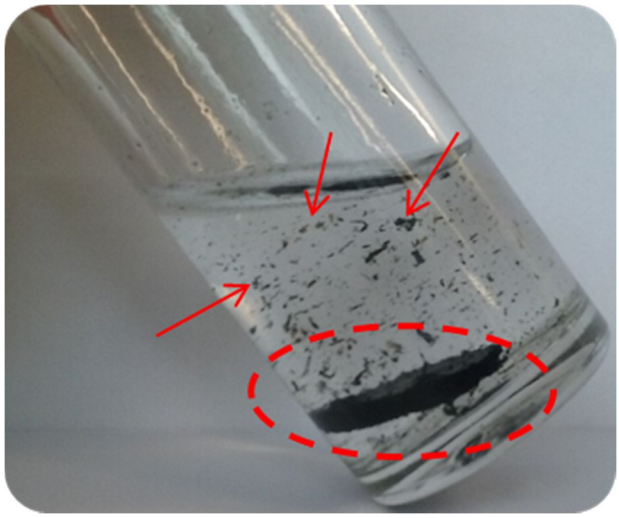

Figure 3.38 10mg vacuum-filtered GO film in de-ionised water after 4 hours. The GO film can be seen to have "puffed up" (red circle) and sections of the film have come away into the solution (red arrows)

As such an alternative method for the production of a stable homogeneous dispersion of Cu-rGO was investigated. A study by (Zhang et al. 2010) showed that GO could be reduced using l-ascorbic acid and that not only would it result in reduction but the homogeneity of the rGO was enhanced by the presence of ascorbic acid acting as a capping agent in the final product. A similar work by (Xiong et al. 2011) showed that $CuCl_2$ could be reduced using l-ascorbic acid to produce stable dispersions of copper nano particles. Combining the principles of both of these studies, a mixture of $CuCl_2$ and GO were sonicated and heated in the presence of l-ascorbic acid. Several formulations with differing concentrations of copper were created with 10, 15, 25 and 40% Cu by weight. As the borohydride reduced composite had been 40% by weight, the objective was to reproduce an immobilisable version. However the concentration of copper present within the composite was shown to play a key role in whether or not the dispersion was homogeneous. All of the as-produced dispersions were capable of film formation except the highest concentration of 40% Cu.

When vacuum-filtering was carried out, the resulting surface was cracked and represented more of a cake than a film (figure 3.39 [B]). In addition, SEM analysis showed large deposits of what are most likely copper particles throughout the material (Figure 3.39[A]).

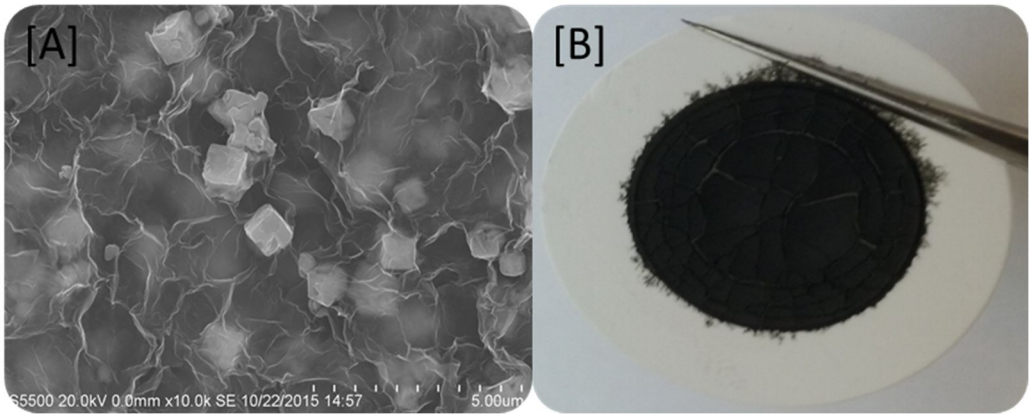

Figure 3.39. [A] SEM micrograph of the 40% copper composite produced via l-ascorbic acid with large chunks of what are most likely copper which can be seen throughout the graphene sheets. [B] An attempt to form a free-standing films with the same dispersion, resulting in a cracked and cake like covering rather than a homogeneous film

As such, the composite containing ~25% copper by weight was chosen as the most ideal to be used for immobilisation. The composite was capable of forming both a stable dispersion which could be vacuum filtered to form a film, or drop cast onto glass fibre membranes to form a coating. The vacuum-filtered films were stable in aqueous solutions for several months.

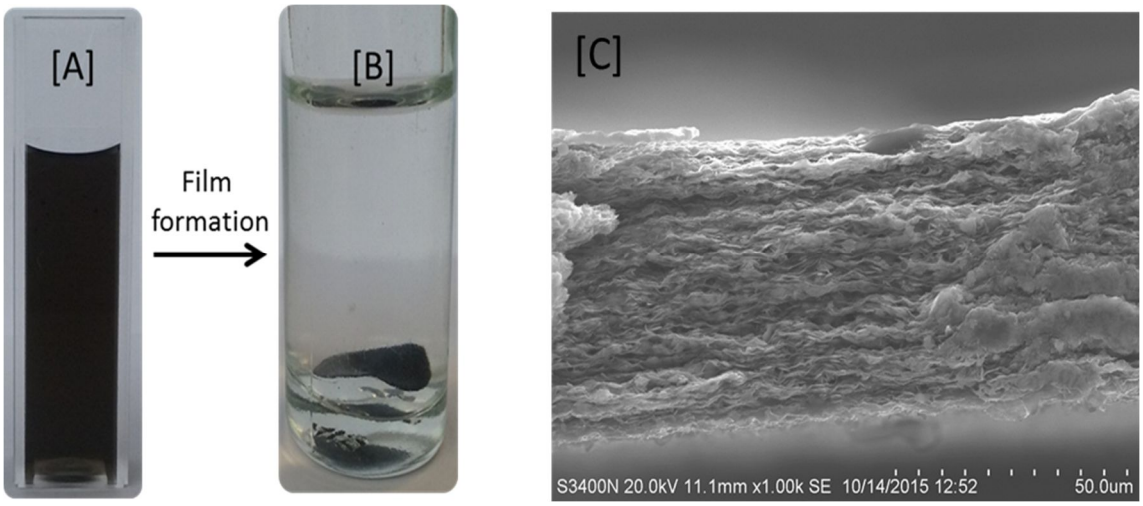

Figure 3.40. [A] The homogeneous dispersion of the 25% Cu content l-ascorbic acid reduced copper composite [B] the 10mg vacuum-filtered film of the same stable in aqueous solution and [C] SEM micrograph of a cross-section of the vacuum-filtered free-standing film with the compacted graphene sheets visible.

3.4 Adsorption Studies

To examine whether or not the composite could be applied as an adsorbent as well as an anti-bacterial agent, the adsorptive potential of each material was examined. This was to ascertain the effect the physical format would have on the effectiveness of each material, as well as examining the effect the formation of a composite would have on graphenes adsorptive capabilities.

The adsorption of methylene blue, famotidine and diclofenac was examined for each of the three materials in three different physical forms. All three materials would be examined in two different formats; as disperse particles in suspension and as vacuum filtered films while the Cu-rGO would also be examined as a coating on a glass fibre membrane. All adsorption studies were carried out in conical flasks and monitored via UV-visible spectroscopy over five days. Removal of diclofenac was found to be minimal while the removal of both methylene blue and famotidine were greater at higher initial concentrations. Free particles were found to be the most effective due to the higher surface area in all cases. The composite coated membranes were found to be more effective than the free-standing films in terms of their adsorptive potential for both famotidine and methylene blue.

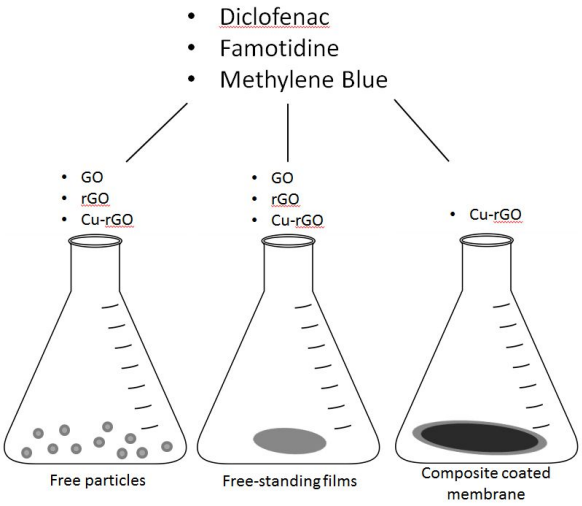

Figure 3.41. Representation of the different three different ways in which the adsorptive potential of the three graphene materials was examined.

3.4.1 Time Dependant adsorption of chemical contaminants by graphene materials

As the free-standing films and the composite coated membranes were created with a view to their incorporation into a water treatment prototype their time-dependant adsorption of each of the materials was also monitored over 8 hours to gauge the speed at which removal would occur.

3.4.1.1 Time-dependant adsorption of methylene blue

The time dependant adsorption of methylene blue was carried out in 10ml at a concentration of 0.0048mg/ml (absorbance = 1) using 10mg free-standing films of each of GO, rGO and Cu-rGO as described in section 2.2.5.1. The time dependant monitoring of the change in concentration showed that within the 8 hour period GO removed 80% (0.038mg), rGO 74.5% (0.035mg) and Cu-rGO 70% (0.033mg). GO showed a greater overall rate of removal compared to the other two materials with Cu-rGO showing the lowest rate and overall removal within the eight hours monitored. However due to the low concentration and volume employed the relative difference in total adsorption of methylene blue is marginal. Monitoring of the change over time has shown that a significant decrease occurs within the initial time period following addition of the films to the solution. The GO rGO and Cu-rGO showed initial removals of 25, 20 and 17% respectively within the first hour.

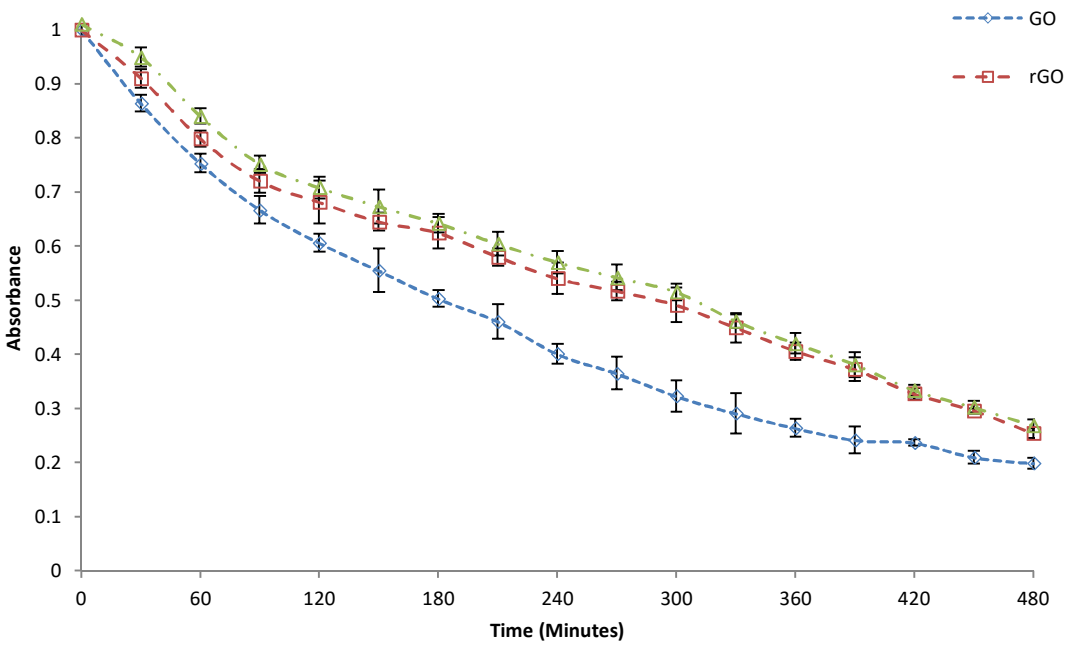

Figure 3.42. Time dependant adsorption of methylene blue by 10mg free-standing films of GO, rGO and Cu-rGO.

As the size and shape of the composite coated membrane was larger than that of the free-standing films, time-dependant monitoring of methylene blue adsorption was carried out in 100ml at the same concentration. A total reduction of 67% (0.321mg) was observed within the eight hours. The trend of a large decrease following the initial exposure was continued with a 17% decrease (0.08mg) occurring within the first hour alone. The overall removal far exceeded that of the free-standing films (an order of magnitude in the difference) which can be attributed to a combination of the larger available surface area present and the greater availability of the methylene blue due to the greater volume.

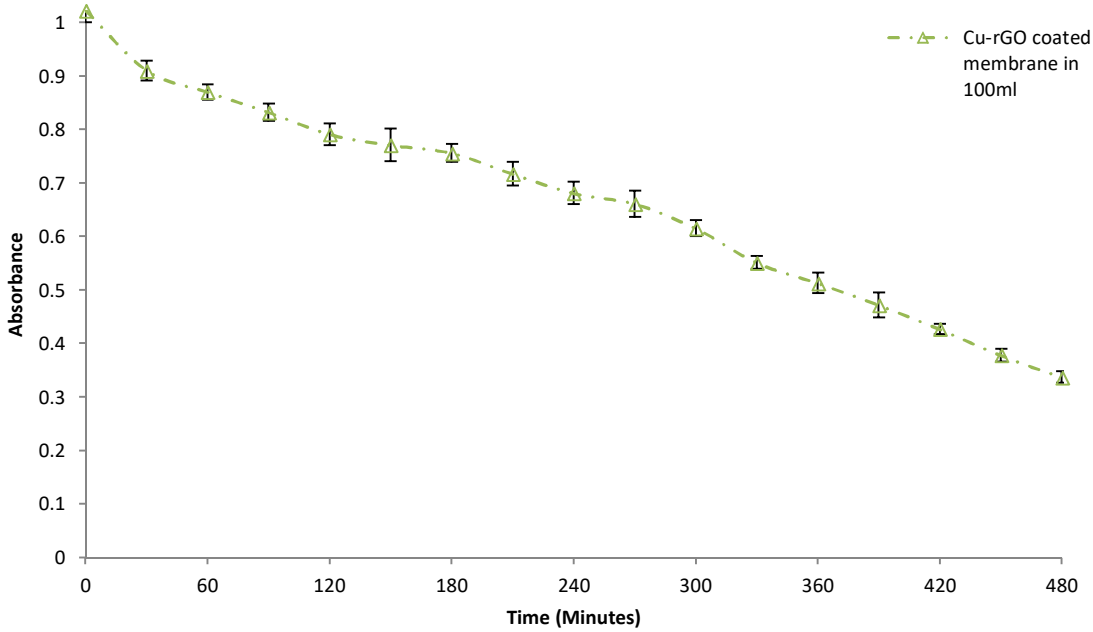

Figure 3.43. Time dependant adsorption of methylene blue by the graphene-copper composite coated Cu-rGO membrane.

3.4.1.2 Time dependant adsorption of famotidine

The time dependant adsorption of famotidine was carried out in 10ml at a concentration of 0.032mg/ml (absorbance = 1) using 10mg free-standing films of each of GO, rGO and Cu-rGO as described in section 2.2.5.1. The time dependant monitoring of the change in concentration showed that within the 8 hour period GO removed 81% (0.26mg), rGO 78.7% (0.25mg) and Cu-rGO 64% (0.2mg). GO once again showed a greater rate of removal compared to the other two materials in a similar trend to that observed with the methylene blue adsorption. The GO rGO and Cu-rGO showed initial removals of 29, 28 and 24% respectively within the first hour showing again that a high percentage of the overall adsorption will occur within the early stages following initial exposure of the materials.

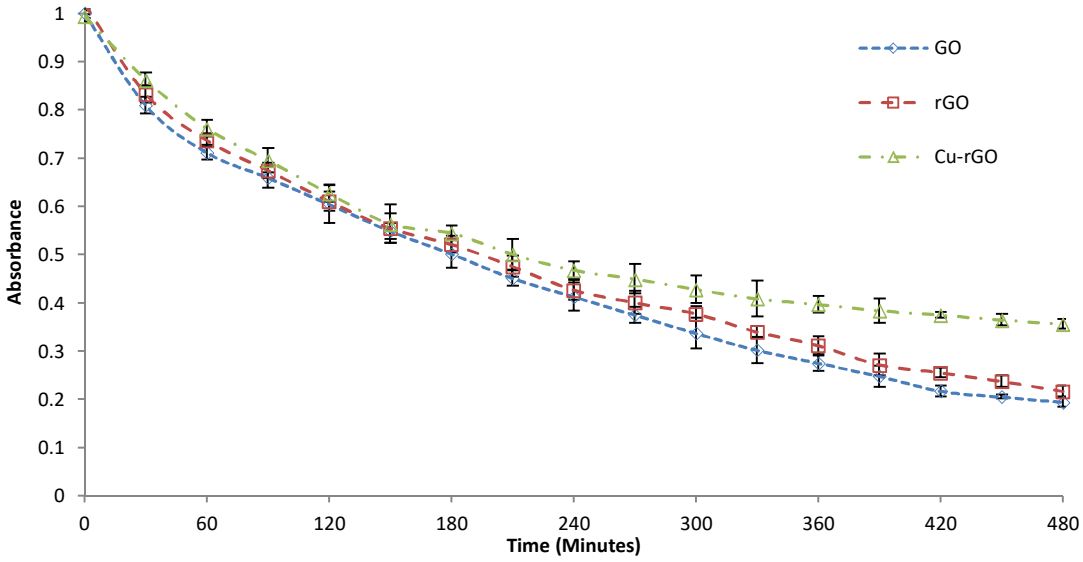

Figure 3.44. Time dependant adsorption of famotidine by 10mg free-standing films of GO, rGO and Cu-rGO

As with the methylene blue analysis the Cu-rGO coated membrane investigation was carried out in 100ml at the same concentration of famotidine as above. A total reduction of 26% (0.8mg) was observed within the eight hours. Almost 10% (0.31mg) of the total concentration was removed within the first hour equally almost 40% of the total removal. The total removal once again exceeded that of the free-standing films though by approximately four times (~0.2 compared to 0.8) and not an order of magnitude as had been seen with the methylene blue.

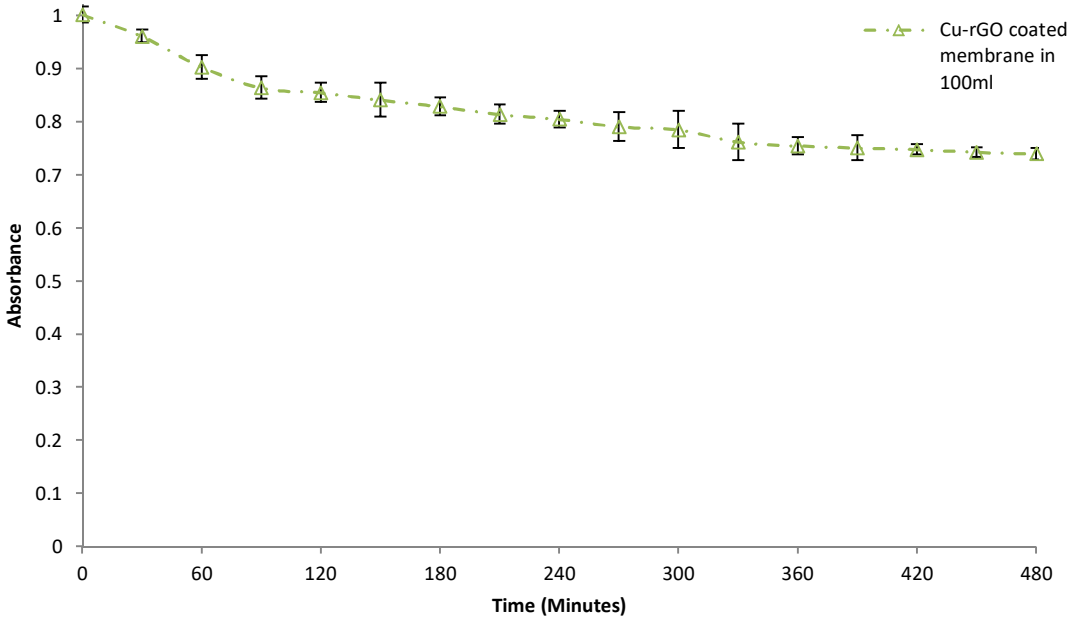

Figure 3.45. Time dependant adsorption of famotidine by 10mg graphene-copper composite coated glass fibre membranes

3.4.1.3 Time dependant adsorption of Diclofenac

There was no significant removal of diclofenac by any of the materials in any format; this can be attributed to the use of de-ionised water as a matrix and its relevant pH. This is no surprise as diclofenac has been shown to adsorb at lower pH's (~pH 3) and the pH of the de-ionised water was at ~7. An investigation carried out with a larger volume to examine whether or not the removal was not observed yielded a similar result. As such the adsorption of diclofenac was not pursued further.

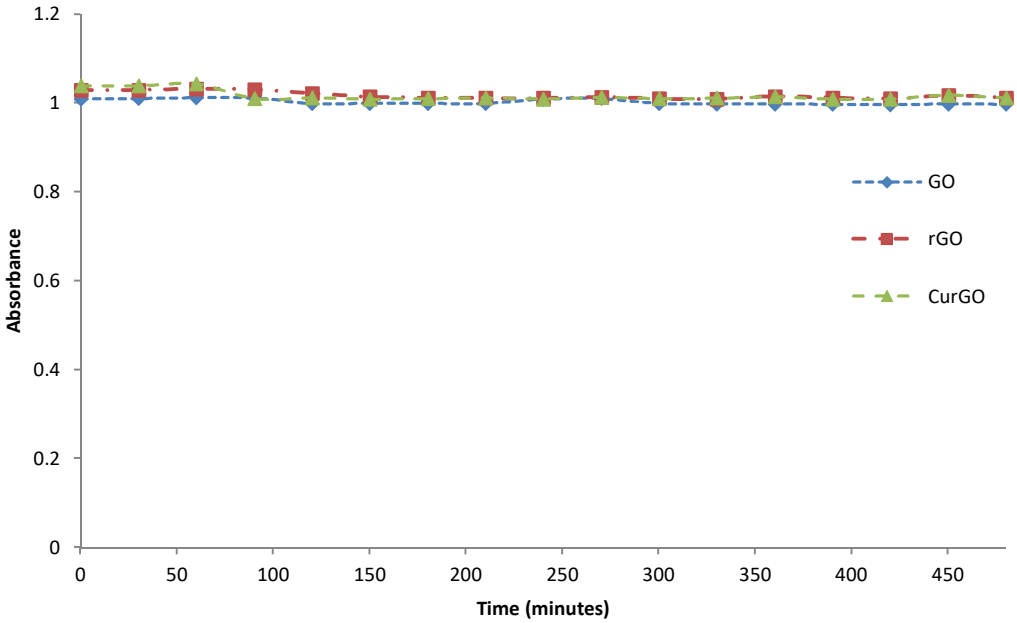

Figure 3.46. Time-dependant removal of Diclofenac by 10mg free-standing films of the graphene-copper composite

3.4.2 Adsorption of famotidine by graphene materials

For the adsorption of famotidine, the rGO performed the best when free-particles were used and had ~5% higher removal across the concentration range compared to GO. The Cu-rGO showed a lower adsorptive potential compared to the other two materials at, which can be attributed to the proportion of copper present which would offer no advantage in terms of removal (figure 3.47.) Most notable in the adsorption of the three materials in film format is the significant decrease in capacity. Compared to the free particles which had capacity in the 200-300mg/g range, the films had significantly reduced adsorption with GO showing the highest at 113mg/g at the highest initial concentration of 3.2mg/ml. Another interesting observation is the much higher performance of the GO compared to the other two materials (Figure 3.48). This is most likely due to the instability of the GO film and its tendency toward expansion in with water. This is due to the presence of the high number of oxidative groups on the surface of the GO compared to the rGO and the composite. As such the GO film was seen

to “puff up” when put into solution. This most likely resulted in a higher overall surface area and as such an adsorption capacity. This however significantly compromises the structural stability of the GO, making it unsuitable as the film will fray and particles will enter the solution which in a water treatment scenario would require further removal at a later stage.

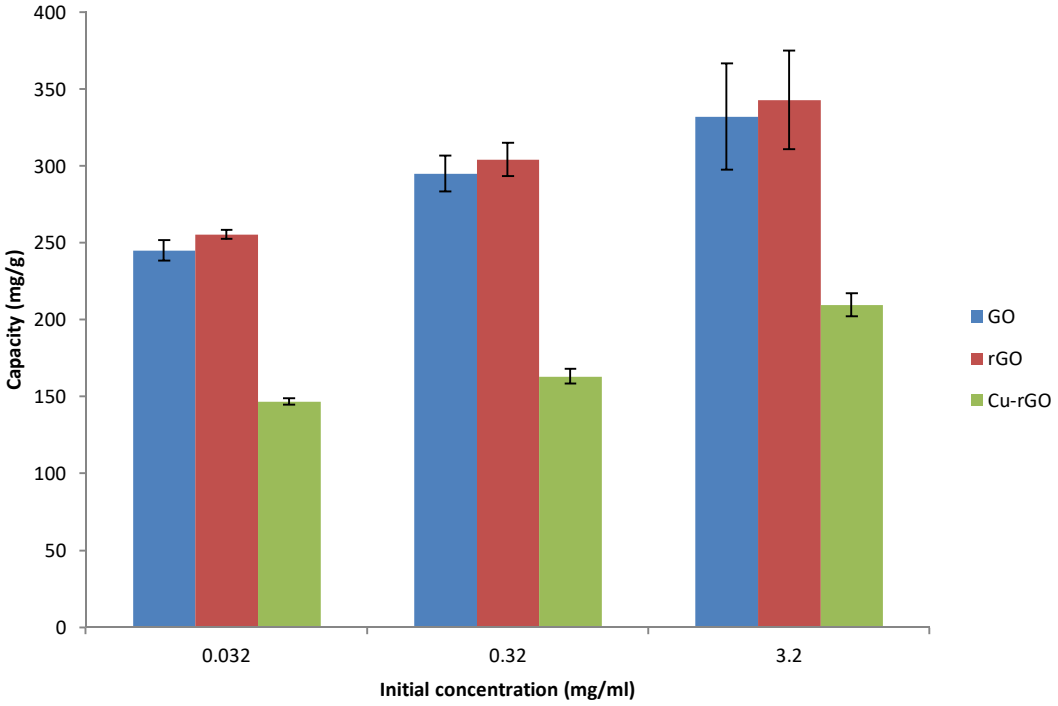

Figure 3.47. Adsorption of famotidine by 10mg of graphene materials dispersed as free particles in de-ionised water at 0.032, 0.32 and 3.2mg/ml in 100ml

The impregnated membranes, having a diameter of 40mm compared to the 15mm of the films, had a much higher adsorption capacity. Though this was lower than the free particles, due to the attachment of the particles to the surface, the removal of famotidine was still significant at 183.62mg/g at a concentration of 3.2mg/ml compared to that of the films (Figure 3.49).

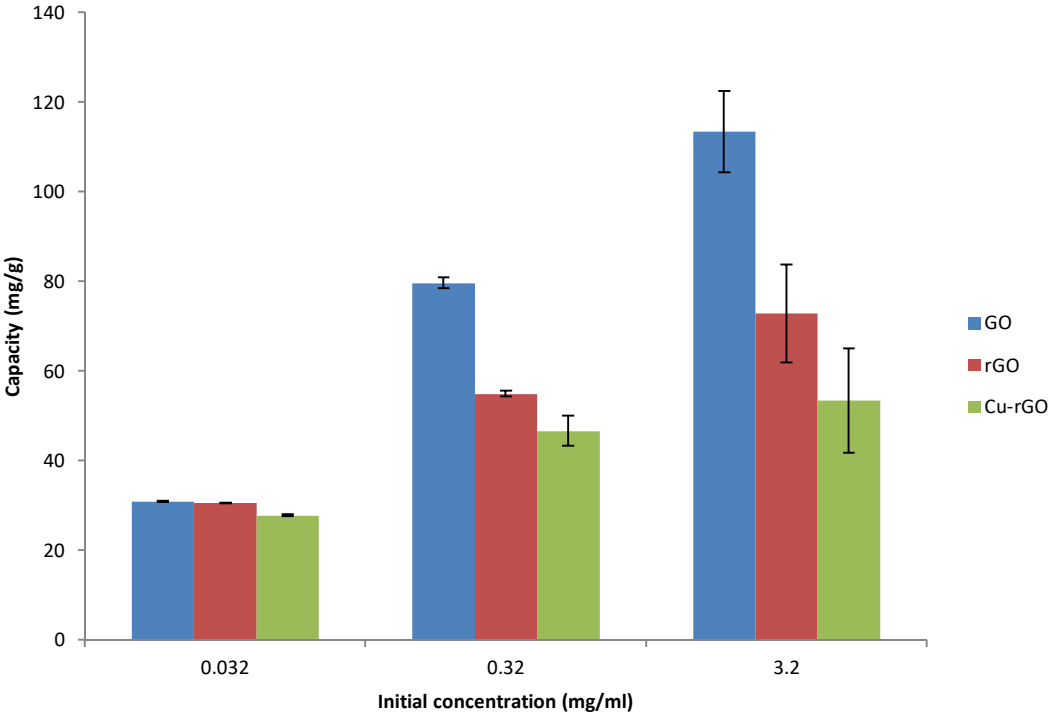

Figure 3.48. Adsorption of famotidine by 10mg free-standing films of graphene materials in 100ml de-ionised water at 0.032 0.32 and 3.2mg/ml.

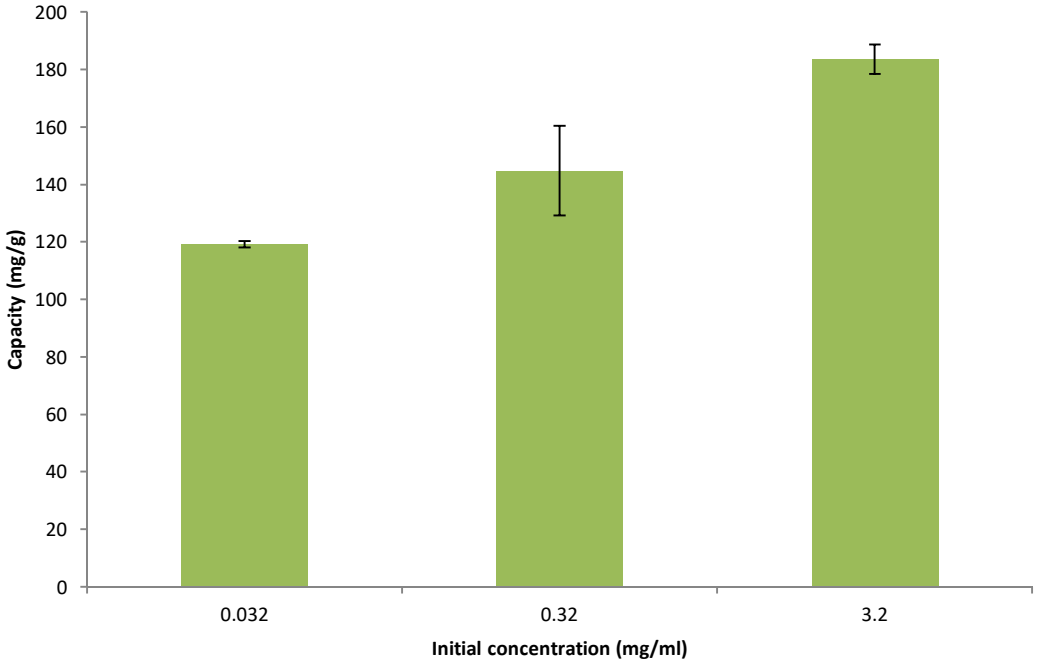

Figure 3.49. Adsorption of famotidine by glass fibre membranes coated with 10mg of the graphene-copper composite in 100ml de-ionised water at 0.032 0.32 and 3.2mg/ml.

3.4.3 Adsorption of methylene blue by graphene materials

Compared to the adsorption of famotidine, the potential for methylene blue removal is far greater. The free particles of GO, rGO and Cu-rGO showed loading capacities of 739,661 and 605mg/g respectively at the highest concentration; 0.48mg/ml. The GO showed the highest adsorptive potential of the three in this format (figure 3.50). Though the Cu-rGO showed the lowest adsorption, again most likely due to the presence of the copper, the relative ratio compared to the loss of adsorptive capacity was lower than that seen with the famotidine with almost total removal at the lowest concentration and >80% at the intermediate concentration of 0.048mg/ml. This may indicate that graphene materials have a higher tendancy toward removal of dyes such as methylene blue.

The adsorption of methylene blue by the various films showed a similar trend to that of the famotidine. The overall adsorption in all cases was reduced compared to the free particles, again due to the loss of relative surface area during the formation of the films. The GO once again showed the highest potential for removal at 194mg/g at the highest concentration (Figure 3.51). This is, again, likely to be the result of the water solubility and the expansion of the GO in solution resulting the in structural instability and an increase in available surface

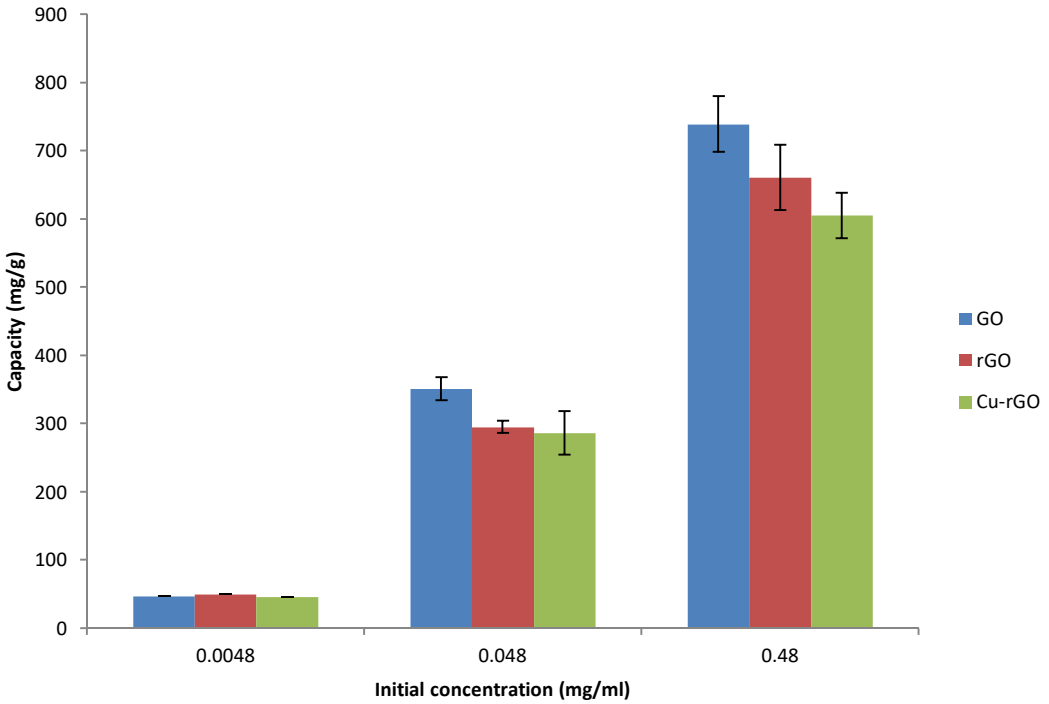

Figure 3.50. Adsorption of methylene blue by 10mg of graphene materials dispersed as free particles in de-ionised water at 0.0048, 0.048 and 0.48mg/ml

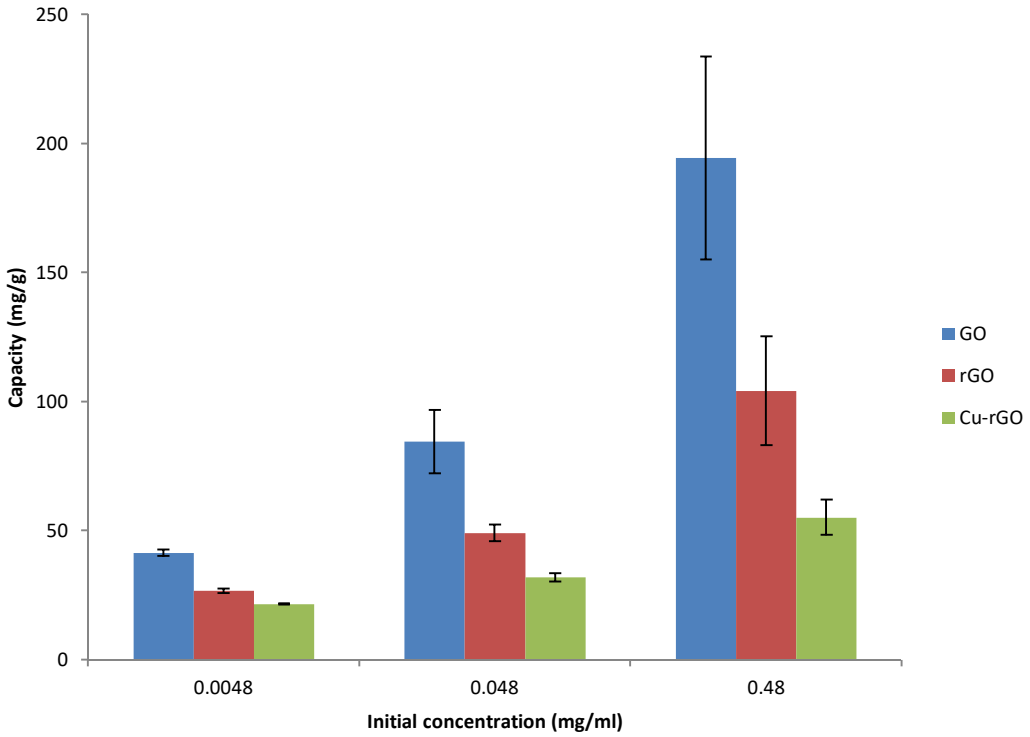

Figure 3.51. Adsorption of methylene blue by 10mg of graphene materials as free-standing films in 100ml de-ionised water at 0.0048, 0.048 and 0.48mg/ml

Finally, the methylene blue removal by the Cu-rGO impregnated membranes showed a marked increase compared to those of the films with the films at the higest concentration of methylene blue showing a loading capacity of 482mg/g (Figure 3.52). This is significantly higher than the 55mg/g shown by the Cu-rGO film at the same concentration (Figure 3.51). This highlights the importance of the format in which the material is used. While the composite films may be robust and usable there is a resultant loss of adsorptive potential due to the loss in surface area. The impregnated membranes offer a higher adsorptive potential than the films while placing the Cu-rGO onto a robust substrate. The larger diameter and relative porosity of the membrane allows for higher contact of the Cu-rGO present with the solution and a higher overall adsorptive capacity.

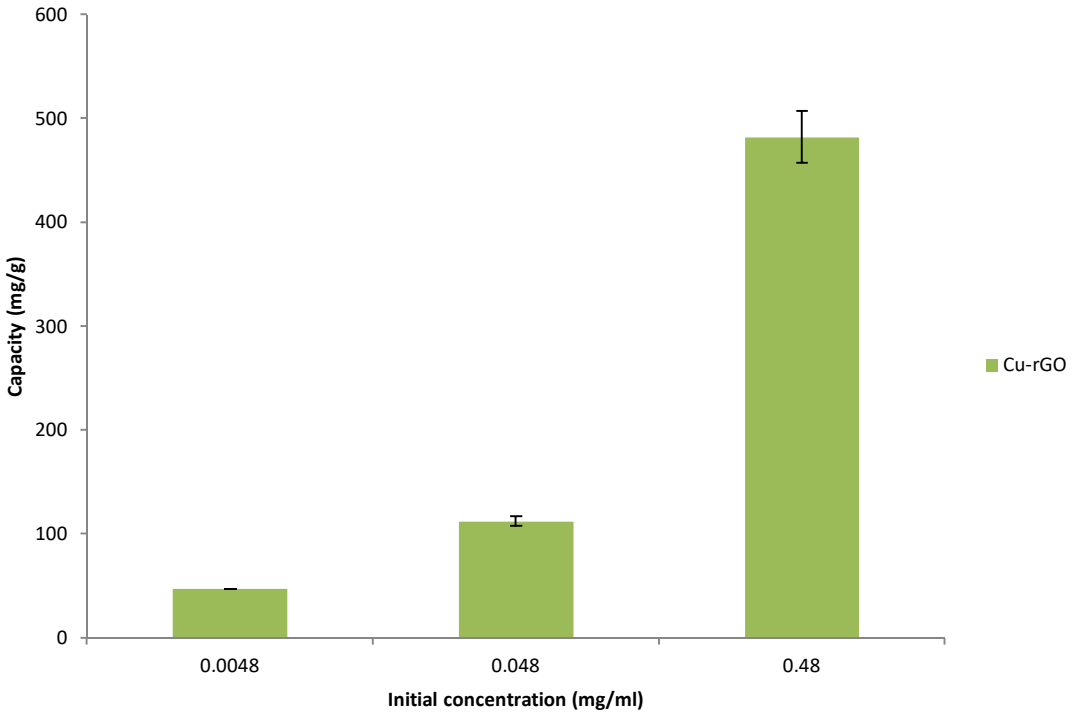

Figure 3.52. Adsorption of methylene blue by glass fibre membranes coated with 10mg of the graphene-copper composite in 100ml de-ionised water at 0.0048, 0.048 and 0.48mg/ml.

3.5 Prototype studies

The final portion of the study was dedicated to the application of the immobilised composite in a water treatment prototype. Initially, the antibacterial efficacy of the immobilised composite was examined via an agar slurry method to establish its effectiveness as an antibacterial surface. The prototypes would take the form of flow-through units, throughout which the immobilised composite would be applied to support structures separating individual chambers. Water would be pumped upward through the unit so as to facilitate contact with the immobilised composite between each chamber. Initial tests were carried out using sterile saline solution inoculated with *E. coli*, however later (and larger volume) tests would be carried out using tap water. Exposure time and flow rates used would be based upon the observed anti-bacterial efficacy of the immobilised composite.

Initially the immobilised composite would be incorporated into the prototype as the free standing films; however refinements would show the composite coated membranes as a more effective method of immobilisation. This improved effectiveness would be attributed to the nature of membranes and their ability to retain the organisms on their surface as well as the greater surface area provided for the interaction of the composite. A total of three different designs were trialled, with the final prototype incorporating nine composite coated membranes. Both the removal of bacteria and their viability in contact with the composite coated membrane was examined along with the capability of the prototype to remove Cryptosporidium. The adsorptive potential of the prototype for both methylene blue and famotidine was also examined during flow-through testing. Volumes of up to 10L were used in the final prototype to examine its structural robustness before the beginning of long-term testing.

Long-term testing was carried out using a tap-water fed reservoir to better accommodate the high volume needed. Throughout long-term testing the prototype would be challenged at a maximum flow-rate in order to examine its physical robustness when operating at maximum capacity. Throughout the long-term testing the flow would be spiked with bacteria and the retention of the organism tested for. The leaching of copper from the prototype would also be analysed as, once again, the ultimate objective it the production of drinking water to which strict limits on the concentration of copper are applied.

3.5.1 Antibacterial analysis of immobilised graphene-copper composite surfaces

Both the free-standing graphene-composite films and the composite coated membranes would be employed in the construction of a prototype. As the composite would be fixed in both cases, it was necessary to evaluate their antibacterial performance when in this state. In order to examine the antibacterial efficacy of the fixed graphene-copper composite as a surface, an agar slurry method, used to ascertain the antibacterial efficacy of surfaces was employed (ASTM standard E2180-07 2012). Both *E. coli* and B. subtilis were found to be completely inhibited after 40 minutes of contact with the Cu-rGO surface. Neither organism was shown to be effected when a similar analysis was carried out using films formed of either GO or rGO. Similarly, a control membrane with no graphene coating was shown to have no impact on the bacterial population when used.

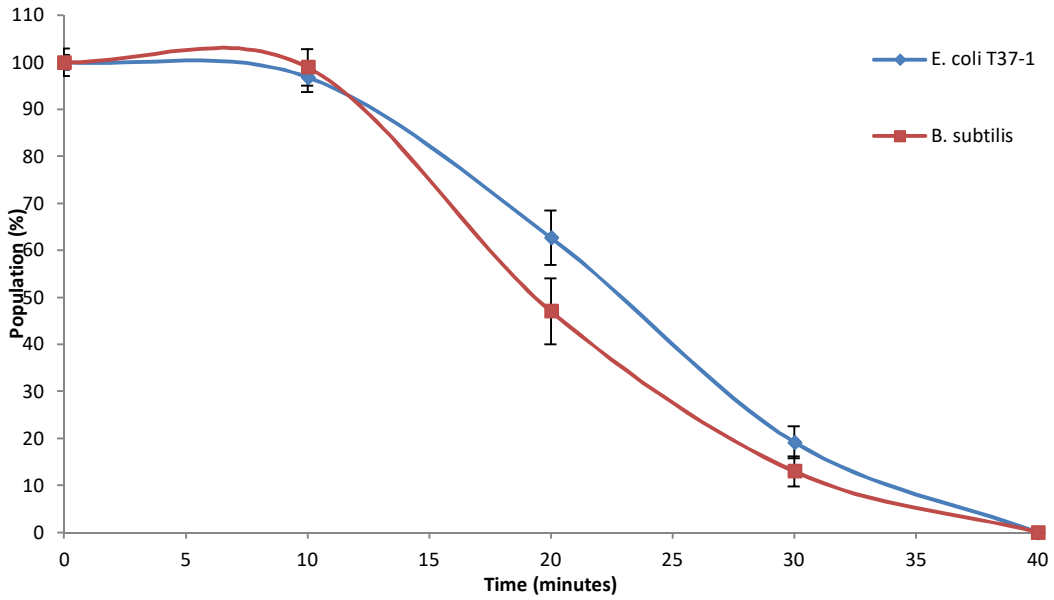

Figure 3.53. Antibacterial activity of the composite films as surfaces against *E. coli* (blue) and *B. subtilis* (red)

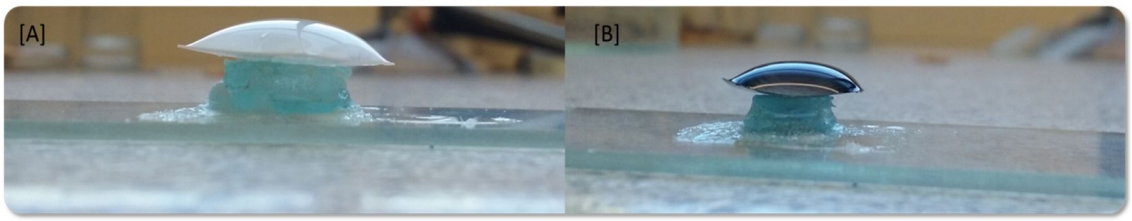

Figure 3.54. The antibacterial surface analysis carried out using the agar slurry method. 1cm^2 squares of the surface on interest were placed onto a custom built stage which had been sterilised by autoclaving. [A] The control membrane with no composite and [B] the free-standing film covered with agar slurry inoculated with *E. coli.*

3.5.2 Prototype construction

All prototypes followed a similar methodology of construction; the unit would be attached to a peristaltic pump via the inlet at the base of the prototype and water flow would be propelled upward. The unit, depending on variety, would consist of several chambers separated by a support structure which would house either the free-sanding composite film or the composite coated glass fibre membrane. Clear commercially available silicone sealant was sufficient for all structural bonding and used throughout, for internal bonding of films or membranes an inert dental glue which would not leach was found to be the most appropriate bonding agent.

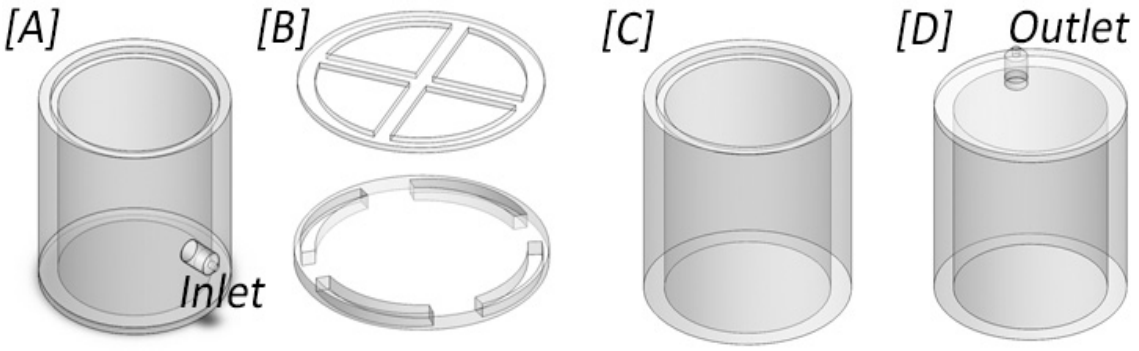

Figure 3.55 The four basic structural sections within each prototype [A] The bottom-most section consisting of the inlet and a rebated inner wall to incorporate a support structure [B] The two varieties of support structure for either the free standing films or the composite coated membranes [C] the central sections with rebated inner wall for inserting support structure and [D] the top section with outlet.

3.5.3 Prototype #1: Incorporating four freestanding composite films

The first prototype incorporated four 10mg free-standing graphene-copper composite films, with three films situated at each of the centre of the support structures, surrounded by four vents (Figure 3.56). Initial antibacterial tests were performed using 700ml saline solution inoculated with *E. coli* at 10^2CFU/ml at a flow rate of 22ml/min equalling one cycle of the total volume every 30 minutes. A thirty minute cycle was chosen as the most apparopriate for initial tests as, based on the observed antibacterial efficacy of the immobilised composite, it would be sufficient time for contact with the free-standing films. The unit showed negligible reduction in bacterial population with only a 23% reduction after six hours and a 41% reduction after 24 hours and an 84% loss of bacterial viability only after 48 hours (Table 3.5). A control unit, which consisted of all structural components of the prototype with the absence of the graphene-copper composite films, was also assembled to determine whether or not the unit itself would affect the bacteria.

Flow-through tests with the control unit showed that no significant impact on the bacterial population occurred. Due to the low reduction in the bacterial population over time the use of a composite coated glass fibre membrane was chosen for incorporation into the second prototype.

Table 3.5. Bacterial population over timer during flow-through tests of both the control unit and the graphene-copper composite film incorporation prototype.

Time (Minutes)	Control Unit (No graphene) CFU/ml	Unit (four composite films) CFU/ml
0	130 ± 15	131 ± 22
30 (ramp-up)	129 ± 13	124 ± 17
60	130 ± 12	118 ± 18
120	130 ± 20	115 ± 12
180	133 ± 19	110 ± 14
240	128 ± 15	107 ± 9
300	129 ± 17	101 ± 16
360	132 ± 19	100 ± 7
24 hours	134 ± 25	74 ± 8
48 hours	122 ± 13	22 ± 3

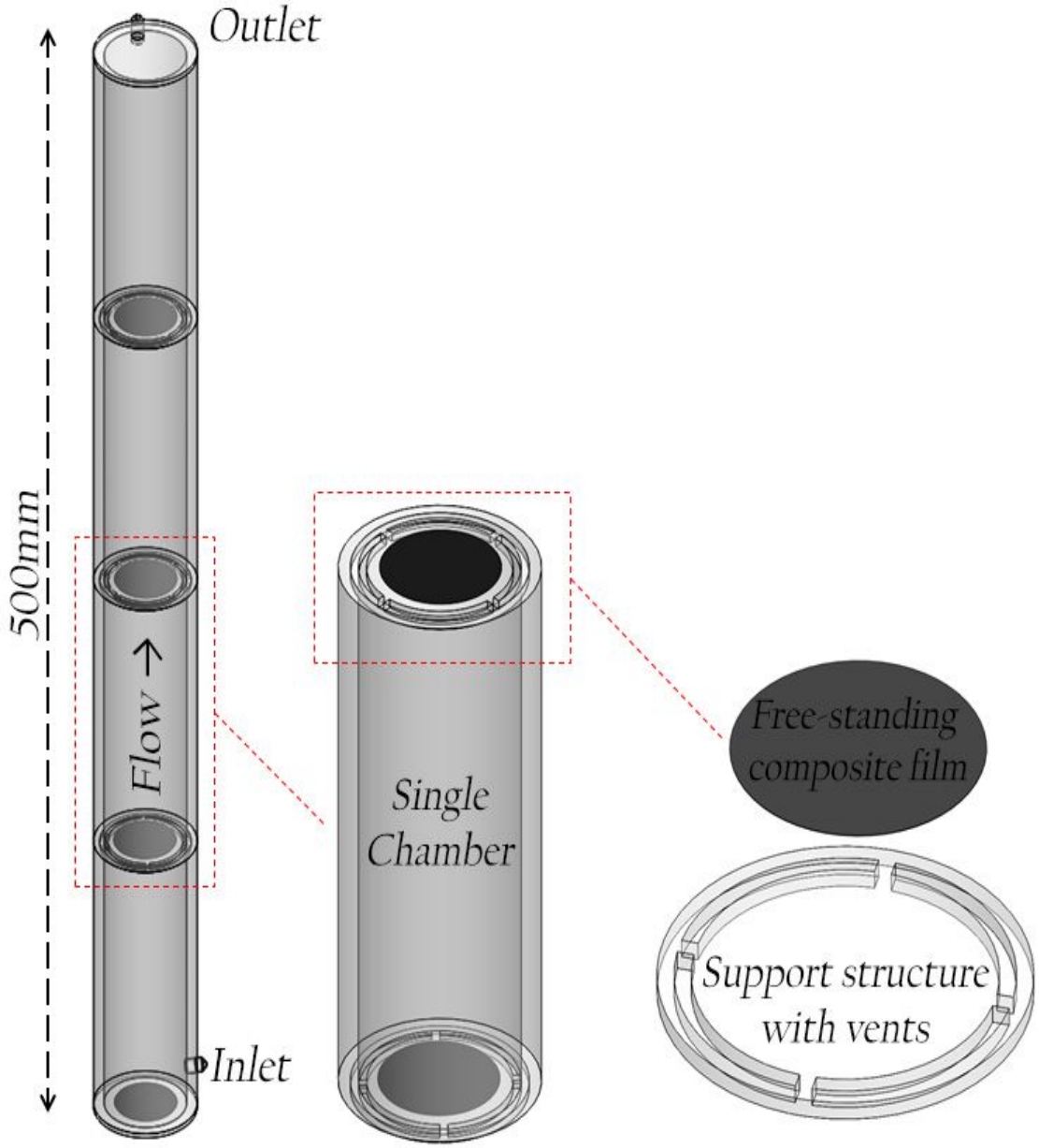

Figure 3.56. The first constructed prorotype which incorporated four free-standing graphene-copper composite films

3.5.4 Prototype #2: Incorporating three composite coated glass fibre membranes

Following the low reduction in the bacterial numbers observed in the initial prototype test, a second prototype, which incorporated three composite coated glass fibre membranes, was constructed and tested using the same parameters (Figure 3.57). One side of the glass fibre membrane was coated with 10mg of the graphene-copper composite by drop casting. Units were constructed with the coated side both face up and face down to investigate the impact the direct exposure of the graphene coating would have on the performance of the prototype. With composite coating oriented upward (not in the direct path of the flow) there was a 79% reduction within 6 hours (Table 3.6). With the coated side oriented into the direction of the flow the reduction was more significant with a >99% reduction in the bacterial population occurring within 6 hours.

With the improved performance of the composite coated membranes compared to the free-standing films a further refinement of the design was carried out which incorporated 9 composite coated membranes within a unit of the same dimensions.

Table 3.6. Bacterial population over time during flow testing of the second prototype, incorporating 3 composite coated glass fibre membranes.

Time (Minutes)	Unit (Coating face-up) CFU/ml	Unit (Coating face-down) CFU/ml
0	139 ± 19	125 ± 14
30	96 ± 7	72 ± 10
60	81 ± 11	59 ± 9
120	60 ± 6	51 ± 7
180	56 ± 3	15 ± 4
240	48 ± 7	12 ± 2
300	34 ± 8	4 ± 1
360	30 ± 4	3 ± 1
24 hours	0	0
48 hours	0	0

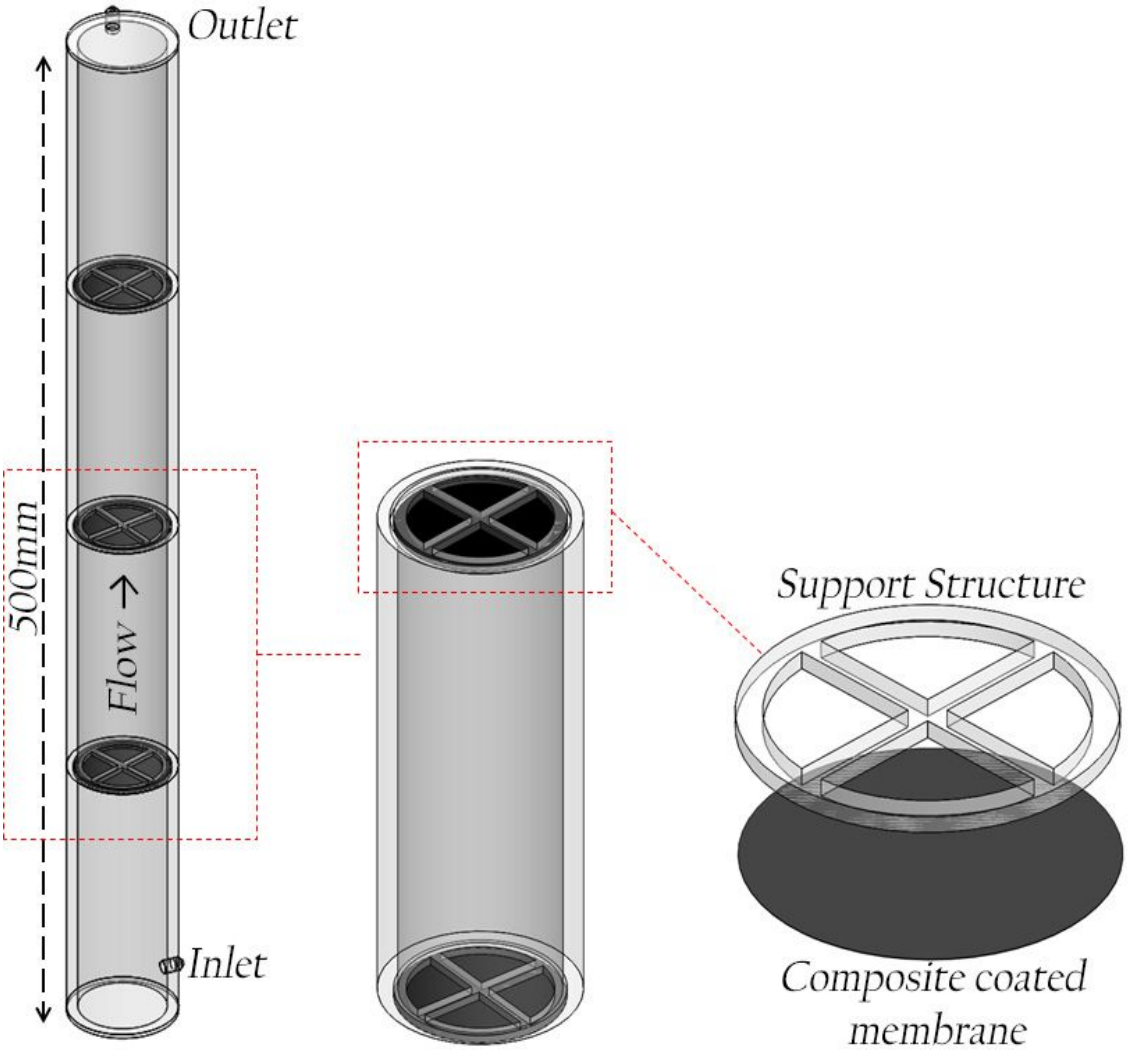

Figure 3.57. A representation of the second iteration of the prototype which incorporated 3 graphene-copper composite coated membranes in a flow through system.

3.5.5 Prototype #3: Final prototype, incorporating nine composite coated glass fibre membranes

In order to promote a more expedient effect on the bacteria present in solution a third prototype was constructed which incorporated nine composite coated glass fibre membranes with the coated side oriented into the flow to maximise exposure. An additional support structure was also incorporated so as to support both sides of the membrane. Preliminary larger volume tests had shown that membrane tearing could occur over longer periods and that a more robust support structure would prevent this occurrence. The removal of both microorganisms and chemical contaminants was examined for using prototype #3.

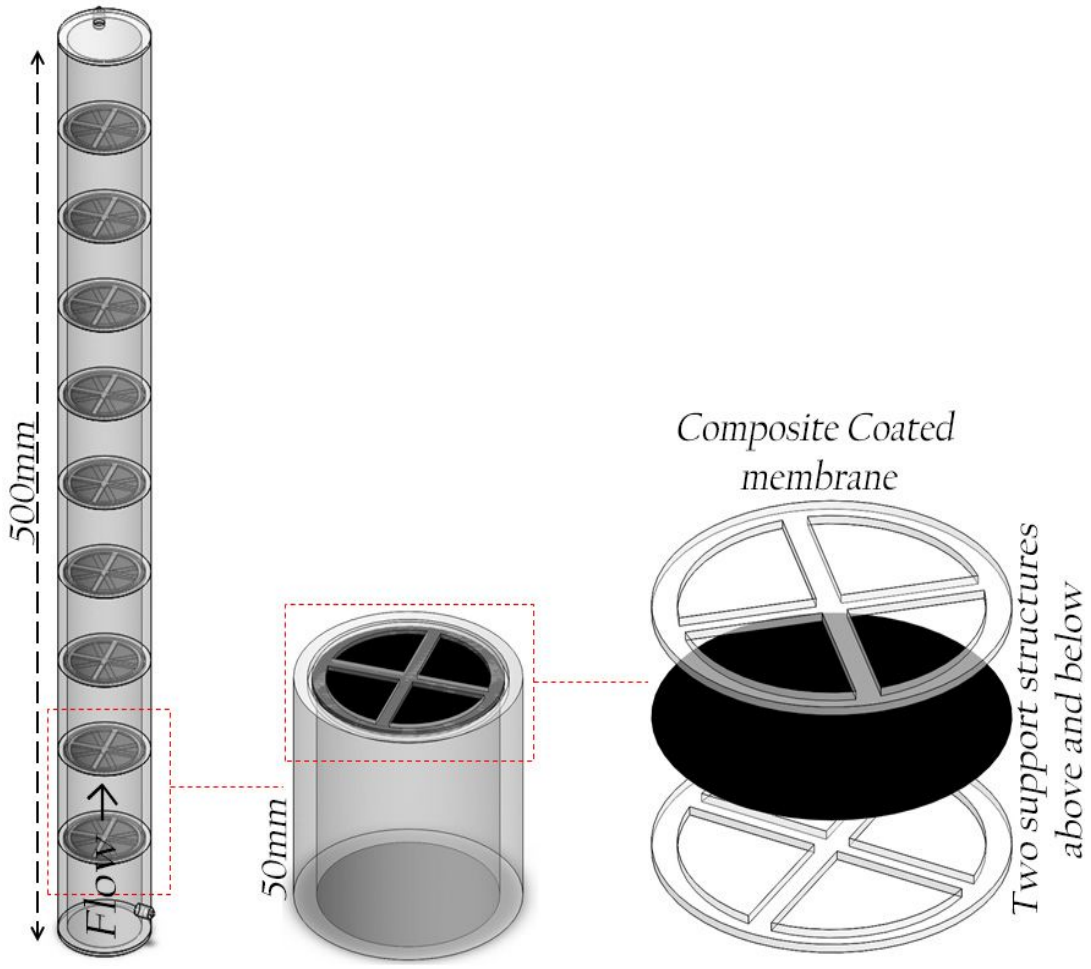

Figure 3.58. A representation of the third and final prototype design employed. Incorporating 10 chambers and nine graphene-copper composite coated membranes

3.5.6 Bacterial removal by final prototype

The third and final prototype (figure 3.58) was tested with a variety of volumes; 700ml, 5L and 10L of saline solution inoculated, as before, with 10^2CFU/ml of *E. coli*. Tests up to 10L showed that the prototype was capable of removing up to >99% of the bacterial population within 30 minutes or one cycle of the total volume and that no bacteria were present in the permeate throughout the flow-through of the 10L.

A control unit, incorporating nine glass fibre membranes uncoated was also tested for comparison. The control unit showed a similar result to that of the composite coated membranes with >99% of the bacteria removed. As such, the viability of the bacteria exposed to the surface of both coated and uncoated membranes was examined.

Table 3.7 Bacterial removal by the third and final prototype, incorporating nine composite coated glass fibre membranes as well as the control unit

Time (Minutes)	700ml	5L	10L	Control (10L)
0	127 ± 15	121 ± 12	129 ± 21	135 ± 17
30	0	0	0	0
60	0	0	0	0

The viability of the organisms retained on each membrane was examined using both R2A and nutrient broth. The results of the viability test in each broth can be seen in table 3.8, control membranes showed growth on all membranes indicating that while bacteria were retained, they were still cultural in minimal and rich growth media. The composite coated membranes however showed no growth in either media, R2A or nutrient broth, except on the first membrane. Indicating that only bacteria present on the surface of first membrane were still viable follow flow-through testing.

Table 3.8. Viability of bacteria attached to both control membranes (with no composite) and the composite impregnated membranes following unit testing. Where ✓ indicates growth and X indicates no growth.

#Membranes	Control Membranes		Composite membranes	
	R2A	NB	R2A	NB
1	✓	✓	✓	✓
2	✓	✓	X	X
3	✓	✓	X	X
4	✓	✓	X	X
5	✓	✓	X	X
6	✓	✓	X	X
7	✓	✓	X	X
8	✓	✓	X	X
9	✓	✓	X	X

3.5.7 Removal of cryptosporidium by prototype

To investigate the response of the prototype to cryptosporidium, the unit was challenged with 10 L of sterile saline (0.85 %) containing 10 oocysts/L. The 10 L volume was then passed through the filtramax filtration unit.

Following microscopic analysis by City Analysts Ltd. no oocysts were detected.

3.5.8 Chemical contaminant removal by prototype

Removal of both methylene blue and famotidine were examined for during two flow-through tests of the final prototype. 700ml of each material were passed through individual units (as described in sections 2.2.6.3) and the change in concentration monitored by UV-vis over eight hours and again at twenty-four hours. During the methylene blue analysis (figure 3.59), a removal of 74% (2.48mg) was found to occur within eight hours, with almost 20% (0.67mg) occurring within the first hour and a total of 95% (3.19mg) reduction in concentration after 24 hours. For the famotidine (figure 3.60), a removal of 35% (7.84mg) was found to occur within the eight hour period, with 13% (2.86mg) occurring within the first hour and a final removal of 46% (10.2mg) over the total twenty-four hour period.

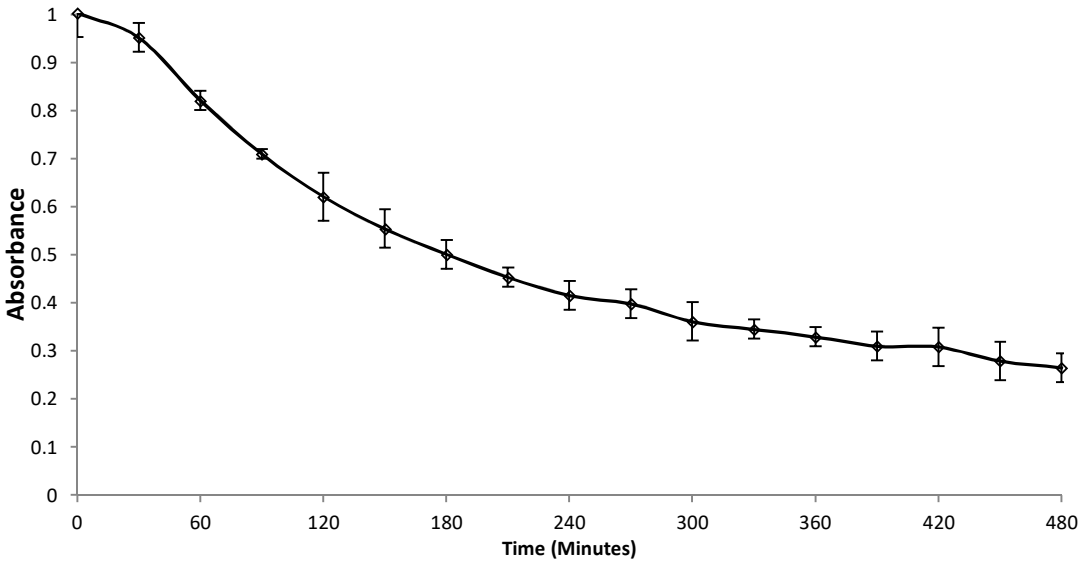

Figure 3.59. Methylene Blue adsorption over time carried out using prototype #3.

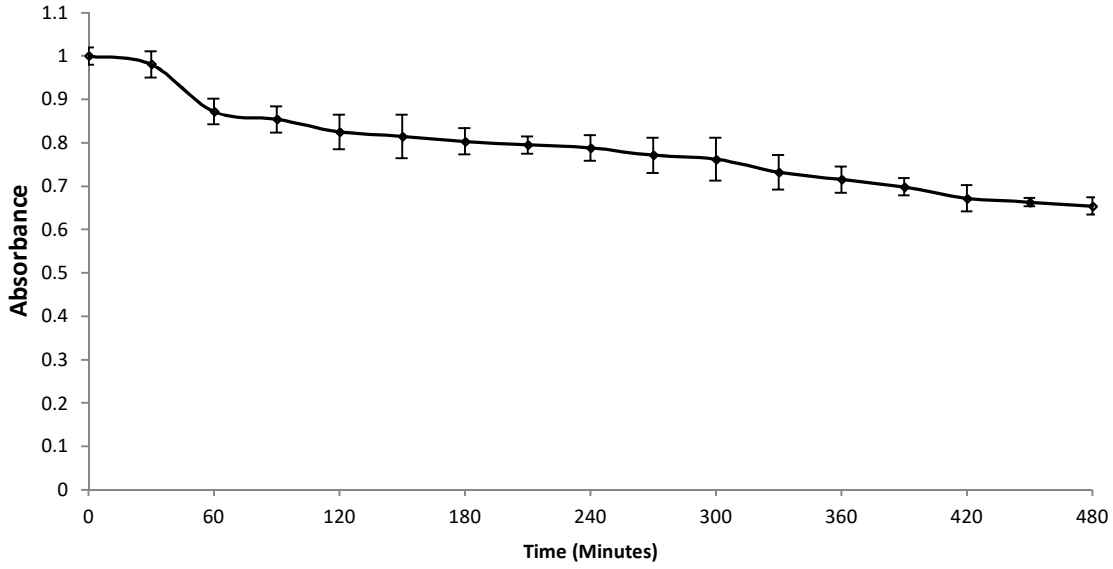

Figure 3.60. Famotidine adsorption over time carried out using prototype #3.

3.5.9 Long-term testing of prototype

The long-term testing of the prototype was carried out using up to 100L of tap water as described in section 2.2.6.5, the primary purpose of which was to examine the physical robustness of the unit when performing at maximum flow-rate over an extended period. In addition to visual observation of the physical state of the prototype, samples were taken for analysis via flame atomic absorption spectroscopy (AAS) to examine the copper concentration in the permeate and spiking with *E. coli* was carried out every ten litres.

Visual observations showed that the prototype was capable of performing well up to ~50L. From ~40 to 50L there was a build-up of bubbles within the first chamber of the unit. This build-up was seen to increase the pressure on the first membrane with it bowing upward. At 50L the first membrane was seen to burst and the build-up began in the following chamber and membrane #2 burst after an additional 10L. Membrane #3 & 4 were seen to burst after another 10L with membranes 5 and 7 following much more quickly within the following 5L. After approximately 80L all 9 membranes had burst, with all ruptures occurring at the centre of the membrane at the cross-section of the two support structures.

Figure 3.61. The build-up of bubbles seen during the long-term test of prototype #3

Bacterial removal during long-term testing

Bacterial removal during long-term testing was monitored every 10L following spiking with *E. coli*. Table 3.9 below shows the results of 1ml samples added to nutrient broth to examine for bacterial growth as described in section 2.2.6.3.5. There was no visible bacterial growth in any of the nutrient broth samples up to 50L. A single sample taken following spiking at 60L showed positive growth and each following sample, from 70 to 100L, was found to be positive. These positive results can be attributed to the physical damage occurring to the membranes during operation and the breakthrough of bacteria into the permeate.

Table 3.9. Results of the bacterial removal analysis from the long-term testing. Three 1ml samples were taken and added to nutrient broth. – indicates no growth within the broth and + indicates positive growth.

	10L	20L	30L	40L	50L	60L	70L	80L	90L	100L
Growth (+ / -)	-	-	-	-	-	-	+	+	+	+
	-	-	-	-	-	+	+	+	+	+
	-	-	-	-	-	-	+	+	+	+

Copper leachate analysis

As water for human consumption would be the ideal output of the prototype, the leaching of copper into the permeate from the unit is of concern. As such, samples were taken every 10L during the long-term testing to analyse for the presence of copper. Samples were analysed via AAS against a set of copper standards and the concentration of copper present calculated. Figure 3.62 shows the copper concentration over time in the permeate. The initial sample taken after the start-up phase of the prototype (i.e. immediately after circulating a full internal volume) showed the highest concentration of copper, 1.3mg/L, with subsequent samples showing concentrations of 0.3mg/L on average and a dip to 0.18mg/L in the final 3 samples taken at 80, 90 and 100L respectively. The results would indicate that a low level of copper leaching occurs during prototype operation but that the initial start-up phase dislodges or washes any unbound composite present on the surface of the membranes.

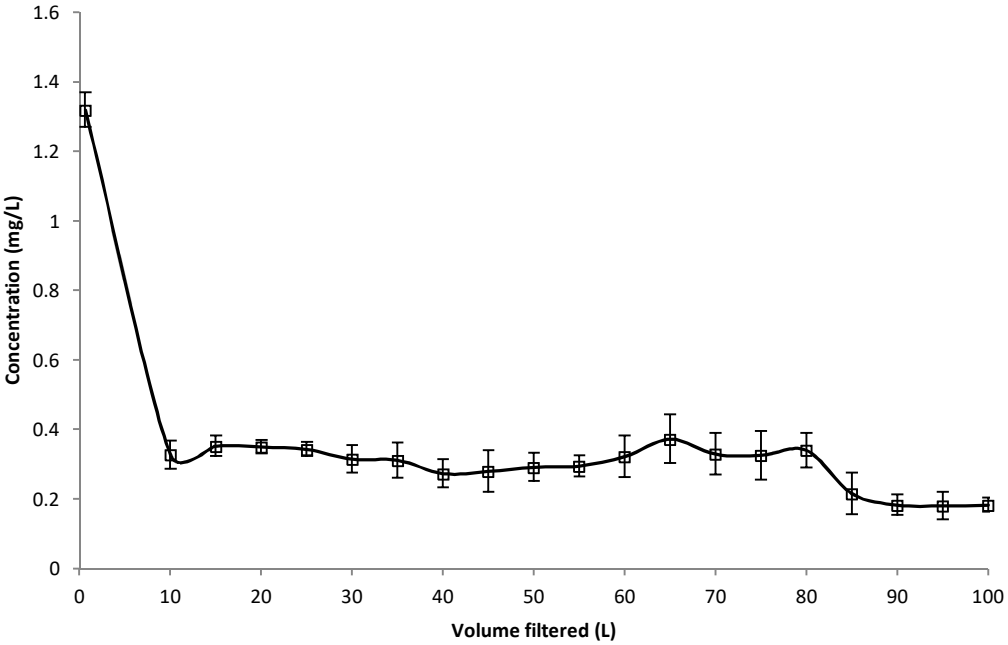

Figure 3.62 Copper concentration in permeate from the prototype during long-term testing.

4. Discussion

4.1 Production and characterisation of materials

4.1.1 Production of graphene materials

For the synthesis of graphene materials, the well-established chemical exfoliation known as the *hummer's method* was used (Hummers *et al.* 1958) along with the addition of microwave expansion of graphite flakes (Liu *et al.* 2013). The chemical exfoliation of graphite is one of the four primary methods for graphene production and is the most commonly applied due to its expedience. Unlike the more complex methods such as chemical vapour deposition (CVD), chemical exfoliation produces graphene of variable sheet size, thickness and levels of oxidation. In situations where pristine graphene is not required, the chemical exfoliation method is ideal as it can be carried out via a relatively simple (albeit time-consuming) bench-top synthesis. As graphene oxide (GO) is the base material produced via chemical exfoliation, its use as an antibacterial agent is an attractive concept due to the ease of production. GO can subsequently be reduced to produce reduced graphene oxide (rGO) or conjugated with any number of other materials to produce composites. The high numbers of oxidative groups present on the surface of graphene oxide also represent potential adsorption sites for the removal of chemical contaminants when applying the material to a water-treatment scenario as is the focus in this project (Zhao *et al.* 2011), (Maliyekkal *et al.* 2013), (Raj Pant et al. 2013). However graphene oxide may not fully represent the characteristics of pristine graphene in terms of its biological interaction. As such, the production of reduced graphene oxide (rGO) was carried out via chemical reduction (Chua *et al.* 2013). The rGO would act as a material more akin to that of pristine graphene so as to better understand its potential interactions with bacteria. In addition to the production of GO and rGO, a graphene-copper composite (Cu-rGO) was also produced to examine it for the potential synergistic effect that copper and graphene may have together in terms of their anti-bacterial potential. While there have been several studies examining the effect of graphene composited with other heavy metals for anti-bacterial applications, the effect of a graphene-copper composite has not been investigated. While the higher anti-bacterial potential of silver nano-particles is reflected in the number of studies examining graphene-silver composites, there have been concerns as to the potential impact of silver on human health and the environment; (Marambio-Jones *et al.* 2010), (Wijnhoven *et al.* 2009). A single study has examined the effect of rGO coupled with both poly-l-lysine and copper nanoparticles for anti-bacterial applications and previous studies have examined the synergistic effect between copper and other carbon-nanomaterials like carbon nanotubes (Ouyang *et al.* 2013), (Mohan *et al.* 2011).

While the production of graphene-copper composites has been reported, their application as anti-bacterial agents has not been investigated (Xu *et al.* 2009), (Chen *et al.* 2011), (M. Wang

et al. 2013). As such the production and use of a graphene-copper composite as an anti-bacterial agent for water treatment is an attractive concept, both due to its novelty and the reduced potential for cytotoxicity compared to silver (Gaetke *et al.* 2003). In addition, a composite material of graphene and copper may offer an advantage in a water treatment application due to its potential dual functionality. The graphene, as a carbonaceous material, would act as an adsorbent for the removal of chemical contaminants and the copper would perform as a biocide. It is important to consider the potential variance in the production of graphene materials via chemical exfoliation. While the Hummers' method may provide the basis, there exists innumerable adaptations and small alterations to the process; thermal exfoliation, microwave exfoliation, different reducing agents, the use of centrifugation or dialysis for washing and the use of different source material. Source material in particular represents a fundamental issue; the sourcing of high quality graphite for graphene production has been highlighted as different sources produce graphene of varying qualities. All these variations potentially influence the biological interactions of graphene materials and it is difficult to countenance the comparability of different studies in any meaningful manner. There exists a lack of standardisation to chemically exfoliated production of graphene materials: this issue underpins the variability in the results of antibacterial assays which have been observed in different studies. This variability also highlights the need for appropriate characterisation in each case so as to develop an understanding of the physio-chemical properties of the graphene produced using a given set of parameters.

4.1.2 Material characterisation via UV-visible spectroscopy

The use of UV-visible spectroscopy for the characterisation of graphene oxide and reduced graphene oxide is well established and is used as an initial method to confirm the production of each material (Krishnamoorthy *et al.* 2012), (Han *et al.* 2013), (Khanra *et al.* 2012), (Luo *et al.* 2009). Graphene oxide possesses a characteristic absorption peak at 230nm corresponding to the π-π* transition in graphene and shows a shoulder at around 300nm which corresponds to the n-π* transition of the C=O bonds present in the oxidative groups on the surface (Lai *et al.* 2012), (Russel *et al.* 1993). Upon reduction of GO to rGO, there is a characteristic red shift in the absorption spectrum with the peak at 230nm moving to ~260nm coinciding with the removal of the oxidative groups present on the surface and a restoration of the sp^2 hybridisation and electronic structure across the sheet (Eda *et al.* 2010). The GO shows the characteristic peak at 230nm with the small yet clear shoulder appearing at the 300nm region. rGO has a similar peak to that of GO albeit at 260nm, indicating the successful reduction of GO to rGO. Cu-rGO however shows a very a distinct spectrum compared to both GO and rGO. While there exists a peak at 260nm, indicative of the rGO present within the composite, the

peak is much broader and extends across to the 400nm region. A previous study by (Christian *et al.* 2010) investigated the formation of copper nanoparticles (CuNPs) via a reduction process similar to that employed here. They stated that their copper metal nanoparticles displayed a distinct peak at 260nm, which in the case of the composite material produced here would overlap with the rGO peak, however they showed that the copper metal readily oxidised in air to Cu_2O. The oxidation of the copper nanoparticles present in the composite is likely and may explain the broadening of the peak at 260nm. An investigation by (Tian *et al.* 2012) into the formation of a graphene-Cu_2O-Cu-CuO composite which contained a mix of copper nanorods in different oxidative states showed a similar result in terms of its UV-vis analysis with a broad peak occuring across the 260 to 400nm region and a study by (Salavati-Niasari *et al.* 2009) showed that Cu_2O nano-particles possess a peak in the 360nm region. It is most likely that the composite produced in this manner contains copper nano-particles reduced from $CuCl_2$ which would have readily oxidised during processing and may contain a mix of copper in different oxidative states. While the use of UV-vis is a quick and easy method to glean an understanding of the constituents of graphene and graphene composites further characterisation via a suite of techniques is required to develop a full knowledge of its elemental composition

4.1.3 Thermogravimetric Analysis

Thermogravimetric analysis is another commonly applied technique for the characterisation of graphene and graphene-composite materials (Zhu *et al.* 2013), (Tai *et al.* 2012), (Vijay Kumar *et al.* 2013), (de Faria *et al.* 2013). The material is heated gradually and the change in mass measured continually, the greater the thermal stability of a material the lower the rate of loss. As graphene oxide contains numerous oxidative functional groups across its surface it inherently has a lower thermal stability than reduced graphene oxide, the removal of these functional groups from the GO during the reduction process results in a partial realignment of the planar carbon surface and a greater degree of thermal and electrical conductivity of the material. This gives reduced graphene oxide a greater thermal capacitance and thus better stability at higher temperatures. The oxidative functional groups on the surface of GO, which will compose a certain percentage of its total mass, are more easily broken down and will be removed at lower temperatures adding to the loss. As such, the use of TGA is an excellent choice to examine whether or not reduction has occurred. In addition, metals such as copper are highly thermally stable and as such a composite of reduced graphene oxide and copper should display a higher thermal stability than rGO alone. Graphene oxide shows a typical thermal decomposition curve with a sudden loss of weight at ~200^{o}C, this can be attributed to the breakdown of the bonds present in the numerous carboxy, epoxyl and hydroxyl functional groups on the surface. The difference between the GO and both the rGO and Cu-rGO is clear,

with the latter two materials having a much higher level of thermal stability. The steep drop at 200^{o}C present in the GO is absent in the rGO which is suggestive of successful reduction and removal of the oxidative groups. The Cu-rGO shows a higher level of thermal stability again compared to the rGO. As copper is an excellent conductor in its own right, the combination of rGO and copper particles appear to have a greater capacitance for thermal distribution affording the material a greater level of thermal stability. This higher level of thermal stability is indicative of the successful creation of the composite. The TGA analysis showed that GO had a typical decomposition as seen in the literature and that it was produced successfully, the increased stability in the rGO sample shows that the successful reduction from GO was achieved. The higher level again observed in the Cu-rGO is indicative of the presence of copper and that the materials in combination have a greater stability than rGO alone. While both the UV-vis analysis and TGA give an indication as to the change in composition following reduction and composite formation, more accurate techniques are required to confirm the change in elemental composition of each of the materials.

4.1.4 Fourier transform infrared spectroscopy

Fourier-transform infrared spectroscopy (FTIR) was used to examine the chemical bonds present within each of the materials and to examine the change in those bonds following the reduction of GO to rGO and after the production of the composite. As FTIR is routinely applied in the characterisation of GO and rGO there exists a wealth of literature for comparison. The GO showed a typical FTIR spectrum with a characteristically large peak at 3204cm^{-1} which is attributed to the O-H deformation in the C-OH groups along with the typical peaks corresponding to C=O, C-O and C-OH bonds (Wang *et al.* (2010), (Stankovich *et al.* 2006), (Fuente *et al.* 2003), (Szab *et al.* 2006), (Mei *et al.* 2011). The absence of these peaks in the rGO spectrum along with the low transmittance associated with rGO was indicative of the reduction of GO to rGO with only small peaks visible at 1570 and 1032cm^{-1} corresponding to the –C=C bonding within the partially restored graphene structure (Kellici *et al.* 2014). The copper composite showed a similar spectrum to that of the rGO with the peaks associated with the oxidative groups present within GO absent. The three spectra are in fact a fingerprint of those shown by (Chen et al. 2011) following their production of a graphene-copper-nanoparticle compoiste. As the copper is not bound chemically, but rather adsorbed by the graphene, there is no chemical bonding which is detectable via FTIR. As such the use of a more quantifiable method to evaluate the elemental composition, and the quantity of copper present, in the composite was required.

4.1.5 Material characterisation via energy dispersive X-ray spectroscopy (EDX)

Energy dispersive X-ray spectroscopy was used to confirm the reduction of GO to rGO via the carbon oxygen ration and to ascertain the level of copper attachment during composite production. EDX analysis is commonly used for the examination of metal nanoparticle decorated graphene as it provides quantitative data on the percentage of metal present and can even be used to examine graphene composited with several metals (Zhang *et al.* 2013) (Bora *et al.* 2013) (Raj Pant *et al.* 2013) (Ocsoy *et al.* 2013). The reduction of GO to rGO can be confirmed as the oxygen percentage present in GO is ~50% average becoming ~29% in the rGO. (Bora *et al.* 2013) reported the successful reduction of GO to rGO when a change of 45 to 15% oxygen content was observed. The chemical reduction of GO via borohydride, while effective; will not result in a total removal of all oxygen containing funciotnal groups present. The average copper content of the composite material was found to be 40% albeit with a large degree of variance across the surface. Five sample sites were examined and varied from 28 to 49% copper content, this variance in the attachment of copper to the surface of the graphene is also illustrated from the SEM analysis as areas of concentrated copper attachment across the sheets can be seen as well as barren areas with little to no copper coverage. To further examine the effect the reduction process had on the form of copper present in the Cu-rGO, the $CuCl_2$ which was used to produce the composite was also subjected to the same reduction process in the absence of graphene. As suggested by (Christian *et al.* 2010), the reduction of metal salts to their base metal form can produce metal nanoparticles. However, they suggested that copper nanoparticles readily oxidise in air. The EDX analysis showed clearly that oxidation of the copper present has occurred and the entirety of the chlorine has been removed following washing. An average oxygen content of 24% was found which is suggestive of a mix of copper in its various oxidative forms, though this cannot be asserted definitively as the analysis does not proved any data on the volume or ratio of the various forms of copper present. This oxygen contained within the oxidised copper nano particles may also explain as to why the carbon oxygen ratio within the composite is not as reduced as is seen the rGO. The graphene may have experienced a comparable reduction during composite production, though it becomes less clear due to the presence of the oxidised copper within the structure of the material. The observed UV-vis spectrum also supports this, showing a broad peak from 260 to 400nm and does bear resemblance to a Cu_2O-graphene composite produced in a study (Tian *et al.* 2012). Though there are visible differences which may be attributed to different levels of oxidation of copper in the two studies or that the copper nanorods used by (Tian *et al.* 2012) altered the absorption spectrum of their composite. However, based off these two methods it is not possible to assert what level of oxidation has occurred with the CuNPs.

The characterisation of graphene and graphene-composite materials can be carried out via a number of methods, depending on the intended application and characteristics of interest. Microscopic methods such as scanning electron microscopy (SEM), transmission electron microscopy (TEM) and atomic force microscopy (AFM) are primarily used to gauge the physical morphology of graphene-based materials and can give a qualitative indication as to size and shape of suspended particles and to highlight the differing profiles of composite materials (Krishnamoorthy *et al.* 2012) (Some *et al.* 2012) (Liu *et al.* 2012) (Lim *et al.* 2012). Particle size distribution analysis methods can be used to glean a more quantitative profile of the size distribution of particles in solution and supplements the more visual representation of the material acquired from microscopic methods (Gurunathan *et al.* 2013). Morphological profiling is particularly important prior to any biological assay as the shape and size of particles can have a profound effect on their cellular interaction. The effect of size and shape of metal nano-particles on their anti-bacterial efficacy and cytotoxicity is well documented and can drastically alter how effective a material is, due mainly to the surface-to-volume ratio (Martínez-Castañón *et al.* 2008) (Pal *et al.* 2007) (Simon-Deckers *et al.* 2009) (Wang *et al.* 2008), Zhao *et al.* (2012). Similarly the size and length of carbon nanotubes has also been shown to have an impact on their anti-bacterial efficacy, this is particularly relevant when considering the potential of graphene as an anti-bacterial agent as the materials are very similar in terms of their chemical structure (Yang *et al.* 2010) (Kang *et al.* 2008). The morphology of nano materials will also have an impact on their surface-to-volume ratio and their available surface area which can have a significant impact upon their adsorptive capabilities.

4.1.6 Material characterisation via scanning electron microscopy (SEM)

Scanning electron microscopy was used to evaluate the differing physical characteristics of each material; GO, rGO and Cu-rGO. Each of the three materials showed a very different morphological profile. The GO shows a typical profile of graphene oxide, thin and translucent with a layered appearance but with well-defined separate sheets in the tens of micrometre range, while the reduced graphene oxide appears much more agglomerated with particles having become compacted. The Cu-rGO showed a much higher level of aggregation compared to the GO and rGO resulting in a material with a much more carbonaceous appearance. This is most likely due to the attachment of copper particles to the surface of graphene sheets which then promotes further aggregation following the reduction process. Small copper particles are visible on the surface of the large aggregated reduced graphene oxide sheets. These typical features of both GO and rGO suggest that both materials were produced successfully (Zhang *et al.* (2010) (Park *et al.* 2011). The aggregation of particles in solutions of reduced graphene oxide has been well reported (Li *et al.* 2008). The decoration of these more agglomerated

graphene sheets with copper particles has been shown in previous reports investigating the production of graphene copper composites (Xu *et al.* 2009) (Chen *et al.* 2011) (M. Wang *et al.* 2013) and the decoration of nano sized metal nanoparticles onto the surface of graphene materials is commonly characterised via microscopic analysis for other metals such as silver (Vijay Kumar *et al.* 2013) (Nguyen *et al.* 2012) (Jiang *et al.* 2012). From this microscopic analysis, the obvious difference in the morphology of the three materials is very clear and it is important to take this into consideration when viewing them from a microbiological and adsorptive perspective. While graphene materials possess a high surface-to-volume ratio, it is apparent that the chemical reduction and subsequent decoration of graphene with copper nanoparticles promotes aggregation of the sheets potentially limiting the available area. While the available surface area of the composite may be limited compared to that of GO, the morphological profile visible from SEM analysis is still suggestive of a high surface-to-volume ratio increasing the potential interaction between the material and bacterial cells compared to copper nano-particles alone. The high surface area of the Cu-rGO decorated with copper nano-particles may provide potential sites of attachment for bacterial cells, increasing the potential contact with the copper, which could then result in inactivation. The high surface area of graphene sheets has already been applied in the production of microbial fuel cells to promote bacterial attachment and biofilm formation (Zhang *et al*. 2011). The same principal could be applied to an anti-bacterial application as the attachment of bacterial cells to the surface would increase the likelihood of the organism coming into contact with the effective biocidal agent.

4.1.7 Particle size distribution

Dynamic light scattering (DLS) was used to evaluate the particle size distribution within solutions of GO, rGO and Cu-rGO. DLS has been used extensively to examine the varying sizes of different particles within colloidal suspensions like graphene, in particular silver nanoparticles, before anti-bacterial testing (Panáček *et al.* 2006) (Kvitek *et al.* 2008) (Martínez-Castañón *et al.* 2008). The size and shape of other nanoparticles has already been shown drastically impact on their anti-bacterial activity (Pal *et al.* 2007). The limitations of DLS should be noted however, particularly when dealing with solutions with high poly-dispersity like the rGO and Cu-rGO. Particles aggregation and occlusion of smaller particles by larger ones can impact greatly on the validity of results. The presence of large variations in solutions is an issue as significantly larger particles can occlude those which are several orders of magnitude smaller. The lack of water-solubility of the materials and their short-term settleability can also interfere with DLS measurements. Several studies have investigated the particle size distribution of GO and rGO via DLS prior to applying those materials to an anti-bacterial

application (Liu *et al.* 2011) (Gurunathan *et al.* 2012) (Gurunathan *et al.* 2013). The particle size distribution of GO is most notably almost identical to that reported by (Gurunthan *et al.* 2013) with 91.8% of particles having being in the range of 0.793µm and the remaining 8.2% around the 0.131µm region. Although they showed the results of the DLS measurements of rGO within their published work, (Guranathan *et al. 2013)* do point out that the lack of reliability in the suspension due to particle agglomeration and that the data is only used as a qualitative indication of the different sized particles present when the materials are dispersed. While these peaks characterise the most commonly occurring particle sizes, the broad band which can be visible in both cases would suggest a variance from the 10 nm range up to the 10 µm range. All three studies mentioned above describe the successful use of DLS for the characterisation of rGO. However, during analysis for this study, it was found that a large particle variance along with a high level of settle-ability and particle aggregation rendered the measurement of rGO and Cu-rGO invalid. As quantifying the particle sizes within each suspension proved difficult due to the large aggregates, light microscopy was used in order to give a broader overview of just how each of the materials looked in suspension.

4.1.8 Optical microscopic analysis

The stability of colloidal suspensions of graphene materials has been examined and questioned extensively and the search for an ideal dispersant for a long-term stable suspension is on-going (Lin *et al.* 2011) (Shih *et al.* 2010) (Paredes *et al.* 2008). The oxidative groups on the surface of graphene oxide lend the material excellent water solubility and dispersbility but even GO will aggregate if left over long periods of time. The removal of those groups to produce rGO hinders the solubility or more-rather the dispersibility of the material in aqueous solution and promotes aggregation. This can pose an issue when processing the material for applications as the lack of homogeneity can impact on consistency, particularly when considering immobilisation. The addition of a metal, like copper in this case, onto the surface of the sheets appears to only promote this aggregative behaviour. Graphene oxide sheets within solution showed individual defined sheets with a few notably laterally large sheets in the 10 µm range giving a clear indication as to the evolution of low number GO sheets, the majority of particles within the solution are barely visible sub-micron sized sheets not quantifiable by light microscopy. The large aggregates within the rGO are within the 100µm range and are composed of many smaller particles which can be clearly seen at x40 magnification. While Cu-rGO shows a similar profile to that of rGO, denser particles, which obscure light entirely, can be seen within the solution. This more compacted darker particle suggests that an even higher tendency toward aggregation within the Cu-rGO solution is present than in the rGO.

4.1.9 Final comments on characterisation

In contrast to the sodium borohydride ($NaBH_4$) reduction method, the l-ascorbic acid (AA) reduction to rGO and Cu-rGO resulted in the materials showing far higher water dispersibility and thus greater potential for immobilisation. The UV-vis spectra of each of the l-ascorbic acid reduced rGO and Cu-rGO showed a less significant "red shift" toward the visible region to ~250nm compared to 260nm as was seen with the borohydride reduction. This is suggestive of a lower number of oxidative groups being removed from the GO due to a milder reduction process. This is not surprising as studies comparing the use of different reducing agents for graphene oxide reduction have shown that strong chemical reducers such as hydrazine and borohydrides are more effective than reducing sugars such as ascorbic acid or sodium citrate (Eigler *et al.* 2013). The lower efficiency of ascorbic acid as a reducing agent compared to borohydride has also been shown with other materials such as gold nanoparticles (Luty-Błocho *et al.* 2011). Despite this lower level of reduction, each of the solutions appeared distinctly black in colour compared to the brown of the GO which is a distinct characteristic following graphene reduction. Similarly, the thermogravimetric analysis of both the ascorbic acid reduced rGO and Cu-rGO showed that a milder reduction had occurred compared to the borohydride method. The rGO reduced using ascorbic acid showed the greatest loss of mass of all the materials bar GO, indicating that while reduction had occurred it was to a lesser degree than the borohydride method and that there was still a large proportion of oxygen remaining within the material. The Cu-rGO produced using AA still had a very high thermal stability having a total mass loss of 34% compared with the 25% loss of the borohydride derived Cu-rGO. This is indicative of the copper content which affords the composite material a higher level of thermal stability compared to rGO alone. The lower level of thermal stability compared to the borohydride derived composite may be as a result of two factors; 1) the lower level of reduction occurring with the AA and 2) the lower concentration of copper present within the material. The EDX analysis showed that the second composite which was selected to be used for immobilisation contained ~25% copper by weight on average. While several iterations of the AA derived composite were produced, 25% was found to be the maximum copper load which facilitated the production of a stable dispersion. Unlike the borohydride derived Cu-rGO, the copper distribution was found to be much more homogeneous with only a variation of ~2-3% across the different sites of analysis. This greater homogeneity of copper across the graphene sheets may have occurred due to a number of factors. The lower level of reduction of the GO would facilitate a lower level of aggregation and thus a greater dispersity of the copper nano particles across the surface. It has however been theorised that the use of different reducing methods can have a significant impact on the morphology of graphene

following reduction from GO. In their study (Shang *et al.* 2015) show that GO reduced by hydrazine, a powerful reducing agent much like borohydride, resulted in crumpled and randomly aggregated sheets of rGO not unlike those seen here following the borohydride reduction. They showed that thermal reduction resulted in a "fluffier" and more expanded sheet by comparison, most likely due to the stationary nature of the GO during reduction and retention of its original morphology. The milder reduction of GO using the l-ascorbic acid may operate through a similar mechanism, the lower level of aggregation allows the nano-particles which are being produced simultaneously to become more evenly spread across the surface and create a more homogeneous final product. The morphological differences between the two methods of production were clearly demonstrated by the transmission electron microscopic (TEM) analysis. The borohydride reduced rGO and Cu-rGO were far more aggregated and resulted in much larger particles making the differentiation of individual sheets difficult. The ascorbic acid reduction however allowed the identification of individual sheets of both rGO and Cu-rGO. In particular the more disperse composite facilitated the observation of the clusters of copper nano-particles attached to the sheets of rGO. While a study examining the reduction of GO to rGO using ascorbic acid by (Gao *et al.* 2010) made use of tryptophan, an amino acid, as a capping agent in their production of stable dispersion of rGO, it was not found to be necessary here as the suspensions of both the rGO and Cu-rGO derived via AA reduction were stable for several months. The study by (J. Zhang *et al.* 2010) which also produced rGO through ascorbic acid production found similar results with AA alone and made the point that, quite often, the addition of capping agents and other materials to promote stability is undesirable as it can hinder the electronic or adsorptive properties of the final product.

Of principal interest was the stability of the composite when immobilised. Unlike the borohydride produced composite, the AA derived Cu-rGO was capable of being vacuum filtered into a free-standing film. While the production of graphene paper and graphene-metal composite such as silver has been carried out previously by different groups, the preparation of an immobilised graphene-copper composite film has not been investigated (Li *et al*. 2013), (Song *et al.* 2007), (Hu *et al.* 2010). When applying an immobilised graphene material in an aqueous environment, as is the objective here, it is vital that the material remain robust. Graphene oxide papers can be produced easily and are commonly applied in areas such as electronics, a dry environment. In an aqueous scenario however the GO, with its associated functional groups, will dissociate into the surrounding media as has been shown in this project. When a vacuum filtered GO film was applied to a vial of de-ionised water, the film became frayed and "puffed up" rapidly. As such there must be sufficient reduction in order for the material to retain its morphology following immobilisation. The AA reduced composite

produced here, while capable of forming a stable workable dispersion was sufficiently reduced and had a homogenous distribution of copper so as to be capable of forming a free-standing film. The free-standing films were stable in an aqueous environment for several months and represented an ideal material for the application of an immobilised graphene-copper composite to a water treatment scenario.

4.2 Antibacterial testing

4.2.1 Isolation of environmental strain of Escherichia coli.

The initial isolation of an environmental strain of *E. coli* provided a representative organism for the study of the anti-bacterial potential of graphene materials. When considering the application of materials for anti-bacterial purposes it is important to choose an appropriate organism which represents the intended target. As *E. coli* is an indicator organism for faecal coliforms which can be cultured quickly and easily, it is an ideal choice when examining potential water treatment scenarios and has been used as an indicator organism for faecal contamination for years (Rompré *et al.* 2002). *E. coli* is routinely used as a model gram-negative organism in the examination of graphene materials as well as metal-composites in both solid and liquid media. As *B. subtilis* is a gram-positive organism, it allows for the examination of how the different composition of the cellular envelope may affect the biocidal potential of the different materials of interest. Previous reports have shown that the intrinsic susceptibility of different environmentally isolated bacterial species to copper containing compounds and other commonly applied disinfectants can vary greatly (Aarestrup *et al.* 2004). This fundamental difference in cell composition necessitates the need for the investigation of various organisms. As the potential application of the antibacterial graphene materials is water treatment, the use of *B. subtilis* presents an additional advantage as it can be used as an indicator organism for *Cryptosporidium.* Due to its ability to form endospores which decrease inactivation susceptibility greatly, it has been suggested that non-pathogenic *B. subtilis* can be used in disinfection testing as an analogue for *Cryptosporidium* (Nieminski *et al.* 2000) (Rice *et al.* 1996). The use of *B. subtilis* as an indicator organism offers several advantages of safety and ease of use compared to directly analysing *Cryptosporidium* which, as a pathogenic protozoan, can be difficult to work with in terms of culturing and dangerous in terms of pathogenicity. The use of a *Cryptosporidium* analogue is topical in terms of Irish drinking water treatment in particular, as it has been a prominent issue in more rural areas over the past decade (Kelly 2014). The recent EPA drinking water report showed that eight different water supplies were on boil water notices at the time of publication as a direct result of *Cryptosporidium* contamination and that over 170,000 people were at direct risk of infection (The

Environmental Protection Agency 2013). It has become such an issue of concern that under new legislative guidelines in Ireland, any positive detection of *Cryptosporidium* must be brought to the immediate attention of the EPA. Using both a gram-positive and gram-negative organism will allow an understanding of different bacteria will interact with the materials to be developed.

4.2.2 Investigations into the anti-bacterial efficacy of graphene materials

While several studies have reported that both graphene oxide and reduced graphene oxide possess anti-bacterial activity in both solid and liquid media, contrasting reports as to the anti-bacterial activity of both are present with some claims of graphene oxide even enhancing the growth of *E. coli* (Ruiz *et al.* 2011). The majority of studies claiming the high anti-bacterial potential of both GO and rGO often investigate the effect of those materials only, while studies examining the effect of graphene-composites tend to find that GO or rGO (used as controls) possess little to no anti-bacterial activity. Several studies also assert that the physical characteristics and morphology of the graphene material employed play a key role in how they exert their anti-bacterial effect and these characteristics are not always highlighted between reports (Liu *et al.* 2012). When examining the anti-bacterial efficacy of a compound the most commonly applied methods are the minimum inhibitory concentration (MIC) test, performed in a 96-well culture plate, or the Kirby-Bauer disk-diffusion method performed on solid growth media (Andrews 2001) (Bonev *et al.* 2008). These methods are ideal when the compound of interest is water-soluble and can form a homogeneous solution. Particulate matter or suspended solids represent an issue in terms of the experimental limitations of these tests and as such it can be difficult to apply them in the same manner. Issues can arise due to light scattering by particles for spectrophotometric methods and solution inhomogeneity can affect dilution factors for multi-well tests due to the small volumes involved. As such the investigation into the anti-bacterial efficacy of particulates necessitates the application of more bespoke methodology. The step-wise evolution of testing the materials within solid media echoes the development of appropriate techniques to express a representative result of the anti-bacterial efficacy of colloidal suspensions of graphene materials. The first stage of the examination of anti-bacterial activity was performed in solid media to gauge whether or not the materials possessed any considerable diffusive anti-bacterial effect. The application of a more free-standing material in terms of a water treatment scenario would also be preferable as it would allow the fixation of the potential agent in a robust manner as opposed to free particles introduced to a liquid which would then require removal or further treatment.

Typically, the investigation into the anti-bacterial efficacy or cytotoxicity of carbon nanomaterials such as graphene is conducted in liquid media (Wang *et al.* 2013) (Jia *et al.*

2005). However there have been several studies which have examined the application of free-standing graphene materials or solid pieces of graphene on solid media for anti-bacterial applications. While these studies have employed similar methods in the examination of anti-bacterial potential, there are conflicting results as to the level of efficacy. The majority of cases reporting a lack of inherent anti-bacterial activity from standalone graphene materials, GO and rGO, are those which are primarily investigating composite materials. Studies examining *only* graphene materials however tend to show more positive results in terms of their anti-bacterial capabilities. There have been no studies investigating the anti-bacterial effect of a graphene-copper composite carried out, with the majority of composite focused studies favouring silver instead and as such no comparative work is available for the copper-composite. Copper chloride ($CuCl_2$) and copper sulphate ($CuSO_4$) were used for comparative purposes as they are commonly applied copper containing salts for antibacterial applications such as Bordeaux mixture and can also be found introduced into animal feed in agriculture; Brun *et al.* (2001). The use of copper nanoparticles for comparative purposes would allow for the observation of any potential synergistic effect between the graphene and the attached nano particles in the composite material.

4.2.3 Anti-bacterial testing in solid media

Several studies examining the effect of graphene composites have performed solid media testing of standalone graphene materials as control experiments against which to gauge the effectiveness of their produced composite (Bao *et al.* 2011) (Tai *et al.* 2012) (Das *et al.* 2011) (Wang *et al.* 2014) (Mondal *et al.* 2012) (Dai *et al.* 2011) (Li et al. 2013). These materials range from chemically exfoliated graphene oxide, "graphene nanosheets" and commercially purchased GO as well as rGO. Testing is typically carried out on agar inoculated with 10^7-10^8CFU/ml of an organism. The majority of these studies have examined both *E. coli* and *S. aureus* with one study from (De Faria *et al.* 2013) examining six others in addition. Preparation of the graphene for placement varies from vacuum filtration to dropping the solution directly onto the media and concentrations vary from 1ug up to 50mg with some tests being carried out using unspecified concentrations. These studies universally reported that little to zones of inhibition were observed when graphene materials were placed directly onto the surface of agar inoculated with *E. coli*, *S. aureus* and other organisms while the composites tested were, in all cases, superior in terms of their anti-bacterial efficacy. One of the principal investigations, carried out by (Hu *et al.* 2010) however examined the anti-bacterial properties of vacuum filtered GO and rGO paper against *E. coli* with no focus on composite materials. They showed that, of the two materials, GO was more capable of inhibiting bacterial growth in solid form with no visible colonies on the surface of paper placed on agar which was inoculated with

10^8CFU/ml. They concluded that vacuum filtered GO paper was a more effective anti-bacterial agent than its rGO counter-part. While this result contrast strongly with those mentioned already, the concentration per unit area for the graphene papers was not specified and it may be that a much greater concentration was present which yielded a more dramatic anti-bacterial effect. It should also be noted that the solid media approach is dependent on the diffusion of the biocide into the surrounding media so as to inhibit the growth of the organism. If a material were to act as a biocide in a physical manner, there would be no observable antibacterial effect.

Well-diffusion assay.

The well diffusion method is simple antibacterial assay whereby wells are cut into agar inoculated with a micro-organism and a material of interest added. It has been employed for both bacterial and fungal testing of biocidal agents previously (Bonev *et al.* 2008) (Magaldi *et al.* 2004), though it has not been employed by any previous studies in the antibacterial investigation of graphene materials. Wells were cut into agar inoculated with 10^8CFU/ml of *E. coli* and *B. subtilis* and had 200µl of each material suspension added, equating to 0.2mg. There was no visible zone formed from either the GO or rGO with either organism. Surprisingly, there was no zone present with either the Cu-rGO or the copper nanoparticles. However, following incubation it was observed that the suspensions which were added to the wells had dried. This drying may have resulted in the suspended particulates falling to the bottom of the well quickly and becoming unavailable to the surrounding media. As this method is commonly applied to antibiotics, which are dissolved solutions rather than suspensions of particulates, the drying of a solution would not be an issue as the active agent present would have already diffused into the surrounding media and thus come into contact with the organism. Additionally, the concentration used may have been insufficient to elicit a response, though the nature of the particulate matter is the more likely reason for the lack of antibacterial action as there was no observable zone from the copper containing compounds. Though an expedient method in terms of antibacterial investigation, the well-diffusion method was found to be unsuitable for use with suspensions of particulate matter.

Disk-diffusion assay.

Following on from the well-diffusion assay, the use of a more traditional disk-diffusion method was employed. Ideally the minimum quantity of a biocidal material should be employed for anti-bacterial purposes, particularly when dealing with a scenario relating to human health such as drinking water treatment. A review from (Borkow *et al.* 2005) concluded that, in terms of their antibacterial potential, copper possessed a greater efficacy than most other heavy metals and was second only to silver. Making use of a GO-zinc composite at concentrations as

low as 0.02mg, Wang *et al.* (2014) showed a positive anti-bacterial response from *E. coli* in solid media using filter paper loaded with their composite. Considering that copper should possess the greater anti-bacterial effect and the minimal quantities used by Wang *et al.* (2014) in their investigation, Cu-rGO should show observable anti-bacterial potential in solid media in concentrations as low as 0.02mg. The area of effect is much lower compared to that of the well-diffusion method and as such a lower quantity of material is required to achieve a higher localised concentration. As such, 20µl equating to 0.02mg of each material were loaded onto to 6mm sterile whatman disks and placed onto agar inoculated with 10^8CFU/ml of *E. coli*. Once again, there was no visible zone with GO or rGO as seen with the well-diffusion assay. However, no zone of inhibition was observed with either Cu-rGO or CuNPs. This may be due to the loading of the suspensions onto the disks which caused the material to become unavailable and unable to interact with the organism. The lower concentrations may also have been insufficient to elicit a response. When considering the concentrations used, particularly in regards to the composite, it is plausible that the concentration of copper present (40w/w% equating to 0.008mg) was insufficient to elicit a response. In particular, the colouration of the loaded disks remained on the top-most surface, indicating that the particulates present in suspension had sat on the top of the disks and may have been unavailable. The incorporation of the bacteria directly into the agar in addition to the limitation of the particulate interaction may also be limiting any observable effect. As such a bacterial lawn spread on the surface of the agar may be more suited to direct contact with the material.

Solid Exposure Assay.

In order to maximise the contact between the material and the organism, a bacterial lawn was used for further antibacterial investigation in solid media. The use of a lawn would guarantee contact between the organism and the material and allow for any inhibition to be more easily observed. In addition, the release of any active ions, such as Cu^+ or Cu^{2+}, as would come from the CuNPs and the composite material would only have to diffuse laterally rather than throughout the media in order for an effect to be observed. The analysis showed that neither GO nor rGO caused the formation od any zone of inhibition for either organism. Cu-rGO and the CuNPs however showed clear zones around each of the solids on the surface. As such it is clear that direct contact between the organisms and the material is required for any antibacterial action to occur. The role of contact killing in terms of coppers' antibacterial action has been highlighted as well as the role that the release of the different copper ions play within that mode of action (Hans *et al.* (2013) (Espírito Santo *et al.* 2011) (Grass *et al.* 2011). It is not surprising given these previous reports that the copper containing compounds require direct contact in order to assert an antibacterial effect. The almost comparable zones of the

Cu-rGO and CuNPs are a good indication that the copper nanoparticles present on the surface of the graphene retain their antibacterial potential following the production process and that the antibacterial functionality of copper can be added to graphene. The lack of any zone around either of the stand-alone graphene materials is indicative of a lack of inherent antiabcerial efficacy within these experimental parameters. It should be noted that *initial* tests carried out with both GO and rGO resulted in clear zones of inhibition, however this response was attributed to the presence of materials remaining from the production process; sulphuric acid (H_2SO_4), Hydrochloric acid (HCl), potassium permanganate ($KMnO_4$) and hydrogen peroxide (H_2O_2) among them, which would all elicit a toxic response to micro-organisms. Following the addition of a more rigorous washing step as well as elemental analyses', there was no observable response from the GO or rGO present, indicating the removal of all undesirable materials. While Hu *et al.* (2010) do specify the use of dialysis to remove residual contaminants it is possible that some material remained which was the cause of the clear anti-bacterial effect in that case. (Mondal *et al.* 2012), who also reported limited zones of inhibition, stated that an "adequate amount of water" was used to wash and remove any undesirable products or residues from their material. In order to perform a more robust study in terms of comparability and quantification, a method to create disks in which a defined concentration of composite material as well as CuNPs needed to be developed, but where the material would be available on the surface for interaction to occur. In order to facilitate this, the vacuum filtration of particulate suspensions onto Whatman cellulose filters followed by the creation of disks was investigated.

Vacuum-filtered disk diffusion assay.

From the tests carried out it was found that direct contact between the material and the organism was a necessity in order to elicit an antibacterial response from the copper containing compounds. Borrowing from the methodology employed by (Lit *et al.* 2013) and their creation of vacuum filtered papers of an rGO-silver composite, solutions of each material were vacuum filtered onto cellulose-acetate filter paper (Whatman 0.2µm pore size). Compared to the standard 6mm disks employed for disk diffusion assays, the cellulose filter paper is much less absorbent and much thinner by comparison, removing the potential issue of material becoming sequestered within the disk as was observed with the disk-diffusion assay. Additionally, the coated filter paper could then be placed face-down ensuring that all of the material present was in direct contact with the organism. Finally, as the solutions were being filtered onto a known area, the concentrations present on disks produced could be controlled. 20ml of 1000ppm of each solution was filtered onto an available area of 35mm resulting in a concentration per unit area of ~20ug/mm^2. 5mm disks were cut which equated to ~0.4mg, a

greater concentration than that employed in both the disk and well diffusion assays but still an order of magnitude lower than the solid exposure assay. This much lower concentration would show whether or not the material would be practical and cost-effective at lower concentrations, particularly when considering the composite which would contain only 8μg/mm^2 of copper. Unsurprisingly at this point, there was no zone of inhibition present with either the GO or rGO with either of the organisms once again. Overall the *B. subtilis* was seen to be more susceptible to all of the copper containing compounds than the *E. coli* with larger zones of inhibition in each case. The greater susceptibility of *B. subtilis* to copper nano particles compared to *E. coli* has been highlighted previously and supports the results observed here, it has even been shown that copper nanoparticles can be more effective than their silver counterparts in this regard (Ruparelia *et al.* 2008) (Yoon *et al.* 2007). The zones surrounding both the Cu-rGO and the CuNPs are smaller and less defined than the copper containing salts. This is indicative of the slower release of copper ions from the surface of the solids compared to the more soluble copper salts which would diffuse more readily into the surrounding media. The formation of a secondary zone surrounding the first where the growth is reduced though not inhibited is supportive of this slower release of the active ions, this secondary zone is particularly noticeable in the *E. coli* exposure from both the Cu-rGO and CuNP disks. The eventual colour change of the CuNP disk from brown to white after ~48 hours is also indicative of the slow solubilisation of the copper into the surrounding media and the slow release of the active ions compared to the copper salts. For both organisms, the CuNPs showed a larger zone of inhibition than the Cu-rGO, this is unsurprising as the composite contains 40% copper by weight and as there was no observable effect from the graphene materials it is reasonable to conclude that only the copper is having any appreciable antibacterial effect. While not as effective as the copper containing salts, the composite and the nanoparticles do show a propensity for a slower diffusive release of the copper from the surface. It may be that this slow release could be beneficial in a practical application such as an antibacterial surface or water treatment scenario where a more sustained lifespan to the material is more desirable than an acute effect.

4.2.4 Liquid Media Studies

As mentioned, there has been no previous study undertaken to examine the anti-bacterial effect of a graphene-copper composite in solid or liquid media. The studies examining the effect of GO and rGO in liquid media, however, are numerous. The majority of these studies examine the effect of graphene materials on *E. coli*, the typical model organism, though some investigations have examined many other organisms including *B. subtili* and plant-borne microorganisms among others (Krishnamoorthy et al. 2012) (Musico et al. 2014) (Wang et al.

2013). Typically the investigation of graphene materials in terms of their anti-bacterial capacity in liquid media is focused on a unique aspect of either material preparation or antibacterial mechanistic examination; lateral sheet size, sheet edge orientation, Oxidative stress and DNA damage and lipid peroxidation are all the foci of different studies on GO and rGO in liquid media (Liu *et al.* 2012) (Akhavan *et al.* 2010) (Liu *et al.* 2011) (Gurunathan *et al.* 2012) (Tu *et al.* 2013). Effective concentrations against *E. coli* range from as little as 0.5mg/L of to 1000mg/L and with numerous results in between (Veerapandian *et al.* 2013) (Mejías Carpio *et al.* 2012). However the major studies purport that a significant loss of bacterial cell viability should be observable with both GO and rGO up to 100mg/L when applied in a saline solution (Liu *et al.* 2011) (Hu *et al.* (2010). There have been studies which have reported that GO and rGO have little to no apparent effect in liquid media, or may even act as a growth enhancer, thus a systematic investigation into the effect of both graphene oxide and reduced graphene oxide as well as the composite material of interest is required to establish what, if any, antibacterial effect each of the materials possesses (Some *et al.* 2012) (Sreeprasad *et al.* 2011) (Ruiz *et al.* 2011). In addition, the antibacterial effect of copper nanoparticles produced via the same method was investigated in order to examine if any possible synergistic effect would occur as has been previously reported with other graphene-metal composites in liquid media (Han *et al.* 2013) (Dinh *et al.* 2015), (Pant *et al.* 2015).

The three materials were examined so as to establish their concentration and time-dependant anti-bacterial effects. PBS was the chosen media as it is a non-growth environment which will retain organisms in a healthy state for time periods within the desired experimental parameters and allowing change in the population to be observed. It is also more representative of a water treatment scenario where organisms would be in a low-nutrient environment unlike rich growth medias such as nutrient broth. It is a more applicable method in terms of intended usage in this regard as it reflects the materials ability to kill an organism rather than inhibit its growth. Shake flask studies have been employed commonly in previous studies to examine the effect of both stand-alone graphene materials as well as composites. Most notably there is no observable antibacterial effect with either organism within the six hour period from the GO or rGO and the same can be seen in both the 24 hour time-points. As the methods employed to examine GO and rGO vary wildly throughout the literature a comparison will be made with those studies which have examined each material via the same method employed here. Only studies which have examined chemically derived GO and rGO (i.e. via the hummers method), challenged an organism in a non-growth scenario such as PBS or saline solution and performed population analysis via plate counting will be discussed in comparison with these observations. Several studies have found similar results to those here, with no reduction from GO or rGO over 24 hours at 100mg/L (Ouyang *et al.* 2013), no

reduction from GO over 2 hours at 100mg/L (L. Liu *et al.* 2011) and no reduction against *E. coli* as well as other organisms such as S. aureus and P. aeruginosa at 5mg/L up to 6 hours (de Faria *et al.* 2013) (Tang *et al.* 2013). However the reports on the concentration and time-dependant activity of GO and rGO vary considerably. Table 4.1 gives an overview of the reported response of each material in a non-growth scenario, as above, at various concentrations over different time periods.

Table 4.1 Studies which examine the effect of GO and rGO against various organisms in a non-growth scenario such as PBS or saline solution.

Reference	***GO***	***rGO***	***Time***	***Organism (% reduction)***	
Tang et al. (2013)	5mg/L	No	2.5 hours	*E. coli*	No reduction
				S. aureus	No reduction
L. Liu et al. (2011)	100mg/L	No	2 hours	*E. coli*	No reduction
Ouyang et al. (2013)	100mg/L	100mg/L	24 hours	*E. coli* (GO)	No reduction
				E. coli (rGO)	No reduction
de Faria et al. (2013)	5mg/L	No	6 hours	P. Aeruginosa	No reduction
Pant et al. (2015)	500mg/L	No	8 Hours	*E. coli*	20%
				S. Aureus	15%
Bao et al. (2011)	45mg/L	No	4 hours	*E. coli*	52%
				S. Aureus	61.30%
S. Liu et al. (2011)	80mg/L	80mg/L	2 hours	*E. coli* (GO)	91.60%
				E. coli (rGO)	76.80%
Gurunathan et al. (2013)	150mg/L	150mg/L	2 hours	*E. coli* (GO)	87%
				E. coli (rGO)	81%
Tu et al. (2013)	100mg/L	No	2.5 hours	*E. coli*	90.90%
Hu et al.(2010)	85mg/L	85mg/L	2 hours	*E. coli* (GO)	98.50%
				E. coli (rGO)	90%
Sedki et al. (2015)	100mg/L	No	4 hours	*E. coli*	Total reduction

The variation in both the concentration and time-dependant response is highlighted in table 4.1 and shows just how different the observations between different studies can be. In terms of the observations in this study, there are a number of reasons as to why no antibacterial action may have been observed. In particular, it should be pointed out that initial studies carried out with both GO and rGO yielded a positive antibacterial response in both solid and liquid media. The positive response in solid media raised suspicions in this regard as to the proposed mechanisms of action required cell membrane interaction which would become difficult to exert if the material was in a fixed state. If some sort of kinetic shear or membrane interaction were to occur, movement would need to be involved. It is possible that the

materials would produce reactive oxygen species which could diffuse into the surrounding media and these may or may not be in concentrations high enough to create a visible zone of inhibition. After additional centrifugal washing with de-ionised water it was found that no antibacterial efficacy remained for either material. It could be that many of the studies mentioned, and others which observe strong antibacterial efficacy with stand-alone graphene materials may be observing false positives in the form of residual material from the production process.

It also may be the case that the organisms examined here, i.e. the environmental strain of *E. coli* and the spore-forming *B. subtilis*, are potentially highly resistant to both of the graphene materials. However the fact that *no reduction* in any way was observed makes this unlikely. The use of PBS rather than a less ion heavy solution such as 0.9% NaCl limits the capability of the materials as suggested by (Wang *et al.* 2012), though the methodology and bacteria employed in their case is quite different and may not reflect the response of the organism as seen above. Also, a study from (Ouyang *et al.* 2013) which observed no response over 24 hours in 0.9% NaCl contradicts the assertion of Wang and as such it is difficult to say whether the different buffer solutions may or may not be a contributing factor. The results of the growth media examination of GO and rGO yielded much the same response, with no observable effect in either case up to 1000mg/L, the lack of any antibacterial action up to this concentration was confirmed via spread plating which yielded a level of growth comparable to the control sample. The obvious production of a bacterial film or pellet and the aggregation of particulates in solution were indicative of uninhibited, or even enhanced, bacterial growth. Taking the trend which had appeared in the literature into account, which seemed to suggest that stand-alone graphene materials would only exert their antibacterial effect in a minimal or saline media, this result is not surprising. It is likely that any potential active sites for oxidation or membrane interaction would be occupied by the contents of the nutrient broth as was suggested by (Hui *et al.* 2014). There has even been suggested MIC values for GO and rGO as high as >10,000mg/L as observed by (Ouyang *et al.* 2013), who had no observable effect at this massive concentration.

It is clear from these observations, and those found during solid media testing that neither GO nor rGO possess any inherent antibacterial properties in the experimental parameters carried out here.

There was an obvious difference in response between the two different organisms against the various copper-containing materials. The gram-positive *B. subtilis* was far more susceptible than the gram-negative *E. coli* with complete reduction in population at the six hour time point for all the materials tested. While the composite showed a less acute effect against the *B. subtilis*, there was still a substantial reduction with >50% of the population killed after 3 hours.

The greater susceptibility of *B. subtilis* to copper nanoparticles compared to *E. coli* has been shown previously, though the reported biocidal values can vary greatly, from 20 to 5000mg/L, and are obviously dependant on the particle size and shape (Baek *et al.* 2011) (Ren *et al.* 2009) (Ruparelia *et al.* 2008) (Yoon *et al.* 2007).

The MIC values from the growth media analysis for each organism with all of the copper containing materials are almost identical with only the $CuCl_2$ showing a greater effect against the *B. subtilis* at 200mg/L and all others having a value of 400mg/L. The composite, which showed MIC values of 1000mg/L for both organisms was the highest concentration needed of any material tested. Considering the copper load of the graphene composite, which is 40%, it is not surprising that this concentration was required. The 1000mg/L of composite is equal to 400mg/L of CuNPs, the observed MIC for the stand-alone nanoparticles. The graphene does not appear to be offering any additional antibacterial effect in terms testing within growth media, as the observed value is most likely a result of the action of the CuNPs bound to the surface of the graphene alone. As mentioned previously, *B. subtilis* can act as an indicator organism for the response of *Cryptosporidium* for toxicity testing. As such the response observed here, which is highly acute, may indicate that the copper containing graphene-composite could act as an effective agent for the inhibition of *Cryptosporidium* in a water treatment scenario. In terms of what has been observed previously, a report from (Young *et al.* 2014) showed values almost identical to those found here with MIC values for both of the copper containing salts at 375mg/L. However a comprehensive report from (Aarestrup *et al.* 2004) on the susceptibility of environmentally isolated bacteria, showed that 169 strains of *E. coli* had MIC values of 20mM of $CuSO_4$ equating to 4990mg/L, substantially higher than the values reported here. They did however show that *S. aureus*, a gram-positive organism, was more much more susceptible with MIC values as low as 2mM (499mg/L) for the majority of strains tested. It would seem that in light of previous reports and what has been observed here that copper-containing compounds, including the composite, are more effective at killing gram-positive bacteria than gram-negative.

A particularly interesting phenomenon can be observed with the response of the *E. coli* to the CuNPs and the Cu-rGO over time. During the six hour incubation, the copper salts have an obviously more acute effect than the two particulate materials. This is most likely due to their water-solubility and homogeneity, allowing for greater immediate interaction with the planktonic bacterial cells present in solution. However at the 24 hour time-point, the CuNPs and the Cu-rGO show a greater overall level of reduction with the CuNPs reducing the population to 20% and the Cu-rGO to 19% compared with a total of 43% and 53% remaining for the $CuCl_2$ and $CusO_4$. Additionally, the Cu-rGO is performing at a comparable rate to the stand-alone nano particles at the same concentration while only containing 40% Cu. This

would suggest that in saline solution and with agitation, the graphene-copper composite is enhancing the activity of the copper nanoparticles present on the surface. It may be that, as a carbonaceous material, the graphene is promoting the attachment of the bacterial cells with the surface, thus increasing the likelihood of contact between the cells and the CuNPs present on the graphene. Particle association and bacterial attachment is particularly relevant in this regard as the formation of bacterial deposits/biofilms on carbon-based materials has been an issue in water treatment for quite some time (Camper 1986) (LeChevallier 1984). The propensity for bacteria to attach to activated carbon surfaces is an issue when the intended operation is the removal of chemical and odorous contaminants. Biofouling in this regard can ultimately reduce the effectiveness of the agent. However, this particular phenomenon, if also applicable to graphene, may be advantageous in this situation. A carbonaceous surface decorated with a biocidal metal which promotes the attachment of bacterial cells, would be more effective than the nano particles alone as well as offering a fixed surface for those particles preventing them from being eluted into the surrounding solution. The use of copper as an antimicrobial surface and its ability to exhibit "contact killing" of bacteria is well documented and has resulted in the application of copper in clinical applications such as self-sterilising surfaces (Espírito Santo *et al.* 2011) (Grass *et al.* 2011). An increased likelihood of the planktonic bacteria coming into direct contact with the copper nanoparticles could only enhance their performance.

The release of copper ions into various buffer solutions was also examined by (Hans *et al.* 2013) and shows results which may have relevance to those seen here. In a comparison between copper immersed in PBS and TRIS, an amino acid containing saline solution, they found that the PBS limited the release of Cu^{+} and Cu^{2+} ions by comparison. The release of ions into the TRIS solution was x17 times higher than that of the PBS. They also found that in liquid media such as PBS, copper will preferentially oxidise to CuO as opposed to Cu_2O as in dry air. This holds implications for the antibacterial efficacy, as they found that CuO was less effective as an antibacterial agent than Cu_2O due to the preferential release of the cupric (Cu^{2+}) ion as opposed to the cuprous (Cu^{+}) ion which is considerably more biocidal. This may hold implications for the application of materials applied here, the investigation into the use of different buffer solutions and minimal media could show how the different surrounding liquid environment effects the release of active ions and fundamentally changes the antibacterial effectiveness of the composite and the nanoparticles. It also highlights the requirement to examine the elution of Cu ions from the composite material, not only to examine the rate for antibacterial concerns but also in terms of the life-span of the composite as a practical material and the potential exposure of the end user. The results have shown that the composite, though acutely effective against the gram-positive *B. subtilis*, requires a significantly longer

period of time to incur a similar effect in the gram-negative *E. coli* and that even after a full 24 hours not all of the organisms present have been killed. This was advantageous in a small way as it allowed the observation of the different rates at which the composite expressed its antibacterial effect compared to the control materials. It highlighted that the composite was just as effective as the equivalent concentration of CuNPs. This synergistic effect appears to have been lost during the growth media determination as the results suggested that the copper was not enhanced by the attachment to the graphene. This may be due to the lack of agitation during exposure or to the fact that it was carried out in a growth media which could inhibit the antibacterial effect by occupying effective sites on the material.

4.2.5 Microscopic analyses of microorganisms

Examination of E. coli exposure to graphene materials via SEM analysis

The effect of each material on the cellular structure of bacteria was also investigated via Scanning Electron Microscopy (SEM). Previous studies have investigated the effect of GO and rGO deposited onto a surface and a similar method was employed here in order to investigate the effect of bacteria in direct contact with each material (Hu *et al.* 2010) (Akhavan *et al.* 2010). In a similar method to that employed by Akhavan and Hu et al, sterile filter paper coated with each of GO, rGO and Cu-rGO were incubated with *E. coli* overnight. Following exposure, the micro-organisms were fixed to the surface and observed for their morphological profile under SEM. Images captured of *E. coli* incubated on the surface of each material showed the morphological profile of the cells. These results were in accordance with those observed from the previous analyses' carried out in this project, where no inhibition was observed in the case of GO or rGO. For both materials, large numbers of cells can be seen to have proliferated across the surface. Bacteria appear to have fully intact membranes, showing a rotund rod shape in both cases and standing proud of the surface which indicates no obvious membrane damage or elution of intracellular material. Though the observations of (S. Liu *et al.* 2011) claim that their SEM images show bacteria with perturbed membranes in contact with rGO, that was not the case here. Although there is no evidence from these results to suggest the wrapping of cells by GO sheets as proposed by Liu, the experimental parameters may not have allowed for such an action to occur before fixation of the cells. The materials were already fixed on a surface before exposure and as such may not have been able to perform this mode of action. In the case of Cu-rGO however the response is very clearly quite different. The shape of the bacteria in contact with the surface is contrasting to those seen on the surface of the GO and rGO. They appear wider and conform to the surface of the material rather than maintaining a stout shape, indicating a loss of membrane integrity. The membranes also appear to be corrugated rather than smooth and their conforming to the surface is indicative

of the elution of intracellular material and the loss of cell viability. These observations are no surprise when taken in the context of the antibacterial results, no inhibition of bacteria was observed by GO or rGO and copper is known to act upon the bacterial membrane. As such the unperturbed membranes and cell proliferation across the two stand-alone graphene materials is to be expected.

Optical and fluorescent microscopic analysis

The optical microscopic analysis also gives an indication as to the bacterial cell interaction with the materials during incubation. Reports from studies such as (Wang *et al.* 2012) have suggested that the agglomeration of graphene-materials in solution can negatively impact on their potential antibacterial effectiveness. Although no antibacterial action has been observed with GO or rGO via plate counting, this line of reasoning may stand in terms of composite materials also, as agglomerated particles of biocide decorated graphene would ultimately be self-limiting due to the loss of exposed surface. This stands to reason as the anti-bacterial effect of these materials is said to be based on surface interaction, over-loading a solution may serve to increase agglomeration and decrease the overall available surface area, limiting potential sites of action. It is quite clear that the organisms have promoted the agglomeration of GO sheets in solution, when compared to microscopic images of the GO sheets alone, as captured during microscopic characterisation of the material. There are bacteria visible across the sheets of GO with few free cells visible in solution. This trend can be seen to continue with the rGO, which showed a different morphological profile to the GO as seen in both the SEM and optical analyses', with more agglomerated, less disperse and larger particles present within solution. Cells can be seen to be attached to these particles in large numbers. Interestingly, the majority of cells attached to the particles are on the rim or edge. This may or may not echo the "entrapment" of bacterial cells by graphene materials in solution as was suggested by (Akhavan *et al.* 2011). For the Cu-rGO the level of particle agglomeration can be seen to be higher again, with the brightfield-image showing opaque large particles blocking the transmittance of light. The association of bacterial cells is consistent with that of the rGO sample and shows that almost no free planktonic cells are present in the surrounding solution. A trend in increasing particle agglomeration with increasing Cu-rGO concentration was also observed. The microscopic images show the level of particle agglomeration is directly proportional to the concentration of particulates present and that Incubation with microorganisms may promote this action. During the microscopic analysis another phenomenon came to light, that of the quenching of the fluorescent dye by the graphene. The higher concentration, 1000mg/L, required the use of longer exposure time as well as higher light intensity in order for a clear image to be captured. This is reflected in how disperse the

light appears in the images due to the difficult imaging conditions. Given the adsorptive nature of graphene it is not surprising that some degree of fluorescent quenching would occur. This raises concerns as to the application of fluorescent probes for quantification during bacterial assays involving graphene as have been employed by other studies previously (Mangadlao *et al.* (2015) (Wu *et al.* 2013) (Y.-W. Wang *et al.* 2013) (Veerapandian *et al.* 2013). When applying a novel nanomaterial like graphene to an application such as water treatment, it is important to consider the potential impacts upon human health. Drinking water in particular is a vector through which potentially toxic materials, even at low concentrations, may be internalised readily. In particular, the presence of mutagens, carcinogens and teratogens are of concern as they can have a significant impact on human health. There is little to no information available as to the carcinogenic or mutagenic potential of graphene materials.

4.2.6 Evaluation of graphene material mutagenicity using the AMES test

Up to this point there have been no investigations carried out into the mutagenicity of graphene materials using bacterial cells or the AMES test specifically. Previous studies have commented on the biocompatibility of graphene materials with mammalian cells (Pinto *et al.* 2013) (Chen *et al.* 2008) (Sreeprasad *et al.* 2012), and graphene based biosensors are an area of intense interest (Mohanty *et al.* 2008) (Tonelli *et al.* 2015). This would seem to suggest that the potential health impact of graphene materials may be low. The AMES test is a mutagenicity test which utilises modified bacterial strains incapable of synthesising important amino acids and was originally developed by Bruce Ames using a modified *Salmonella Typhimurium* (Maron & Ames 1983). More recent modified tests have been developed utilising non-pathogenic strains of *Escherichia coli* (Mortelmans *et al.* 2000). In each case the organism is incapable of producing an essential amino acid for cell proliferation; histidine for *S. typhimurium*, and tryptophan for *E. coli.* The assay is a so called “reverse mutation” assay as it relies upon the mutagenic compound of interest reverting the organism to a state in which the amnio acid can be produced and growth observed i.e. the more growth observed, the greater the mutagenic potential of the compound. While the Ames test was originally developed using a solid agar, more modern techniques and commercially available kits have opted to employ aqueous based media to reduce workload, facilitate greater cell interaction with the mutagen and to allow higher throughput.

The commercially available kit used here (AMES-MOD ISO) employs a liquid based assay. GO, rGO and Cu-rGO were tested at concentrations of 0.1, 1 and 10ppm. These concentrations were selected as the expected final use of the materials would be as an immobilised compound. As the free-standing films and composite coated membranes produced during the project employed 10mg of compound, any concentrations within suspension than those tested

above would represent a serious dissolution of the material into the water stream which was hoped would not occur. The strain employed was S. typhimurium (TA-100), a strain sensitive to base-pair substitution and DNA oxidation. As one of the primary modes of action suggested within the literature of the biological interaction of graphene materials is oxidative stress, this organism was selected as an ideal model. Results of the mutagenicity testing can be seen in table 3.6 (section 3.3.8). The negative control represents the level of spontaneous revertants which will occur naturally during testing and is used as background. Each of the materials, graphene oxide (GO), reduced graphene oxide (rGO) and the composite (Cu-rGO) showed results comparable to that of the negative control with less than 15 positive wells in all concentrations tested. As such, it can be said that there is no mutagenic potential from any of the materials employed here at the concentrations tested. While there are no reports on the mutagenicity of graphene materials currently available, a study by (Clift *et al.* 2012) analysed both single walled carbon nanotubes (SWCNTs) and multi-walled carbon nano tubes (MWCNTs) using the AMES test and found that no mutagenic properties were present in either material. A comprehensive review by (Toyokuni 2013) on the carcinogenicity of both MWCNTs and SWCNTs concluded that only MWCNTs possess carcinogenic effects while SWCNTs do not. As graphene materials are more similar in structure to SWCNTs it may be that this this lack of mutagenic action is shared by the two materials.

4.3 Adsorption studies

The investigations into the adsorptive potential of each of the graphene materials were carried out for a number of reasons. Much like activated carbon, charcoal and other carbonaceous materials, graphene has a high adsorptive potential and can be effective in the removal of chemical contaminants. The primary focus of the adsorptive studies was not only to examine the loading capacity of each of the three materials but to examine how the immobilisation impacted upon their effectiveness. In addition, there was a focus on comparing the effectiveness of the three graphene materials in terms of their adsorptive potential. The composite and how the addition of copper would impact on its adsorption of chemical contaminants was of particular interest. As such three chemical contaminants of interest; methylene blue, diclofenac and famotidine were used as model agents for the removal of chemical contaminants from water.

- *Famotidine* is a widely available and used pharmaceutical used to inhibit acid production within the stomach and used to treat but ulcerous conditions and acid-reflux. Its presence and fate within waterways, treatment plants and activated sludge

systems has been highlighted in recent years and is coming into focus in terms of its environmental impact (Radjenović *et al.* 2009) (Jelic *et al.* 2011).

- *Diclofenac* is a widely used anti-inflammatory medication which is available over the counter is probably most notable in products such as Voltarol™ in Ireland. It has been classed as a "*substance of emerging concern*" by the European union and is one of the first on a list of chemical contaminants to be labelled as such (Environmental Quality Standards Directive 2008/105/EC).

- *Methylene Blue* is a commonly used compound in both research and medical applications. It is used commonly used as a redox indicator in chemistry, can be used for photodynamic therapy, is used in fish tanks but may also act as a teratogen and is undesirable in waste streams (Bishop *et al.* 1997). However it may have a high occurrence within water ways due to its prevalent usage.

4.3.1 Time-dependant adsorption

The most notable result which can be seen from the preliminary findings of the time dependant examinations is that the removal of diclofenac was negligible for all three materials. Previous studies have shown that the adsorption of diclofenac onto graphene and other carbon materials is pH sensitive and is greatly lessened at around pH7 (Beltrán *et al.* 2009) (Jauris *et al.* 2016). As this examination was carried out in de-ionised water with an unadjusted pH, the results are not surprising in light of the literature. However, when considering the final practical application of the graphene materials in this case; water treatment, the adjustment of pH in order to more greatly understand the interactions of the material with the contaminant becomes a moot consideration. In a water treatment scenario, pH adjustment can be done, however at cost, workload and time. It would not be feasible to apply a pH change in a prototype water treatment scenario and as such no further investigations into the removal of diclofenac were carried out.

4.3.2 Adsorption of methylene blue

The adsorption and removal of methylene blue by graphene materials within the literature has predominantly focused on the production of graphene-composites (such as titanium dioxide (TiO_2)) for photocatalytic breakdown in conjunction with the adsorptive potential (Lee *et al.* 2012) (Liu *et al.* 2010) (Zhang *et al.* 2009). This dual functionality of adsorption onto graphene and subsequent photo-breakdown is a popular approach, much like the interest in applying

graphene as both an adsorptive agent and an antibacterial material as is the focus in this project. Some studies have focused on the adsorption alone of graphene materials of methylene blue however. Studies from both (Yang *et al.* 2011) and (Ramesha *et al.* 2011), have reported removal efficiencies of up to >99% at concentrations of up to 40mg/L and loading capacities of >700mg/g of methylene blue onto graphene oxide. The results seen in this study are in-line with these findings; section 3.3.3 shows the adsorptive potential of the three graphene materials with methylene blue. It is un-surprising that the free-particles, having the greatest available surface area, showed the highest removal rates with GO possessing a capacity of 739mg/g, while the Cu-rGO showed only a marginally lower capacity with a loading capacity of 605mg/g. In terms of the use of the composite as a dual-function material these results are very positive as the 25% w/w copper content does not impact heavily on the loading capacity of methylene blue. The trade-off in terms of overall material functionality can certainly be said to be acceptable as the material can be seen to be effectively antibacterial. The most notable change in adsorptive capacity is in the free-standing films; where a large drop, compared to that of the free-particles, can be seen in the loading capacity; with GO showing ~200mg/g loading capacity albeit with a *high* level of error involved as can be seen in figure. 3.46. This high level of error associated with this analysis can be attributed to the dissolution of the GO film within the aqueous solution, as has been mentioned during the discussion of the immobilisation of the graphene materials. The break-up of the GO film within the solution significantly increases its relative surface area but due to the random nature of this dissolution, the consistency across replicates is lost and thus the high error. It can also explain the large difference in loading capacities between the unstable GO film and the stable rGO and Cu-rGO films which had 104 and 55mg/g respectively, far lower than the GO film and far lower again compared to the free particles. This would suggest that the formation of the film and the packing of graphene sheets results in a huge loss of surface area and thus adsorption sites. The Composite coated films showed promising results compared to those of the free-standing films with a loading capacity of 482mg/g at the highest concentration tested. While still lower than that of the free-particles, the composite coated membrane performance would certainly make it the immobilisation method of choice between the two methods investigated here.

4.3.3 Adsorption of famotidine

There is very little literature available literature on the removal of famotidine from environmental or water scenarios in any format, with only some studies focusing on the breakdown of famotidine via activated carbon-TiO_2 adsorption and photo degradation (Keane *et al.* 2011). In fact, an exhaustive review by (Rivera-Utrilla *et al.* 2013) on the removal of

pharmaceuticals from water doesn't include any comment on famotidine due to the lack of available literature. Compared to the methylene blue, the famotidine had a lower loading capacity with all three of the graphene materials. The highest loading capacity was found to be with the rGO free particles at the highest concentration used (3.2mg/ml) and a loading capacity of 342mg/g. The Cu-rGO had a significantly reduced loading capacity in this case with an adsorption capacity of only 209mg/g at the highest concentration with the free particles. The greater variation between the materials is most likely due to the lower overall loading capacity of famotidine onto the graphene material and as such the composite, with the copper present within its structure, has a more prominent drop in adsorption capacity compared to the GO and rGO. In the examination of the films, the GO showed the highest adsorptive potential (as with the methylene blue) with a loading capacity of 113mg/g which is most likely due to the expansion of the film within the aqueous solution. Finally, the composite coated membranes showed a higher adsorptive potential than that of the films but less than the free-particles with a loading capacity of 183mg/g at the highest concentration once again indicating that in terms of integration into a system that the coated membranes with their higher surface area would be the method of choice for immobilisation.

The adsorption studies have shown clearly that while there is little difference between the adsorptive potentials of GO and rGO, the GO had a higher affinity for the methylene blue than the rGO. The rGO may have had a higher potential for famotidine adsorption in the free particle analysis but the expansion of the GO film showed that surface area plays a key role. While the Cu-rGO did not perform as well as the other two materials as both free-particles and free-standing films, the composite coated membranes performed excellently and showed that applying the composite as a coating over a larger surface can serve to improve the available adsorption sites and thus the overall potential of the immobilised material. The testing of each material in the different physical formats showed an obvious relationship between surface-area and adsorption capacity; free particles > coated membranes > free-standing films, indicating that in terms of the application of the composite for adsorption, the membranes far out-performed the films and that the loss compared to free particles is not highly impactful. This is not surprising when simply considering the surface area. The vacuum-filtered films are 15mm diameter with a total surface area (both sides) of ~352mm^2 while the composite coated membranes have a total area (both sides) of ~2513mm^2, a far greater area. Not only that but that vacuum-filtered films are far more compacted compared to the coating on the porous glass fibre membrane. The compacted graphene within the structure of the film becomes unavailable and unable to perform any adsorption. The composite coated onto the membrane however not only has the greater overall area but the less compacted graphene spread onto

the porous structure will be exposed to the solution via the soaking of the membrane and the ability of the liquid to pass through it.

4.4 Prototype Studies

The application of graphene to water treatment has seen different formats across previous studies. Primarily there is a lot of speculation as to the application of graphene for desalination and this is reflected in the volume of literature available. The preparation of graphene for water treatment has seen a plethora of high sophistication methods applied. While the production of graphene based coatings on polymer surfaces has been applied for water separation, they involve functionalization and cross-linking to facilitate production of graphene films (Hu *et al.* 2013). Similarly, "punching holes" into graphene sheets using electron beams and gallium ions so as to create separation membranes is equally complex and requires sophisticated equipment (Wang *et al.* 2012) (Cohen-Tanugi et al. 2012). A driving principle behind the current project was to develop a simple method of fixation so as to apply the graphene-copper composite to a water treatment prototype. As such, the idea of free-standing films or surface coatings was the most attractive. Other free standing varieties of graphene have also been produced for water treatment such as bi-layered foams making use of graphene sandwiched between hydrogels (Jiang *et al.* 2016). The production of graphene oxide based water filtration membranes has also been carried out previously. The process by which these membranes are produced involves shear alignment of individual graphene sheets onto a fixed substrate and is highly dependent on the viscosity and physical characteristics of the dispersion; (Akbari *et al.* 2016). As the primary goal in this case was to apply the composite, these techniques which deal with pure dispersions of graphene were unsuitable and as such the use of vacuum filtration for the formation of the films and drop-casting for the creation of the membrane coatings was favoured. Ideally, the composite would be incorporated alone i.e. with no supports or substrates and as such the initial prototype would focus on the use of the free-standing composite films. The use of free-standing films would not only simplify the immobilisation process but also theoretically increase the availability of the graphene.

4.4.1 Antibacterial analysis of immobilised graphene-copper composite surfaces

As the format in which the graphene-copper composite would be incorporated would be that of a surface, either free-standing films or composite coated membranes, the antibacterial performance of the composite in this format was tested before the construction of a prototype. The ASTM method "Standard test method for the determining the activity of incorporated antimicrobial agent(s) in polymeric or hydrophobic materials" is designed for use with surfaces such as polymers which include anti-microbial agents as part of their structure

(ASTM standard E2180-07 2012). It has been used for examining the antimicrobial properties of silver-nano-particle incorporating chitosan membranes and for silver containing meat packages for example (Dehnavi *et al.* 2013) (Kuuliala *et al.* 2015). As the immobilised composite fits within these parameters, due to the inclusion of the copper nanoparticles, this method was chosen as the most appropriate so as to reflect the antibacterial activity of the surface more accurately than the aqueous or solid media based assays which had been used for the disperse composite. The method makes use of semi gelatinous agar slurry (like a gel) which is inoculated with bacteria and placed onto a known area of the material of interest. As had been found in the solid media studies done previously, the requirement for direct contact with the composite in order for antibacterial action to occur would be facilitated by the contact between the gel and the surface. The results of the analysis showed that both *B. subtilis* and *E. coli* were completely inhibited within forty minutes. Comparatively, copper surfaces have been shown to operate within a similar time-frame for a comparable number of bacteria, further reinforcing the evidence of a good distribution of the copper throughout the material (Hans *et al.* 2013). As with the previous antibacterial examinations, films of both GO and rGO were also tested with no significant reduction in bacterial numbers occurring. The time taken for total inhibition to occur in this scenario is significant as it would influence the parameters in which the first prototype (incorporating the free-standing films) would be operated. Considering the fact that the concentration of bacterial cells present on the surface of the film is relatively high at 10^4CFU/cm^2, much higher than would be expected in a tertiary water treatment scenario, an exposure time of 30 minutes within the unit was thought to be sufficient to achieve a total inactivation with a much lower concentration of bacteria.

4.4.2 Prototype 1

This first prototype included four 10mg free-standing graphene-copper composite films. One film was placed at the base of the unit and a film was situated on each support structure separating the four chambers. It was decided to use an upward flow-system so as to allow for maximum exposure of the films during testing and to prevent unwanted movement of water throughout the unit due to gravity, particularly during the initial start-up phase. The support structures would sport four vents around their circumference to allow for flow-through. A structural rebate or indent on the inside wall would allow the placement of the support structure into the unit and each section was sealed using silicone sealant. The driving principle in the design is that a low flow-rate, filling the unit from the bottom up will allow sufficient time for bacteria to contact each of the films and become inactivated. A concentration of 10^2CFU/ml of *E. coli* was used to better reflect low bacterial numbers which may be seen in a tertiary water treatment scenario. The antibacterial analysis of the films showed that they

were capable of inactivating *E. coli* at a concentration of 10^4CFU/cm^2 (equating 10^8CFU/ml) within 40 minutes. As such, it was assumed that four films placed evenly throughout the unit would provide sufficient surface area to inactivate the much lower concentration of bacteria within 30 minutes. With this in mind a flow rate of 22 ml/min was chosen so as to have a single cycle of the unit equate to 30 minutes. The total volume would be recycled and the effect on the bacterial population monitored. The control unit with no composite films included was operated in parallel and resulted in no reduction in bacterial numbers. This showed that the materials used for construction would not inherently retain the bacteria and any observed reduction in bacterial numbers could be attributed to the films. The first prototype design would prove to be lack-lustre in terms of its performance over short time periods with a reduction of only 23% in the bacterial population occurring within six hours and the majority of the bacterial population still remaining even after twenty-four hours. This result was certainly at odds with the anti-bacterial performance of the films in the antibacterial surface test, however it can be rationalised by several factors. Principally the media of exposure is different, while the surface testing method is designed to better reflect the antibacterial potential of the contacted surface, the low volume employed (150µl) could have resulted in the rapid build-up of copper ions within the gel. The elution of copper ions from copper has been shown previously to have a significant role in its anti-bacterial action (Chatterjee *et al.* 2014) (Rispoli *et al.* 2010). The large volume employed in the prototype test (700ml) would result in a much lower concentration per millilitre overall when considering the elution of copper ions from the composite. In addition, the location of the films (on top of the support structures) may not have been the optimal choice. The flow is proceeding upward and the force may be carrying the bacteria away from the surfaces as the water moves upward. While some bacteria are coming into contact with the films, as denoted by the drop in population, the majority are carried upward and away from the films. While simply attaching the films to the underside of the support structures may have improved performance, the very low reduction in the bacterial population necessitated a more comprehensive re-design. With this in mind, a movement toward the use of the composite coated glass fibre membranes was done with the next version of the prototype.

4.4.3 Prototype 2

As the inclusion of the films in the first prototype proved insufficient, the second design would include three copper composite coated glass fibre membranes. In order to consistently examine and compare the effect of the composite, 10mg was drop cast onto each of the membranes. The thinking was that the greater surface area combined with the retentive nature of the membranes would enhance the performance of the unit compared to the first

prototype. The antibacterial tests had shown the adsorption potential of the composite in terms of bacterial cell attachment; this would theoretically facilitate a greater interaction of the cells with the surface in this case also. As the previous test suggested the upward movement of the bacteria would not facilitate their contact with an upward facing structure, the composite coated membranes were placed faced down, with the coated side directed into the flow so as to maximise exposure. In addition, another unit was constructed which included the membranes with the composite coating face-up so as to examine how the coating would affect the retention performance of the membrane. No membrane was placed at the bottom of the unit as had been done with the films as this was deemed redundant. The membranes would be fixed to a cross-shaped support in order to maximise the available surface. The second prototype was shown to be far more effective than the first with > 99% of the bacterial population removed within 6 hours and over 50% gone within the first hour. In addition the coating was shown to improve the retention of the bacteria with the upward facing coated membranes showing a lower retention of bacteria of 80% after six hours. While clearly more effective than the prototype which incorporated the free-standing films, the second design still required ~6 hours (12 cycles) to completely remove all of the bacteria from the 700ml volume. The GFA glass fibre membranes have a particle retention of ~1.6µm, much larger than the typical 0.45µm pore size used for bacterial retention in environmental analyses'. The time required reflects the low retention potential of the membranes despite the small improvement offered by the graphene-composite coating. The use of membranes with relatively larger pore sizes, like thoe employed here, has been shown historically to be less effective at retaining bacteria like *E. coli* (Bobbitt *et al.* 1992).

4.4.4 Prototype 3

As the second prototype had achieved a 50% reduction in the population within the first hour using three coated membranes, the third prototype would incorporate 9 membranes with the objective of removing all bacteria immediately from the initial start-up phase. During the operation of the second prototype some obvious bowing of the glass fibre membranes was observed which may have also impacted upon their performance. With this in mind, the membranes incorporated into the third prototype would be sandwich between two cross-shaped supports in a hatched pattern to ensure sufficient support on both sides. Initial tests of the unit using the same parameters as those before showed that the third prototype was indeed capable of removing >99% of the population within 30 minutes and that no bacteria were present in subsequent samples up to six hours of the volume being recycled. Larger volume tests were carried out at higher flow-rates to examine the robustness of the membranes and whether or not the prototype would be suitable for longer and more

demanding operational times and parameters. It was found that in the current setup a flow-rate of between 95 and 100ml/min would result in the membranes being burst due to pressure. As such a maximum flow-rate of 90ml/min was chosen as the most appropriate to examine the structural robustness of the prototype over longer period tests. Results of tests of both 5 and 10L at 90ml/min showed that no bacteria were present in the permeate, indicating that all of the bacteria were either retained within the unit or inactivated. A control unit, which included nine uncoated membranes showed a similar response and it was clear that the bacteria were indeed being retained by the membranes. As such, the focus turned to the viability of the organisms retained on the surface of both the coated and uncoated membranes. Following flow-through testing the membranes were removed, cut into two with each half added to both nutrient and (Reasoners') R2A broth. R2A broth is primarily used for the culturing of organisms which may not grow in richer media or for organisms which have been exposed to environmental stress (Reasoner *et al.* 1985). Should the organisms be culturable in these conditions rather than in the richer nutrient broth, growth would be observed. Following the ten litre tests, viability tests showed that positive growth in both media was observed for the control membranes, indicating that while bacteria were retained within the unit, they were still viable. The composite coated membranes however showed that there was no growth from eight out of the nine membranes. Only the first membrane, the one closest to the inlet, showed positive growth in both the nutrient and R2A broths. This would indicate that the composite coating was capable of inactivating the organism upon surface contact. The growth on the first membrane is most likely due to its position, as the first membrane it is more likely to retain a greater number of organisms. As a build-up occurs, particularly over larger volumes, the active biocidal sites may become unavailable which may explain the growth in the viability test. The larger volume tests however showed that the unit and the membranes were physically robust enough to be tested at the higher flow rate over a greater volume. As the unit had proven to be both robust physically and capable of removing bacteria, the third design was then selected for further testing. In addition to examining the removal of bacteria, the capability of the unit to remove *Cryptosporidium* was also investigated. Cryptosporidium is a pathogenic protozoan and is particularly relevant in the context of water quality in Ireland. The west of Ireland in particular has seen several outbreaks of the organism over the past ten years (Callaghan *et al.* 2009). *Cryptosporidium* oocysts are not inactivated by concentrations of chlorine typically used for disinfection in drinking water (Chauret *et al.* 2001), as such the use of an alternative method like that employed here may be useful for the removal of this pathogenic protozoa. While there are no specific acceptable limits for the presence of *Cryptosporidium*, Irish water has stated that any detection within 1000L is deemed as an exceedance (Irish Water 2016). Limits in the United Kingdom and

Northern Ireland are more specific however and are set at 1 oocysts per 10L and 0.1 oocysts per 10L, respectively, as not permissible. In their work outlining the risk associated with Cryptosporidium defined an “extreme contamination event” as 1 to 15 oocysts/10L (Cummins *et al.* 2010). As such a concentration of 10 oocysts/L in ten litres was used to examine the capability of the prototype. The Cryptosporidium analysis was carried out in conjunction with City analysts Ltd. who performed a quantitative microscopic analysis for the presence or absence of oocycts following testing. It was found that, following testing with the prototype, there were no *Cryptosporidium* oocysts present in the permeate. The analysis was microscopic only and analysis of the viability of the oocysts retained within the unit was not possible. However, as *B. subtilis* can be taken as an analogue for *Cryptosporidium*, its response in the antibacterial surface testing showed that it was inactivated upon contact with the composite and this may be the case with the *Cryptosporidium* also.

The capability of the prototype to remove both methylene blue and famotidine was also examined to see whether or not the flow-through system would impact on the adsorptive potential compared to the bench top analyses’. The removal of methylene blue was unaffected, with a 95% removal occuring over 24 hours. The rate at which the methylene blue was removed in the flow-through system was greater than that observed in the shake flask method employed during the bench top analysis. The unit showed a reduction of 74% in total concentration over 8 hours compared to the 67% in the bench top method. This may be due to increased exposure as the liquid passes through the membranes though it is most likely due to the volume to membrane ratio. In the bench top analysis a composite coated membrane was added to 100ml of methylene blue solution and in the case of the flow through test, there are nine composite coated membranes treating 700ml. However the test *did* show that the membranes, installed within the prototype, still retained their capabilities for adsorption of methylene blue. A similar trend was observed with the famotidine; from the bench-top adsorption studies the composite coated membranes had a capacity of ~1.2mg of famotidine when placed into a solution at 0.032mg/ml and as such nine membranes would theoretically remove 10.8mg at this concentration. The total removal of famotidine in the flow-through test was ~46% from the 700ml equating to 10.2mg. While a relatively small loss of ~0.6mg was seen compared to the bench top tests, the composite coated membranes retained the majority of their adsorptive capabilities. This small loss is most likely due to the area of the coated surface which is covered by the attachment of the membrane to the support structure.

Having examined the capabilities of the prototype to remove bacteria, Cryptosporidium and chemical contaminants, the focus then moved on to its long-term robustness. While the five and ten litre tests had shown the prototype capable of handling these volumes at the higher flow-rate of 90ml/min, a more long-term test to challenge the unit was then carried out.

To facilitate a continuous flow, a tap-water fed reservoir was used during long-term testing, the purpose of which was to examine the capability of the prototype to retain bacteria over longer periods of operation and to ascertain if it was robust enough structurally for continuous operation at the higher flow-rate. In addition to testing the removal of bacteria the leaching of copper into the permeate was also examined for and monitored via flame atomic absorption spectroscopy (AAS). The bacterial analysis was carried out via spiking every ten litres throughout the operation of the unit. As a flow rate of 90ml/min was used, a single cycle of the unit would equate to ~8 minutes and as such three samples were taken over the course of ten minutes following spiking with *E. coli* to examine for the elution of any bacteria in the permeate. The unit was shown to remove all bacteria following spiking up to 50L. At the 60L mark there was a single sample which showed positive growth out of three. At that point there-after there was found to be positive growth in all samples and at 100L the operation of the unit was stopped as it was clear the membranes had failed. During operation the physical structure of the membranes was monitored visually and there was a noticeable build-up of bubbles which formed into air pockets under the membranes. This build-up was noticed under the first membrane at ~40L, with the membrane obviously being pushed upward and rupturing at around the 50L mark along with smaller levels of build-up under each membrane throughout the unit. Following the rupture of membrane #1, this build-up then proceeded to occur underneath the second membrane. Despite the first membrane having ruptured, the unit was still capable of retaining bacteria as there was no visible growth in any of the samples at 50L. The rupture of membrane one seemed to cause a cascade however, with each of the membranes rupturing with greater frequency and the final membrane being ruptured at the 80L mark. Despite using a peristaltic pump in order to create as stable a flow as possible, this build-up of bubbles may have been cause by turbulence within the flow or air coming in from the tap-fed reservoir. The membranes were seen to consistently have ruptured in the centred along the cross-section of the two support structures between which the membrane was sandwiched. This consistency indicates that the design used for the two support structures may have contributed to the failure of the membranes along with the air build-up.

4.4.5 Copper leachate

While copper is a useful biocidal tool and an essential nutrient in small quantities, higher concentrations of copper can present a danger to human health (Halliwell *et al.* 1984), and the current limit on copper in Ireland in drinking water is set at 2mg/L (The European Union Drinking Water Regulations S.I. 122 2014). Samples were taken following the start-up phase of the unit and at 10L intervals thereafter, these samples were acidified with nitric acid (HNO_3) to under pH2 for preservation before analysis. The analysis, which showed an average copper

concentration of ~0.3mg/L throughout the majority of the long-term test revealed that the copper leachate concentration was well below that of the present limits. Only the initial sample, taken directly after the start-up phase, showed a higher concentration at 1.3mg/L. Though higher than the average concentration seen throughout the test, 1.3mg/L is still within the acceptable limits for drinking water and that should the coated membranes be applied to water treatment, the leaching of copper from the composite may not be an issue for concern. Additionally, the elution of copper ions into the solution at the concentration range seen may be advantageous for disinfection. The use of copper ionisation systems for example creates a concentration range of between 0.2 and 0.8mg/L to inhibit *Legionella pneumophelia* growth in water (Lin *et al.* 2015). The average concentration found here 0.3mg/L, lies within this range. As all nine membranes are required to retain the bacteria, their movement through the unit while exposed to this concentration of copper ions within solution may further assist in their inactivation.

5. Conclusions and future work

Conclusions

1. Analysis of graphene oxide, reduced graphene oxide and a graphene copper composite was carried out using ultraviolet-visible spectroscopy (UV-vis), thermogravimetric analysis (TGA), dynamic light scattering, scanning electron microscopy (SEM), fourier transform infrared spectroscopy (FTIR), energy dispersive x-ray spectroscopy (EDX) and verified that the materials were successfully produced (Section 3.1).

2. Graphene oxide and reduced graphene oxide showed no antibacterial activity (Section 3.2).

3. The copper composite showed antibacterial activity at 100ppm which was attributed to the presence of the copper and the adsorptive potential of the graphene (Section 3.3.4).

4. The use of l-ascorbic acid was effective at producing a homogeneous suspension of the graphene-copper for immobilisation. The immobilised composite was effective as an antibacterial surface, capable of inactivating *E. coli* and *B. subtilis* within 40 minutes (Section 3.5.1).

5. Adsorption studies showed that the composite material had reduced adsorption capacities for both famotidine and methylene blue compared to GO and rGO. The available surface area was shown to play a key role in the adsorption potential with the free particles showing the highest adsorption of both contaminants, followed by the composite coated membranes and finally the free-standing films (Section 3.4).

6. A prototype incorporating nine composite coated membranes was effective at inactivating *E. coli* in up to 10L at a flow rate of 90ml/min and the prototype was shown to be capable of removing *Cryptosporidium* at a concentration of 10 oocysts/L. Copper leachate from the prototype was shown to be minimal with a maximum concentration of 1.3mg/L (Section 3.5.5).

Recommendations for future work

Areas of future development with the prototype include:

- The investigation of alternative methods for composite production. The use of alternative “greener” methods of composite production would reduce the environmental impact of the overall production process and yield a greater quantity of product per unit of energy used.

- The examination of the antibacterial effect against other micro-organisms. The examination of a suite of different microorganisms would give a good overall indication as to the biocidal potential of the graphene copper composite.

- The use of a more robust substrate for immobilisation. The use of different substrates may the the solution to the rupturing observed in the third prototype and improve the lifespan of the prototype.

- Alternative matrixes for flow-through testing such as different water types to examine membrane fouling. The investigation as to the impact of different water types on the performance of the unit would give a more robust understand as to the potential lifespan of the unit in a “real world” situation.

6. Bibliography

Aarestrup, F. M. & Hasman, H. (2004). Susceptibility of different bacterial species isolated from food animals to copper sulphate, zinc chloride and antimicrobial substances used for disinfection. *Veterinary Microbiology*, *100*(1-2), 83–9.

Agarwal, S., Zhou, X., Ye, F., He, Q., Chen, G. C. K., Soo, J. Chen, P. (2010). Interfacing live cells with nanocarbon substrates. *Langmuir*, *26*(4), 2244–2247.

Ahamed, M., Alsalhi, M. S., & Siddiqui, M. K. J. (2010). Silver nanoparticle applications and human health. *Clinica Chimica Acta; International Journal of Clinical Chemistry*, *411*(23-24), 1841–8.

Akbari, A., Sheath, P., Martin, S. T., Shinde, D. B., Shaibani, M., Banerjee, P. C., Majumder, M. (2016). Large-area graphene-based nanofiltration membranes by shear alignment of discotic nematic liquid crystals of graphene oxide. *Nature Communications*, *7*, 10891.

Akhavan, O. & Ghaderi, E. (2009). Photocatalytic Reduction of Graphene Oxide Nanosheets on TiO2 Thin Film for Photoinactivation of Bacteria in Solar Light Irradiation. *The Journal of Physical Chemistry C*, *113*, 20214–20220.

Akhavan, O. & Ghaderi, E. (2010). Toxicity of graphene and graphene oxide nanowalls against bacteria. *ACS Nano*, *4*(10), 5731–6.

Akhavan, O. & Ghaderi, E. (2012). Escherichia coli bacteria reduce graphene oxide to bactericidal graphene in a self-limiting manner. *Carbon*, *50*(5), 1853–1860.

Akhavan, O. Ghaderi, E., & Akhavan, A. (2012). Size-dependent genotoxicity of graphene nanoplatelets in human stem cells. *Biomaterials*, *33*(32), 8017–25.

Akhavan, O., Ghaderi, E. & Esfandiar, a. (2011). Wrapping bacteria by graphene nanosheets for isolation from environment, reactivation by sonication, and inactivation by near-infrared irradiation. *The Journal of Physical Chemistry. B*, *115*(19), 6279–88.

Allen, M. J., Tung, V. C., & Kaner, R. B. (2010). Honeycomb carbon: a review of graphene. *Chemical Reviews*, *110*(1), 132–45.

Andrews, J. M. (2001). JAC Determination of minimum inhibitory concentrations. *Journal of Antimicrobial Chemotherapy*, *48*, 5–16.

ASTM standard E2180-07. (2012). *"Standard Test Method for Determining the Activity of Incorporated Antimicrobial Agent(s) In Polymeric or Hydrophobic Materials."* ASTM International, West Conshohocken, PA, 2003.

Baek, Y. W., & An, Y. J. (2011). Microbial toxicity of metal oxide nanoparticles (CuO, NiO, ZnO, and Sb to Escherichia coli, Bacillus subtilis, and Streptococcus aureus. *Science of the Total Environment*, *409*(8), 1603–1608.

Bao, Q., Zhang, D., & Qi, P. (2011). Synthesis and characterization of silver nanoparticle and graphene oxide nanosheet composites as a bactericidal agent for water disinfection. *Journal of Colloid and Interface Science*, *360*(2), 463–70.

Barbolina, I., Woods, C. R., Lozano, N., Kostarelos, K., Novoselov, K. S., & Roberts, I. S. (2016). Purity of graphene oxide determines its antibacterial activity. *2D Materials*, *3*(2), 025025.

Beltrán, F. J., Pocostales, P., Alvarez, P., & Oropesa, A. (2009). Diclofenac removal from water with ozone and activated carbon. *Journal of Hazardous Materials*, *163*(2-3), 768–776.

Bianco, A., Cheng, H.-M., Enoki, T., Gogotsi, Y., Hurt, R. H., Koratkar, N., Zhang, J. (2013). All in the graphene family – A recommended nomenclature for two-dimensional carbon materials. *Carbon*, *65*, 1–6.

Bishop, J. B., Witt, K. L., & Sloane, R. a. (1997). *Genetic toxicities of human teratogens*. *Mutation Research - Fundamental and Molecular Mechanisms of Mutagenesis* (Vol. 396).

Bobbitt, J. a., & Betts, R. P. (1992). The removal of bacteria from solutions by membrane filtration. *Journal of Microbiological Methods*, *16*(3), 215–220.

Bonev, B., Hooper, J., & Parisot, J. (2008). Principles of assessing bacterial susceptibility to antibiotics using the agar diffusion method. *The Journal of Antimicrobial Chemotherapy*, *61*(6), 1295–301.

Bora, C., Bharali, P., Baglari, S., Dolui, S. K., & Konwar, B. K. (2013). Strong and conductive reduced graphene oxide/polyester resin composite films with improved mechanical strength, thermal stability and its antibacterial activity. *Composites Science and Technology*, *87*, 1–7.

Borkow, G. & Gabbay, J. (2005). Copper as a biocidal tool. *Current Medicinal Chemistry*, *12*(18), 2163–2175.

Brun, L. a., Maillet, J., Hinsinger, P., & Pépin, M. (2001). Evaluation of copper availability to plants in copper-contaminated vineyard soils. *Environmental Pollution*, *111*(2), 293–302.

Cai, X., Lin, M., Tan, S., Mai, W., Zhang, Y., Liang, Z., Zhang, X. (2012). The use of polyethyleneimine-modified reduced graphene oxide as a substrate for silver nanoparticles to produce a material with lower cytotoxicity and long-term antibacterial activity. *Carbon*, *50*(10), 3407–3415.

Cai, X., Tan, S., Lin, M., Xie, A., Mai, W., Zhang, X., Liu, Y. (2011). Synergistic antibacterial brilliant blue/reduced graphene oxide/quaternary phosphonium salt composite with excellent water solubility and specific targeting capability. *Langmuir : The ACS Journal of Surfaces and Colloids*, *27*(12), 7828–35.

Cai, X., Tan, S., Yu, A., Zhang, J., Liu, J., Mai, W., & Jiang, Z. (2012). Sodium 1-naphthalenesulfonate-functionalized reduced graphene oxide stabilizes silver nanoparticles with lower cytotoxicity and long-term antibacterial activity. *Chemistry – An Asian Journal*, *7*(7), 1664–1670.

Callaghan, M., Cormican, M., Prendergast, M., Pelly, H., Cloughley, R., Hanahoe, B., & O'Donovan, D. (2009). Temporal and spatial distribution of human cryptosporidiosis in the west of Ireland 2004-2007. *International Journal of Health Geographics*, *8*, 64.

Camper, A. (1986). Bacteria associated with granular activated carbon particles in drinking water. *Applied and Environmental Microbiology*, *52*(3), 434–438.

Cao, B., Cao, S., Dong, P., Gao, J., & Wang, J. (2013). High antibacterial activity of ultrafine TiO2/graphene sheets nanocomposites under visible light irradiation. *Materials Letters*, *93*, 349–352.

Carpenter, C., Fayer, R., Trout, J., & Beach, M. J. (1999). Chlorine disinfection of recreational water for Cryptosporidium parvum. *Emerging Infectious Diseases*, *5*(4), 579–584.

Carvalho, R.N. et al. (2015). *Development of the first Watch List under the Environmental Quality Standards Directive 2015 Report EUR*,

Casey, A., Herzog, E., Davoren, M., Lyng, F. M., Byrne, H. J., & Chambers, G. (2007). Spectroscopic analysis confirms the interactions between single walled carbon nanotubes and various dyes commonly used to assess cytotoxicity. *Carbon*, *45*(7), 1425–1432.

Chatterjee, A. K., Chakraborty, R., & Basu, T. (2014). Mechanism of antibacterial activity of copper nanoparticles. *Nanotechnology*, *25*(13), 135101.

Chauret, C. P., Radziminski, C. Z., Lepuil, M., Creason, R., & Andrews, R. C. (2001). Chlorine Dioxide Inactivation of Cryptosporidium parvum Oocysts and Bacterial Spore Indicators. *Applied and Environmental Microbiology*, *67*(7), 2993–3001. 3

Chen, H., Müller, M. B., Gilmore, K. J., Wallace, G. G., & Li, D. (2008). Mechanically strong, electrically conductive, and biocompatible graphene paper. *Advanced Materials*, *20*(18), 3557–3561.

Chen, Q., Zhang, L., & Chen, G. (2011). Facile preparation of graphene-copper nanoparticle composite by in situ chemical reduction for electrochemical sensing of carbohydrates. *Analytical Chemistry*, *84*, 171–178.

Chook, S. W., Chia, C. H., Zakaria, S., Ayob, M. K., Chee, K. L., Huang, N. M., Rahman, R. (2012). Antibacterial performance of Ag nanoparticles and AgGO nanocomposites prepared via rapid microwave-assisted synthesis method. *Nanoscale Research Letters*, *7*(1), 541.

Christian, P., & Bromfield, M. (2010). Preparation of small silver, gold and copper nanoparticles which disperse in both polar and non-polar solvents. *Journal of Materials Chemistry*, *20*(6), 1135.

Chu, K., & Jia, C. (2014). Enhanced strength in bulk graphene-copper composites. *Physica Status Solidi (A) Applications and Materials Science*, *211*(1), 184–190.

Chua, C. K., & Pumera, M. (2013). Reduction of graphene oxide with substituted borohydrides. *Journal of Materials Chemistry A*, *1*(5), 1892.

Clift, M. J. D., Raemy, D. O., Endes, C., Ali, Z., Lehmann, A. D., Brandenberger, C., Rothen-Rutishauser, B. (2012). Can the Ames test provide an insight into nano-object mutagenicity? Investigating the interaction between nano-objects and bacteria. *Nanotoxicology*, *7*(February), 1–13.

Cohen-Tanugi, D., & Grossman, J. C. (2012). Water desalination across nanoporous graphene. *Nano Letters*, *12*(7), 3602–3608.

Cummins, E., Kennedy, R., & Cormican, M. (2010). Quantitative risk assessment of Cryptosporidium in tap water in Ireland. *Science of the Total Environment*, *408*(4), 740–753.

Dai, C., Yang, X., & Xie, H. (2011). One-step synthesis of reduced graphite oxide–silver nanocomposite. *Materials Research Bulletin*, *46*(11), 2004–2008.

Das, M. R., Sarma, R. K., Borah, S. C., Kumari, R., Saikia, R., Deshmukh, A. B., Boukherroub, R. (2013). The synthesis of citrate-modified silver nanoparticles in an aqueous suspension of graphene oxide nanosheets and their antibacterial activity. *Colloids and Surfaces. B, Biointerfaces*, *105*, 128–36.

Das, M. R., Sarma, R. K., Saikia, R., Kale, V. S., Shelke, M. V, & Sengupta, P. (2011). Synthesis of silver nanoparticles in an aqueous suspension of graphene oxide sheets and its antimicrobial activity. *Colloids and Surfaces. B, Biointerfaces*, *83*(1), 16–22.

De Faria, A. F., Martinez, D. S. T., Meira, S. M. M., de Moraes, A. C. M., Brandelli, A., Filho, A. G. S., & Alves, O. L. (2013). Anti-adhesion and antibacterial activity of silver nanoparticles supported on graphene oxide sheets. *Colloids and Surfaces. B, Biointerfaces*, *113C*, 115–124.

Dehnavi, A. S., Aroujalian, A., Raisi, A., & Fazel, S. (2013). Preparation and characterization of polyethylene/silver nanocomposite films with antibacterial activity. *Journal of Applied Polymer Science*, *127*(2), 1180–1190.

Dellieu, L., Lawarée, E., Reckinger, N., Didembourg, C., Letesson, J., Sarrazin, M., Colomer, J. F. (2015). Do CVD grown graphene films have antibacterial activity on metallic substrates? *Carbon*, *84*, 310–316.

Deng, C.-H., Gong, J.-L., Zeng, G.-M., Niu, C.-G., Niu, Q.-Y., Zhang, W., & Liu, H.-Y. (2014). Inactivation performance and mechanism of Escherichia coli in aqueous system exposed to iron oxide loaded graphene nanocomposites. *Journal of Hazardous Materials*, *276*, 66–76.

Dinh, N. X., Chi, D. T., Lan, N. T., Lan, H., Van Tuan, H., Van Quy, N., Le, A.-T. (2015). Water-dispersible silver nanoparticles-decorated carbon nanomaterials: synthesis and enhanced antibacterial activity. *Applied Physics A*, *119*(1), 85–95.

Driedger, A., Staub, E., Pinkernell, U., Mariñas, B., Köster, W., & Gunten, U. Von. (2001). Inactivation of bacillus subtilis spores and formation of bromate during ozonation. *Water Research*, *35*(12), 2950–2960.

Duffy, M. (2015). "Tests confirm presence of Cryptosporidium in Westport water supply" Retrieved May 15, 2015 from http://www.mayonews.ie/news/21957-tests-confirm-presence-of-cryptosporidium-in-westport-water-supply

Durán, N., Marcato, P., & Conti, R. De. (2010). Potential use of silver nanoparticles on pathogenic bacteria, their toxicity and possible mechanisms of action. *Journal of Brazilian Chemistry*, *21*(6), 949–959.

Eda, G., & Chhowalla, M. (2010). Chemically derived graphene oxide: towards large-area thin-film electronics and optoelectronics. *Advanced Materials*, *22*(22), 2392–415.

Eigler, S., Grimm, S., Enzelberger-Heim, M., Muller, P., & Hirsch, A. (2013). Graphene oxide: efficiency of reducing agents. *Chemistry Communications*, *49*(67), 7391–7393.

Espírito Santo, C., Lam, E. W., Elowsky, C. G., Quaranta, D., Domaille, D. W., Chang, C. J., & Grass, G. (2011). Bacterial killing by dry metallic copper surfaces. *Applied and Environmental Microbiology*, *77*(3), 794–802.

Fang, J., Lyon, D. Y., Wiesner, M. R., Dong, J., & Alvarez, P. J. J. (2007). Effect of a fullerene water suspension on bacterial phospholipids and membrane phase behavior. *Environmental Science and Technology*, *41*(7), 2636–2642.

Feng, L., Chen, Y., & Chen, L. (2011). Easy-to-Operate and Low-Temperature Synthesis ofGram-Scale Nitrogen-Doped Graphene and Its Application as Cathode Catalyst in Microbial Fuel Cells. *ACS Nano*, *5*(12), 9611–9618.

Fuente, E., Menéndez, J. a., Díez, M. a., Suárez, D., & Montes-Morán, M. a. (2003). Infrared Spectroscopy of Carbon Materials: A Quantum Chemical Study of Model Compounds. *Journal of Physical Chemistry B*, *107*, 6350–6359.

Gaetke, L., & Kung Chow, C. (2003). Copper toxicity, oxidative stress, and antioxidant nutrients. *Toxicology*, *189*(1-2), 147–163.

Gao, J., Bao, F., Feng, L., Shen, K., Zhu, Q., Wang, D., Yan, C. (2011). Functionalized graphene oxide modified polysebacic anhydride as drug carrier for levofloxacin controlled release. *RSC Advances*, *1*(9), 1737.

Gao, J., Liu, F., Liu, Y., Ma, N., Wang, Z., & Zhang, X. (2010). Environment-friendly method to produce graphene that employs vitamin C and amino acid. *Chemistry of Materials*, *22*(7), 2213–2218.

Gao, P., Ng, K., & Sun, D. D. (2013). Sulfonated graphene oxide-ZnO-Ag photocatalyst for fast photodegradation and disinfection under visible light. *Journal of Hazardous Materials*, *262*, 826–35.

Graphene-Flagship.eu. (2013). Graphene-Flagship. Retrieved November 12, 2013, from http://graphene-flagship.eu/

Grass, G., Rensing, C., & Solioz, M. (2011). Metallic copper as an antimicrobial surface. *Applied and Environmental Microbiology*, *77*(5), 1541–7.

Gurunathan, S., Han, J. W., Dayem, A. A., Eppakayala, V., & Kim, J.-H. (2012). Oxidative stress-mediated antibacterial activity of graphene oxide and reduced graphene oxide in Pseudomonas aeruginosa. *International Journal of Nanomedicine*, *7*, 5901–14.

Gurunathan, S., Han, J. W., Dayem, A. A., Eppakayala, V., Park, M.-R., Kwon, D.-N., & Kim, J.-H. (2013). Antibacterial activity of dithiothreitol reduced graphene oxide. *Journal of Industrial and Engineering Chemistry*, *19*(4), 1280–1288.

Halliwell, B., & Gutteridge, J. M. C. (1984). Oxygen toxicity, oxygen radical, transition metals and disease. *Biochemical Journal*, *219*, 1–14.

Han, Y., Luo, Z., Yuwen, L., Tian, J., Zhu, X., & Wang, L. (2013). Synthesis of silver nanoparticles on reduced graphene oxide under microwave irradiation with starch as an ideal reductant and stabilizer. *Applied Surface Science*, *266*, 188–193.

Hans, M., Erbe, A., Mathews, S., & Chen, Y. (2013). Role of copper oxides in contact killing of bacteria. *Langmuir*, *29*, 16160–16166.

Harley, J. P., & Prescott, L. M. (1990). *Laboratory exercises in microbiology*. Wm. C. Brown Publishers.

He, G., Wu, H., Ma, K., Wang, L., Sun, X., Chen, H., & Wang, X. (2013). Photosynthesis of Multiple Valence Silver Nanoparticles on Reduced Graphene Oxide Sheets With Enhanced Antibacterial Activity. *Synthesis and Reactivity in Inorganic, Metal-Organic, and Nano-Metal Chemistry*, *43*(4), 440–445.

He, W., Huang, H., Yan, J., & Zhu, J. (2013). Photocatalytic and antibacterial properties of Au-TiO2 nanocomposite on monolayer graphene: From experiment to theory. *Journal of Applied Physics*, *204701*, 1–13.

Hegab, H. M., Elmekawy, A., Zou, L., Mulcahy, D., Saint, C. P., & Ginic-Markovic, M. (2016). The controversial antibacterial activity of graphene-based materials. *Carbon*, *105*, 362–376.

Hong, B., Jung, H., & Byun, H. (2013). Preparation of Polyvinylidene Fluoride Nanofiber Membrane and Its Antibacterial Characteristics with Nanosilver or Graphene Oxide. *Journal of Nanoscience and Nanotechnology*, *13*(9), 6269–6274(6).

Hu, M., & Mi, B. (2013). Enabling graphene oxide nanosheets as water separation membranes. *Environmental Science and Technology*, *47*(8), 3715–3723.

Hu, W., Peng, C., Luo, W., Lv, M., Li, X., Li, D., Fan, C. (2010). Graphene-based antibacterial paper. *ACS Nano*, *4*(7), 4317–23.

Hui, L., Piao, J.-G., Auletta, J., Hu, K., Zhu, Y., Meyer, T., Yang, L. (2014). Availability of the basal planes of graphene oxide determines whether it is antibacterial. *ACS Applied Materials & Interfaces*, *6*(15), 13183–90.

Hummers Jr, W. S., & Offeman, R. E. (1958). Preparation of graphitic oxide. *Journal of the American Chemical Society*, *80*(6), 1339–1339.

Irish Water. (2016). What is tested for in drinking water? Retrieved December 21, 2016, from https://www.water.ie/water-supply/water-quality/parameters/

Jauris, I. M., Matos, C. F., Saucier, C., Lima, E. C., Zarbin, a J. G., Fagan, S. B., Zanella, I. (2016). Adsorption of sodium diclofenac on graphene: a combined experimental and theoretical study. *Physical Chemistry Chemical Physics*, *18*(3), 1526–1536.

Jelic, A., Gros, M., Ginebreda, A., Cespedes-Sánchez, R., Ventura, F., Petrovic, M., & Barcelo, D. (2011). Occurrence, partition and removal of pharmaceuticals in sewage water and sludge during wastewater treatment. *Water Research*, *45*(3), 1165–1176.

Jia, G., Wang, H., Yan, L., & Wang, X. (2005). Cytotoxicity of carbon nanomaterials: single-wall nanotube, multi-wall nanotube, and fullerene. *Environmental Science & Technology*, *39*(5), 1378–83.

Jiang, B., Tian, C., Song, G., Chang, W., Wang, G., Wu, Q., & Fu, H. (2012). A novel Ag/graphene composite: facile fabrication and enhanced antibacterial properties. *Journal of Materials Science*, *48*(5), 1980–1985.

Jiang, B., Tian, C., Song, G., Chang, W., Wang, G., Wu, Q., & Fu, H. (2013). A novel Ag/graphene composite: facile fabrication and enhanced antibacterial properties. *Journal of Materials Science*, *48*(5), 1980–1985.

Jiang, Q., Tian, L., Liu, K. K., Tadepalli, S., Raliya, R., Biswas, P. & Singamaneni, S. (2016). Bilayered Biofoam for Highly Efficient Solar Steam Generation. *Advanced Materials*, *28*(42), 9400–9407.

Jiao, Y., Qian, F., Li, Y., Wang, G., Saltikov, C. W. & Gralnick, J. A. (2011). Deciphering the electron transport pathway for graphene oxide reduction by Shewanella oneidensis MR-1. *Journal of Bacteriology*, *193*(14), 3662–5.

Kang, S., Herzberg, M., Rodrigues, D. F. & Elimelech, M. (2008). Antibacterial effects of carbon nanotubes: size does matter! *Langmuir : The ACS Journal of Surfaces and Colloids*, *24*(13), 6409–13.

Kang, S., & Mauter, M. S. (2009). Microbial Cytotoxicity of Carbon-Based Nanomaterials : Implications for River Water and Wastewater Effluent. *Environmental Science and Technology*, *43*(7), 2648–2653.

Kang, S., Pinault, M., Pfefferle, L. D. & Elimelech, M. (2007). Single-Walled Carbon Nanotubes Exhibit Strong Antimicrobial Activity. *Langmuir*, *23*, 8670–8673.

Kavitha, T., Gopalan, A. I., Lee, K. P., & Park, S.Y. (2012). Glucose sensing, photocatalytic and antibacterial properties of graphene–ZnO nanoparticle hybrids. *Carbon*, *50*(8), 2994–3000.

Keane, D., Basha, S., Nolan, K., Morrissey, A., Oelgemöller, M., & Tobin, J. M. (2011). Photodegradation of famotidine by integrated photocatalytic adsorbent (IPCA) and kinetic study. *Catalysis Letters*, *141*(2), 300–308.

Kellici, S., Acord, J., Ball, J., Reehal, H. S., Morgan, D., & Saha, B. (2014). A single rapid route for the synthesis of reduced graphene oxide with antibacterial activities. *RSC Advances*, *4*, 14858–14861.

Kelly, L. (2014). “Cryptosporidium will continue to contaminate unless drastic improvements are made.” Retrieved January 1, 2015, from http://www.independent.ie/irish-news/cryptosporidium-will-continue-to-contaminate-unless-drastic-improvements-are-made-expert-30627797.html

Kemp, K. C., Seema, H., Saleh, M., Le, N. H., Mahesh, K., Chandra, V., & Kim, K. S. (2013). Environmental applications using graphene composites: water remediation and gas adsorption. *Nanoscale*, *5*(8), 3149–71.

Khanra, P., Kuila, T., Kim, N. H., Bae, S. H., Yu, D., & Lee, J. H. (2012). Simultaneous bio-functionalization and reduction of graphene oxide by baker’s yeast. *Chemical Engineering Journal*, *183*, 526–533.

Kholmanov, I. N., Stoller, M. D., Edgeworth, J., Lee, W. H., Li, H., Lee, J., Stoller, M. (2012). Nanostructured Hybrid Transparent Conductive films with antibacterial properties. *ACS Nano*, *6*(6), 5157–5163.

Krishnamoorthy, K., Veerapandian, M., Zhang, L. H., Yun, K., & Kim, S. J. (2012). Antibacterial Efficiency of Graphene Nanosheets against Pathogenic Bacteria via Lipid Peroxidation. *The Journal of Physical Chemistry C*, *116*(32), 17280–17287.

Kumar, S., Ghosh, S., Munichandraiah, N., & Vasan, H. N. (2013). 1.5 V battery driven reduced graphene oxide-silver nanostructure coated carbon foam (rGO-Ag-CF) for the purification of drinking water. *Nanotechnology*, *24*(23), 235101.

Kuuliala, L., Pippuri, T., Hultman, J., Auvinen, S. M., Kolppo, K., Nieminen, T., Jääskeläinen, E. (2015). Preparation and antimicrobial characterization of silver-containing packaging materials for meat. *Food Packaging and Shelf Life*, *6*, 53–60.

Kvitek, L., & Panáček, A. (2008). Effect of surfactants and polymers on stability and antibacterial activity of silver nanoparticles (NPs). *The Journal of Physical Chemistry C*, *112*, 5825–5834.

Lai, Q., Zhu, S., Luo, X., Zou, M., & Huang, S. (2012). Ultraviolet-visible spectroscopy of graphene oxides. *AIP Advances*, *2*(3), 032146.

Landrygan, J., James, P. a, Brooks, D., & Kubiak, E. M. (2002). Reproducibility of control organism zone diameters for batches of IsoSensitest agar manufactured from 1996 to 2000 using the BSAC disc susceptibility test method. *The Journal of Antimicrobial Chemotherapy*, *49*, 391–394.

LeChevallier, M. (1984). Disinfection of bacteria attached to granular activated carbon. *Applied and Environmental Microbiology*, *48*(5), 918–923.

LeChevallier, M. (1988). Inactivation of biofilm bacteria. *Applied and Environmental Microbiology*, *54*(10), 2492–2499.

Lee, J. S., You, K. H., & Park, C. B. (2012). Highly photoactive, low bandgap TiO_2 nanoparticles wrapped by graphene. *Advanced Materials*, *24*(8), 1084–1088.

Li, D., Müller, M. B., Gilje, S., Kaner, R. B., & Wallace, G. G. (2008). Processable aqueous dispersions of graphene nanosheets. *Nature Nanotechnology*, *3*(2), 101–5.

Li, J., Wang, G., Zhu, H., Zhang, M., Zheng, X., Di, Z., Wang, X. (2014). Antibacterial activity of large-area monolayer graphene film manipulated by charge transfer. *Scientific Reports*, *4*, 4359.

Li, Q., Mahendra, S., Lyon, D. Y., Brunet, L., Liga, M. V, Li, D., & Alvarez, P. J. (2008). Antimicrobial nanomaterials for water disinfection and microbial control: potential applications and implications. *Water Research*, *42*(18), 4591–602.

Li, S.-K., Yan, Y.-X., Wang, J.-L., & Yu, S.H. (2013). Bio-inspired in situ growth of monolayer silver nanoparticles on graphene oxide paper as multifunctional substrate. *Nanoscale*, *5*(24), 12616–23.

Li, X., Cai, W., An, J., Kim, S., Nah, J., Yang, D., Ruoff, R. S. (2009). Large-area synthesis of high-quality and uniform graphene films on copper foils. *Science*, *324*(5932), 1312–4.

Lim, H. N., Huang, N. M., & Loo, C. H. (2012). Facile preparation of graphene-based chitosan films: Enhanced thermal, mechanical and antibacterial properties. *Journal of Non-Crystalline Solids*, *358*(3), 525–530.

Lin, S., & Shih, C. (2011). Molecular insights into the surface morphology, layering structure, and aggregation kinetics of surfactant-stabilized graphene dispersions. *Journal of the American Chemical Society* , *133*, 12810–12823.

Lin, Y. E., Stout, J. E., Yu, V. L., LinPhD, Y. E., StoutPhD, J. E., YuMD, V. L., Yu, V. L. (2015). Controlling Legionella in Hospital Drinking Water: An Evidence-Based Review of Disinfection Methods. *Infection Control & Hospital Epidemiology*, *32*(02), 166–173.

Liu, J., Bai, H., Wang, Y., Liu, Z., Zhang, X., & Sun, D. D. (2010). Self-assembling tio2 nanorods on large graphene oxide sheets at a two-phase interface and their anti-recombination in photocatalytic applications. *Advanced Functional Materials*, *20*(23), 4175–4181.

Liu, L., Bai, H., Liu, J., & Sun, D. D. (2013). Multifunctional graphene oxide-TiO2-Ag nanocomposites for high performance water disinfection and decontamination under solar irradiation. *Journal of Hazardous Materials*, *261*, 214–23.

Liu, L., Liu, J., & Sun, D. D. (2012). Graphene oxide enwrapped Ag3PO4 composite: towards a highly efficient and stable visible-light-induced photocatalyst for water purification. *Catalysis Science & Technology*, *2*, 2525–2532.

Liu, L., Liu, J., Wang, Y., Yan, X., & Sun, D. D. (2011). Facile synthesis of monodispersed silver nanoparticles on graphene oxide sheets with enhanced antibacterial activity. *New Journal of Chemistry*, *35*(7), 1418.

Liu, S., Hu, M., Zeng, T. H., Wu, R., Jiang, R., Wei, J., Chen, Y. (2012). Lateral dimension-dependent antibacterial activity of graphene oxide sheets. *Langmuir : The ACS Journal of Surfaces and Colloids*, *28*(33), 12364–72.

Liu, S., Ng, A. K., Xu, R., Wei, J., Tan, C. M., Yang, Y., & Chen, Y. (2010). Antibacterial action of dispersed single-walled carbon nanotubes on Escherichia coli and Bacillus subtilis investigated by atomic force microscopy. *Nanoscale*, *2*(12), 2744–50.

Liu, S., Zeng, T. H., Hofmann, M., Burcombe, E., Wei, J., Jiang, R., Chen, Y. (2011). Antibacterial activity of graphite, graphite oxide, graphene oxide, and reduced graphene oxide: membrane and oxidative stress. *ACS Nano*, *5*(9), 6971–80.

Liu, X., Liu, J., Zhan, D., Yan, J., Wang, J., Chao, D., Shen, Z. (2013). Repeated microwave-assisted exfoliation of expandable graphite for the preparation of large scale and high quality multi-layer graphene. *RSC Advances*, *3*(29), 11601.

Loh, K. P., Bao, Q., Ang, P. K., & Yang, J. (2010). The chemistry of graphene. *Journal of Materials Chemistry*, *20*(12), 2277.

Lu, B., Li, T., Zhao, H., Li, X., Gao, C., Zhang, S., & Xie, E. (2012). Graphene-based composite materials beneficial to wound healing. *Nanoscale*, *4*(9), 2978.

Luo, Z., Lu, Y., Somers, L. A., & Johnson, C. (2009). High yield preparation of macroscopic graphene oxide membranes. *Journal of the American Chemical Society*, *131*(3), 898–899.

Luty-Błocho, M., Fitzner, K., Hessel, V., Löb, P., Maskos, M., Metzke, D., Wojnicki, M. (2011). Synthesis of gold nanoparticles in an interdigital micromixer using ascorbic acid and sodium borohydride as reducers. *Chemical Engineering Journal*, *171*(1), 279–290.

Lyon, D. Y., & Alvarez, P. J. J. (2008). Fullerene Water Suspension (nC 60) Exerts Antibacterial Effects via ROS-Independent Protein Oxidation. *Environmental Science and Technology*, *42*(21), 8127–8132.

Ma, J., Zhang, J., Xiong, Z., Yong, Y., & Zhao, X. S. (2011). Preparation, characterization and antibacterial properties of silver-modified graphene oxide. *Journal of Materials Chemistry*, *21*(10), 3350.

Macguire, E., & Knight, M. "*Graphene the nano-sized material with a massive future*" Retrieved April 30, 2014, from http://edition.cnn.com/2013/04/29/tech/graphene-miracle-material/

Magaldi, S., Mata-Essayag, S., Hartung de Capriles, C., Perez, C., Colella, M., Olaizola, C., & Ontiveros, Y. (2004). Well diffusion for antifungal susceptibility testing. *International Journal of Infectious Diseases*, *8*(1), 39–45.

Maliyekkal, S. M., Sreeprasad, T. S., Krishnan, D., Kouser, S., Mishra, A. K., Waghmare, U. V, & Pradeep, T. (2013). Graphene: a reusable substrate for unprecedented adsorption of pesticides. *Small*, *9*(2), 273–83.

Mangadlao, J. D., Santos, C. M., Felipe, M. J. L., de Leon, a C. C., Rodrigues, D. F., & Advincula, R. C. (2015). On the antibacterial mechanism of graphene oxide (GO) Langmuir-Blodgett films. *Chemical Communications*, *51*(14), 2886–9.

Marambio-Jones, C., & Hoek, E. M. V. (2010). A review of the antibacterial effects of silver nanomaterials and potential implications for human health and the environment. *Journal of Nanoparticle Research*, *12*(5), 1531–1551.

Maron, D. M., & Ames, B. N. (1983). Revised methods for the Salmonella mutagenicity test. *Mutation Research*, *113*(3-4), 173–215.

Martínez-Castañón, G. a., Niño-Martínez, N., Martínez-Gutierrez, F., Martínez-Mendoza, J. R., & Ruiz, F. (2008). Synthesis and antibacterial activity of silver nanoparticles with different sizes. *Journal of Nanoparticle Research*, *10*(8), 1343–1348.

Mei, X., & Ouyang, J. (2011). Ultrasonication-assisted ultrafast reduction of graphene oxide by zinc powder at room temperature. *Carbon*, *49*(15), 5389–5397.

Mejías Carpio, I. E., Santos, C. M., Wei, X., & Rodrigues, D. F. (2012). Toxicity of a polymer-graphene oxide composite against bacterial planktonic cells, biofilms, and mammalian cells. *Nanoscale*, *4*(15), 4746–56.

Meyer, J. C., Geim, a K., Katsnelson, M. I., Novoselov, K. S., Booth, T. J., & Roth, S. (2007). The structure of suspended graphene sheets. *Nature*, *446*(7131), 60–3.

Mohan, R., Shanmugharaj, a M., & Sung Hun, R. (2011). An efficient growth of silver and copper nanoparticles on multiwalled carbon nanotube with enhanced antimicrobial activity. *Journal of Biomedical Materials Research. Part B, Applied Biomaterials*, *96*(1), 119–26.

Mohanty, N., & Berry, V. (2008). Graphene-based single-bacterium resolution biodevice and DNA transistor: Interfacing graphene derivatives with nanoscale and microscale biocomponents. *Nano Letters*, *8*(12), 4469–4476.

Mondal, T., Bhowmick, A. K., & Krishnamoorti, R. (2012). Chlorophenyl pendant decorated graphene sheet as a potential antimicrobial agent: synthesis and characterization. *Journal of Materials Chemistry*, *22*(42), 22481.

Morones, J. R., Elechiguerra, J. L., Camacho, A., Holt, K., Kouri, J. B., Ramírez, J. T., & Yacaman, M. J. (2005). The bactericidal effect of silver nanoparticles. *Nanotechnology*, *16*(10), 2346–53.

Mortelmans, K., & Riccio, E. S. (2000). The bacterial tryptophan reverse mutation assay with Escherichia coli WP2. *Mutation Research*, *455*(1-2), 61–9.

Musico, Y. L. F., Santos, C. M., Dalida, M. L. P., & Rodrigues, D. F. (2014). Surface modification of membrane filters using graphene and graphene oxide-based nanomaterials for bacterial inactivation and removal. *Sustainable Chemistry & Engineering*, (2), 1559–1565.

Narayan, R. (2010). Use of nanomaterials in water purification. *Materials Today*, *13*(6), 44–46.

Nguyen, D. D., Tai, N. H., Lee, S.B., & Kuo, W.-S. (2012). Superhydrophobic and superoleophilic properties of graphene-based sponges fabricated using a facile dip coating method. *Energy & Environmental Science*, *5*(7), 7908.

Nguyen, V. H., Kim, B.K., Jo, Y.-L., & Shim, J.J. (2012). Preparation and antibacterial activity of silver nanoparticles-decorated graphene composites. *The Journal of Supercritical Fluids*, *72*, 28–35.

Nieminski, E. C., Bellamy, W. D., & Moss, L. R. (2000). Using surrogates to improve plant performance. *Journal / American Water Works Association*, *92*(3), 67–78.

Novoselov, K., Geim, A., & Morozov, S. (2004). Electric field effect in atomically thin carbon films. *Science*, *306*(5696), 666–669.

Novoselov, K., & Jiang, D. (2005). Two-dimensional atomic crystals. *Proceeedings of the National Academy of Sciences of the USA*, *102*(30), 10451–10453.

Oberdörster, G., Stone, V., & Donaldson, K. (2007). Toxicology of nanoparticles: A historical perspective. *Nanotoxicology*, *1*(1), 2–25.

Ocsoy, I., Paret, M. L., Ocsoy, M. A., Kunwar, S., Chen, T., You, M., & Tan, W. (2013). Nanotechnology in Plant Disease Management: DNA-Directed Silver Nanoparticles on Graphene Oxide as an Antibacterial against Xanthomonas perforans. *ACS Nano*, *7*(10), 8972–80.

Ocsoy, I., Paret, M., Ocsoy, M., & Kunwar, S. (2013). Nanotechnology in plant disease management: DNA-directed silver nanoparticles on graphene oxide as an antibacterial against Xanthomonas perforans. *ACS Nano*, (10), 8972–8980.

Ouyang, Y., Cai, X., Shi, Q., Liu, L., Wan, D. & Tan, S. (2013). Poly-L-lysine-modified reduced graphene oxide stabilizes the copper nanoparticles with higher water-solubility and long-term additively antibacterial activity. *Colloids and Surfaces. B, Biointerfaces*, *107*, 107–14.

Pal, S., Tak, Y. K., & Song, J. M. (2007). Does the antibacterial activity of silver nanoparticles depend on the shape of the nanoparticle? A study of the Gram-negative bacterium Escherichia coli. *Applied and Environmental Microbiology*, *73*(6), 1712–20.

Panáček, A., Kvitek, L., & Prucek, R. (2006). Silver colloid nanoparticles: synthesis, characterization, and their antibacterial activity. *The Journal of Physical Chemistry. B*, *110*, 16248–16253.

Pandey, H., Parashar, V., Parashar, R., Prakash, R., Ramteke, P. W., & Pandey, A. C. (2011). Controlled drug release characteristics and enhanced antibacterial effect of graphene nanosheets containing gentamicin sulfate. *Nanoscale*, *3*(10), 4104–8.

Pant, B., Pokharel, P., Tiwari, A. P., Saud, P. S., Park, M., Ghouri, Z. K., Kim, H.-Y. (2015). Characterization and antibacterial properties of aminophenol grafted and Ag NPs decorated graphene nanocomposites. *Ceramics International*, *41*(4), 5656–5662.

Paredes, J. & Villar-Rodil, S. (2008). Graphene oxide dispersions in organic solvents. *Langmuir*, (24), 10560–10564.

Park, S., An, J., Potts, J. R., Velamakanni, A., Murali, S., & Ruoff, R. S. (2011). Hydrazine-reduction of graphite- and graphene oxide. *Carbon*, *49*(9), 3019–3023.

Park, S., Mohanty, N., Suk, J. W., Nagaraja, A., An, J., Piner, R. D., Ruoff, R. S. (2010). Biocompatible, robust free-standing paper composed of a TWEEN/graphene composite. *Advanced Materials, 22*(15), 1736–40.

Peplow, M. (2013). The quest for super carbon. *Nature*, *503*, 327–329.

Pinto, A. M., Gonçalves, I. C., & Magalhães, F. D. (2013). Graphene-based materials biocompatibility: A review. *Colloids and Surfaces B: Biointerfaces*, *111*, 188–202.

Radjenović, J., Petrović, M., & Barceló, D. (2009). Fate and distribution of pharmaceuticals in wastewater and sewage sludge of the conventional activated sludge (CAS) and advanced membrane bioreactor (MBR) treatment. *Water Research*, *43*(3), 831–841.

Raj Pant, H., Pant, B., Joo Kim, H., Amarjargal, A., Hee Park, C., Tijing, L. D., Sang Kim, C. (2013). A green and facile one-pot synthesis of Ag–ZnO/RGO nanocomposite with effective photocatalytic activity for removal of organic pollutants. *Ceramics International*, *39*(5), 5083–5091. d

Ramesha, G. K., Vijaya Kumara, a., Muralidhara, H. B., & Sampath, S. (2011). Graphene and graphene oxide as effective adsorbents toward anionic and cationic dyes. *Journal of Colloid and Interface Science*, *361*(1), 270–277.

Reasoner, D. J., & Geldreich, E. E. (1985). A new medium for the enumeration and subculture of bacteria from potable water. *Applied and Environmental Microbiology*, *49*(1), 1–7.

Ren, G., Hu, D., Cheng, E. W. C., Vargas-Reus, M. a, Reip, P., & Allaker, R. P. (2009). Characterisation of copper oxide nanoparticles for antimicrobial applications. *International Journal of Antimicrobial Agents*, *33*(6), 587–90.

Rice, E. W., Fox, K. R., Miltner, R. J., Lytle, D. a., & Johnson, C. H. (1996). Evaluating plant performance with endospores. *Journal / American Water Works Association*, *88*(9), 122–130.

Richardson, S. D., Fasano, F., Ellington, J. J., Crumley, F. G., Buettner, K. M., Evans, J. J., Plewa, M. J. (2008). Occurrence and mammalian cell toxicity of iodinated disinfection byproducts in drinking water. *Environmental Science and Technology*, *42*(22), 8330–8338.

Richardson, S. D., Plewa, M. J., Wagner, E. D., Schoeny, R., & DeMarini, D. M. (2007). Occurrence, genotoxicity, and carcinogenicity of regulated and emerging disinfection by-products in drinking water: A review and roadmap for research. *Mutation Research - Reviews in Mutation Research*, *636*(1-3), 178–242.

Rispoli, F., Angelov, A., Badia, D., Kumar, A., Seal, S., & Shah, V. (2010). Understanding the toxicity of aggregated zero valent copper nanoparticles against Escherichia coli. *Journal of Hazardous Materials*, *180*(1-3), 212–6.

Rivera-Utrilla, J., Sánchez-Polo, M., Ferro-García, M. Á., Prados-Joya, G., & Ocampo-Pérez, R. (2013). Pharmaceuticals as emerging contaminants and their removal from water. A review. *Chemosphere*, *93*(7), 1268–1287.

Rizzo, L., Manaia, C., Merlin, C., Schwartz, T., Dagot, C., Ploy, M. C., Fatta-Kassinos, D. (2013). Urban wastewater treatment plants as hotspots for antibiotic resistant bacteria and genes spread into the environment: A review. *Science of the Total Environment*, *447*, 345–360.

Rompré, A., Servais, P., & Baudart, J. (2002). Detection and enumeration of coliforms in drinking water: current methods and emerging approaches. *Journal of Microbiological methods*, *49*, 31–54.

Ruiz, O. N., Fernando, K. a S., Wang, B., Brown, N. a, Luo, P. G., McNamara, N. D., Bunker, C. E. (2011). Graphene oxide: a nonspecific enhancer of cellular growth. *ACS Nano*, *5*(10), 8100–7.

Ruparelia, J. P., Chatterjee, A. K., Duttagupta, S. P., & Mukherji, S. (2008). Strain specificity in antimicrobial activity of silver and copper nanoparticles. *Acta Biomaterialia*, *4*(3), 707–16.

Russell, M. A; Clark, B. J; Ultraviolet Spectrometry Group (Great Britain); Frost, T. (1993). *UV spectroscopy: techniques, instrumentation, data handling* (1st ed.). London, New York: Chapman & Hall 1993.

Salas, E. C., Sun, Z., Lu, A., & Tour, J. M. (2010). Reduction of Graphene Oxide via Bacterial Respiration. *ACS Nano*, *4*(8), 4852–4856.

Salavati-Niasari, M., & Davar, F. (2009). Synthesis of copper and copper(I) oxide nanoparticles by thermal decomposition of a new precursor. *Materials Letters*, *63*(3-4), 441–443.

Sedki, M., Mohamed, M. B., Fawzy, M., Abdelrehim, D. a., & Abdel-Mottaleb, M. M. S. a. (2015). Phytosynthesis of silver–reduced graphene oxide (Ag–RGO) nanocomposite with an enhanced antibacterial effect using Potamogeton pectinatus extract. *RSC Advances*, *5*(22), 17358–17365.

Shang, Y. U., Zhang, D., Liu, Y., & Guo, C. (2015). Preliminary comparison of different reduction methods of graphene oxide. *Bulletin of Material Science*, *38*(1), 7–12.

Shen, J., Li, T., Shi, M., Li, N., & Ye, M. (2012). Polyelectrolyte-assisted one-step hydrothermal synthesis of Ag-reduced graphene oxide composite and its antibacterial properties. *Materials Science and Engineering C*, *32*(7), 2042–2047.

Shen, J., Shi, M., Li, N., Yan, B., Ma, H., Hu, Y., & Ye, M. (2010). Facile synthesis and application of Ag-chemically converted graphene nanocomposite. *Nano Research*, *3*, 339–349.

Shih, C., & Lin, S. (2010). Understanding the stabilization of liquid-phase-exfoliated graphene in polar solvents: molecular dynamics simulations and kinetic theory of colloid aggregation. *Journal of the American Chemical Society*, (132), 14638–14648.

Shukman, D. (2013). "*Is graphene really a wonder-material?*" Retrieved January 15, 2014, from http://www.bbc.co.uk/news/science-environment-21014297

Simon-Deckers, A., Loo, S., & Mayne L'Hermite, M. (2009). Size-, composition-and shape-dependent toxicological impact of metal oxide nanoparticles and carbon nanotubes toward bacteria. *Environmental Science & Technology*, *43*, 8423–8429.

Some, S., Ho, S., Dua, P., Hwang, E., & Shin, Y. (2012). Dual Functions of Highly Potent Graphene Derivative-Poly-L-Lysine Composites to Inhibit Bacteria and Support Human Cells. *ACS Nano*, *6*(8), 7151–7161.

Song, J., Wang, X., & Chang, C.T. (2007). Preparation and characterization of graphene oxide paper. *Journal of Nanomaterials*, *448*(7152), 457–60.

Sreeprasad, T. S., Maliyekkal, M. S., Deepti, K., Chaudhari, K., Xavier, P. L., & Pradeep, T. (2011). Transparent, luminescent, antibacterial and patternable film forming composites of graphene oxide/reduced graphene oxide. *ACS Applied Materials & Interfaces*, *3*(7), 2643–54.

Sreeprasad, T. S., & Pradeep, T. (2012). Graphene for Environmental and Biological Applications. *International Journal of Modern Physics B*, *26*(21), 1242001.

Stankovich, S., Piner, R. D., Nguyen, S. B. T., & Ruoff, R. S. (2006). Synthesis and exfoliation of isocyanate-treated graphene oxide nanoplatelets. *Carbon*, *44*(15), 3342–3347.

Szab, T., Tombcz, E., Ills, E., & Dkny, I. (2006). Enhanced acidity and pH-dependent surface charge characterization of successively oxidized graphite oxides. *Carbon*, *44*(3), 537–545.

Tai, Z., Ma, H., Liu, B., Yan, X., & Xue, Q. (2012). Facile synthesis of Ag/GNS-g-PAA nanohybrids for antimicrobial applications. *Colloids and Surfaces. B, Biointerfaces*, *89*, 147–51.

Tang, J., Chen, Q., Xu, L., & Zhang, S. (2013). Graphene oxide–silver nanocomposite as a highly effective antibacterial agent with species-specific mechanisms. *ACS Applied Materials & Interfaces*, *5*, 3867–3874.

The Environmental Protection agency. (2013). *Drinking Water Report*, Wexford, Ireland.

The Environmental Protection agency. (2017). *Focus on private water supplies*, Wexford, Ireland.

The Oireachtas. European Union (Drinking Water) Regulations, 2014 (S.I. 122/2014) (2014).

Tian, J., Li, H., Xing, Z., Wang, L., Luo, Y., Asiri, A. M., … Sun, X. (2012). One-pot green hydrothermal synthesis of CuO–Cu2O–Cu nanorod-decorated reduced graphene oxide composites and their application in photocurrent generation. *Catalysis Science & Technology*, *2*(11), 2227.

Tonelli, F. M., Goulart, V. A., Gomes, K. N., Ladeira, M. S., Santos, A. K., Lorençon, E., … Resende, R. R. (2015). Graphene-based nanomaterials: biological and medical applications and toxicity. *Nanomedicine (London, England)*, *10*(15), 2423–50.

Toyokuni, S. (2013). Genotoxicity and carcinogenicity risk of carbon nanotubes. *Advanced Drug Delivery Reviews*, *65*(15), 2098–2110.

Tu, Y., Lv, M., Xiu, P., Huynh, T., Zhang, M., Castelli, M., Zhou, R. (2013). Destructive extraction of phospholipids from Escherichia coli membranes by graphene nanosheets. *Nature Nanotechnology*, (July), 1–8.

Uang, C.H. & Edlak, D., 2001. Analysis of estrogenic hormones in municipal wastewater effluent and surface water using enzyme linked immunosorbent assay and gas chromatography / tandem mass spectrometry. *Environmental Toxicology*, 20(1), pp.133–139.

Veerapandian, M., Zhang, L., Krishnamoorthy, K., & Yun, K. (2013). Surface activation of graphene oxide nanosheets by ultraviolet irradiation for highly efficient anti-bacterials. *Nanotechnology*, *24*(39), 395706.

Verstraete, W., & Rabaey, K. (2006). Critical Review Microbial Fuel Cells : Methodology and Technology. *Environmental Science & Technology*, *40*(17), 5181–5192.

Vijay Kumar, S., Huang, N. M., Lim, H. N., Marlinda, a. R., Harrison, I., & Chia, C. H. (2013). One-step size-controlled synthesis of functional graphene oxide/silver nanocomposites at room temperature. *Chemical Engineering Journal*, *219*, 217–224.

Wang, E. N., & Karnik, R. (2012). Water desalination: Graphene cleans up water. *Nature Nanotechnology*, *7*(9), 552–554.

Wang, G., Qian, F., Saltikov, C. W., Jiao, Y., & Li, Y. (2011). Microbial reduction of graphene oxide by Shewanella. *Nano Research*, *4*(6), 563–570.

Wang, H., Liu, J., Wu, X., Tong, Z., & Deng, Z. (2013). Tailor-made Au@Ag core-shell nanoparticle 2D arrays on protein-coated graphene oxide with assembly enhanced antibacterial activity. *Nanotechnology*, *24*(20), 205102.

Wang, H., Liu, Y., Li, M., Huang, H., Xu, H. M., Hong, R. J., & Shen, H. (2010). Multifunctional TiO2 nanowires-modified nanoparticles bilayer film for 3D dye-sensitized solar cells. *Optoelectronics and Advanced Materials, Rapid Communications*, *4*(8), 1166–1169.

Wang, M., Huang, J., Tong, Z., Li, W., & Chen, J. (2013). Reduced graphene oxide–cuprous oxide composite via facial deposition for photocatalytic dye-degradation. *Journal of Alloys and Compounds*, *568*, 26–35.

Wang, S., Lu, W., Tovmachenko, O., Rai, U. S., Yu, H., & Ray, P. C. (2008). Challenge in Understanding Size and Shape Dependent Toxicity of Gold Nanomaterials in Human Skin Keratinocytes. *Chemical Physics Letters*, *463*(1-3), 145–149.

Wang, S., Sun, H., Ang, H. M., & Tadé, M. O. (2013). Adsorptive remediation of environmental pollutants using novel graphene-based nanomaterials. *Chemical Engineering Journal*, *226*, 336–347.

Wang, W., Liu, Y., Zhang, H., Qian, Y., & Guo, Z. (2017). Re-investigation on reduced graphene oxide/Ag2CO3 composite photocatalyst: An insight into the double-edged sword role of RGO. *Applied Surface Science*, *396*, 102–109.

Wang, W., Yu, J., & Xia, D. (2013). Graphene and g-C3N4 nanosheets cowrapped elemental α-sulfur as a novel metal-free heterojunction photocatalyst for bacterial inactivation under visible-light. *Environmental Science & Technology*, *47*, 8724–8732.

Wang, X., Liu, X., & Han, H. (2012). Evaluation of antibacterial effects of carbon nanomaterials against copper-resistant Ralstonia solanacearum. *Colloids and Surfaces. B, Biointerfaces*, *103*, 136–42.

Wang, Y. W., Cao, A., Jiang, Y., Zhang, X., Liu, J.H., Liu, Y., & Wang, H. (2014). Superior antibacterial activity of zinc oxide/graphene oxide composites originating from high zinc concentration localized around bacteria. *ACS Applied Materials & Interfaces*, *6*(4), 2791–8.

Wang, Y. W., Fu, Y., Wu, L.J., Li, J., Yang, H.-H., & Chen, G.-N. (2013). Targeted photothermal ablation of pathogenic bacterium, Staphylococcus aureus, with nanoscale reduced graphene oxide. *Journal of Materials Chemistry B*, *1*(19), 2496.

WHO. (2015). *Water, sanitation and hygiene in health care facilities Status in low- and middle-income countries and way forward*.

Wijnhoven, S. W. P., Peijnenburg, W. J. G. M., Herberts, C. A., Hagens, W. I., Oomen, A. G., Heugens, E. H. W., Geertsma, R. E. (2009). Nano-silver – a review of available data and knowledge gaps in human and environmental risk assessment. *Nanotoxicology*, *3*(2), 109–138.

Wörle-Knirsch, J. M., Pulskamp, K., & Krug, H. F. (2006). Oops they did it again! Carbon nanotubes hoax scientists in viability assays. *Nano Letters*, *6*(6), 1261–1268.

Wu, M., Deokar, A., Liao, J., Shih, P., & Ling, Y. (2013). Graphene-based photothermal agent for rapid and effective killing of bacteria. *ACS Nano*, (2), 1281–1290.

Xiang, Q., Yu, J., & Jaroniec, M. (2012). Synergetic E ff ect of MoS 2 and Graphene as Cocatalysts for Enhanced Photocatalytic H 2 Production Activity of TiO 2 Nanoparticles. *Journal of the American Chemical Society*, *134*, 6575–6578.

Xiong, J., Wang, Y., Xue, Q., & Wu, X. (2011). Synthesis of highly stable dispersions of nanosized copper particles using l-ascorbic acid. *Green Chemistry*, *13*(4), 900.

Xu, C., Wang, X., Yang, L., & Wu, Y. (2009). Fabrication of a graphene–cuprous oxide composite. *Journal of Solid State Chemistry*, *182*(9), 2486–2490.

Xu, W.-P., Zhang, L.C., Li, J. P., Lu, Y., Li, H., Ma, Y.-N., Yu, S. H. (2011). Facile synthesis of silver@graphene oxide nanocomposites and their enhanced antibacterial properties. *Journal of Materials Chemistry*, *21*(12), 4593.

Yang, C., Mamouni, J., Tang, Y., & Yang, L. (2010). Antimicrobial activity of single-walled carbon nanotubes: length effect. *Langmuir : The ACS Journal of Surfaces and Colloids*, *26*(20), 16013–9.

Yang, S. T., Chen, S., Chang, Y., Cao, A., Liu, Y., & Wang, H. (2011). Removal of methylene blue from aqueous solution by graphene oxide. *Journal of Colloid and Interface Science*, *359*(1), 24–29.

Yang, S.-T., Chang, Y., Wang, H., Liu, G., Chen, S., Wang, Y., Cao, A. (2010). Folding/aggregation of graphene oxide and its application in Cu2+ removal. *Journal of Colloid and Interface Science*, *351*(1), 122–7. doi:10.1016/j.jcis.2010.07.042

Yang, X., Zhang, X., Ma, Y., Huang, Y., Wang, Y., & Chen, Y. (2009). Superparamagnetic graphene oxide–Fe3O4 nanoparticles hybrid for controlled targeted drug carriers. *Journal of Materials Chemistry*, *19*(18), 2710.

Yang, Y., Li, B., Ju, F., & Zhang, T. (2013). Exploring variation of antibiotic resistance genes in activated sludge over a four-year period through a metagenomic approach. *Environmental Science and Technology*, *47*(18), 10197–10205.

Yoon, K.-Y., Hoon Byeon, J., Park, J.-H., & Hwang, J. (2007). Susceptibility constants of Escherichia coli and Bacillus subtilis to silver and copper nanoparticles. *The Science of the Total Environment*, *373*(2-3), 572–5.

Yoon, Y. Westerhoof, P., Snyder, S.A, Wert, E. C. (2003). Pharmaceuticals, Personal Care Products, and Endocrine Disruptors in Water: Implications for the Water Industry. *Environmental Engineering Science*, 20(5), pp.449–469.

Young, M., & Santra, S. (2014). Copper (Cu)-silica nanocomposite containing valence-engineered Cu: A new strategy for improving the antimicrobial efficacy of cu biocides. *Journal of Agricultural and Food Chemistry*, *62*(26), 6043–6052.

Yu, L., Zhang, Y., Zhang, B., Liu, J., Zhang, H., & Song, C. (2013). Preparation and characterization of HPEI-GO/PES ultrafiltration membrane with antifouling and antibacterial properties. *Journal of Membrane Science*, *447*, 452–462.

Zhang, D., Liu, X., & Wang, X. (2011). Green synthesis of graphene oxide sheets decorated by silver nanoprisms and their anti-bacterial properties. *Journal of Inorganic Biochemistry*, *105*(9), 1181–1186.

Zhang, H., Lv, X., Li, Y., Wang, Y., & Li, J. (2009). P25-Graphene Composite as a High Performance Photocatalyst. *ACS Nano*, *4*(1), 380–386.

Zhang, J., Yang, H., Shen, G., Cheng, P., Zhang, J., & Guo, S. (2010). Reduction of graphene oxide via l-ascorbic acid. *Chemical Communications*, *46*(7), 1112–1114.

Zhang, K. (2012). Fabrication of copper nanoparticles/graphene oxide composites for surface-enhanced Raman scattering. *Applied Surface Science*, *258*(19), 7327–7329.

Zhang, K., Zhang, L. L., Zhao, X. S., & Wu, J. (2010). Graphene/Polyaniline Nanofiber Composites as Supercapacitor Electrodes. *Chemistry of Materials*, *22*(4), 1392–1401.

Zhang, Y., Mo, G., Li, X., Zhang, W., Zhang, J., Ye, J., Yu, C. (2011). A graphene modified anode to improve the performance of microbial fuel cells. *Journal of Power Sources*, *196*(13), 5402–5407.

Zhang, Y., Tang, Z., Fu, X., & Xu, Y. (2010). TiO2 - Graphene Nanocomposites for Gas-phase photocatalytic degradation of colatile aromatic pollutant: Is TiO2-graphene Truly different from other TiO2-carbon composite materials? *ACS Nano*, *4*(12), 7303–7314.

Zhang, Z., Zhang, J., Zhang, B., & Tang, J. (2013). Mussel-inspired functionalization of graphene for synthesizing Ag-polydopamine-graphene nanosheets as antibacterial materials. *Nanoscale*, *5*(1), 118–23.

Zhao, C., & Wang, W. (2012). Size-dependent uptake of silver nanoparticles in Daphnia magna. *Environmental Science & Technology*, *46*, 11345–11351.

Zhao, G., Li, J., & Ren, X. (2011). Few-layered graphene oxide nanosheets as superior sorbents for heavy metal ion pollution management. *Environmental Science & Technology*, *45*, 10454–10462.

Zhao, J., Deng, B., Lv, M., Li, J., Zhang, Y., Jiang, H., Fan, C. (2013). Graphene oxide-based antibacterial cotton fabrics. *Advanced Healthcare Materials*, *2*(9), 1259–66.

Zhu, Z., Su, M., Ma, L., Ma, L., Liu, D., & Wang, Z. (2013). Preparation of graphene oxide-silver nanoparticle nanohybrids with highly antibacterial capability. *Talanta*, *117*, 449–55.

7. Appendix

Publications and conferences

Oral presentations

- McGlade, D., Morrissey, A., Nolan, K., Lawler, J., Quilty, B., 2016, Immobilising a graphene copper composite for use in water treatment applications. Environ 2016, University of Limerick.

- McGlade, D., Morrissey, A., Nolan, K., Lawler, J., Quilty, B., 2016 A graphene-copper composite as an anti-bacterial agent for potential water treatment applications. Advanced Materials World Congress 2016, Stockholm, Sweden.

- McGlade, D., Morrissey, A., Nolan, K., Lawler, J., Quilty, B., 2015, A graphene-copper composite as an anti-bacterial agent for potential water treatment applications, Environ 2015, IT Sligo, Ireland.

Poster Presentations

- McGlade, D., Morrissey, A., Nolan, K., Lawler, J., Quilty, B., 2014, Investigation of the antimicrobial activity of graphene and graphene composites for use in drinking water treatment. Environ 2014, Febuary 26-28th, Trinity College Dublin, Dublin, Ireland.

- McGlade, D., Morrissey, A., Nolan, K., Lawler, J., Quilty, B., 2014, Investigation of the anti-microbial activity of graphene and graphene composites for use in drinking water treatment Graphene.study 2014, Obergurgl, Austria

- McGlade, D., Morrissey, A., Nolan, K., Lawler, J., Quilty, B., 2013, Investigation of the anti-microbial activity of graphene oxide and reduced graphene oxide. Environ 2013, National University of Ireland, Galway, Ireland.

- McGlade, D., Morrissey, A., Nolan, K., Lawler, J., Quilty, B., 2013, Investigation of the anti-microbial activity of graphene and graphene composites for use in drinking water treatment. ATWARM 2013, The Helix, Dublin City University, Dublin, Ireland.

Workshops & Courses

- Graphene.study Winter School 2014. January 2014, Obergurgl, Austria.

Journal Articles

- M. Kumar, D. McGlade, J Lawler. Functionalised chitosan derived novel positively charged organic-inorganic hybrid ultrafiltration membranes for protein separation. RSC Advances 2014, 42, 4, 21699-21711.

- M. Kumar, D. McGlade, M. Ulbricht, J Lawler. Quaternized polysulfone and graphene oxide nanosheet derived low fouling novel positively charged hybrid ultrafiltration membranes for protein separation. RSC Advances 2015, 63, 5, 51208-51219.